June 2018

Therapeutic modulation of Alzheimer's disease with biological (HUCBS) and pharmacological (LISPRO) approaches

Md Ahsan Habib
University of South Florida, mhabib1@health.usf.edu

Therapeutic modulation of Alzheimer's disease with biological (HUCBS) and

pharmacological (LISPRO) approaches

by

Md Ahsan Habib

A dissertation submitted in partial fulfillment
of the requirements for the degree of
Doctor of Philosophy
with a concentration in Neuroscience
Department of Molecular Pharmacology and Physiology
Morsani College of Medicine
University of South Florida

Major Professor: Jun Tan, M.D., Ph.D.
Thomas Taylor-Clark, Ph.D.
Brian Giunta, M.D., Ph.D.
Jaya Padmanabhan, Ph.D.
Kevin Nash, Ph.D.

Date of Approval:
June 26, 2018

DEDICATION

To My Mother

TABLE OF CONTENTS

iv

LIST OF FIGURES

vi

LIST OF ABBREVIATIONS

AAS... Atomic Absorption Spectroscopy
ABP.. Adult Blood Plasma
ABS.. Adult Blood Serum
ADAM .... A Disintegrin and Metalloproteinase
AgBP...Aged Blood Plasma
AgBS...Aged Blood Serum
AgBSF... Aged Blood Serum Fraction
AICD..APP Intracellular Domain
AD... Alzheimer's disease
ANOVA ....One-Way Analysis of Variance
APP .... Amyloid Precursor Protein
Aβ...Amyloid beta
BACE1 ....Beta-site Amyloid Precursor Protein Cleaving Enzyme 1
BDNF... Brain Derived Neurotrophic Factor
CBP... Cord Blood Plasma
CBS .... Cord Blood Serum
CBSF...Cord Blood Serum Fraction
CD40L..Cluster of Differentiation 40 Ligand
CHO/APPwt... Chinese Hamster Ovary Cells expressing Wild-type APP
COX2 ....Cyclooxygenase 2
CNS... Central Nervous System
CSF ....Cerebrospinal fluid
CTF ....C-Terminal Fragment
Ctrl .... Control
DMEM ....Dulbecco's modified Eagle's medium
ELISA ....Enzyme-Linked Immunosorbent Assay
EPM……………………………………………………………………….Elevated Plus Maze
FACS.. Fluorescence Activated Cell Sorting
fAPP... Full-length APP
FBS ....Fetal Bovine Serum
FC... Fear Conditioning
FDA.. Food and Drug Administration
FITC..Fluorescein Isothiocyanate
GFAP .... Glial Fibrillary Acidic Protein
GSK3.. Glycogen Synthase Kinase 3
HUCBC..Human Umbilical Cord Blood Cells
HUCBS ....Human Umbilical Cord Blood Serum
IFN ....Interferon
IHC... Immunohistochemistry
IL...Interleukin

viii

ABSTRACT

Dementia is the top global public health threat of the twenty first century. Within the dementia spectrum, Alzheimer's disease (AD) is the most common type of dementia that occurs with aging and accounts for about 60% - 80% of diagnosed cases. But currently available discoveries failed to develop disease-modifying therapies for all patients living with AD. Recent discoveries can only partially slow down cognitive decline in a small subset of patients with limited effectiveness. The heterogeneity and complexity of the pathophysiology of AD indicate that a single drug approach may not be sufficient to prevent disease onset and progression. Human umbilical cord blood cells (HUCBC) and lithium treatment have shown promise against numerous neurological conditions, including AD. Yet, they also show significant unwanted, adverse effects. To address this barrier to yield successful treatments, we employed two key modifications to these two treatment strategy. We used human umbilical cord blood derived serum (HUCBS, also labeled as CBS) rather than HUCBC. We also utilized ionic cocrystal of lithium salicylate l-proline (LISPRO, also labeled as LP) instead of usual lithium salt. Both HUCBS and LISPRO have been shown to have strong neuroprotective, anti-inflammatory properties in separate studies conducted in transgenic AD mouse models. The studies detailed herein independently investigated the effectiveness of biological (HUCBS) and pharmacological (LISPRO) approaches in modulating the pathology and cognitive impairments in AD mouse models (e.g., 5XFAD, 3XTg-AD, APPswe/PS1dE9, and Tg2576).

While administration of HUCBC stimulate anti-inflammatory pathways shown in previous studies, we found that HUCBS markedly promoted neurotrophic soluble amyloid precursor protein alpha (sAPPα) through non-amyloidogenic amyloid precursor protein (APP) processing pathway compared to adult (ABS) and aged blood serum (AgBS) in Chinese hamster ovary cells expressing wild type APP (CHO/APPwt). Using chromatographic fractionation, mass-spectrometry, and targeting complement proteins in cord blood serum fraction (αCBSF), we discovered the source of sAPPα in HUCBS as C1 complement protein. Further, intraperitoneal administration of αCBSF *via* osmotic minipump for 6 weeks showed prevention of cognitive impairment in 5XFAD mice assessed by novel object recognition, and Y-maze test.

A series of recent studies have shown that lithium can prevent both AD- and age-associated cognitive decline. But, current United States Food and Drug Administration-approved lithium pharmaceutics (carbonate and citrate forms) have a narrow therapeutic window and unstable pharmaceutics that can cause toxicity without monitoring. Here we investigated the safety, pharmacokinetics, and therapeutic efficacy of LISPRO (LP), lithium salicylate (LS), and lithium carbonate (LC) in cell culture and mouse (B6129SF2/J, Tg2576, and 3xTg-AD) models. Cytokine profiles from the brain, plasma and splenocytes demonstrated that 8-week oral treatment with LISPRO downregulates pro-inflammatory cytokines, upregulates anti-inflammatory cytokines and suppress renal cyclooxygenase 2 (COX2) expression in Tg2576 mice. Pharmacokinetic studies indicated that LISPRO provides significantly higher brain and more steady plasma lithium levels in both B6129SF2/J and transgenic Tg2576 mice compared with lithium carbonate. Oral administration of LISPRO for 28 weeks significantly reduced β-amyloid plaques and tau phosphorylation. In addition, LISPRO significantly elevated pre-synaptic (synaptophysin) and post-synaptic protein (post synaptic density protein 95) expression in brains from transgenic

3XTg-AD mice. Moreover, female APPswe/PS1dE9 mice at 4 months of age were orally treated with LP, LS, or LC for 8- to 9- months at 2.25 mmol lithium/kg/day followed by measuring body weight, internal organs' growth, and cognitive and non-cognitive function. LISPRO treatment prevented cognitive decline compared with transgenic APPswe/PS1dE9 cohort, as shown by shorter escape latency during training and probe trials in the Morris water maze and longer contextual freezing time during fear conditioning. As expected, LISPRO treatment also reduced depression assayed by tail suspension test and irritability assessed with the touch escape test. But, lithium treatment did not alter anxiety or locomotor activity as assessed by open field, elevated plus maze or accelerated rotarod tests.

Taken together, these data indicate that both biological HUCBS and pharmacological LISPRO treatment may prove to be viable effective strategy for ameliorating Alzheimer's like pathology and cognitive impairment in preclinical models.

CHAPTER 1

INTRODUCTION

Note to reader:

Portion of this chapter has been previously published in Journal of Neuroscience Research, Habib *et al.,* (2017) 95(4): 971–991 (Restoring Soluble Amyloid Precursor Protein α Functions as a Potential Treatment for Alzheimer's Disease) and has been reproduced with permission from Wiley Periodicals, Inc.

Alzheimer's disease (AD): Overview

Alzheimer's disease (AD) is a chronic neurodegenerative disorder that severely affects cognition with no disease modifying treatments. The pathological features of AD currently include: (a) extracellular amyloid plaques composed largely of amyloid-β (Aβ) peptides [1], (b) intracellular neurofibrillary tangles (NFTs) composed of hyperphosphorylated microtubule associated protein tau (p-tau) [2], (c) dysmorphic synapses, (d) inflammation, and (e) neuronal loss [3]. The clinical symptoms of AD comprise difficulties with thinking, internalizing information, memory, language, and other cognitive skills that affect the ability to live independently. These cognitive-processing difficulties occur, because neurons in different parts of the brain associated with cognition have become irreversibly damaged. Changes in mood and personality may be an initial, early sign of AD following a gradual decline in memory. With more substantial memory

decline, individuals often become disoriented to time and space and show disrupted sleep-wake cycle. People with more prominent memory decline begin to forget recent conversations, names or events at early stages, while later stages show additional symptoms including impaired verbal communication, poor judgment, losing or misplacing things, lose the ability to work, and ultimately unable to carry out activities of daily living, such as speaking and walking. A person in the final stage of the disease is bed-bound and usually requires intensive care. AD accounts for the sixth-leading cause of death in the United States. According to Alzheimer's association data, an estimated 5.7 million Americans of all ages are currently living with AD in 2018. The percentage of people with AD increases with age with a prevalence rising from 3% at the age of 65 and 32% at the age of 85. Total number of AD cases will be nearly 14 million in the United States, as the older population is expected to double by 2050. Although five drugs have U.S. federal approval to manage AD symptoms, there still remains no permanent cure for AD. Therefore, the management cost of the disease will exceed 20 trillion USD in 2050, if we do not find effective treatments [4].

Alzheimer's disease (AD): Pathology

The major pathological hallmark of AD is amyloid plaque, which is an extracellular deposit of a short peptide called Aβ. According to amyloid cascade hypothesis, the proteolytic cleavage of APP by two different enzymes, β- (also called beta-site amyloid precursor protein cleaving enzyme 1, BACE1) and γ-secretases, is a critical step to develop AD. In the non-amyloidogenic pathway, most APP is cleaved at the plasma membrane by α-secretase, which precedes Aβ formation but produces a large secreted, 105-125 kDa N-terminal ectodomain of APP (sAPPα) and small membrane-bound α-C-terminal fragment (CTF) [5]. Alpha (α) secretase proteolytic enzymes are members of a disintegrin and metalloproteinase domain (ADAM) family that cleaves

numerous cell surface proteins including APP. Then, the membrane-bound α-CTF is cleaved by γ-secretase complex (presenilin-1, nicastrin, anterior pharynx-defective 1, presenilin enhancer 2) inducing release of P3 peptide (3 kDa) and AICD (APP intracellular domain). In the amyloidogenic pathway, the remaining uncleaved APP is processed into endosomal-lysosomal compartments by β-secretase, producing soluble sAPPβ and membrane-bound β-CTF [6]. Subsequent action of γ- secretase on β-CTF produces Aβ $_{1-40/42}$ peptides and AICD. In addition to α-, β- and γ- secretase cleavage, some studies have identified that APP can be cleaved by the metalloprotease meprin β, which generates soluble N-terminal truncated APP (N-APP) and N-terminally truncated Aβ$_{2-x}$ peptide variants [7][8][9]. These latter proteins show increased aggregation potential compared to non-truncated Aβ$_{40}$ peptides. Cleavage of APP by meprin β occurs prior to endocytosis, and different APP mutants affect the catalytic properties of the enzyme. More specifically, Swedish mutant APP does not undergo this cleavage and is unable to produce these truncated Aβ variants. One recent study showed that APP can also be cleaved by matrix metalloproteinases such as MT5-MMP, referred to as η-secretase, which releases a long-truncated ectodomain (sAPPη) and a membrane-bound CTF, termed CTFη. The membrane-bound CTFη is further cleaved by α- and β-secretases releasing both a long (Aη-α) and a short (Aη-β) peptide, respectively. The cleavage of η occurs far from the N-terminus of the β-secretase cleavage site and produces fragments of 92 or 108 amino acids, which end at either the β- or α- secretase site, respectively [10] [Figure 1-1].

The major pathological hallmark of AD is amyloid plaque, which is an extracellular deposit of a short peptide called Aβ. A number of *in vitro* and *in vivo* studies demonstrated the toxic properties of Aβ peptides, since the APP gene was first identified in 1987 [6][11][12]. Administration of Aβ peptides [13], their structural mimetics, and anti-Aβ antibodies [14] have

supported the toxic functions of the peptide in terms of promoting cognitive deficits. Yankner *et al.,* (1989) showed that Aβ-expressing PC-12 cells grow normally without any cellular degeneration. Interestingly, after treatment with nerve growth factor (NGF), these Aβ-expressing PC-12 cells differentiated into neuronal cells and started to degenerate slowly. Further, cultured neuronal cells treated with conditioned medium collected from Aβ-expressing PC-12 cells also degenerated at a slower rate. Pre-treatment with the anti Aβ antibody blocked the Aβ-induced degeneration in PC-12 cells. This findings indicated that Aβ peptide induces neurodegeneration and eventual cell death [15]. Subsequently, other studies confirmed that this was the same oligomeric Aβ peptides cause neuronal cell death *in vitro* and *in vivo*. Further, substantial evidence demonstrates that elevated levels of soluble Aβ can initiate the disruption of synaptic connections between neurons, which then lead to neuronal loss and cognitive impairment (reviewed by [16][17]). No strong correlation exists between the total number of plaques and degree of cognitive impairment in AD patients [18], however a series of recent studies demonstrated that prefibrillar soluble Aβ are found to be more toxic than their insoluble Aβ fibril forms [19][20].

The other hallmark of AD is neurofibrillary tangles, which form inside the neurons and are composed of abnormally hyperphosphorylated tau [2]. The primary component of the neurofibrillary tangle is the microtubule-associated protein tau. In the central and peripheral nervous system, microtubules participate in many cellular processes such as cell structure, division, motility, and intracellular transport of proteins [21]. Tau, a highly expressed axonal protein responsible for maintaining physiology and stability of microtubule structure [22], becomes modified in AD [23]. Among different modifications of tau, phosphorylation rigorously affects its normal physiological functions in the brain. The tau phosphorylation state influences its ability to bind and stabilize microtubules, as hyperphosphorylation produces detachment and self-

aggregation of tau into neurofibrillary tangles and microtubule depolymerization [24][25]. Several

independent studies have extensively characterized the tangle pathology over the past few decades.

As AD progresses, the number and size of tangles increase throughout the whole brain. The extent

and distribution pattern of tangles well correlate with the stage and degree of cognitive impairment

in AD [26][18]. The detail findings of those study fall beyond the scope of this study herein.

Alzheimer's disease (AD): Risk Factors

The exact etiology of AD remains unclear. Only 1% of AD cases arise from known genetic

mutations in three predominant genes such as APP, presenilin 1, and 2 (reviewed by [27]). Down

syndrome patients, who have an extra APP molecule at chromosome 21, often get AD at a very

early age (reviewed by [28]). The remaining 99% of patients have no genetic component and

presumably arise through unknown environmental factors. It is thought that interaction among

genetic, environmental, and lifestyle factors for many years with the aging likely trigger changes

in the brain. Evidences suggest that the brain is particularly vulnerable to the effects of aging, as

increasing age is the greatest known risk factor for AD to date. It is generally believed that AD is

not a part of normal aging, rather the risk for AD onset increases significantly after age 65. After

age 85, the probability of AD onset is nearly 40%. Early-onset AD, or familial AD, comprises 1-

5% cases and arises through mutations in three predominant genes. In contrast, the greatest known

risk factor for late-onset sporadic AD is older age. Most studies confirmed that a family history

and carrying the ApoE4 allele increases the risk of AD. Genome-wide association studies have

identified multiple genes with single nucleotide polymorphisms or variants associating with AD,

including ABCA7, BIN1, CASS4, CD33, CD2AP, CELF1, CLU, CR1, DSG2, EPHA1,

FERMD4A, FERMT2, HLA-DRB5/DRB1, INPP5D, MS4A, MEF2C, NME8, PICALM, PLD3,

PTK2B, SLC24H-RIN3, SORL1, TRIP4, TREM2, and ZCWPW1 (reviewed by [29]). Data also

indicates an association between AD and head injury. Yet, other data demonstrate an association between AD and infection. Cardiovascular disease risk factors, such as high cholesterol and high blood pressure, also increase the risk to develop AD.

Alzheimer's disease (AD): Treatment

No pharmacological treatments or therapeutic strategies delay or stop the progression of AD. Evidence suggests that AD begins over a decade before clinical symptoms appear which supports the importance of early intervention to modify disease progression. Current FDA-approved drugs acetylcholinesterase inhibitor and NMDA-receptor antagonist for AD, e.g., donepezil, galantamine, tacrine, rivastigmine, and memantine, partially improve symptoms in small subset of patients. Acetylcholinesterase inhibitor is used for mild to moderate cases while NMDA-receptor antagonist used for moderate to severe dementia. Although these drugs have demonstrated significant clinical benefit, they are unable to stop, inhibit, or reverse the core neuropathology of AD. According to clinical trial registry, a total of 244 drugs have been tested in clinical trial between 2002 and 2012. Among all of these drugs, only one drug received approval from the FDA (reviewed by [30][31]). This indicates that we must develop new therapeutic targets and develop novel treatments to address this health crisis [4].

Alzheimer's disease (AD): Biological and pharmacological treatments

Human umbilical cord blood derived serum (HUCBS) treatment as a biological approach to modulate AD

HUCBS: Isolation

Human umbilical cord blood-derived serum (HUCBS) was collected from umbilical cord blood and is blood that remains in the placenta and in the attached umbilical cord, after the cord has been detached from the newborn at the time of childbirth. HUCBS is separated from umbilical

cord blood by allowing clotting for 5-10 h in red top tubes with no anticoagulation followed by centrifugation at 3500 rpm for 5-10 min at 4 ^{0}C. Before treatment, all the samples were passed through a 0.22 µm pore size filter. In a recent study, we found that HUCBS produce increased levels of sAPPα compared to the adult (ABS, 25-30 years old) or aged (AgBS, >75 years old) blood serum in Chinese hamster ovary cells overexpressing wild-type APP (CHO/APPwt). First, we examined the enzymatic activity of α-secretase-like enzyme in HUCBS, ABS, and AgBS by comparing the levels of sAPPα upon treating CHO/APPwt cells. We hypothesized that HUCBS may contain novel enzyme protein that is responsible for this effect. In order to identify the source of the enzyme, we enriched a fraction (termed as αCBSF) with highest sAPPα producing capacity using multi-step chromatographic separation techniques. Further investigation using LC-MS/MS analyses showed that HUCBS-derived APP α-secretase cleavage activity is mediated by C1 complement. Infusion of αCBSF *via* intraperitoneal osmotic minipump ameliorates cognitive impairments and associated-amyloid pathology in transgenic 5XFAD mouse model.

HUCBS: Anti-AD therapeutic properties of sAPPα, HUCBC, and HUCBS

HUCBC induce embryonic, post-natal, and adult neurogenesis in preclinical models [32] and clinical study [33], and has been recommended as a treatment option for specific conditions. A series of recent study in HUCBC in treating different neurological conditions [34][35] opened new opportunities for AD research [36]. In our prior work in an AD mouse model, we found that multiple low-dose peripheral infusions of HUCBC reduced amyloid plaques, cerebral vascular Aβ astrocytosis, and improved cognition [37]. In a subsequent study, we demonstrated that HUCBC-derived monocytes ameliorate amyloid pathology and cognitive impairment in Tg2576 AD mouse model [38]. Nevertheless, the possibility of causing graft versus host disease [39] and low yield of HUCBC makes the use of this cell-based therapy less attractive in many circumstances. In a recent

work using a sophisticated parabiosis experiment, Wyss-Coray and his colleagues have showed that blood plasma from old mice reduces neurogenesis and impairs cognitive functions in young mice brain [40]. In a follow-up study, the same group has reversed age-related impairments by infusing plasma from young mice into old mice [41]. We also believe that HUCBS possess anti-AD therapeutic potential for reducing inflammation, pathology, and cognitive deficits. In our prior study, we found that sAPPα can inhibit amyloid [42] and tau pathology [43] by modulating BACE1 and GSK3β enzyme activity.

HUCBS: Neuroprotective effect of sAPPα and HUCBS

The level of sAPPα in the cerebrospinal fluid (CSF) and brain often serves as a predictive biomarker for AD patients. Almost all of the animal and human studies reported lower levels of sAPPα in AD brain compared to age-matched controls [44][45]. Many studies have reported the protective function of sAPPα against a variety of extracellular insults in cell cultures and *in vivo* models. However, the exact neuroprotective mechanisms of sAPPα that provide protection are unclear. Overall, sAPPα contributes to numerous protective functions in the brain including neuroprotection [46][47], increase long-term potentiation (LTP) [48], synaptic plasticity [49], stimulate neurite outgrowth [50][51], and proliferation of neuronal [52][53], and non-neuronal cells [54][55], which appear to be disrupted in Alzheimer's patients [56]. Initial studies on cultured rat hippocampal slices showed neuroprotection against glucose-deprivation and glutamate mediated toxicity [57]. This finding indicates that sAPPα can protects cultured neuronal cells from excitotoxicity; this fact is further supported by increased secretion of sAPPα in response to electrical depolarization on rat hippocampal slices. Subsequently, the sAPPα-mediated neuroprotective mechanism in neuronal environment was identified. Using whole-cell patch-clamp and imaging techniques, Furukawa and his colleagues have shown that sAPPα activates K^+

channel and suppress N-methyl-D-aspartate (NMDA) currents, which subsequently prevents neuronal excitability and glutamate-induced excitotoxicity [58][59]. Barger and Mattson have found that sAPPα decreases Ca^{2+} and NMDA currents in hippocampal neurons by elevating cyclic guanosine monophosphate, which protect against hypoglycemic damage and glutamate-induced excitotoxicity [60]. In line with the cell culture findings, *in vivo* studies confirmed the protective function of sAPPα. One study showed that ventricular administration of sAPPα in a rat model reduced hippocampal neuronal cell death against ischemic [61], spinal cord [62] and traumatic brain injury (TBI) [63][64]. Surviving neuronal cells synthesized new proteins visualized by amino acid autoradiography in the cell bodies of hippocampal neuronal cells [64]. Another study found that sAPPα treatment attenuated amyloid pathology, improved cognition, and motor functions in a moderately brain-injured APP knockout mouse model [65]. Subsequent studies by the Cappai group showed that the heparin binding site of sAPPα (amino acid residues 96-110) provides protection against TBI [66]. In addition, signaling pathway activation followed by gene transcription is another mechanism by which sAPPα elicits its protective function. A number of different studies demonstrated that sAPPα activates several signaling pathways involving phosphatidylinositol-3-kinase (PI3K)-PKB/Akt [67][68][69], nuclear factor kappa-light-chain-enhancer of activated B cells (NF-κβ) [70], extracellular signal regulated kinase (ERK) [71][67] and inhibits stress-induced inhibition *via* c-Jun N-terminal kinase [72]. Moreover, sAPPα also activates several neuroprotective genes, such as insulin-like growth factor 2, manganese superoxide dismutase, catalase, and transthyretin [73]. To identify the downstream effector molecules, Hartl and his colleagues have analyzed sAPPα-induced proteome changes in primary neuronal cell culture. The study demonstrated that sAPPα downregulates cyclin-dependent kinase 5 expression and induces cytoprotective chaperone 150-kDa oxygen regulated protein as a

protective response [74]. Furthermore, a recent study found that sAPPα can activate an Akt survival pathway by interacting with G-protein-coupled receptors and cell surface APP [69].

Increasing research demonstrates that blood plasma factors play an important role in age-associated diseases, particularly in dementia and AD. In previous work, a research team led by Dr. Wyss-Coray from Stanford University demonstrated that administration of young mouse plasma *via* tail vein injection into old mice improved hippocampal learning and memory function [40]. They concluded that young blood could be a source of growth factors that might have benefited the old mice. In a new study by the same group demonstrated that older mice received human umbilical cord blood plasma showed improved hippocampal learning and memory function. They then identified the specific factor in umbilical cord blood plasma that makes the old mice brain young, and found that tissue inhibitor of metalloproteases 2 is responsible for rejuvenating hippocampal spatial memory function in older mice [75]. Wyss-Coray and his colleagues further compared umbilical, adult (19- to 24 year-olds) and aged (61- to 82 year-olds) blood plasma, and found an age-associated change in several proteins. They found that these age-associated changes in proteins might affect the hippocampal function in the brain. Recently, we found that HUCBS contain α-secretase-like enzyme that either directly or indirectly activates α-secretase and produces sAPPα significantly in cell culture and cell free system.

HUCBS: Anti-inflammatory effects of HUCBC

Microglia, the main immune cells in the brain, play a critical role in the etiology of several neuroinflammatory conditions [76]. Preclinical and postmortem analyses implicate inflammatory process as causative factor in neuronal cell death in a number of neurodegenerative diseases, such as Multiple sclerosis [77], Parkinson's disease [78], Bipolar disorder [79], Alzheimer's disease [80]. Activated microglia typically removes damaged cells from the brain either by recruiting

10

soluble factors or phagocytosis [81]. But, it remains unclear whether microglia plays a beneficial or detrimental role in diseased conditions. Current proposals state that acute microglial activation is beneficial to eliminate pathogens and damaged cells. But, chronic microglial activation cause damage through secretion of proinflammatory cytokines, complement proteins, and reactive species [82]. So, suppressing inflammatory cytokines released by microglia are considered an effective therapeutic approach in neuroinflammatory diseases. Several neuroprotective and anti-inflammatory approaches can suppress microglial activation in the brain following inflammation. Our prior work showed that flavonoid compounds such as luteolin [83], diosmin [84], and epigallocatechin-3-gallate [85], have disease modifying properties through modulation of inflammatory pathways. In recent years, our lab and others have identified the immunomodulatory properties of HUCBCs in several neurodegenerative conditions particularly in AD [37]. The exact molecular mechanism behind these immunomodulatory effects of HUCBC remains unclear. More recently, HUCBC–derived stem cells have the potential to differentiate into neuronal and glial cells in experimental conditions. HUCBC opposes pro-inflammatory T helper cell type 1 response and stimulate anti-inflammatory T helper cell type 2 responses in a rat stroke model [86]. HUCBC can also reduce proinflammatory CD40-CD40 ligand interaction, which reduces Aβ deposition in Tg2576 and PSAPP AD mouse models [37]. Furthermore, HUCBC reduces proinflammatory reactive microgliosis, associated astrocytosis, and increased anti-inflammatory cytokines IL-10, transforming growth factor β1 (TGF-β1), and NGF in the brain [37]. Like HUCBC, we believe that HUCBS will also demonstrate its AD-modulating properties through anti-inflammatory function.

Ionic co-crystal of lithium salicylate l-proline (LISPRO) treatment as a pharmacological approach to modulate AD

LISPRO: Formulation

The active pharmaceutical ingredient of LISPRO is lithium. Briefly, lithium salicylate salt and l-proline were dissolved in hot deionized water. The resulting solution was maintained at 75-90 ^{0}C on a hot plate. The colorless crystal formed in the plate after slow evaporation of solvent. Lithium is a divalent cation with the anion being salicylic acid, which is a derivative of acetyl salicylic acid (aspirin). The amino acid l-proline works as a coformer. *In vivo* pharmacokinetics data showed that LISPRO produced very steady lithium plasma and brain lithium levels for 48 h compared to lithium carbonate in Sprague Dawley rat model [87].

LISPRO: Anti-AD therapeutic properties of lithium

Diverse preclinical studies provide consistent evidence supporting the neuroprotective effects of lithium to prevent neurodegenerative diseases, including AD. Several mechanisms may underlie lithium's potential neuroprotective efficacy for AD. One important mechanism is that lithium inhibits certain enzymes in a noncompetitive manner by displacing the required divalent cation, magnesium [88]. Klein and Melton identified GSK3β as a key molecular target of lithium [89]. In the context of AD, this enzyme phosphorylates tau at most of the serine and threonine residues in the paired helical filaments. GSK3 activity contributes both to Aβ production and Aβ-mediated neuronal cell death [90]. Therapeutic doses of lithium block production of Aβ by interfering with APP cleavage at the γ-secretase step without inhibiting Notch processing by targeting GSK3α [91]. Lithium also blocks Aβ accumulation in brains of mice overexpressing APP by inhibiting GSK3β, which further implicates its requirement to process APP [92]. Since GSK3β also phosphorylates the tau protein, inhibition of GSK3β offers a new approach to reduce the formation of both β-amyloid plaques and neurofibrillary tangles. Interestingly, lithium

treatment can prevent prefibrillar tau-aggregates in double transgenic mice that overexpress GSK3β and tau with a triple frontotemporal dementia with parkinsonism-17 (FTDP-17) mutation [93].

LISPRO: Neuroprotective effects of lithium

Lithium induces its cellular and molecular effects by activating neurotrophic and neuroprotective pathways and its associated signaling mechanisms [94]. These neuroprotective effects are secondary to the two main effects, inhibition of GSK3β and inositol phosphatase. As GSK3β induces amyloid and tau pathology, lithium-induced inhibition of GSK3β offers a novel approach to modulate formation of both amyloid plaques and neurofibrillary tangles. More specifically, lithium inhibits GSK3β in a noncompetitive fashion by displacing the divalent cation, Mg^{2+} [95]. Lithium can modify cyclic adenosine monophosphate (cAMP)-mediated signaling by increasing adenylyl cyclase and protein kinase A (PKA), which subsequently activates the nuclear transcription factor cAMP response element binding protein (CREB) and increases brain derived neurotrophic factor (BDNF) expression. In addition, it has been demonstrated that chronic administration of lithium upregulates BDNF expression in rat and human studies. Increased BDNF activity may restore learning and memory function through neurogenesis and LTP. Binding with tropomyosin receptor kinase B receptor, BDNF activates extracellular signal-regulated kinase/mitogen-activated protein kinase (ERK/MAPK) signaling pathway which inhibit GSK3β and pro-apoptotic Bcl-2-associated death promoter protein (BAD). This signaling further increases nuclear CREB expression, which subsequently stimulates expression of anti-apoptotic bcl-2 and neuroprotective BDNF through feedback mechanisms. Mitochondrial bcl-2 inhibits BAD protein and also inhibits calcium and cytochrome c release into the cytoplasm. Lithium exerts neuroprotection by inhibiting inositol phosphatase enzymes, which regulate cellular inositol

13

triphosphate (IP3) levels. IP3 acting as a second messenger regulates several cellular processes through calcium signaling pathways. Lithium also downregulates calcium release from the endoplasmic reticulum (ER) *via* the IP3 pathway, which increases bcl-2 levels and prevents activation of apoptotic pathways. Another neuroprotective mechanism of lithium is attenuating pro-inflammatory cytokine generation, like IL-1β and TNFα, in activated microglia. This is particularly significant since inflammation commonly occurs in AD (reviewed by [94]) [Figure. 1-2].

LISPRO: Anti-inflammatory effects of lithium

Increasing evidence suggests that inflammation plays a key role in the pathological processes in AD. Among multiple mechanisms of action that underlie lithium's therapeutic efficacy, anti-inflammatory effects of lithium play a critical role in preventing several inflammatory brain diseases including AD. As lithium has multiple targets in the brain, it is unclear which target mediates its therapeutic efficacy in a specific condition. The arachidonic acid-prostaglandin pathway contributes to brain inflammation and anti-inflammatory treatment of AD [96]. Several lines of evidence demonstrated anti-inflammatory properties of lithium by modulating prostaglandin pathways [97]. Lithium can reduce COX2 expression and lipopolysaccharide induced prostaglandin E2 production and also increases anti-inflammatory 17-hydroxy-docosahexanoic acid in different parts of the brain in preclinical models and primary cell cultures [98][99][100]. However, other studies reported either no effect or increased COX2 expression in other tissue sites of action [101][102]. Nitric oxide (NO) is an important signaling molecule involved in multiple cellular processes. The NO pathway is implicated in brain inflammation [103]. Other studies showed that lithium treatment enhances nitric oxide synthase expression and NO production [104][105]. However, most studies demonstrated that lithium

inhibits nitric oxide synthase-nitric oxide inflammatory pathway [106][107]. Tumor Necrosis Factor-α (TNF-α), IL-1β, IL-4 and IFN-γ are major pro-inflammatory cytokines involved in neural inflammatory processes. Some studies indicate that lithium stimulates TNF-α production [108][109]. However, most studies showed that lithium significantly inhibits TNF-α synthesis in the brain [110][111][112]. Similar to TNF-α, most of the studies showed that lithium can inhibit IL-1β [113], IL-4 [114] and IFN-γ [115] synthesis. IL-2 and IL-10 are important anti-inflammatory cytokines found in the human immune system. Numerous studies found that lithium increases IL-2 [116][117], and IL-10 [118] synthesis, indicating a profound anti-inflammatory effect for lithium. Lithium also can modulate other inflammatory markers, such as IL-1α, IL-1 receptor antagonist, IL-3, IL-6 and IL-17. As very few studies have investigated the effect of lithium on these mediators, no conclusive findings available in this context. Several studies investigated the effects of lithium on microglial expression and function in the brain [119][120]. Lithium inhibits microglial and astrocytes activation in a mouse model of AD [121]. GSK3β dysregulation plays a critical role in the development of several inflammatory diseases including AD [122]. The exact anti-inflammatory therapeutic mechanism of action of lithium remains unclear. Accumulating evidence suggests that GSK3β enhances the activity of transcription factor NF-κβ, which increased inflammatory processes in animal models [123]. Pharmacological inhibition of GSK3β attenuated inflammatory NF-κβ activity and pro-inflammatory cytokine production under different experimental conditions [124]. In fact, GSK3β phosphorylates NF-κβ and accelerates proteasomal degradation of this transcription factor. Inhibiting NF-κβ activation by GSK3β further suppressed LPS-induced TNF-α, COX2 and nitric oxide synthase expression [110][125]. Inhibiting GSK3β activity by lithium downregulates the pro-inflammatory cytokine signal transducer and activator of transcription (STAT) pathway [126]. Taken together, the above findings indicate that lithium

suppresses inflammatory pathways in many experimental conditions. Despite these anti-inflammatory potential, many other studies show that lithium has pro-inflammatory effects in the cells. Further studies will elucidate the effects of lithium on inflammation. Our studies should also investigate the inflammatory effects of the related compound, salicylic acid, a derivative of aspirin and further investigate whether it will enhance the anti-inflammatory effects of LISPRO in AD.

Rationale: GSK3β is a target for both sAPPα and lithium

GSK3 is a serine/threonine protein kinase initially identified as playing a key role in glycogen metabolism [127]. The phosphorylation state and growth factor signaling regulate GSK3β activity, as phosphorylation at tyrosine 216 increases [128] and serine 9 residue decreases [129] its activity. GSK3β kinase has many different kinds of physiological functions in neuronal cells. GSK3β has specific functions during neuronal development [130], neuronal apoptosis [131][132], and synaptic dysfunction [133]. Partial inhibition of GSK3β using various approaches showed positive effects in different pathologies including psychiatric disorders and is now recommended as treatment for specific conditions [134][135]. Since GSK3β induces both amyloid formation and tau hyperphosphorylation [136], it acts as a bridge between amyloid and tau pathology [137][138]. Partial inhibition of GSK3 signaling significantly reduced Aβ deposition, plaque formation, and rescued memory deficits in a double transgenic AD mouse model [134]. GSK3β also induces tau phosphorylation in various different conditions [139]. So, inhibition of GSK3β emerged as a putative therapeutic target option for AD. Numerous studies identified different modulators that can modulate Aβ and tau hyperphosphorylation. However, *in vitro* and *in vivo* studies show that not many of these modulators can reduce both amyloid and tau pathologies together. A potential agent that modulates both amyloid and tau pathologies together will be a promising therapeutic tool for the treatment of AD.

Our recent laboratory data demonstrated that sAPPα producing capacity of HUCBS is not mediated by ADAM and ADAM17 (TACE) metalloprotease function in cell culture and cell free system. Alpha (α) -secretases are members of the ADAM family of proteins with cysteine-rich, disintegrin, and zinc metalloproteinase domains in their ectodomain [140]. Two members of this family e.g., ADAM10 and ADAM17 are primarily responsible for the α-secretase activity [141]. Both ADAM10 and ADAM17 can cleave several transmembrane proteins and promote tumor growth in the cell [142]. ADAM10, in particular, cleaves various transmembrane proteins in the vascular system, including the platelet-activating collagen receptor glycoprotein VI [143][144] and endothelial transmembrane proteins CX3CL1 and CXCL16 [145]. Inhibition of ADAM10 is a potential therapeutic target for prevention of cancer and inflammation. ADAM17 is responsible for TNFα secretion [146], and act as a therapeutic target in cancer, inflammatory, and vascular diseases. AD is the only disease where increasing α-secretase activity is favorable. The cleavage of substrates other than APP seems the primary obstacle to enhance α-secretase enzymatic activity in AD therapeutics [147]. Thus, we hypothesized that HUCBS treatment as a novel biological approach will modulate pathology and cognitive impairments in cell culture and AD mouse models by restoring sAPPα, and other neurotrophic growth factors. Our prior work and others have demonstrated that sAPPα-mediated inhibition of BACE1 activity reduces β-amyloid [42], and GSK3β-mediated inhibition of BACE1 expression reduces AD-like pathology. Further, a recent study using human primary neurons from sporadic AD patients showed that purified neurons treated with β-secretase inhibitors, but not γ-secretase inhibitors, significantly reduced phospho-tau (Thr 231) and GSK3β levels. These results suggest a direct relationship between APP proteolytic processing, but not Aβ, in GSK3β activation and tau phosphorylation in human neurons [148].   Additionally, we have demonstrated that sAPPα reduces GSK3β-mediated tau

phosphorylation in cell culture and transgenic mouse overexpressing sAPPα crossed with PSAPP mice [43]. As sAPPα can reduce both amyloid and tau pathology, we hypothesized that restoring sAPPα with HUCBS will reduce both amyloid and tau pathology in AD preclinical mouse models. Taken together, we believe that HUCBS-derived α-secretase will provide a novel therapeutic tool to treat AD through production of sAPPα, and other neurotrophic factors [Figure 1-3].

Lithium inhibits GSK3β activity by competitively inhibiting magnesium (Mg^{2+}) [95] and increasing inhibitory GSK3 (Ser9) phosphorylation through activation of protein kinase B/Akt signaling pathway. One of the main limitations of lithium pharmaceutics (carbonate and citrate) is that they have narrow therapeutic window 0.6-1.5 (mmol/L or mEq/L). The therapeutic ranges are based on the steady-state plasma lithium concentrations found 12 h after a dose. In addition, a plasma lithium level of ($\geq$ 1.5 mmol/L) or more is associated with serious toxicity. To improve therapeutic efficacy and reduce inflammation, one of our collaborators at University of South Florida investigated the pharmacokinetics of lactate, salicylate, and carbonate salts of lithium [149]. The study data indicated that lithium carbonate produces a very sharp peak and rapid elimination with undetectable levels at 48 h in Sprague Dawley rat model. This results explains the required multiple administrations of lithium carbonate to reach the target therapeutic concentration. In contrast, lithium salicylate produced elevated plasma and brain levels of lithium at 48 h after administration without any sharp peak. The hygroscopic property of parent lithium salicylate inspired to modify this salt using crystal engineering technology, and made an ionic cocrystal of lithium salicylate with amino acid l-proline (abbreviated as LISPRO or LP) [87]. Together, we believe that LISPRO will ameliorate Alzheimer's like β-amyloid and associated pathologies through inhibition of GSK3β and anti-inflammatory cytokines stimulation [Figure 1-4].

Hypothesis and project aims

In this study, we propose to explore the therapeutic efficacy of biological HUCBS (Aim 1 & 2) and pharmacological LISPRO (Aim 3 & 4) treatment in cell culture and AD mouse models in stated aim below.

Aim 1, Identify and characterize novel APP specific α-secretase enzyme from HUCBS. Aim1 outcome, we expect that the proposed studies using separation techniques such as chromatography, centrifugation, and sodium dodecyl sulfate polyacrylamide gel electrophoresis (SDS-PAGE) will isolate α-secretase enzyme from HUCBS.

Aim 2, Investigate whether αCBSF derived from HUCBS ameliorates AD pathology and cognitive impairments in AD mouse models. Aim 2 outcome, we expect that αCBSF administration will ameliorate pathology and cognitive impairment in transgenic AD (5XFAD, 3XTg-AD) mice.

Aim 3, Investigate and compare the safety, pharmacokinetics, and therapeutic efficacy of LISPRO treatment with carbonate and salicylate lithium salts in cell culture and rodent models. Aim 3 outcome, we expect that LISPRO treatment will showed better safety profile compared to lithium carbonate through inhibition of inflammatory COX2. We also expect that LISPRO will show stable lithium levels in the blood plasma compared to lithium carbonate in rodent models. Finally, we also expect that LISPRO treatment will reduce amyloid and tau pathology in transgenic Tg2576 and 3XTg-AD mouse models through inflammatory pathway inhibition.

Aim 4, Examine and compare the effect of LISPRO treatment in improving cognitive- and non-cognitive behavioral impairments in transgenic APPswe/PS1dE9 AD mice with carbonate, and salicylate salt of lithium. Aim 4 outcome, we expect that LISPRO treatment will prevent cognitive and non-cognitive functional decline in transgenic APPswe/PS1dE9 AD mouse model.
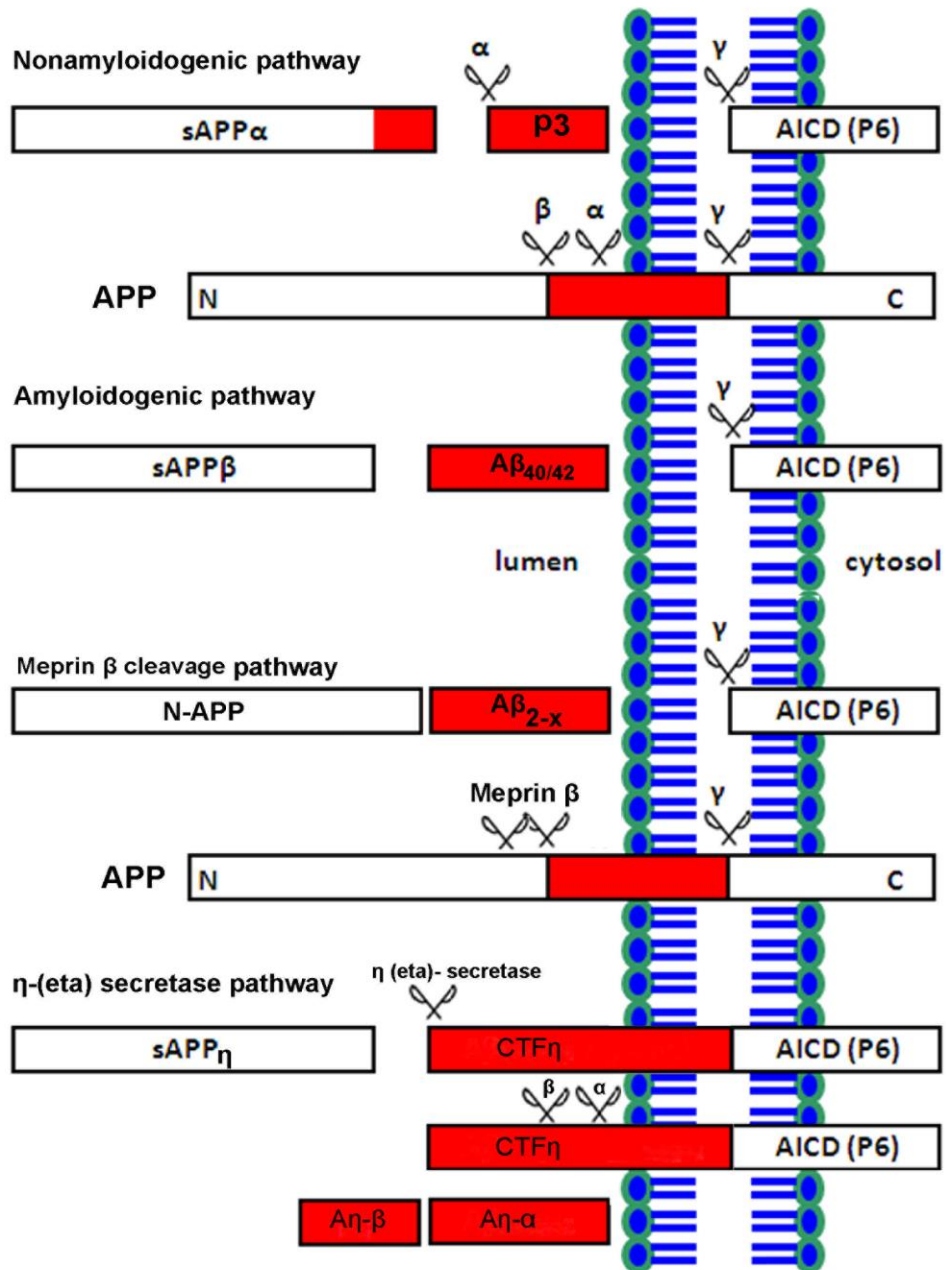
Figure 1-1 Schematic diagram of amyloid precursor protein (APP, middle) processing pathways and cleavage products.

The non-amyloidogenic APP processing pathway (upper) involves cleavages by α- and γ-secretases. Sequential cleavage of APP by α-secretase generates sAPPα and c-terminal fragment C83 (not shown). The subsequent cleavage of C83 by γ-secretase complex generate APP intracellular domain (AICD) and a short fragment called P3. The amyloidogenic APP processing pathway (lower) involves cleavages by β- and γ-secretases. Cleavage of APP by β-secretase generate sAPPβ and c-terminal fragment C99 (not shown). Subsequent cleavage of C99 by γ-

secretase complex generate toxic species Aβ (40 or 42, depends on the cutting site) and AICD. This is termed as amyloidogenic pathway due to generation and accumulation of Aβ species into plaque inside the brain. In addition to α-, β- and γ-secretases cleavage, APP is cleaved by metalloprotease meprin β, generating soluble N-terminal truncated APP (N-APP) or $Aβ_{2-X}$ variants. In addition to meprin β cleavage, the cleavage of APP by several matrix metalloproteinases such as MT5-MMP, referred to as η-secretase, releases a long-truncated ectodomain (sAPPη) and a membrane-bound carboxy-terminal fragment (CTF), termed CTFη. The membrane-bound CTFη is further cleaved by α- and β- secretases and release a long (Aη-α) and a short (Aη-β) peptide, respectively.

[**Note to reader:** Adapted from Habib *et al.,* 2017 [56]*,* Restoring Soluble Amyloid Precursor Protein α Functions as a Potential Treatment for Alzheimer's Disease. Journal of Neuroscience Research 2017; 95(4):973-991 with permission from Wiley Periodicals, Inc. © Copyright 2016.]
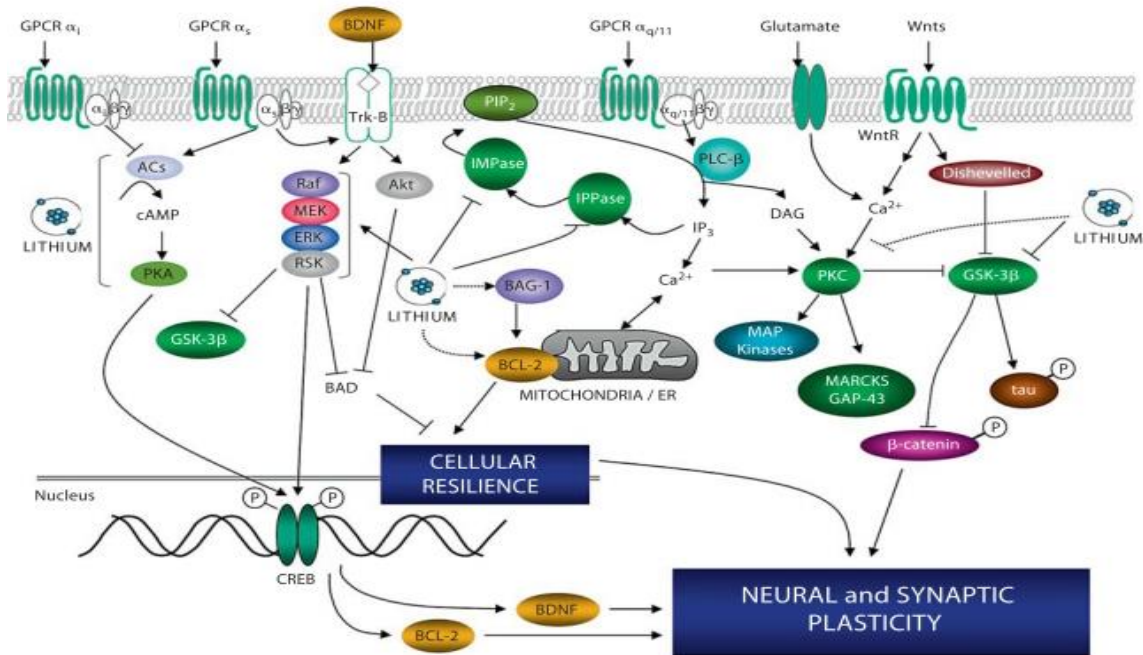
Figure 1-2 Neurotrophic and neuroprotective pathways targeted by lithium.

BDNF receptor (Trk-B) activation activates the ERK/MAPK pathway, which inhibits GSK3β and BAD protein. This activation increases the expression of CREB, which facilitates the expression of neuroprotective proteins such as bcl-2, and BDNF. Mitochondrial bcl-2 inhibits pro-apoptotic activation of BAD, and subsequent mitochondrial increases of calcium influx and cytochrome c release. Dysregulated intracellular calcium levels, may increases the risk of apoptosis, have been associated with the pathophysiology of bipolar disorder. Lithium downregulates endoplasmic reticulum (ER) calcium release via an IP3 receptor dependent pathway also increases bcl-2 expression, which improves mitochondrial stability and prevents activation of apoptotic pathway. IMPase directly inhibited by lithium, recycles IP3. In addition, cellular signaling through Wnt glycoproteins and frizzled receptors inhibits GSK3β. Lithium's inhibition of GSK3β prevents β-catenin phosphorylation and stimulates its translocation to the nucleus, and activating transcription of neurotrophic and synaptogenesis genes. Lithium also indirectly inhibits PKC.

[Note to reader: Adapted from Quiroz *et al.,* 2010 [94]. Novel Insights into Lithium's Mechanism of Action: Neurotrophic and Neuroprotective Effects; Neuropsychobiology (2010) 62 (1):50-60; with permission from S. Karger AG, BASEL]
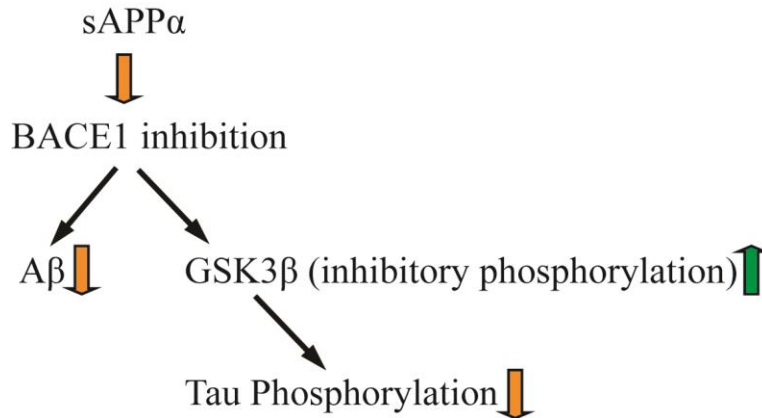
Figure 1-3 Hypothesized pathways for sAPPα-mediated reduction of amyloid and tau pathology

Soluble amyloid precursor protein alpha (sAPPα) increases GSK3β inhibitory phosphorylation (decrease GSK3β activity) by inhibiting BACE1 and followed by reduction of tau phosphorylation. sAPPα mediated BACE1 inhibition also results in a decrease of Aβ production and amyloid plaque load.

[**Note to reader:** Adapted from Deng & Habib *et al.,* 2015 [43], Soluble Amyloid Precursor Protein α Inhibits Tau Phosphorylation through Modulation of GSK3β Signaling Pathway. Journal of Neurochemistry 2015; 135: 630-637 with permission from John Wiley & Sons, Inc. Copyright © 1999-2018.]
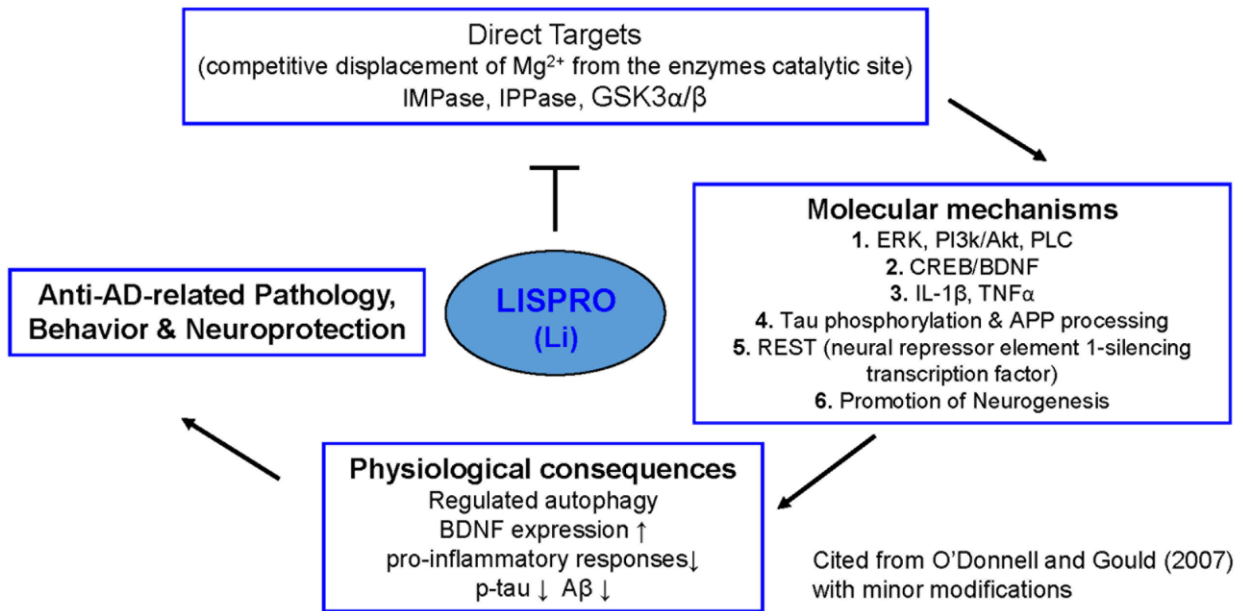
Figure 1-4 Schematic illustration of the lithium targeted cellular and molecular mechanism by activating several neurotrophic and associated signaling in Alzheimer's disease.

Lithium inhibit GSK3 (both α and β isoforms) and inositol mono/polyphosphatase (IMPase, IPPase) activity. The inhibition of GSK3 by lithium reduces tau phosphorylation and production of Aβ peptides by interfering γ-secretase cleavage of APP processing. In addition, inhibition of inositol monophosphatase by lithium may regulate clearance of aggregated phosphorylated tau and Aβ peptides. Moreover, lithium increases the expression of BDNF, which activates the ERK/MAPK pathway and further increases the expression of nuclear transcription factor cAMP response element (CREB). Accordingly, activation of BDNF may up-regulates neurogenesis and down-regulates pro-inflammatory responses (IL-1β, and TNFα) in Alzheimer's disease

[**Note to reader:** Adapted from Habib *et al.,* 2017 [150], LISPRO mitigates β-amyloid and associated pathologies in Alzheimer's mice. Cell Death & Disease 2017; 8(6): e2880]

24

CHAPTER 2

Human umbilical cord blood serum derived α-secretase: Functional testing in Alzheimer's disease mouse models

Permission statement

The information in chapter 2, "Human umbilical cord blood serum derived α-secretase: Functional testing in Alzheimer's disease mouse models" has been legally reproduced under the Creative Commons Attribution (CC-BY) license. This means the publication is accessible online without any restrictions and can be re-used in any way subject only to proper citation.

Habib A, Hou H, Mori T, Tian J, Zeng J, Fan S, Giunta B, Sanberg PR, Sawmiller D, Tan J Human umbilical cord blood serum derived α-secretase: Functional testing in Alzheimer's disease mouse models. Cell Transplantation (2018); Jan 1: doi: 10.1177/0963689718759473

Chapter synopsis

Alzheimer's disease (AD) is an age-related disorder that affects cognition. Our previous studies showed that the neuroprotective fragment of amyloid procurer protein (APP) metabolite, soluble APPα (sAPPα), interferes with β-site APP cleaving enzyme 1 (BACE1, β-secretase) cleavage and reduces amyloid-β (Aβ) generation. In an attempt to identify approaches to restore sAPPα levels, we found that human cord blood serum (CBS) significantly promotes sAPPα

production compared with adult blood serum (ABS) and aged blood serum (AgBS) in Chinese hamster ovary cells stably expressing wild-type human APP (CHO/APPwt). Interestingly, CBS selectively mediated the α-secretase cleavage of human neuron-specific recombinant APP_{695} ($fAPP_{695}$) in a cell-free system with independent from TNFα converting enzyme (TACE) [a disintegrin and metalloproteinase domain-containing protein 17 (ADAM17)] and ADAM. Subsequently, using three-step chromatographic separation techniques (*i.e.*, diethylaminoethanol, size exclusion, and ion-exchange chromatography), we purified and ultimately identified a CBS specific fraction with enhanced α-secretase catalytic activity (termed αCBSF), and found that αCBSF has more than 3,000 fold increased α-secretase catalytic activity compared with the original pooled CBS. Furthermore, intracerebroventricular injection of αCBSF markedly increased cerebral sAPPα levels together with significant decrease in cerebral Aβ production and abnormal tau (Thr^{231}) phosphorylation compared with AgBSF treatment in 3XTg-AD mice. Moreover, aged blood serum fraction with enhanced α-secretase activity administered intraperitoneally to 5XFAD mice *via* an osmotic mini pump for 6 weeks ameliorated β-amyloid plaques and reversed cognitive impairment measures. Together, our results propose necessity for the further study aimed at identification and characterization of the-α-secretase in CBS for novel and effective AD therapy.

Background

The neuropathological hallmarks of AD that differentiate it from other dementia include: extracellular β-amyloid plaques composed largely of amyloid-β (Aβ) peptides [1] and intracellular neurofibrillary tangles (NFTs) composed of the hyperphosphorylated microtubule associated protein tau [2]. Successive cleavage of APP by β- and γ-secretases produce Aβ peptides of variable length ($Aβ_{x-40, 42}$), soluble APPβ (sAPPβ), membrane-bound β-C-terminal fragment (β-CTF, C99),

and APP intracellular cytoplasmic/C-terminal domain (AICD) [6]. The Aβ peptide fragments, which accumulate as plaques in the brain, induce neuroinflammation, synaptic dysfunction, and neuronal cell death that affects cognitive function [11]. In contrast, most of the APP is cleaved by α- and γ-secretases which not only precludes Aβ generation but also produce a secreted soluble APPα (sAPPα), membrane-bound α-C-terminal fragment (α-CTF, C83), P3 peptide and AICD [5]. Overall, sAPPα has been shown to be involved in numerous physiological functions in the brain, which appear to be interrupted in AD. Several studies have shown that neurotrophic fragment sAPPα not only prevents Aβ generation [42] and tau phosphorylation [43] but is also known to be a neuroprotective APP metabolite, including but not limited to proliferation, neurite outgrowth, and long term potentiation [56][151][152]. Thus, we hypothesized that therapeutic interventions or approaches that has potential to produce sAPPα markedly could improve AD pathology and cognitive function.

Several studies have shown that human umbilical cord blood cell (HUCBC) has therapeutic potential in numerous age-related neuroinflammatory conditions, including AD. In line with those studies, we showed that single as well as multiple low-dose infusion of HUCBC significantly reduced amyloidogenic APP processing, Aβ and β-amyloid plaque accumulation, glial neuroinflammation, and cognitive impairments in preclinical AD mice models [37][153]. Additionally, HUCBC treatment changed microglial phenotypes from pro-inflammatory to anti-inflammatory, increased microglial Aβ phagocytosis, increased anti-inflammatory cytokines in the brain [*i.e.*, interleukin-10 (IL-10), transforming growth factor β1 (TGFβ1), and nerve growth factor (NGF)], and reduced CD40-CD40L interaction that is important for Aβ-induced pro-inflammatory microglial activation [38]. To identify the specific HUCBC responsible for this neuroprotective effect, we found that cord blood-derived monocyte reduces β-amyloid pathology and improves

27

cognition with much more effectively than monocyte-deficient cord blood in AD mouse model [38]. In line with the findings of above studies, several recent reports underscored the role of young blood and/or plasma in aging and age-associated neurodegenerative conditions. Among those, Wyss-Coray and other labs have reported that exposing old mice to a young systemic environment by parabiosis increased synaptic plasticity, improved pathology, and behavioral recovery such as contextual fear conditioning and spatial learning in old mice. More interestingly, they also found that it is not the blood cells rather the soluble factors are getting into the mice brain. They pooled plasma from young mice as well as young human and injected into old mice, which successfully rejuvenated old mice brain structure and cognition tested by Barnes maze memory test [41][154][155][156][157]. In a follow-up study, they showed that human cord blood plasma as well as plasma enriched in tissue inhibitor of metalloproteinases 2 improves synaptic plasticity and hippocampal dependent cognitive function in old mice [75].

Based on our preliminary laboratory findings, we hypothesized that human cord blood serum (CBS) possesses novel APP-specific α-secretase-like enzyme, reflected by marked production of sAPPα level. As CBS contains many different small molecules, growth factors, proteins, inhibitors, hormones, enzymes, and other unknown substances, we also hypothesized that infusion of characterized CBS fraction will ameliorate AD-like pathology and cognitive impairments in mouse models. Here, we show that CBS markedly enhanced sAPPα production in Chinese hamster ovary (CHO) cells stably expressing wild-type human APP (CHO/APPwt cells) as well as mediated α-secretase cleavage of human neuron-specific APP_{695} ($fAPP_{695}$) in a cell-free system, which effects are not seen with normal adult or aged blood serum (ABS or AgBS). Additionally, we have been successfully able to characterized a CBS fraction with enhanced α-secretase-like catalytic activity (refer to αCBSF) using sequential DEAE-affinity column, size-

28

exclusion, and anion-exchange chromatographic fractionation processes. Moreover, we found that αCBSF infusion increased sAPPα levels, decreased Aβ production/β-amyloid plaque formation, prevent neuronal loss and abnormal tau (Thr^{231}) phosphorylation in the cortex, and improved cognitive function in Alzheimer's mouse models. Our findings indicate that CBS fraction with enhanced α-secretase-like activity holds immense therapeutic potential for treatment of AD.

Materials and methods

Reagents and antibodies

CBS was obtained from Lee Biosolutions (St. Louis, MO, USA) and human umbilical cord blood plasma (CBP) was obtained from STEMCELL Technologies Inc. (Vancouver, BC, V5Z 1B3, Canada). Human Cord Blood is aspirated from the umbilical cord vein into a cord blood collection bag containing citrate-phosphate-dextrose as an anticoagulant. Individual lot of cord blood plasma (CBP) is prepared from a single cord blood sample. Three to five different lots of CBP samples were pooled in as "pooled cord blood plasma". CBP is separated from umbilical cord blood centrifugation at 3500 rpm for 5-10 min. CBP is aliquoted and frozen at -20°C first, and then transferred to a -80°C freezer after 24 h at 4°C. There is no placement into -80°C for a snap freeze. Frozen CBP are not heat inactivated. There is no analysis performed to determine the number of platelets in each sample, therefore the plasma cannot be specifically characterized as 'low platelet' or 'platelet poor' plasma. Frozen CBP samples were thawed in a 37°C water bath before used in experiment. Cord blood serum (CBS) was collected from umbilical cord blood and is blood that remains in the placenta and in the attached umbilical cord, after the cord has been detached from the newborn at the time of childbirth. CBS is separated from umbilical cord blood by allowing clotting for 5-10 h in red top tubes with no anticoagulation followed by centrifugation at 3500 rpm for 5-10 min at 4°C. CBS sample was passed through a filter membrane with a pore

size of 0.22 µm. Individual CB serum was prepared from a single sample. More than ten serum samples of CBS were pooled in as "pooled cord blood serum". Normal human adult blood serum (ABS, 25-30 years old) and aging blood serum (AgBS, >75 years old) as well as their plasma (ABP and AgBP, respectively) were obtained from Florida Blood Services (Tampa, FL, USA). Antibodies include: specific anti-sAPPα monoclonal antibody (2B3; IBL, Minneapolis, MN, USA, Cat# 11088 RRID: AB_494690), anti-APP C-terminal polyclonal antibody (pAb751/770; EMD Millipore, La Jolla, CA, USA, Cat# 171610, RRID: AB_211444), anti-APP N-terminal monoclonal antibody (22C11; Merck Millipore, Billerica, MA, USA, Cat# MAB348B, RRID: AB_11204540), anti-N-terminal Aβ monoclonal antibody (6E10; Covance Research Products, Emeryville, CA, USA), anti-Aβ$_{16–26}$ monoclonal antibody (4G8; Covance Research Products, Cat# SIG- 39200, RRID: AB_10175149), anti-phospho-tau antibody (Thr^{231}; Merck Millipore, Cat# AB9668, RRID: AB_570891), anti-DDK antibody (Cell Signaling Technology, Danvers, MA, USA, Cat# 2908, RRID: AB_1905079), anti-NeuN antibody (Merk Millipore, Cat# ABN90, RRID: AB_11205592), and anti-β-actin monoclonal antibody (Sigma-Aldrich, St. Louis, MO, USA, Cat# A5316, RRID: AB_476743). Human recombinant full-length APP$_{695}$ (fAPP, 100 ng)-tagged with C-terminal MYC/DDK was purchased from OriGene Technologies, Inc. (Rockville, MD, USA).

Cell culture

Chinese hamster ovary (CHO) cell line with stable expression of human wild-type APP (CHO/APPwt) was a generous gift from Drs. Stefanie Hahn and Sascha Weggen (University of Heinrich Heine, Düsseldorf, Germany). At the beginning of the experiment, CHO/APPwt cells were genotyped and confirmed the genetic make-up. The cells were cultured in Dulbecco's modified Eagle's medium (DMEM) with 10% fetal bovine serum (FBS), 1 mM sodium pyruvate

and 100 U/mL of penicillin/streptomycin. For treatment, the cells were plated in a 24-well plate at 2×10^5 cells /well for overnight incubation, washed and treated with CBS (0-10%), Inact CBS (5%), ABS (0-10%), AgBS (0-10%), or αCBSF (0-1%) in DMEM. After treatment, supernatants were collected and the cells were washed with ice cold PBS 3X and lysed with cell lysis buffer (20 mM Tris, pH 7.5, 150 mM NaCl, 1mM EDTA, 1 mM EGTA, 1% v/v Triton X-100, 2.5 mM sodium pyrophosphate, 1 mM β-glycerolphosphate, 1 mM Na$_3$VO4, 1 μg/mL leupeptin, and 1 mM PMSF) (Cell Signaling Technology). Both cell supernatants and lysates were used for sAPPα analysis by ELISA. For immunoprecipitation, 100 ng of fAPP$_{695}$ was incubated with αCBSF at 37ºC for 1 h and then the sAPPα/αCBSF-derived immune complex was immunoprecipitated using 2B3 sAPPα specific antibody or anti-DDK antibody. The supernatants were then collected and used for treatment of CHO/APPwt cells.

Cell-free α-secretase assay

In order to determine the α-secretase activity of CBS reflected by sAPPα level, human recombinant full-length APP$_{695}$ tagged with C-terminal MYC/DDK (fAPP$_{695}$, 100 ng; OriGen Biomedical, Austin, TX, USA) was incubated with CBS, heat inactivated CBS (inact CBS, 56ºC for 30 minutes), AgBS, fetal bovine serum (FBS), or αCBSF at 37ºC for 5 h in the presence or absence of protease inhibitor cocktail (PI, 1X; Sigma-Aldrich), TNFα converting enzyme (TACE) inhibitor [(TAPI-0, 1 μM; abcam, Cambridge, MA, USA), or a disintegrin and metalloproteinase domain-containing protein (ADAM) inhibitor (GM6001, 1 μM; Sigma-Aldrich)]. The reaction mixtures were then subjected to Western blot (WB) analysis for APP α-secretase processing. In addition, TACE and ADAM10 cleavage activity of αCBSF was determined using TACE (AnaSpec, Fremont, CA, USA) and ADAM10 cleavage activity kits (AnaSpec), according to manufacturer's instructions.

CBS fractionation

Next, in order to purify and characterize the α secretase in - CBS or AgBS, the Econo-Pack Serum IgG purification kit, and 10DG columns (Bio-Rad, Philadelphia, PA, USA) were initially employed to remove highly abundant IgG and salts. The desalted serum was applied to DEAE Affi-Gel blue columns and residual IgG was eluted according to the instructions. Then 20 additional protein fractions were collected by eluting with an ionic strength gradient of NaCl buffer ranging from 0.1 M to 2.0 M. The remaining proteins on the column were eluted by the regeneration buffer included in the kit and collected as the regeneration fraction. The 0.8 M NaCl eluted protein fractions were combined together and sent to Moffitt Cancer Center Protein Purification Core for further separation by size exclusion chromatography, employing analytic Superdex 200 columns and eluting with PBS, and ion-exchange chromatography, employing Q-Sepharose columns and eluting with 500 mM NaCl, 50 mM Tris, pH 7.6. The final enzyme containing fractions were exchanged to PBS buffer by Ultracel-10 membranes (10 kDa, Merck Millipore) for further experimentation and referred to as αCBSF or AgBSF.

Animal models

Both 5XFAD [MMRC Stock No: 34840-JAX; RRID IMSR_JAX: 006554] and 3xTg [MMRC Stock No: 34830-JAX] mice of male and female were purchased from Jackson laboratory (Bar harbor, Maine, USA). In this preclinical study to investigate whether CBS fractionation changes AD-like pathology and associated behavioral deficits, five-month old 5XFAD mice were used that harbor five mutations [APP KM670/671NL (Swedish), APP I716V (Florida), APP V717I (London), PSEN1 M146L, and PSEN1 L286V] [158], rapidly develop AD-like pathology including accumulation of high levels of extracellular β-amyloid plaques, neurodegeneration, and behavioral impairments. In order to investigate whether CBS fractionation administration changes

both Aβ and tau phosphorylation, 3XTg-AD mice were used which harbor presenilin-1 (PS1/M146V), APP (KM670/671NL), and tau (P301L) mutants. These mice progressively develop β-amyloid and NFT pathology which potentially synergize to accelerate neurodegeneration by 6 months of age [159]. At the beginning of the experiment all mice were confirmed as mutant by PCR. One male and four female mice were housed in a single cage separately. All animal experiments were performed in accordance with the guidelines of the National Institutes of Health and were approved by USF Institutional Animal Care and Use Committee (IACUC reference number: IS00000438). Transgenic mice used for aging studies may exhibit signs such as ruffled hair coat, hair loss, excessive weight gain and/or loss. When one of these signs is observed, mice will be monitored more closely and will be weighed twice weekly. Mice exhibiting multiple clinical signs or showing >20% weight loss will be excluded from the study. As per our previous practice, if a mouse appears overtly sick or in pain as indicated by ruffled, matted, or dull hair, hunched back or head pressing, failure to move about the cage, failure to respond to stimuli, rapid, shallow, labored breathing, twitching or trembling, or to experience seizure, a veterinarian will be consulted in order to ensure timely intervention and treatment, or removal from the study. All mice were maintained on a 12-h light/12-h dark cycle at ambient temperature and humidity and housed in the Morsani College of Medicine Animal Facility at the University of South Florida (USF) with ad libitum access to food and water.

Stereotaxic intracerebroventricular injection

In order to determine whether αCBS fraction could modify Aβ and tau pathology, cohorts of seventeen (n = 17, 9♂/8♀) triple transgenic 3XTg-AD mice were arbitrary anesthetized with isoflurane (2 - 3% induction, 1% maintenance). After reflexes were checked to ensure that mice were unconscious, they were positioned on a stereotaxic frame (Stoelting Lab Standard™, Wood

33

Dale, IL, USA) with ear-bars positioned and jaws fixed to a biting plate. The axis coordinates were taken from a mouse brain atlas, and the needle of a Hamilton microsyringe was implanted into the left lateral ventricle delimited from the stereotaxic coordinates (coordinates relative to bregma: −0.6 mm anterior/posterior, +1.2 mm medial/lateral, and −3.0 mm dorsal/ventral) using the stereotaxic device. αCBSF (0.5 µg/mouse, n = 6, 3♂/3♀),), AgBSF (0.5 µg/mouse, n = 6, 3♂/3♀),) and PBS (1 µL/mouse, n = 5, 3♂/2♀),) were administered at 1 µL/minute. After administration, the syringe was removed slowly to prevent bleeding and further brain damage. The lesions were closed with 1-2 staples and observed until anesthesia had cleared. Seventy two hour after the intracerebroventricular (i.c.v.) injections animals were sacrificed with isoflurane, then transcardially perfused with ice-cold PBS, and brains were harvested for biochemical, histochemical, and immunohistochemical analyses.

Intraperitoneal administration with an osmotic mini pump

Mice were labeled using tail tattooing by veterinarian who was blinded about the entire experiment. In order to determine whether CBS fractionation changes AD-like pathology and associated behavioral deficits, cohort of even-number labeled 5XFAD mice were randomly assigned into two experimental groups of six mice each, receiving αCBSF (n = 6, 3♂/3♀), or AgBSF (n = 6, 3♂/3♀) treatment by an Alzet® osmotic mini pump (Alzet 2004, DURECT Corporation, Cupertino, CA, USA). A third group of WT control mice was received to αCBSF (n = 6) by the same administration route. Mice were briefly anesthetized with isoflurane as previously, an area of the abdomen was shaved, a 1-cm abdominal incision was made and an Alzet® osmotic mini pump filled with 100 µL of CBSF, or AgBSF was implanted intraperitoneally (i.p.). The pump delivered these fractionated sera at a constant rate of 0.15 µL/h for 6 weeks, yielding a treatment dose of 1 mg/kg/day or 30 µg/mouse/day. At the end of 4-5 weeks treatment

34

(6 months of age), cognitive evaluations were conducted in these mice with our established behavioral battery. After 6 weeks treatment, mice were sacrificed with isoflurane, then transcardially perfused with ice-cold PBS, and brains were removed to assess β-amyloid plaque pathology.

Behavioral assessments

Novel object recognition test

Novel object recognition is based on the spontaneous tendency of a mouse to explore a new object compared with an old object. At first, during the habituation phase (day 1), each mouse was acclimatized with the testing apparatus box for 10 minutes. Next, during the training day (day 2) each mouse was familiarized with two similar objects (4 cm x 4 cm x 4 cm) for 10 minutes. Finally, during the testing day (day 3) one of the objects was replaced with a new object and tested for 10 minutes. The amount of time spent exploring the new and old objects during the test phase was quantified by video tracking (ANY-Maze; Stoelting Lab Standard™) and provides an index of recognition memory. Discrimination index was calculated as frequency of exploration of new *versus* original objects.

Y-maze test

Y-Maze testing was performed as described previously [160]. This task was used to assess basic mnemonic processing by spontaneous percent alternation and exploratory activity of mice placed into a black Y-maze. The arms of this maze were 21 cm-long and 4 cm-wide with 40 cm-high walls. Each mouse was placed in one of the arms and allowed one five-minute trial of free exploration of the three alleys in the maze. The number of total arm choices and sequence of arm choices were recorded.

Histochemical and immunohistochemical analyses

Mice were euthanized with isoflurane and then transcardially perfused with ice-cold PBS. Brains were rapidly isolated, and one hemisphere was frozen immediately in liquid nitrogen and stored at -80°C. For molecular analysis, brain hemispheres were sonicated in RIPA buffer (Cell Signaling Technology), centrifuged at 14,000 rpm for 1 h at 4°C and supernatants were isolated for WB analyses. The other hemisphere was placed in 4% paraformaldehyde for cryostat sectioning. The 25-μm free-floating coronal sections were collected and stored in PBS with 100 mM sodium azide at 4°C. Immunohistochemical staining was performed using various primary antibodies in conjunction with the VECTASTAIN *Elite* ABC kit (Vector Laboratories, Burlingame, CA, USA) coupled with diaminobenzidine substrate. A set of sections without adding primary antibody were used as negative staining control. Sections were also stained with Congo red dye and Thioflavin-S fluorescence dye for detecting fibrillary Aβ species as described previously [161][85]. Images of five 25-μm sections (150 μm apart) through hippocampus and neocortex were captured and a threshold optical density was obtained that discriminated staining from background. Data are reported as percentage of immunolabeled area captured (positive pixels divided by total pixels captured). Quantitative image analysis was performed by a single examiner (T.M.) blinded to sample identities.

WB analysis and ELISA

WB analyses and quantification were performed as previously described [84]. Briefly, the proteins from the cell-free suspensions, cell lysates, and homogenized tissue were electrophoretically separated using 10% bicine/tris gel (8 M urea) for proteins less than 5 kDa or 10% tris/SDS gels for larger proteins. Electrophoresed proteins were transferred to nitrocellulose membranes (Bio-Rad), washed and blocked for 1 h at room temperature in tris-buffered saline

containing 5% (w/v) nonfat dry milk (TBS/NFDM). After blocking, membranes were hybridized overnight with various primary antibodies, washed and incubated for 1 h with the appropriate HRP-conjugated secondary antibody in TBS/NFDM. Blots were developed using the luminol reagent (Thermo Fisher Scientific, Waltham, MA, USA). sAPPα ELISA (IBL) was performed according to manufacturer's instruction.

Statistical analysis

Comparisons between two groups were performed by Student's *t*-test analysis. For more than two groups, one-way analysis of variance (ANOVA) followed by LSD *post hoc* analysis was used to compare each other for statistical significance. Alpha was set at 0.05 for all analyses. The significance level of p value was set at $p < 0.05$ for all analyses. All the mice experiment were repeated three times in parallel to attain the above significant difference. Data are expressed as mean ± SEM. The statistical package for the social sciences release IBMSPSS 23.0 (IBM, Armonk, NY, USA) was used for all data analyses.

Results

CBS dose-dependently promotes α-cleavage in CHO/APPwt cells

Our previous studies indicate that both single and multiple low-dose infusions of HUCBC as well as HUCBC-derived monocytes can significantly reduce β-amyloid plaques and cognitive impairments in AD mouse models. Having shown that HUCBC can reduce β-amyloid pathology, we next set out to determine whether human umbilical-derived CBS could also reduce β-amyloid pathology through alteration of APP processing. CHO/APPwt cells were treated with different concentrations (0-10%, six different doses) of CBS, ABS, or AgBS for 4 h (Figure 2-1a and b, left panels). The conditioned media were collected and subjected to sAPPα ELISA and also sAPPα WB analysis using 2B3 sAPPα specific antibody. CBS dose-dependently promoted sAPPα levels

with greater than that elicited by ABS and AgBS. Similarly, CHO/APPwt cells were treated with 5% CBS, ABS, or AgBS for six different time points (0-4 h, Figure 2-1a and b, right panels). CBS time-dependently promoted sAPPα levels with greater than that elicited by ABS and AgBS. To see whether the factor present in the serum mediating α-secretase activity is proteinaceous in nature, we treated CHO/APPwt cells with heat inactivated serum (inact CBS) for 4 h. As expected, heat inactivation limited the sAPPα producing capacity of CBS, as shown by ELISA (Figure 2-1c, upper panel) and WB (Figure 2-1c, lower panel). Therefore, CBS possesses α-secretase, reflecting sAPPα level in a dose- and time-dependent fashion and the factor mediating this activity is heat labile and most likely a protein. These results confirm that FBS also contains a heat sensitive α-secretase.

CBS mediates α-cleavage of neuron specific APP$_{695}$ independent of ADAM activity

Next, we tested whether the α-secretase in CBS is mediated by TACE (ADAM17) or ADAM. Human recombinant full-length APP$_{695}$ (fAPP, 100 ng)-tagged with C-terminal MYC/DDK was incubated with CBS, inactivated CBS (inact CBS), or AgBS at 37ºC for 5 h in the presence or absence of different inhibitors [protease inhibitor cocktail (PI, 1X), TACE inhibitor (TAPI-0, 1 µM), or ADAM inhibitor (GM6001, 1 µM)] (Figure 2-2a). The reaction mixtures were subjected to sAPPα WB analysis using 2B3 sAPPα specific antibody (Figure 2-2a, upper panel) and total APP analysis using 6E10 anti-Aβ$_{1-17}$ antibody (Figure 2-2a, lower panel). PI cocktail significantly limited CBS derived α-secretase catalytic activity, as reflected by sAPP$_{695}$ level, but this activity was not limited by TACE or ADAM inhibitors (Figure 2-2a, upper panel). In addition, full-length APP (fAPP$_{695,}$ 100 ng) was incubated with 5% CBS, FBS, or inactivated CBS for 1, 5, or 24 h. CBS α-secretase increased the level of sAPP$_{695}$ in a time-dependent manner, measured

by 2B3 antibody (Figure 2-2b, upper panel). As shown, the level of sAPP$_{770}$ represents endogenous sAPPα.

Removal of high and low abundance proteins increases activity of CBS α-secretase

To purify and ultimately identify the target protein/complex mediating CBS α-secretase catalytic cleavage, three-step chromatographic separation techniques were employed. Initially, removal of highly abundant immunoglobulins and desalting were performed using Bio-Rad Econo-Pack Serum IgG purification kit and 10DG columns. Desalted CBS was then applied to DEAE Affi-Gel blue columns to completely remove IgGs and collect 20 additional protein fractions, and eluted with increasing strengths of NaCl buffer. CHO/APPwt cells were treated with each fraction for 2 h to determine α-secretase activity by ELISA. In addition, unfractionated whole and desalted CBS (dCBS) positive control as well as PBS negative control was used to treat cells. These sequential approaches significantly increased α-secretase, with the fractions showing the highest α-secretase catalytic activity, as reflected by sAPPα level eluting around 0.6-0.9 M NaCl concentrations (Figure 2-3a). As shown in Figure 2-3c, 0.7-0.9 M NaCl fractions from 10 CBS lots increased sAPPα levels at least with maximum fivefold higher than the whole CBS. In addition, the fractionated and whole CBS were run in SDS-PAGE, demonstrating numerous proteins remaining in each CBS fraction (Figure 2-3c, right upper panel). Therefore, we selected the 0.8 M NaCl eluted fraction for further purification. As shown in Figure 2-3b, the level of total protein concentration represents in (mg/mL) in CBS fraction.

Further purification of CBS α-secretase using size-exclusion and anion-exchange chromatography

The 0.8 M NaCl eluted fraction of CBS was subjected to size-exclusion chromatography using Superdex 200 prep grade columns (XK 16/40, GE Healthcare, USA) packed with cross-

linked agarose and dextran. The mobile phase was 20 mg/mL acetone in distilled water, and detection was performed at UV280 nm. Approximately 100 mg of protein from the 0.8 M NaCl fraction was applied to the column and 48 fractions were eluted with PBS. The catalytic activity of α-secretase was greatly enhanced, as tested on CHO/APPwt cells by measuring sAPPα production. Fractions #11 and 12 produced sAPPα $\geq$ fivefold higher compared with the original 0.8 M NaCl eluted fraction as well as all other fractions, as determined by WB (upper panel) and ELISA (lower panel, Figure 2-4a). To confirm the enhancement of α-secretase, we determined the sAPPα in fractions #8-18 along with the original 0.8 M NaCl eluted fraction from three different CBS lots. Fractions #10-13 showed α-secretase activity 15 fold more than the original 0.8 M NaCl eluted fraction, as measured by ELISA (Figure 2-4c). As determined by SDS-PAGE, the molecular mass of the #10-13 fractions was 177-275 kDa (Figure 2-4c).

To examine the charge of α-secretase protein/complex in CBS, the size exclusion fractions containing the highest α-secretase catalytic activities, as reflected by sAPPα levels (#10 to 13) were further subjected to anion-exchange chromatography using Q-Sepharose columns. Protein from the size exclusion fractions were applied to the column and 82 fractions were eluted with 0.5 M NaCl. Fractions #53-56 showed $\geq$ eightfold higher α-secretase catalytic activity, as reflected by sAPPα level than the original size-exclusion fraction, as determined in CHO/APPwt cells by WB and ELISA (fractions #2-4 in Figure 2-5a, upper and lower panels, respectively). To further compare the enzymatic activity of CBS samples before and after anion-exchange chromatography, we collected fractions #1-5 and #23 from three different samples and determined the sAPPα level in each, indirect measurement of CBS α-secretase activity. Combined fractions #2-4 produced sAPPα $\geq$ 50 fold higher than the original eluted (#23) fraction, as measured by ELISA (Figure 2-

5c). Combined fractions #2-4, referred to hereafter as αCBSF, were therefore used for further analysis.

αCBSF promotes non-amyloidogenic APP processing

Human recombinant full-length APP (fAPP$_{695}$) was incubated with five different concentrations (0-1%) of αCBSF at 37ºC for 2 h. The reaction mixtures were subjected to sAPPα WB analysis using 2B3 antibody as well as full length APP and αCTF analyses using pAPP751/770 antibody (an anti-APP C-terminal antibody, Figure 2-6a). This analysis showed that αCBSF increases sAPPα as well as α-CTF fragments and decreases (full-length) holo APP with increasing doses.

In order to confirm that αCBSF mediates novel α-secretase cleavage independent of TACE or ADAM, fAPP$_{695}$ was incubated with αCBSF in t3e absence or presence of ADAM (GM6001, 1 µM) or TACE inhibitor (TAPI-0, 1 µM) for 1 h. αCBSF treatment alone increased the levels of APP-processing fragments such as sAPPα and α-CTF, and decreased the level of holo APP as determined by WB, which effects did not alter significantly by GM6001 and TAPI-0 combined treatment with αCBSF (Figure 2-6b). In addition, TACE and ADAM10 enzymatic activities of αCBSF were measured by TACE and ADAM10 cleavage activity kits. TACE (25 µg/mL) in the presence or absence of TACE inhibitor (TAPI-0, 1 µM) and ADAM10 (50 µg/mL), in the presence or absence of ADAM inhibitor (GM6001, 1 µM), were included as positive controls. Results suggest that αCBSF has very little TACE or ADAM10 activity (Figure 2-6c and d).

Immunoprecipitation of fAPP$_{695}$/CBS specifically limits APP α-secretase cleavage

To determine whether immunoprecipitation could specifically limit α-secretase of αCBSF, 100 ng of fAPP$_{695}$ was incubated with 0.125 µg of αCBSF at 37°C for 1 h and the sAPPα/αCBSF

immune complex was immunoprecipitated using anti-DDK antibody, 2B3 or nonspecific IgG. CHO/APPwt cells were treated in the FBS free condition for 2 h with the supernatants collected from the immune complex or PBS as reference control, and then conditioned media were analyzed by sAPPα WB using anti-N-terminal APP antibody (22C11, Figure 2-7a) and sAPPα ELISA (Figure 2-7b) to determine α-secretase in CBS. Immunoprecipitation of the sAPPα/αCBSF with anti-DDK antibody significantly reduced α-secretase activity of αCBSF, indicating that immunoprecipitation limits the CBS-mediated APP α-secretase cleavage. In contrast, immunoprecipitation of sAPPα/αCBSF with 2B3 did not reduce CBS α-secretase, indicating that αCBSF does not form an immune complex with sAPPα. In addition, there was no notable or significant difference in sAPPα production elicited by 0.5% supernatant from αCBSF IP with control IgG and 2.5 % (equivalent to 0.5% Super.) αCBSF alone (data not shown).

αCBSF reduces β-cleavage, promotes α-cleavage of APP, and stabilizes tau phosphorylation in 3XTg-AD mice

To test whether αCBSF suppresses β-site APP cleaving enzyme 1 (BACE1)-mediated APP processing *in vivo,* four-month old 3XTg-AD mice were treated αCBSF, AgBSF (0.5 μg/mouse), or PBS control (1 μL/mouse) with i.c.v. injections. After 72 h of treatment, in homogenates prepared from the right hemisphere (non-injection side), WB analysis using $A\beta_{1-17}$ antibody (6E10) shows that αCBSF reduced Aβ (Figure 2-8a) and β-CTF production (Figure 2-8c), whereas enhancing sAPPα production (Figure 2-8b), compared with AgBSF and PBS control. Compared with AgBSF and PBS, αCBSF also reduced tau (Thr^{231}) phosphorylation in these mice (Figure 2-8d).

42

αCBSF ameliorates β-amyloid pathology in 5XFAD mice

To determine the effect of αCBSF on β-amyloid pathology, transgenic 5XFAD mice at five months of age were continuously treated with αCBSF or AgBSF *via* i.p. osmotic mini pump for 6 weeks. Immunohistochemical staining using 4G8 antibody showed that αCBSF treatment substantially decreases cortical and hippocampal β-amyloid plaques (Figure 2-9a, upper panel), and reduces fibrillary Aβ species visualized by Thioflavin-S histochemical staining (Figure 2-9a, lower panel) compared with AgBSF treatment. Moreover, the αCBSF-treated cohort also revealed less β-amyloid plaque pathology than the AgBSF-treated cohort, as determined by Congo red histochemical staining (Figure 2-9a, middle panel). Quantitative analysis disclosed that αCBSF therapy significantly ameliorated β-amyloid pathology, as determined by 4G8 antibody staining in both neocortex and hippocampus regions compared with AgBSF treatment (Figure 2-9b).

Neuroprotective effects of αCBSF

5XFAD mice undergo neuronal loss in the neocortex and hippocampus that is associated with behavioral deficits. We examined whether continuous delivery of αCBSF by i.p. osmotic mini pump can elicit a neuroprotective effect in 5XFAD mice. Treatment with αCBSF partially prevented neuronal loss in the neocortex region compared with AgBSF treatment, as demonstrated by NeuN antibody immunohistochemical staining, thus indicating that αCBSF may confer neuroprotective ability for AD brain (Figure 2-10a and b).

αCBSF improves learning, memory, and cognitive function in 5XFAD mice

5XFAD mice were received to continuous treatment with αCBSF or AgBSF *via* i.p. osmotic mini pump for 4 weeks, and evaluated for cognitive function by Novel object recognition and Y-maze tests. Novel object recognition test showed that αCBSF-treated 5XFAD mice spent

more time with the novel *versus* old objects, whereas AgBSF-treated 5XFAD mice spent the same period of time with both novel and old objects (Figure 2-11a). Thus, discrimination index (%) was enhanced by αCBSF compared with AgBSF treatment (Figure 2-11b). Notably, improvement was complete, because there was no significant difference ($p > 0.05$) from WT control mice (NTg). In addition, αCBSF treatment significantly increased the number of entries (Figure 2-11c) and spontaneous alterations in 5XFAD mice compared with the AgBSF-treated cohort (Figure 2-11d), as determined by Y-maze test, thus confirming that αCBSF treatment improved learning and working memory in this AD mouse model.

Discussion

Recent progress in HUCBC therapy for different neurological diseases [34][35] opened new opportunities for AD research [36]. We have previously found that multiple low-dose peripheral infusion of HUCBC reduced cerebral β-amyloid plaques, cerebral amyloid angiopathy, and astrocytosis, whereas these treatments improved cognitive impairments in the PSAPP AD mouse model [37] and enhanced neurogenesis in the aged rat brain [32]. In a subsequent study, we have reported that HUCBC-derived monocytes reduced cerebral β-amyloid pathology and cognitive impairments [38]. In addition, we have shown that HUCBC-derived monocyte more effectively removed Aβ by phagocytosis than the aged-blood monocyte, whereas sAPPα enhanced Aβ phagocytosis by the aged monocyte by forming a complex with Aβ *via* the help of monocyte scavenger receptor [38]. In support of these findings, we demonstrated that overexpression of sAPPα significantly reduces both cerebral β-amyloid [42] and tau pathology in crossing Tg-sAPPα with PSAPP mice [43]. Meanwhile, using a sophisticated parabiosis mouse model, Wyss-Coray and colleagues showed that blood serum from old mice reduces neurogenesis and impairs cognitive functions when administered into young mice [40]. Subsequently, several groups reversed age-

related cognitive impairments in aged mice by infusing plasma from young into old mice [41][154][155] as well as AD pathology [157]. More specifically, Wyss-Coray group have published several articles over the last few years [41][75] showing the potential of young and/or umbilical cord plasma in ameliorating aged-associated cognitive impairments. In those experiments, they have either joined the young and aged mice thorough parabiosis or injected young and/or umbilical cord blood derived plasma into aged mice via tail vein injection. Interestingly, only three to four injections within 3-4 weeks period of time improved cognitive impairments in those experiments. These results encouraged us to determine whether human CBS could effectively reduce AD pathology *in vitro* (*i.e.*, cell culture and cell-free systems) as well as *in vivo* (*i.e.*, 3X-TgAD and 5XFAD mouse models) by enhancing sAPPα production.

Our preliminary findings indicate that CBS possesses α-secretase-like enzyme in cell culture and cell-free systems. In CHO/APPwt cells, CBS produces greater amount of sAPPα production compared with ABS and AgBS in a concentration- and time dependent manner (Figure 2-1a and b). Since α-secretase is proteinaceous and heat-labile, we hypothesized that α-secretase-like enzyme displayed by CBS is also inactivated by heat treatment. As expected, heat inactivation significantly limited the sAPPα producing capacity of CBS (Figure 2-1c). These results suggest that α-secretase-like enzyme of CBS is most likely a single complex protein that interacts with and cleaves APP. Subsequent study indicated that CBS mediates α-secretase cleavage of neuron-specific APP_{695} in a cell-free system, further suggesting that this activity is mediated by an endogenous enzyme (Figure 2-2a and b).

To purify, characterize, and ultimately identify this α-secretase-like content in CBS, we employed three-step affinity column, size-exclusion, and anion-exchange chromatography techniques in a sequential manner (Figure 2-3, 2-4, and 2-5). These sequential purification steps

enhanced the catalytic activity more than 3,000 fold compared with original CBS. The fractions containing highest α-secretase catalytic activity, as reflected by sAPPα level were combined and termed as "αCBSF" for the further study. SDS-PAGE analysis of the fractions from size-exclusion and anion-exchange chromatography yielding the highest α-secretase indicated size of our unknown enzyme could be around 177-275 kDa (Figures 2-4 and 2-5). It is not easy for a 177-275 kDa protein to cross the blood brain barrier through intraperitoneal mini pump administration without any inhibition. However we do not believe the protein is larger than 275 kDa based on the markers in for our gels. However, the SDS-PAGE also showed some low molecular-weight compounds which cannot be ruled out as well, which warrant further investigation. Interestingly, TACE (ADAM17) and ADAM inhibitors did not alter α-secretase in CBS, indicating that the enzyme is not TACE or ADAM, whereas the activity was dramatically reduced by protease inhibitor/cocktail, confirming that the activity is mediated by a protease (Figures 2-2 and 2-6). Moreover, immunoprecipitation of αCBSF with 2B3 antibody (anti-C-terminal of sAPPα) showed significant reduction of sAPPα levels, indicating that α-secretase-like enzyme αCBSF physically interacts with sAPPα (Figures 2-7).

Previously, we and others have shown that sAPPα reduces β-amyloid pathology via inhibition of BACE1 [42]. In a recent article, we have shown that sAPPα decreases tau phosphorylation via BACE1 inhibition and GSK-3β-mediated inhibitory phosphorylation [43]. This study prompted us to investigate the functional efficacy of fractionated CBS (αCBSF) in 5XFAD and 3XTg-AD mouse models. We have shown that αCBSF significantly reduced Aβ and tau phosphorylation (p-tau-Thr^{231}) in 3X-Tg AD mice, whereas αCBSF enhanced α-secretase cleavage products (*i.e.*, sAPPα and α-CTF), indicating that α-secretase-like content in CBS promotes APP non-amyloidogenic processing *in vivo* (Figure 2-8b and c). In 5XFAD mice being

aggressive β-amyloid deposition and plaque formation, αCBSF reduced β-amyloid plaque pathology in both neocortex and hippocampus regions, and reduced neural loss in the neocortex region, compared with AgBSF-treated mouse brains (Figures 2-9 and 2-10). By carrying-out sequential fractionation, we markedly enhanced CBS derived α-secretase (termed αCBS) and infused into 5XFAD mice via osmotic mini pump over the period of 6 weeks. Behavioral analyses in 5XFAD mice indicate that αCBS treated mice showed improved episodic memory, as determined by novel object recognition test (Figure 2-11a and b) as well as spatial working memory, as determined by Y-maze test (Figure 2-11c and d) compared with AgBSF treatment. Our work is in line with the work of Villeda et al. 2014 [41] and Castellano et al. 2017 [75] where improvement of performance in cognitive impairment was found in aged-mice treated with young plasma. Notwithstanding, we are not quite sure how CBS fraction (αCBSF) ameliorates β-amyloid pathology and cognitive functioning in 5XFAD and tau pathology in 3XTg-AD mouse model. The effect we observe may or may not be from CBS α-secretase-like enzyme. One of the plausible explanation of this effects are may be a direct action from CBS α-secretase-like enzyme or could be an indirect effect through peripheral sink hypothesis which demand further investigation. Although we do not know the exact molecular mechanism, however, we believe that human cord blood derived serum and/or plasma protein functions as a master regulator of several genes involved in the proliferation of cells, and blood vessels that might reduce neuroinflammation, Aβ, and improve synaptic plasticity by affecting multiple pathways. Overall, our results show beneficial effects of αCBSF in ameliorating β-amyloid pathology and cognitive functioning in 5XFAD and reducing tau phosphorylation in 3XTg-AD mouse model.

It is well known that members of the membrane-bound zinc-dependent metalloproteinase ADAM family are α-secretase enzymes that cleave APP for the non-amyloidogenic pathway. In

47

particular, three different members of this family, ADAM9, ADAM10, and ADAM17, possess APP α-secretase activity [141]. The ADAM family constitutes a large family of multidomain membrane proteins that have both cysteine-rich, disintegrin, and zinc metalloprotease domains in their ectodomain [140]. The main function of ADAM family is to shed the ectodomain of different membrane proteins, and has growth factors-like function *via* intracellular signaling cascade. However, it should be noted that numerous other substrates also have been linked to these ADAM family. These functions of ADAM family either protect against AD or promote AD pathogenesis *via* activation of different cytokines. One of the enzymes, ADAM17 is also known as TACE, responsible for secreting the main pro-inflammatory cytokine, TNFα [146]. Thus, TACE (ADAM17) is a therapeutic target for multiple diseases. Additionally, both ADAM10 and ADAM17 cleave various other membrane proteins and promote tumor in the cell [142]. ADAM10, in particular, cleaves many different kinds of transmembrane proteins in the vascular system, including the platelet-activating collagen receptor glycoprotein VI, [144][143] and endothelial proteins, including transmembrane chemokines (*i.e.*, CX3CL1 and CXCL16) [145]. These two chemokines are known for angiogenesis, inflammation, and immune cell recruitment [162][163]. Likewise, ADAM9 cleaves and releases a number of molecules with important roles in tumorigenesis and angiogenesis. Taken together, whereas the known α-secretase enzymes, mainly ADAM10 and ADAM17 (TACE) and in some degree ADAM9, are involved in APP α-secretase cleavage, they are not APP specific and cleave various substrates associated with inflammation, tumor formation, and progression. Thus, whereas AD is the only pathology in which an increased α-secretase activity has been proposed to be favorable, the nonspecific nature of the known α-secretases has made this strategy for AD treatment thus far unsuitable [147].

In sum, our study has presumably discovered an umbilical cord blood derived α-secretase which is independent on TACE or ADAM, thus making it a suitable candidate for the further study as a therapeutic target for AD treatment. This α-secretase-like enzyme activity either directly or indirectly activates α-secretase or produce sAPPα in cell culture and AD animal models. In addition, we believe this α-secretase appears to be mediated by novel enzymes residing within the sera which decline with age. We expect that our study using fractionation, chromatographic separation and mass-spectrometry (MS) techniques would identify the target enzyme as well as other interacting partners from CBS. However, identification of a target protein or enzyme with a particular function from a complex mixture of serum is a challenging task due to multiple factors, including the high complexity and wide dynamic range of proteins as well as the presence of contaminating proteins of high abundance. Despite this, here we show that our purification techniques significantly enhanced the α-secretase of CBS. Further MS based sophisticated purification techniques will completely purify, identify, and characterize the factor mediating this α-secretase in CBS.
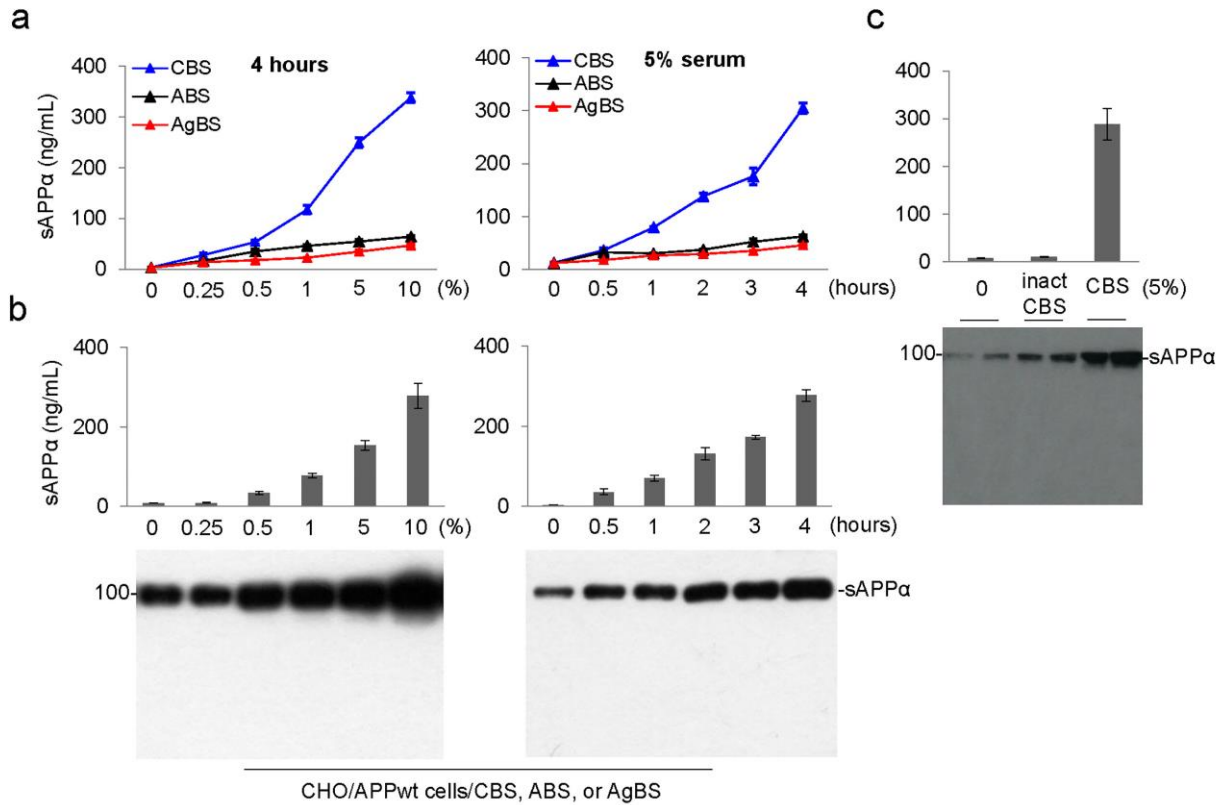
Figure 2-1 CBS, but not ABS or AgBS, markedly promotes APP α-cleavage in a time-, dose- and temperature-dependent manner.

(a) CHO/APPwt cells were treated with 0, 0.25, 0.5, 1, 5 and 10% CBS, ABS, or AgBS (left panel). In addition, CHO/APPwt cells were treated with 5% CBS, ABS, or AgBS between 0 and 4 h, as indicated (right panel). (b) CHO/APPwt cells were treated with CBS at different concentration (0-10%) for 4 h (left panel) or treated with 5% CBS for different time point (0 - 4) h, as indicated (right panel). Conditioned media were subjected to sAPPα ELISA (Figure 2-1A and B, top panel) and WB analyses (Figure 2-1B, bottom panel) with 2B3 antibody (c) CHO/APPwt cells treated with heat inactivated serum (inact CBS) or CBS for 4 h. Conditioned media were subjected to sAPPα ELISA (Figure 2-1C, top panel) and WB analyses (Figure 2-1C, bottom panel) with 2B3 antibody. Data are presented as mean (± S.D.) of sAPPα produced (ng/mg) from 5 independent experiments in triplication. Human umbilical cord blood plasma (CBP) produced similar results (data not shown). APP α-secretase activity of pooled CBS or CBP or individualized CBS or CBP was similar (data not shown).

50

Figure 2-2 CBS directly mediates α-cleavage of neuron specific APP$_{695}$, but this activity is not mediated by ADAM and TACE.

CBS directly mediates α-cleavage of neuron specific APP$_{695}$, but this activity is not mediated by ADAM and TACE. (a) Human recombinant full-length APP$_{695}$ tagged with C-terminal MYC/DDK (fAPP$_{695}$, OriGen, 100 ng) was incubated with 5% CBS, inact CBS, or AgBS at 37ºC for 5 h in the presence or absence of a protease inhibitor cocktail (PI, 1 X), TACE (ADAM17) inhibitor (TAPI-0, 1 µM), or ADAM inhibitor (GM6001, 1 µM). Lane 1-4 represent CBS (1), inact CBS (2), AgBS (3), and FBS (4) sample only control without substrate fAPP$_{695}$. Lane 5 represent fAPP$_{695}$ (5) substrate only control without any serum sample. Lane 6-11 represent substrate fAPP$_{695}$ with CBS (6), inact CBS (7), CBS with PI (8), CBS with TAPI-0 (9), CBS with GM6001 (10), and AgBS (11). Lane 12-14 represent (lane 12-14; PI (12), TAPI-0 (13), and GM6001 (14) inhibitor and substrate control respectively, without any serum sample. The reaction mixtures were subjected to sAPPα WB analysis using 2B3 antibody (top panel) and total APP using 6E10 (an anti-Aβ$_{1-17}$ antibody; lower panel). sAPP$_{770}$ refers to the endogenous α-secretase cleavage product of CBS or AgBS, whereas sAPP$_{695}$ refers to the α-secretase cleavage product of fAPP$_{695}$. (b) 100 ng of fAPP$_{695}$ was incubated with 5% CBS for 1, 5, or 24 h, or 5% FBS or inact. FBS for 24 h, and then subjected to sAPPα and total APP WB analysis using 2B3 (top panel) and 6E10 (lower panel), respectively. sAPP$_{770}$ refers to the endogenous α-secretase cleavage product of CBS or AgBS, whereas sAPP$_{695}$ refers to the α-secretase cleavage product of fAPP$_{695}$.
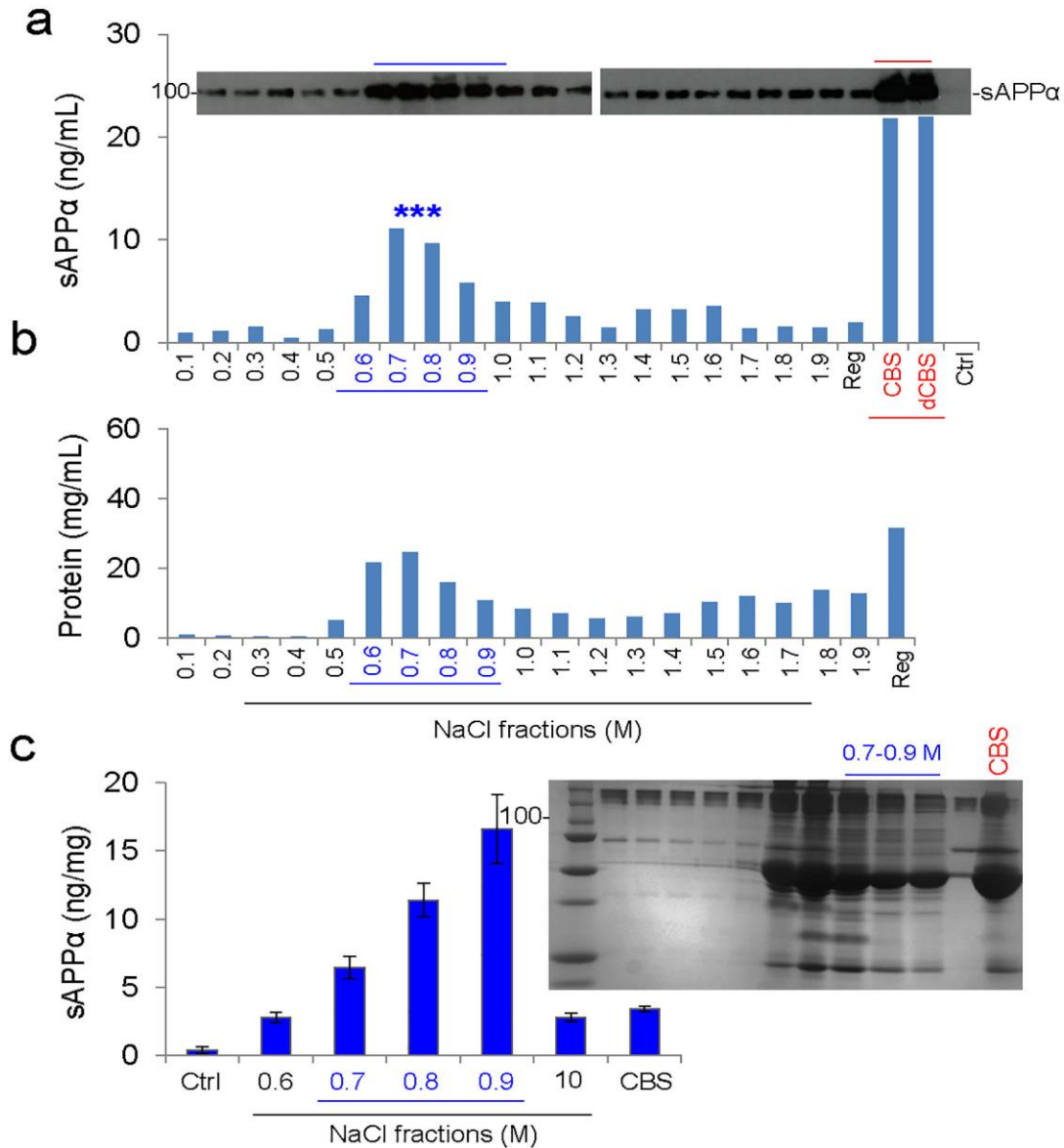
Figure 2-3 Fractionation of APP specific α-secretase activity in CBS.

To purify and eventually identify the α-secretase activity in CBS, the Econo-Pack Serum IgG purification kit (Bio-Rad) was initially employed to remove highly abundant IgG. CBS was then desalted using Econo-Pack 10DG columns. The desalted serum was applied to DEAE Affi-Gel blue columns to remove residual IgG and collect 20 additional protein fractions, by eluting with an increasing ionic strength gradient of NaCl buffer ranging from 0.1 M to 2.0 M. The remaining proteins on the column were eluted by the regeneration buffer included in the kit and collected as the regeneration fraction (Reg). (a) CHO/APPwt cells were cultured in 24-well plates and treated with 10 μL of each protein fraction for 2 h. Conditioned media were then collected and analyzed by sAPPα WB (upper panel) and ELISA (lower panel). 10 μL CBS, desalted CBS (dCBS), and phosphate buffered saline (PBS; Ctrl) were included under the same cell culture conditions as

52

positive and negative controls respectively. Cell lysates were also prepared from each fraction-treated cell culture as an additional reference to evaluate sAPPα production levels (data not shown). (b) Protein concentration of each fraction. (c) CHO/APPwt cells were treated with the 0.6 to 1.0 M NaCl eluted fractions from 10 different CBS lots, as well as whole CBS and PBS (Ctrl), for 2 h and the conditioned media were collected for sAPPα ELISA. The results were presented as mean (± S.D.) sAPPα produced (ng/mg protein). In addition, each protein fraction was also subjected to SDS PAGE to assess total protein fractionation (c, right panel).
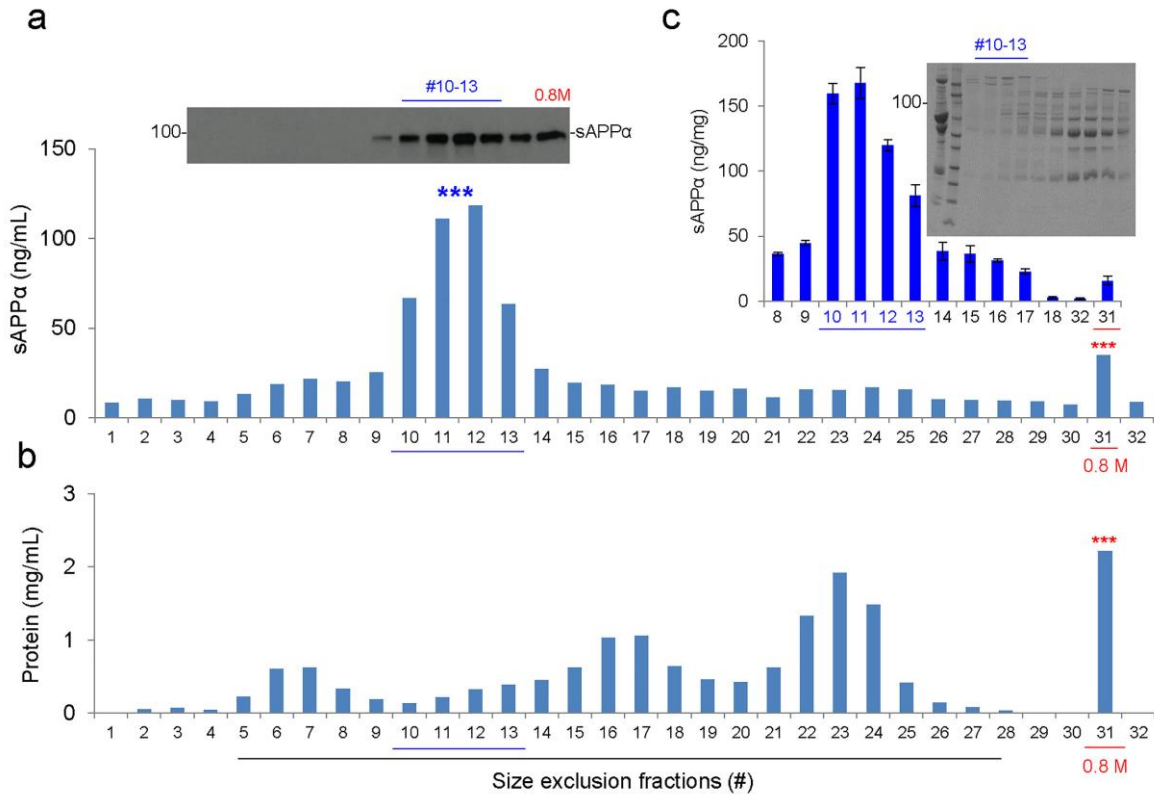
Figure 2-4 Protein size-exclusion chromatography by preparative-grade Superdex 200 column.

The 0.8 M NaCl eluted protein fraction of CBS was further subjected to size exclusion chromatography by analytic Superdex 200 column. Approximately 100 mg of protein from the 0.8 M NaCl fraction was applied to the column and 48 fractions were eluted with PBS. (a) CHO/APPwt cells were cultured in 24-well plates and treated with 40 µL of each protein fraction for 2 h. The conditioned media were collected and analyzed by sAPPα WB (upper panel) and ELISA (lower panel). In parallel, the 0.8 M NaCl eluted fraction (#31) and PBS (#32) were included under the same cell culture conditions as positive and negative controls respectively. Cell lysates were also prepared from each fraction-treated cell culture as an additional reference to evaluate sAPPα production levels. (b) Protein concentration of each size fraction. (c) CHO/APPwt cells were treated with #8 to 18 size fractions prepared from 3 independent experiments, as well as the original 0.8 M NaCl fraction (#31) and PBS (#32), and then conditioned media were collected and analyzed by sAPPα ELISA. The results were presented as mean (± S.D.) sAPPα produced (ng/mg protein). In addition, each size fraction was subjected to SDS PAGE analysis to assess total protein fractionation (C, right panel).

54
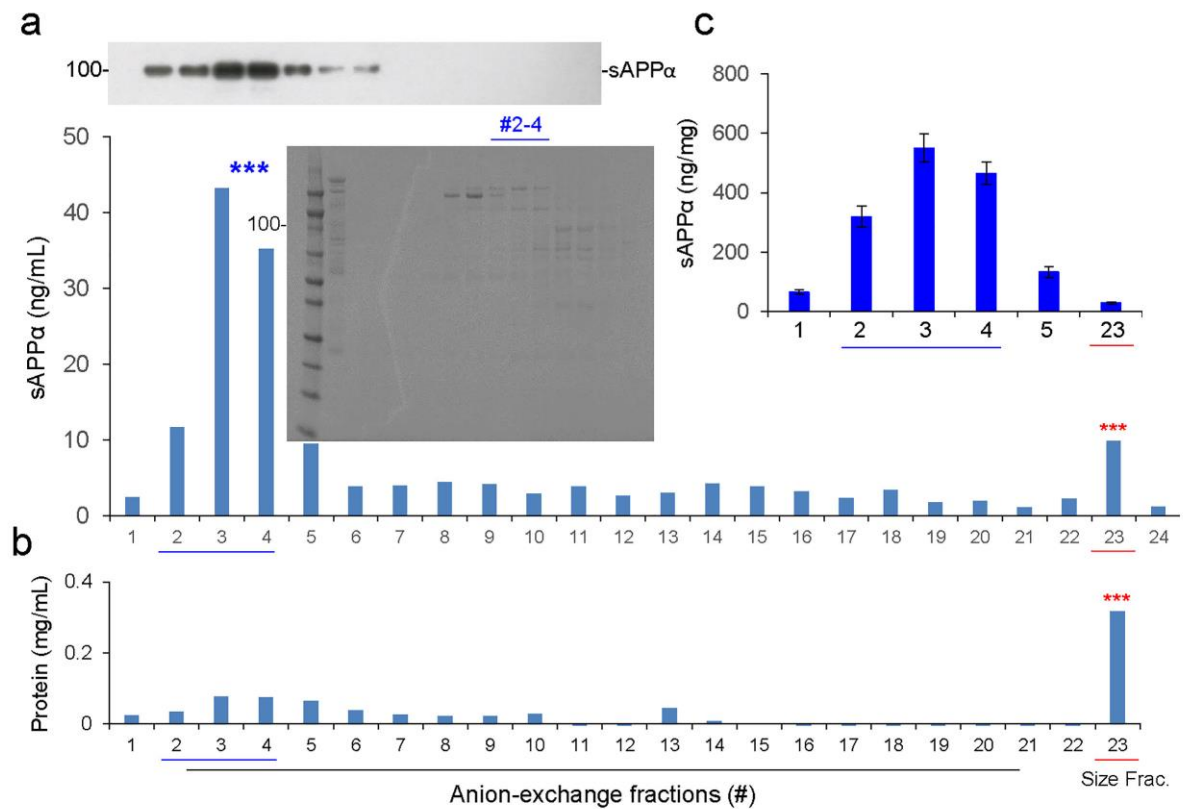
Figure 2-5 Further fractionation by anion-exchange chromatography.

The size exclusion fractions containing the highest APP α-secretase activities (#10 to 13) were further subjected to anion-exchange chromatography using Q-Sepharose columns. Approximately 10 mg of protein from the size exclusion fraction(s) was applied to the column and 82 fractions were eluted with buffer containing 50 mM Tris, 500 mM NaCl, pH 7.6. (a) CHO/APPwt cells were treated with 40 μL of each protein fraction for 2 h and conditioned media and cell lysates were analyzed by sAPPα WB (upper panel) and ELISA (lower panel). The original size exclusion eluted fraction (#23) and PBS (#24) were included as positive and negative controls respectively. In addition, SDS-PAGE of #2-4 anion-exchange fractions showed the presence of multiple proteins (middle panel). (b) Protein concentration of each fraction. (c) CHO/APPwt cells were treated with the #1 to 4 anion-exchange fractions prepared from 3 independent experiments and then conditioned media were subjected to sAPPα ELISA. The results are presented as mean (± S.D.) sAPPα produced (ng/mg protein). The original size exclusion eluted fraction (#23) was included as a positive control. Combined fractions #2 to 4, referred to as αCBSF, and were used for further analysis.

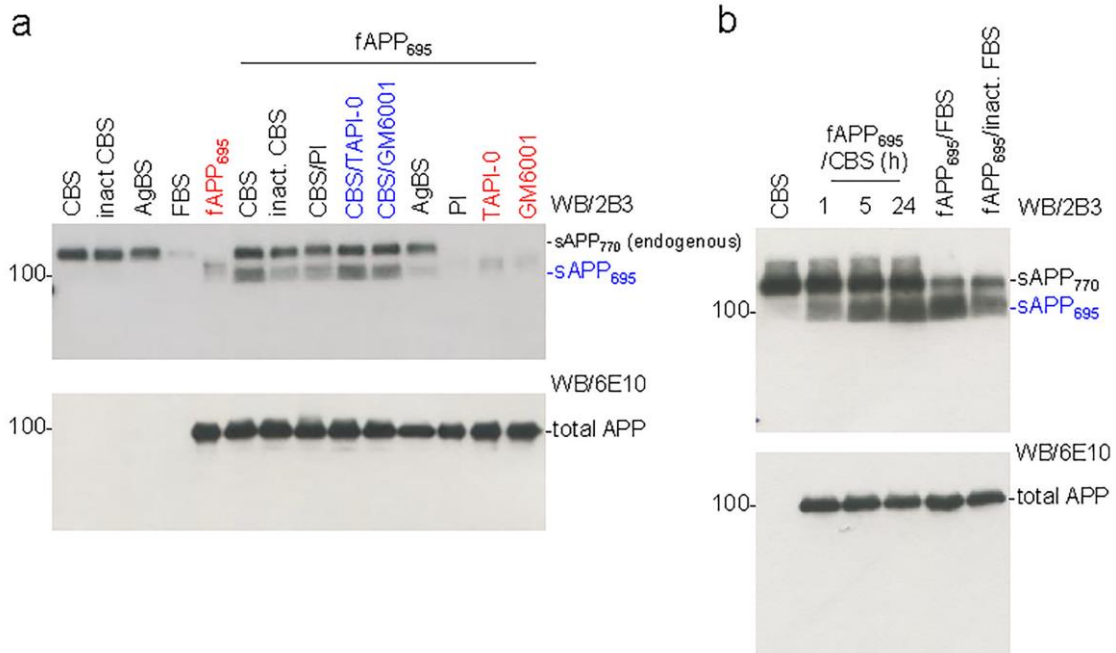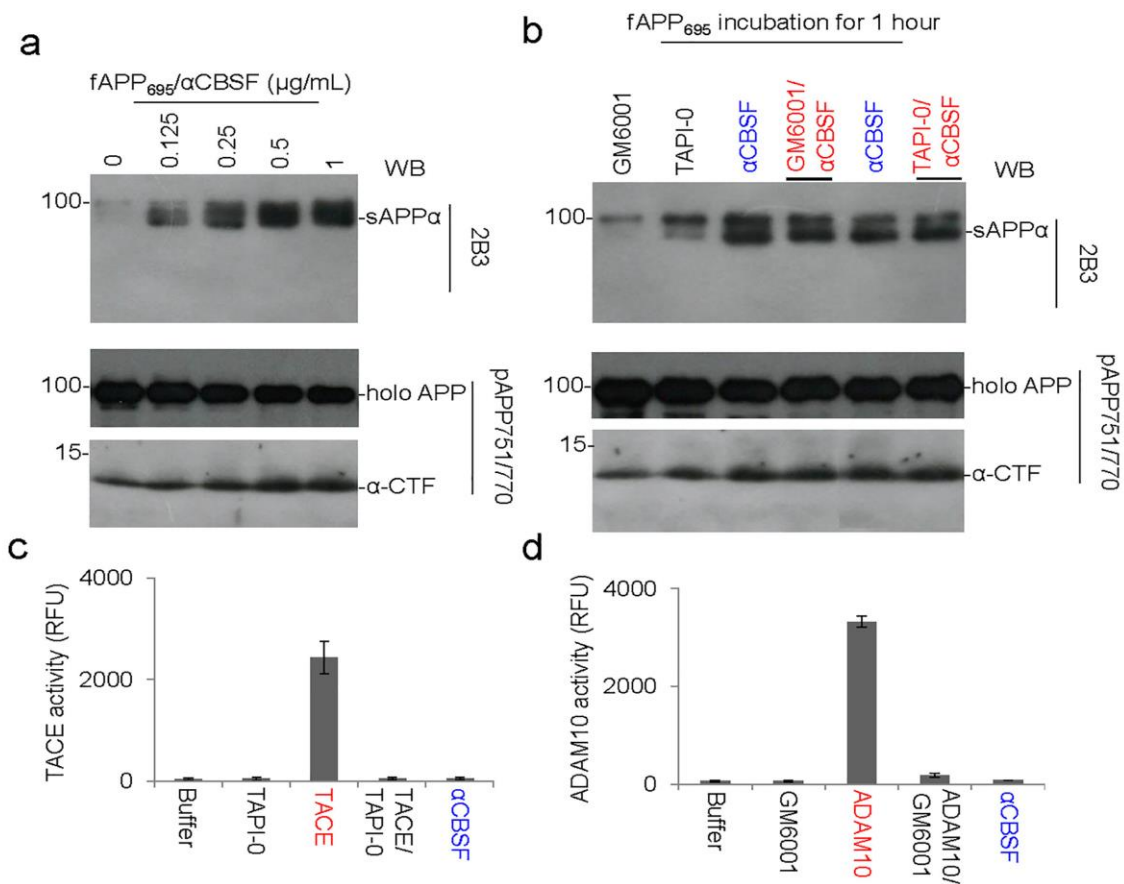**Figure 2-6 αCBSF directly mediates α-cleavage of neuron specific APP₆₉₅, but this activity is not mediated by ADAM or TACE.**

(a) Human recombinant full-length APP$_{695}$ (fAPP$_{695}$, 100 ng) was incubated with 0, 0.125, 0.25, 0.5, or 1 µg of αCBSF. at 37°C for 2 h. The reaction mixtures were subjected to sAPPα WB analysis using 2B3 (top panel) and holo APP and α-CTF analysis using pAPP751/770 antibody (lower panel). (b) fAPP$_{695}$ (100 ng) was incubated with 0.125 µg of αCBSF in the absence or presence of ADAM (GM6001, 1 µM) or TACE inhibitor (TAPI-0, 1 µM) for 1 h and then subjected to sAPPα, holo APP and α-CTF WB analysis using 2B3 (top panel) and pAPP751/770 (lower panel). α-CTF of APP was further confirmed by an additional WB using an antibody specifically against Aβ$_{17-26}$ (4G8). In addition, incubating human recombinant full-length APP$_{751}$ with αCBSF produces similar results (data not shown). (c) The TNFα converting enzyme (TACE or ADAM17) activity of αCBSF was measured by TACE cleavage activity kit. TACE (25 µg/mL) secretase in the presence or absence of TACE inhibitor (TAPI-0, 1 µM) was included as positive control. (d) In parallel the ADAM10 activity of the αCBSF was measured by ADAM10 cleavage activity kit. ADAM10 (50 µg/mL) secretase, in the presence or absence of ADAM inhibitor (GM6001, 1 µM), was included as positive control. TACE, ADAM17, and ADAM10 cleavage activities were determined for 1 h and expressed as relative fluorescence units (RFU). These results are presented as mean (± S.D.) of three independent experiments with triplicates for each condition.
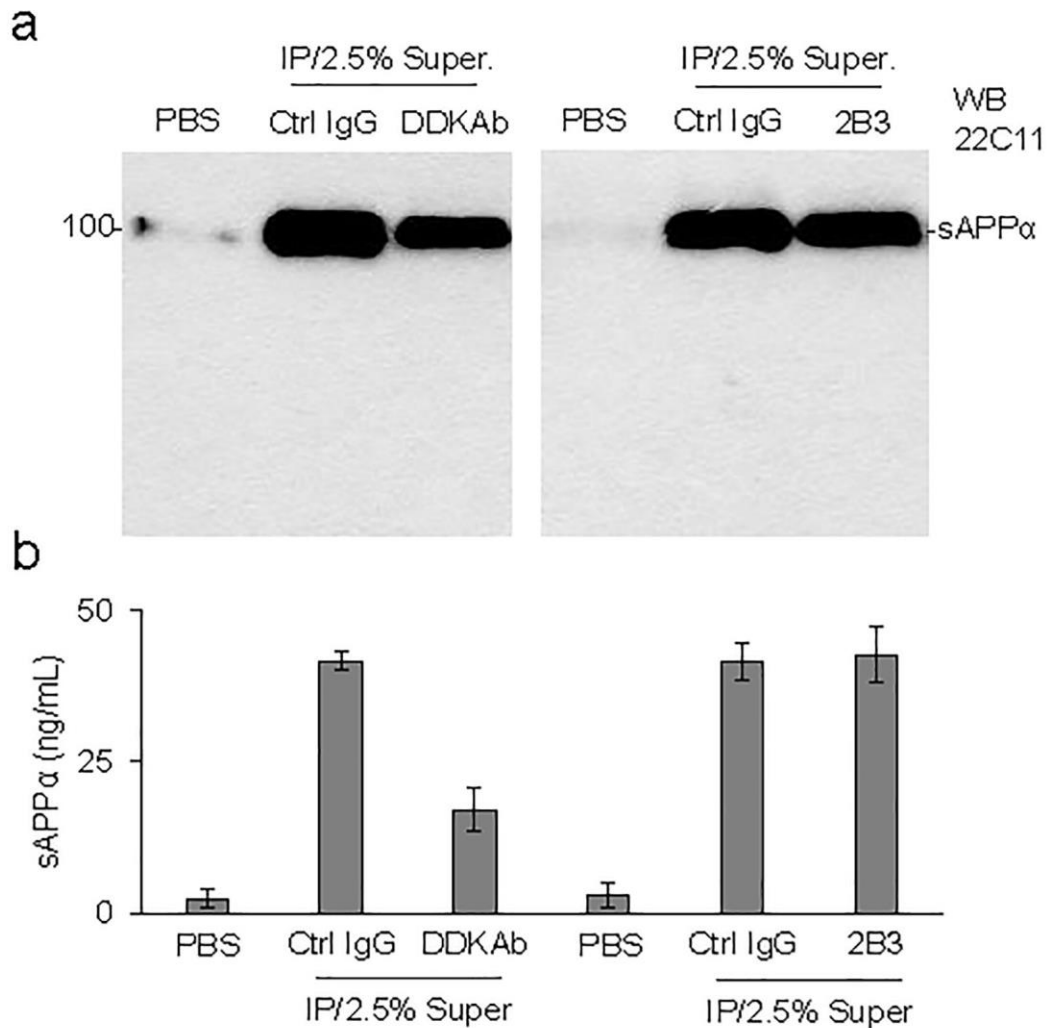
Figure 2-7 Immunoprecipitation of fAPP$_{695}$/αCBSF specifically limits APP α-secretase activity of αCBSF.

To determine whether immunoprecipitation could limit the ability of αCBSF to promote APP α-cleavage, we incubated 100 ng of fAPP$_{695}$ with 0.125 μg of αCBSF at 4°C for overnight and then immunoprecipitated (IP) the sAPPα/αCBSF immune complex using an anti-DDK antibody (DDKAb), an sAPPα specific antibody (2B3), or nonspecific IgG. CHO/APPwt cells were treated with the supernatants (Super.) from each immune complex, or PBS as control, in the FBS free condition. Two h after treatment, conditioned media were collected and analyzed by sAPPα WB using anti-N-termnal APP antibody (22C11, a) and sAPPα ELISA (b). For (b), the results were presented as mean (± S.D.) of sAPPα production (ng/mL) in the conditioned media from three independent experiments with triplicates for each condition. There was no notable or significant difference in sAPPα production elicited by 0.5% supernatant from αCBSF immunoprecipitated with control IgG (Ctrl) and 2.5 % (equivalent to 0.5% Super.) of αCBSF alone, as determined by sAPPα WB and ELISA analysis (data not shown).
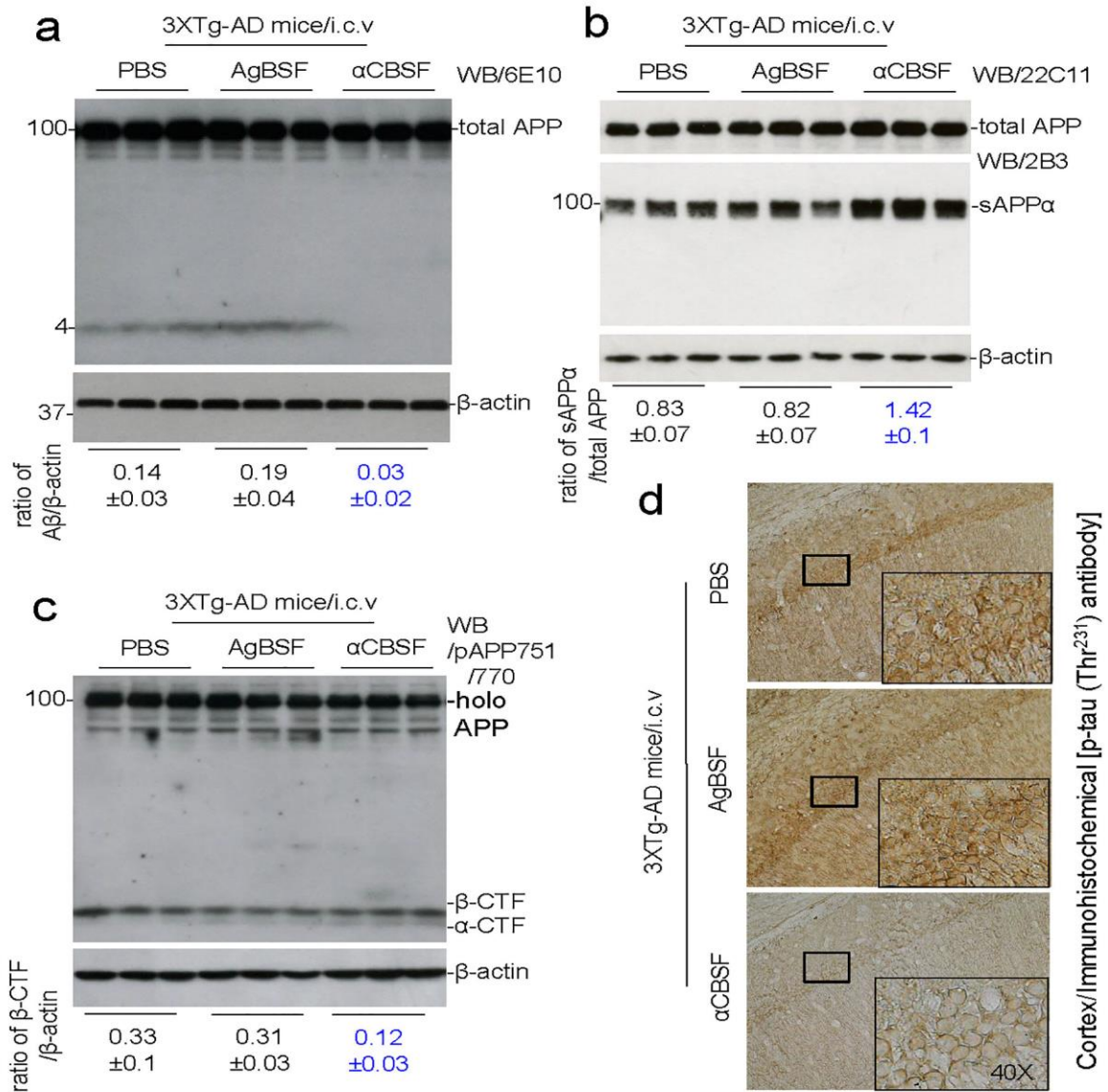
Figure 2-8 αCBSF promotes APP α-secretase processing *in vivo*.

3XTg-AD female mice at 4 months of age were treated with αCBSF, AgBSF (0.5 μg/mouse; $n = 6$), or PBS control (1 μL/mouse; $n = 5$ female) by i.c.v. injection and euthanized 72 h later. Mouse brain homogenates were then prepared from the right half of the brain (non-injection side). (a) WB analysis using $A\beta_{1\text{-}17}$ antibody (6E10) shows total APP and Aβ species. (b) WB analysis using an sAPPα specific antibody (2B3) or anti-N-terminal APP antibody (22C11) shows sAPPα or total APP, respectively. (c) WB analysis using pAb751/770 shows full-length APP (holo APP) and two bands corresponding to β-CTF and α-CTF. (d) Mouse brain cortices from each treatment group were stained with anti-phospho-tau [p-tau (Thr[231])] antibody. In addition, percentages [p-tau (Thr[231]) positive area/total area; mean ± S.D.] of anti-p-tau antibody positive cells were quantified by image analysis ($p < 0.005$) (data not shown). WB data presented here are representative of results obtained from 5 to 6 female mice per group.
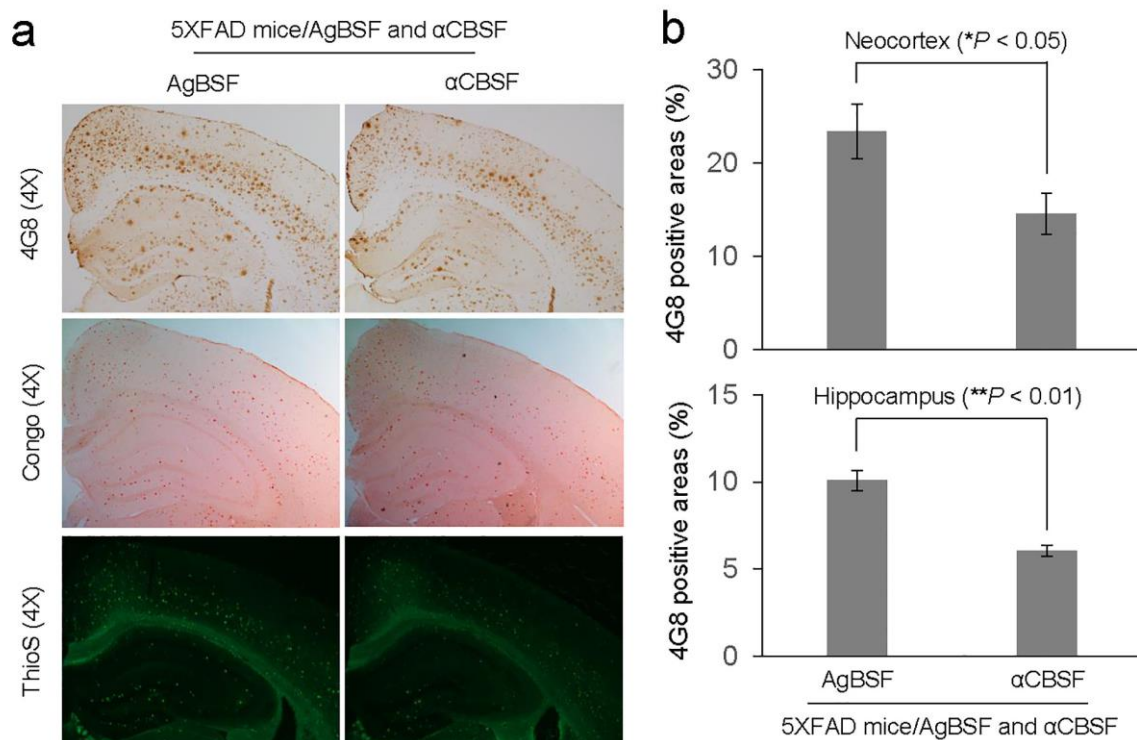
Figure 2-9 αCBSF reduces β-amyloid plaques in 5XFAD mice.

Five month old 5XFAD female mice were treated i.p. with αCBSF (n = 5 to 7) and AgBSF (n = 5 to 6) *via* osmotic mini pump at 30 µg/mouse/day for 6 weeks. (a) Mouse brain sections from each group were stained with 4G8, Congo red, and Thio-S. (b) Percentages of 4G8 positive areas were quantitatified by image J analysis for neocortex and hippocampus, showing that αCBSF treatment significantly reduced plaque area compared with AgBSF treatment (*t*-test for independent samples; *p < 0.05, **p < 0.01).
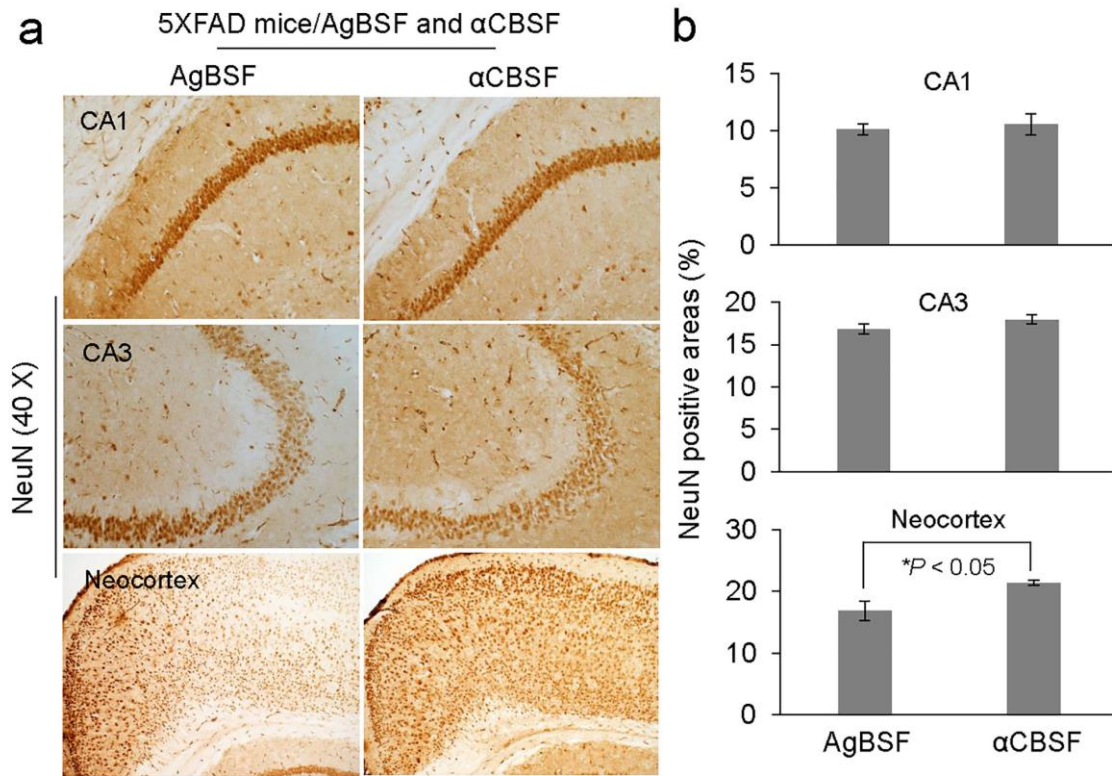
Figure 2-10 Neuroprotective Effects of αCBSF.

5XFAD female mice at 5 months of age were treated i.p. with αCBSF ($n = 7$) or AgBSF ($n = 6$) *via* osmotic mini pump for 6 weeks. (a) Mouse brain sections from αCBSF and AgBSF treated groups were stained with NeuN. (b) Quantification of NeuN positive cells in the CA1, CA3, and neocortex revealed that αCBSF treatment significantly increased NeuN positive cells compared with AgBSF treatment in neocortex *(t-test for independent samples; *$p < 0.05$).
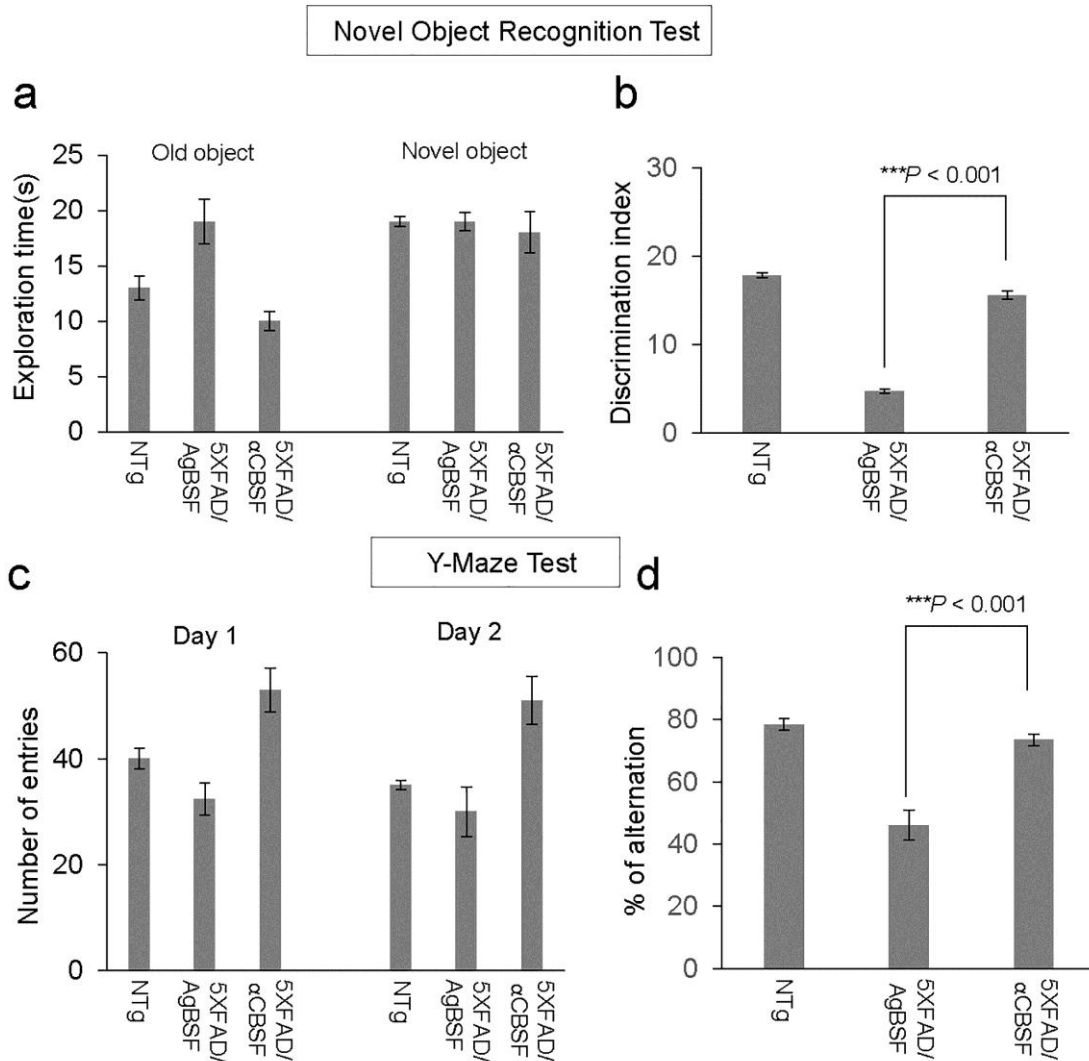
Figure 2-11 αCBSF improves cognitive function in 5XFAD mice.

5XFAD female mice at 5 months of age were treated with αCBSF and AgBSF (30 μg/mouse/day) i.p. by osmotic mini pump for 6 weeks. Each treatment groups as well as nontransgenic WT controls (NTg) were subjected to Novel Object Recognition and Y-maze behavioral testing. (a) Times spent exploring old and novel objects during the test phase of NOR was recorded for each treatment group. (b) Discrimination index, calculated as the frequency of exploring new object vs. original objects, was significantly reduced in 5XFAD mice treated with AgBSF, but not in those treated with αCBSF, compared with NTg controls. (c) Total number of arm entries for Y-maze was recorded for each treatment group. (d) Percent alternations was significantly reduced in 5XFAD mice treated with AgBSF, but not in those treated with αCBSF, compared with NTg controls. Significance level determined by ANOVA for a total of $n = 5$ NTg mice, $n = 7$ αCBSF treated 5XFAD mice, and $n = 6$ AgBSF treated 5XFAD mice (***$p < 0.001$).

CHAPTER 3

Human cord blood serum-derived APP α-secretase cleavage activity is mediated by C1 complement

Permission statement

The information in chapter 3, "Human cord blood serum-derived APP α-secretase cleavage activity is mediated by C1 complement" has been legally reproduced under the Creative Commons Attribution (CC-BY) license. This means the publication is accessible online without any restrictions and can be re-used in any way subject only to proper citation.

Habib A, Sawmiller D, Hou H, Kanithi M, Tian J, Zeng J, Zi D, He ZX, Sanberg PR, Tan J Human Cord Blood Serum-Derived APP α-Secretase Cleavage Activity is Mediated by C1 Complement. Cell Transplantation (2018): May: doi: 10.1177/0963689718775941

Chapter synopsis

Alzheimer's disease (AD) is the leading cause of dementia in the elderly. In healthy individuals amyloid precursor protein (APP) is cleaved by α-secretase generating soluble alpha amyloid precursor protein (sAPPα), which contribute neuroprotective functions in the neuronal environment. In contrast, in the neurodegenerative environment of AD patients, amyloid-β-peptide (Aβ) of either 40 or 42 residues are generated by increased activity of beta and gamma

secretase. These proteins amalgamate in specific regions of the brains, which disrupt neuronal functions and lead to cognitive impairment. Our most recent work studied the impact of umbilical cord blood serum (CBS) on modulation of sAPPα production. Heat-sensitive CBS significantly promoted sAPPα production indicating heat-sensitive factor(s) plays a role in this process. Liquid chromatography with tandem mass spectrometry (LC-MS/MS) analysis was used to determine the molecular source of α-secretase in purified CBS and aged blood serum (AgBS) fraction. Of the proteins identified, the subunits of C1 complex (C1q, C1r, and C1s) and alpha-2-macroglobulin showed significantly greater levels in purified αCBS fraction (αCBSF) compared with AgBS fraction (AgBSF). Specifically, C1 markedly increased sAPPα and alpha-carboxyl-terminal fragment (α-CTF) production in a dose-dependent fashion, whereas C1q alone only minimally increased and C3 did not increase sAPPα production in the absence of sera. Furthermore, C1q markedly increased sAPPα and αCTF, while decreasing Aβ, in CHO/APPwt cells cultured in the presence of whole sera. These results confirm our initial assumption that APP α-secretase activity in human blood serum is mediated by complement C1, opening a potential modality of therapeutic for the future of AD.

Background

AD is the most common neurodegenerative disorder characterized by the presence of intracellular neurofibrillary tangles, extracellular β-amyloid plaques and neuronal loss throughout the entire brain. Aβ, a 4 kDa peptide, is one of the major components of β-amyloid plaques. Under physiological conditions, α-secretase cleaves APP within the Aβ domain, thereby preventing generation of Aβ and releasing soluble neurotrophic sAPPα [56]. sAPPα has been shown to reduce Aβ generation and plaque deposition by interfering with beta-site APP cleaving enzyme 1

(BACE1), also known as beta (β)-secretase [42][164]. In addition, sAPPα has also been shown to inhibit tau phosphorylation through modulation of GSK3β signaling pathway [43]. In neurodegenerative environment of AD, sequential cleavage of APP by β- and gamma (γ)-secretases generate Aβ peptides, comprising either 40 or 42 residues in length and which aggregate in the brain [1]. Eventually, these protein aggregates trigger neuroinflammation and neurodegeneration ultimately leading to cognitive impairment and memory dysfunction [165]. One of the prominent facets of AD neuropathology is the colocalization of activated inflammatory proteins of the complement pathways with the disease pathology [166].

Human umbilical cord blood cells (HUCBC) have emerged as a potential immunomodulatory therapy in various diseases, including ischemia and neurodegeneration [167]. The many benefits of HUCBC include attenuation of amyloidogenic APP processing and reduction of Aβ levels in PSAPP and Tg2576 mice models of AD [37]. Importantly, multiple low-dose HUCBC infusion have also been shown to improve cognitive functions in transgenic PSAPP mice [153]. Our most recent work showed that CBS significantly promoted sAPPα production whereas heat-inactivation eliminated this effect. Furthermore, sAPPα production was found to be increased by the removal of serum immunoglobulins and salts. To further understand what exactly in CBS was promoting sAPPα, we isolated the specific fraction of CBS found to have the highest α-secretase activity (αCBSF) by a three step chromatographic process. The proteolytic α-secretase activity in αCBSF was found to not be mediated by TNF-α converting enzyme (TACE) or a disintegrin and metalloproteinase domain-containing protein (ADAM)10. Immunoprecipitation studies indicated the presence of α-secretase-like enzyme, which physically interacts with APP [168]. As first reported, following the administration of αCBSF by intracerebroventricular (icv) injection, both Aβ levels and tau phosphorylation were reduced in 3XTg-AD mice. Amyloid

64

plaque numbers were decreased in the neocortex and hippocampus of 5XFAD mice through αCBSF intraperitoneal minipump administration in comparison with mouse brain treated with the corresponding AgBSF. Furthermore, icv administration of αCBSF enhanced non-amyloidogenic APP processing in 3xTg-AD mouse, providing a neuroprotective effect. These results combined with reduced neuronal loss in the neocortex of the 5XFAD mice model following αCBSF administration reveal a therapeutic potential for improving synaptic plasticity and neuroinflammation [168].

The complement system is a major part of the innate immune system involved in neuroprotection *via* activation of immunomodulatory pathways [169]. In fact, a growing body of evidence suggests that complement proteins have neuroprotective effects in the developing and adult brain [170][171]. Neurogenesis and synapse elimination are heavily influenced by the complement system, particularly in the early stages of the neurodevelopment [170][172]. Complement protein C1 complex is most commonly known for its neuroprotective role in enhancing and refining the neural network through phagocytosis of apoptotic cells and immune complexes [173]. The C1 complex is composed of a C1q and two each of C1r and C1s molecules. C1q, the largest subcomponent of the cascade initiator of C1 pathway, is composed of 6 of each A, B and C chains comprising 18 polypeptide chains [174]. In addition to a role in synaptic elimination, complement protein subcomponent C1q has been shown to increase neuronal survival and branching in absence of other complement components [175] and this effect could be mediated *via* upregulation of genes associated with neurotrophic factors (neural growth factor, and neurotrophin 3), cytoskeletal (syntaxin-3), and cholesterol metabolism (cholesterol-25-hydroxylase) [176]. During development C1q is expressed in synaptic regions, and synapse elimination is mediated by C1q during the period of synaptic pruning. Therefore deficiencies in

C1q or downstream complement components can lead to neuronal defects and other detrimental effects [172]. These data confirm a direct neuroprotective role of C1q in the physiological condition. In peripheral phagocytes C1q downregulates proinflammatory cytokine expression and supports the overall clearance of cellular debris. C1q binds to apoptotic cells flagging them to be cleared out before they release neurotoxic components [177]. Despite several physiological functions, dysregulated activation of the complement pathways in the central nervous system (CNS) have been usually considered detrimental in various conditions including AD [178]. Treatment with a cyclic hexapeptide C5a receptor antagonist (PMX205) has been shown to reduce fibrillary amyloid deposition and glial activation, while rescuing cognitive impairment in passive avoidance task in Tg2576 Swedish mutant mice [179]. Neuronal C1q is normally down-regulated in adult CNS, but is found to be upregulated in the advent of injury or early stages of disease [170]. Interestingly, C1q is found to be induced in the brain in response to neuronal injuries in AD and blocks fibrillary forms of Aβ neurotoxicity *in vitro* [180]. Benoit *et al*. demonstrated that C1q protect both immature and mature primary neurons against fibrillary and oligomeric Aβ toxicity [181]. Depending on the timing and environment, C1q can either be neuroprotective or induce an inflammatory environment leading to neurodegeneration in adult brain. Loeffler *et al*., reported that C3b and iC3b (i.e., proteolytically inactive product of C3b which prevent complement cascade activation) are also accumulated on AD-affected neurons, much like C1q [182].

Given that sAPPα has anti-amyloidogenic properties, the primary known α-secretases which cleave APP are non-specific and stimulating them could generate unwanted off-target effects. Our preliminary data show that α-secretase-like enzymatic activity in CBS is not mediated by ADAM10 or TACE, the major α-secretases that cleave APP in AD. In addition, we purified and identified a CBS specific fraction αCBSF, with more than thousand fold increased α-secretase

activity, which markedly increased cerebral sAPPα, decreased Aβ production and abnormal tau phosphorylation and ameliorated cognitive impairment in two (3xTg-AD and 5XFAD) AD mouse models [168]. In support of this hypothesis, we have tested further for the identification of the heat-sensitive protein factor(s) exerting this novel enzymatic function. Here, we have recently identified a novel role for complement protein C1 complex in the CNS. Multi-step fractionations followed by LC-MS/MS analyses of CBS have identified several proteins compared to AgBS, each of which could potentially generate sAPPα by cleaving APP in cellular system. Utilizing *in vitro* CHO/APPwt, N2a/APPwt, and TgAPPwt primary neuronal cell lines, we found that α-secretase-like enzymatic activity promoting sAPPα may be in part mediated by complement protein C1 complex. These results point to a novel neurotrophic function of complement protein C1 complex which requires further investigation.

Materials and methods

Reagents and antibodies

CBS was obtained from Lee Biosolutions (St. Louis, MO, USA). CBS was separated from umbilical cord blood by allowing clotting for 5-10 h in tubes without anticoagulant followed by centrifugation at 3,500 rpm for 5-10 min and filtration through a membrane with a pore size of 0.22 μm. Individual CBS samples were prepared from a single lot of cord blood, and more than ten samples of CBS were combined as "pooled CBS". Normal human aged blood serum (AgBS, >75 years old) were obtained from Florida Blood Services (Tampa, FL, USA). All sera were heat-activated. Heat inactivation of human sera was conducted at 56 ^{0}C for 30 min. Complement proteins, complement depleted sera, and complement inhibitors were acquired from the following sources. Human complement protein C1 inhibitor (Cat# GF178), complement protein C1 from

human serum (Cat# 204873), complement protein C3-depleted human serum (Cat# 234403), and complement protein C1q-depleted human sera (Cat# 234401) from MilliporeSigma, St. Louis, MO, USA. Complement protein C3 from human serum (Cat# A113), and complement iC3b from human serum (Cat# A115) are from Complement Technology, Inc. Tyler, Texas, USA. Complement protein C1q from human serum (Cat# 204876) from Calbiochem, UK. Compstatin, complement protein C3b inhibitor human (Cat# SB 431542) was acquired from Tocris Bioscience, Minneapolis, MN, USA. Sera from C1qa deficient (def) mice (129P2/OlaHsd, 3 months age) were kindly provided by Dr. Andrea J. Tenner (University of California, Irvine, USA). Antibodies used in this studies include: specific anti-sAPPα monoclonal antibody (2B3; IBL, Minneapolis, MN, USA, Cat# 11088 RRID: AB_494690), anti-APP C-terminal polyclonal antibody (pAb751/770; EMD Millipore, La Jolla, CA, USA, Cat# 171610, RRID: AB_211444), anti-N-terminal Aβ monoclonal antibody (6E10; Covance Research Products, Emeryville, CA, USA), and anti-β-actin monoclonal antibody (Cat# A5316, RRID: AB_476743) from MilliporeSigma, St. Louis, MO, USA. Human sAPPα ELISA assay kit was purchased from IBL AMERICA, MN, USA.

CBS and AgBS fractionation

In order to purify and characterize the α-secretase in CBS or AgBS, the Econo-Pack Serum IgG purification kit, and 10 DG columns (Bio-Rad, Philadelphia, PA, USA) were initially employed to remove highly abundant IgG and salts. The desalted serum was applied to DEAE Affi-Gel blue columns and residual IgG was eluted according to the instructions. Then 20 additional protein fractions were collected by eluting with an ionic strength gradient of NaCl buffer ranging from 0.1 M to 2.0 M. The remaining proteins on the column were eluted by the regeneration buffer included in the kit and collected as the regeneration fraction. The 0.8 M NaCl eluted protein fractions were combined together and sent to Moffitt Cancer Center protein

purification core for further separation by size exclusion chromatography, employing analytic Superdex 200 columns and eluting with PBS, and ion-exchange chromatography, employing Q-Sepharose columns and eluting with 500 mM NaCl, 50 mM Tris, pH 7.6. The final enzyme containing fractions were exchanged to PBS buffer by Ultracel-10 membranes (10 kDa, Merck Millipore) for further experimentation and referred to as αCBSF or AgBSF (Figure 3-1).

LC-MS/MS

Briefly each lane gel slices were destained using acetonitrile and subjected to tris 2-carboxyethy-phosphine (TCEP) reduction and iodoacetamide alkylation followed by in-gel trypsin digestion, extraction and vacuum centrifugation concentration. A nanoflow liquid chromatograph (U3000, Dionex, Sunnyvale, CA) coupled to an electrospray ion trap mass spectrometer (LTQ-Orbitrap, Thermo, San Jose, CA) was used for tandem mass spectrometry peptide sequencing experiments. Total 5 µL sample was first loaded onto a pre-column (5 mm x 300 µm ID packed with C18 reversed-phase resin, 5 µm, 100Å) and washed for 8 min with aqueous 2% acetonitrile and 0.04% trifluoroacetic acid. Next, the trapped peptides were eluted onto the analytical column, (C18, 75 µm ID x 15 cm, Pepmap 100, Dionex, Sunnyvale, CA). The 120-min gradient was programmed as: 95% solvent A (2% acetonitrile + 0.1% formic acid) for 8 min, solvent B (90% acetonitrile + 0.1% formic acid) from 5% to 50% in 90 min, then solvent B from 50% to 90% B in 7 min and held at 90% for 5 min, followed by solvent B from 90% to 5% in 1 min and re-equilibrate for 10 min (60-min gradient setup). The flow rate on analytical column was 300 nl/min. Five tandem mass spectra were collected in a data-dependent fashion following each survey scan. The MS scans were performed in Orbitrap to obtain accurate peptide mass measurement and the MS/MS scans were performed in linear ion trap using 60 second exclusion for previously sampled peptide peaks. The LC-MS/MS data were submitted to a local MASCOT server Swiss-Prot

Human database for MS/MS protein identification search *via* ProteomeDiscoverer software. Two trypsin missed cleavages were allowed, the precursor mass tolerance was 1.08 Da. The MS/MS mass tolerance was 0.8 Da. The incorrect detection rate in each LC-MS/MS analysis was set to be less than 1%.

Cell culture

Chinese hamster ovary (CHO) cell line with stable expression of human wild-type APP (CHO/APPwt) was a generous gift from Drs. Stefanie Hahn and Sascha Weggen (University of Heinrich Heine, Düsseldorf, Germany). These cells were initially genotyped to confirm their genetic make-up. The cells were cultured in Dulbecco's modified Eagle's medium (DMEM) with 10% fetal bovine serum (FBS), 1 mM sodium pyruvate and 100 U/mL of penicillin/streptomycin. For treatment, the cells were plated in 24-well plate at 2×10^5 cells /well for overnight incubation, washed and treated with CBS, heat inactivated (56 ^{0}C, 30 min) CBS, AgBS, or αCBSF, AgBSF in DMEM. After treatment, supernatants were collected and the cells were washed with ice cold PBS 3X and lysed with cell lysis buffer (20 mM Tris, pH 7.5, 150 mM NaCl, 1mM EDTA, 1 mM EGTA, 1% v/v Triton X-100, 2.5 mM sodium pyrophosphate, 1 mM β-glycerolphosphate, 1 mM Na$_3$VO4, 1 µg/mL leupeptin, and 1 mM PMSF; Cell Signaling Technology). Both cell supernatants and lysates were used for sAPPα analysis by ELISA. In addition, murine N2a cells transfected with APPwt (N2a/APPwt) and primary neuronal cells were obtained from cerebral cortices of TgAPPwt mouse embryos, between 15 and 17 days *in utero*, as described previously [85]. For TgAPPwt mouse-derived cortical neurons, cerebral cortices were isolated from TgAPPwt mice between 15 and 17 days *in utero* and mechanically dissociated in trypsin (0.25%) individually after incubation for 15 min at 37 ^{0}C. Cells were collected after centrifugation at 1200 g, suspended in DMEM supplemented with 10% fetal calf serum, 10% horse serum, uridine (33.6

70

mg/ml, Sigma-Aldrich), and fluorodeoxyuridine (13.6 mg/ml, Sigma-Aldrich) and seeded in 24-well collagen-coated culture plates at 2.5 x 10^5 cells per well. After reaching confluence (~70–80%). these cells were treated with purified human complement C1 at 0, 5, 10, or 20 µg/mL for 4h, supernatants were collected for sAPPα measurement by ELISA and cells were washed with ice cold PBS 3X and lysed with cell lysis buffer followed by western blotting using 6E10 and pAb751/770 antibodies.

Transgenic APPwt mice

Transgenic wild-type B6.Cg-Tg (PDGFB-APP) 5Lms/J strain (TgAPPwt) male and female mice were purchased from the Jackson Laboratory (Bar Harbor, ME, USA). All mice were housed in the Animal Facility in College of Medicine at the University of South Florida and maintained on a 12-h light/12-h dark cycle at ambient temperature and humidity with ad libitum access to food and water. All animal experiments involving mice were performed in compliance with the US Department of Health and Human Services Guide for the Care and Use of Laboratory Animals and in accordance with the guidelines of the University of South Florida Institutional Animal Care and Use Committee.

WB analysis and ELISA

WB analyses and quantification were performed as previously described. Briefly, the proteins from the cell-free suspensions, cell lysates, and homogenized tissue were electrophoretically separated using 10% bicine/tris gel (8 M urea) for proteins less than 5 kDa or 10% tris/SDS gels for larger proteins. Electrophoresed proteins were transferred to nitrocellulose membranes (Bio-Rad), washed and blocked for 1 h at room temperature in tris-buffered saline containing 5% (w/v) nonfat dry milk (TBS/NFDM). After blocking, membranes were hybridized

71

overnight with various primary antibodies, washed and incubated for 1 h with the appropriate HRP-conjugated secondary antibody in TBS/NFDM and developed using the luminol reagent (Thermo Fisher Scientific, Waltham, MA, USA). Soluble sAPPα in the media was quantified with the IBL human sAPPα colorimetric sandwich ELISA kit according to the manufacturer's instructions.

Statistical analysis

Comparison between two groups was performed by Student's *t*-test analysis. For more than two groups, one-way analysis of variance (ANOVA) followed by LSD *post hoc* analysis was used to compare each other for statistical significance. Alpha was set at 0.05 for all analyses. All molecular analyses were repeated three times in parallel. Data are expressed as mean ± SEM. The statistical package for the social sciences release IBM SPSS 23.0 (IBM, Armonk, NY, USA) was used for all data analyses.

Results

Heat-sensitive APP α-secretase activity in CBS

In order to identify the source of α-secretase in CBS, we initially confirmed that CBS possesses heat-labile α-secretase activity. CHO/APPwt cells were treated with CBS (2%) for 0, 5, 10, 15, 30, 60, and 120 min, followed by determination of sAPPα in conditioned medium by ELISA. CBS caused a time-dependent increase in sAPPα release from CHO/APPwt cells that was significantly greater than the control treatment (Figure 3-2a; $*p < 0.05$, $**p < 0.01$, $***p < 0.001$). Similarly, CHO/APPwt cells were treated for 2 h with 0, 0.25, 0.5, 1, 2, and 5% CBS, followed by determination of sAPPα in conditioned medium by ELISA. CBS caused dose-dependent release

of sAPPα in culture medium from CHO/APPwt cells that was significantly greater than the control treatment (Figure 3-2b; *$p < 0.05$, **$p < 0.01$, ***$p < 0.001$). Next, we wanted to determine if heat inactivation of serum reduces sAPPα producing capacity of CBS. CHO/APPwt cells were treated with 2% whole or heat-inactivated CBS or AgBS (56 ^{0}C for 30 min) for 2 h followed by determination of sAPPα in conditioned media by ELISA. Both CBS and AgBS heat-inactivation significantly limited sAPPα releasing capacity (Figure 3-2c; *$p < 0.05$, **$p < 0.01$, ***$p < 0.001$). Furthermore, CHO/APPwt cells were treated with 2% whole or heat-inactivated αCBSF or AgBSF for 2 h followed by determination of sAPPα in conditioned media by ELISA; Figure 3-2d; *$p < 0.05$, **$p < 0.01$, ***$p < 0.001$). As shown most recently, purification significantly enhanced the sAPPα producing capacity of CBS and AgBS, which again was significantly limited by heat inactivation. These results confirm that CBS possesses an enhanced level of heat-sensitive α-secretase activity.

Proteomic analyses of CBSF and AgBSF

Having shown that CBSF possesses an enhanced α-secretase activity, we next set out to determine the molecular source of α-secretase in CBSF and AgBSF by LC-MS/MS analysis. From 142 major proteins identified, we selected those most likely to exhibit α-secretase activity. Several of the major proteins identified in αCBSF and AgBSF are shown in Figure 3-3. Of these proteins, the subunits of complement protein C1 complex (C1q, C1r and C1s) and alpha-2-macroglobulin showed significantly greater levels in αCBSF compared with AgBSF (Figure 3-3; *$p < 0.05$, **$p < 0.01$). Notably, the levels of complement proteins C3, C4, C5, C6 and C8 complexes, ApoE, ApoB100 and full-length APP (fAPP) were not significantly different between αCBSF and AgBSF ($p > 0.05$). Complement proteins C1 and C3b complex have proteolytic

activity, which can be inactivated at 56 ºC for 30 min. These proteins play important roles in neurodevelopment and provide early protection against stress or disease, including AD. Thus, we hypothesized that the heat-labile α-secretase activity in CBS is mediated in part by complement protein C1 complex or C3b.

CBS-mediated α-secretase-like cleavage of APP is independent of complement C3b

In order to determine if α-secretase activity of CBS is mediated by activation of complement protein fragment C3b, we investigated whether depletion of complement protein C3 could limit the α-secretase-like activity of CBS. CHO/APPwt cells were treated with C3 depleted CBS (2%) for 0, 15, 30, 60, and 120 min followed by determination of sAPPα in conditioned medium by ELISA. Depletion of C3 complement protein did not change sAPPα producing capacity of CBS in CHO/APPwt cells (Figure 3-4d; $*p < 0.05$, $**p < 0.01$, $***p < 0.001$). In order to confirm that C3b complement does not mediate α-secretase activity in CBS, we pre-incubated whole or C3 depleted CBS (2 %) with the C3b inhibitor compstatin at 0, 6, 12, 25, 50, and 100 µM for 15 min at $37\,^{0}$C and then treated CHO/APPwt cells with these premix complexes separately for 2 h. Compstatin did not alter sAPPα production significantly elicited by whole (Figure 3-4a; $p > 0.05$) or C3-depleted serum (Figure 3-4b; $p > 0.05$). Therefore, CBS α-secretase-like activity is independent of enzymatic activity of complement C3b protein.

In order to determine if complement protein component C3b acts an inhibitor of CBS α-secretase-like activity, CHO/APPwt cells were treated for 2 h with premixes of CBS (2%) and iC3b (0, 1.25, 2.5, 5, 10, and 20 µg/mL), the proteolytically inactive product of C3b which prevents complement cascade activation. The sAPPα producing capacity of CBS was not altered by iC3b as determined by sAPPα ELISA (Figure 3-4c; $p > 0.05$), indicating that complement C3b protein does not act as a potent CBS α-secretase inhibitor.

CBS α-secretase-like activity is mediated in part by complement protein C1 complex

To determine if α-secretase-like activity in CBS is mediated by complement protein C1 complex, we determined CBS α-secretase activity in the presence of complement protein C1 inhibitor. CHO/APPwt cells were treated with αCBSF (1 and 2%) in the presence of complement protein C1 inhibitor at 0, 50, 100, and 200 µg/mL for 2 h. C1 inhibitor markedly reduced sAPPα released by αCBSF (1 and 2%) in a dose-dependent fashion, as determined by ELISA (Figure 3-5a; $*p < 0.05$, $**p < 0.01$, $***p < 0.001$) and WB (2% CBS; Figure 3-5b; $*p < 0.05$, $**p < 0.01$, $***p < 0.001$; *quantification not shown*), indicating that α-secretase-like activity in CBS is mediated in part by complement C1 protein. In addition, we determined the effect of purified human C1 complement protein on sAPPα production in N2a/APPwt and TgAPPwt/primary neuronal cells in absence of sera. Complement protein C1 dose-dependently increased sAPPα and α-CTF production in N2a/APPwt cells (Figure 3-5c-e; $**p < 0.01$, $***p < 0.001$) and TgAPPwt/primary neuronal cells (Figure 3-5f-h; $*p < 0.05$, $**p < 0.01$) in absence of serum, as determined by ELISA and WB. These results indicate that complement protein C1 complex mediates α-secretase-like activity in CBS.

In order to confirm that complement C1 but not C3 protein has α-secretase-like activity, CHO/APPwt cells were treated with purified human complement C1 or C3, or C1q subunit, at 0, 2.5, 5, 10, and 20 µg/ml in serum free media for 2 h followed by determination of sAPPα in conditioned medium by ELISA. As expected, complement protein C1 significantly increased sAPPα production in a dose-dependent fashion, whereas C1q alone minimally increased and complement protein C3 did not increase sAPPα production in serum free medium (Figure 3-6a, $*p < 0.05$, $**p < 0.01$). In contrast, both complement C1 and C1q protein component significantly increased sAPPα production in CHO/APPwt cells cultured in C1q depleted sera (Figure 3-6b, $**p$

< 0.01, ***p < 0.001), and complement protein C1 significantly increased sAPPα and α-CTF level, while decreasing Aβ and β-CTF level in CHO/APPwt cells in presence of whole sera as determined by WB (Figure 3-6c).

In order to investigate the role of complement protein C1 in mediating α-secretase activity in whole blood plasma, CHO/APPwt cells were treated with plasma from C1qa deficient mice or age-matched wild-type littermates. Interestingly, the production of sAPPα elicited by plasma from male C1qa deficient mice was not significantly different (Figure 3-6d, p > 0.05) whereas that elicited by plasma from female C1qa deficient mice was significantly greater than that elicited by age- and gender-matched plasma from wild-type littermates (Figure 3-6d, **p < 0.01). Therefore, plasma α-secretase activity is not significantly altered by C1qa deficient in male mice but significantly enhanced by C1qa deficient in female mice. These results are consistent with C1-mediated α-secretase playing an important role in male and female individuals but that other α-secretases compensate in its absence. In addition, the elevated sAPPα production capacity in female compared to male C1qa deficient mice indicate a unknown function of this neurotrophic fragment in the peripheral system of females.

Altogether, these results confirm that APP α-secretase-like activity in human blood serum is mediated by complement protein C1 complex. The inability of C1q to rescue α-secretase activity in serum free media is likely due to the absence of components C1s and C1r, which are required to complex with C1q in C1 for proteolytic activity.

Discussion

In our previous study, we have shown that peripheral administration of HUCBC [37] as well as HUCBC-derived monocytes [38] reduce cognitive impairments and β-amyloid plaques in

PSAPP AD mice. In a subsequent study, we showed that human CBS also has α-secretase-like activity which likewise reduces cognitive impairment, tau hyperphosphorylation and plaque deposition in AD mice [168] [183]. The present study further investigated the component of CBS that attenuates β-amyloid plaques, especially through the increased production of the neurotrophic sAPPα. Our results confirm the presence of α-secretase-like enzyme activity within the CBS, reflected by elevated production of sAPPα. Interestingly, heat-inactivation of α-secretase activity of CBS at 56 ^{0}C for 30 min inspired us to assume that α-secretase-like activity is mediated by a complement protein. This is further reinforced by the result of LC-MS/MS data, which indicate the dominance of complement protein C1 subcomponents (C1q, C1r, and C1s), C3b, and C4 proteins in αCBSF as well as AgBSF (Figure 3-3). Further investigations using complement inhibitors and C1 complement protein depleted serum reveal that endogenous C1 complex enhances sAPPα production in cell culture and primary neuronal cell line, including CHO/APPwt (Figure 3-5b), N2a/APPwt (Figure 3-5c-e), and TgAPPwt/primary neuronal cells (Figure 3-5f-h). As previously mentioned, complement protein C1 is composed of a C1q, and two each of C1r and C1s. C1q is composed of 6 of each A, B and C chains comprising 18 polypeptide chains [174]. Modifying various factors revealed that C1q depleted serum elicited less sAPPα production in comparison with the whole serum, highlighting the crucial nature of C1q-mediated α-secretase activity in CBS (Figure 3-6a-c). Interestingly, our results indicate that the inability of C1q to rescue α-secretase-like activity in serum free media is likely due to the absence of C1s and C1r subcomponents, which are required to form complex with C1q in C1 for proteolytic activity (Fig 3-6a). It should be noted that C1r and C1s, are serine proteases, which form the complete initiation complex of C1qC1r2C1s2 when activated by C1q binding to an immune complex [184].

Initially, C1q synthesis serves to be protective by aiding in clearance of apoptotic cells and regulating the environment to prevent further neurotoxicity from spreading [180]. It has been proposed that C1q and C3 opsonisation [185][186] accelerate clearance of Aβ. In addition, C1q-mediated protection against Aβ is associated with expression of low-density lipoprotein receptor-related protein 1B and G-protein-coupled receptor 6 as early as 2 months of age in 3XTg-AD mouse model [181]. Despite the critical role C1q plays in immune regulation and neuroprotection, evidence has also suggested that C1q could potentially be proinflammatory [187]. C1q is synthesized when there is an injury in the CNS [188]. By binding with β-sheet fibrillary plaques, C1q activates the complement cascade that can have detrimental inflammatory consequences *via* production of the chemotactic factor C5a and recruitment and activation of microglial cells to the site of injury. This activation requires association of C1q with C1r and C1s as in the C1 complex. As the disease pathology continues to progress, it causes more of the complement pathways to be activated [189]. High density of negative charges in various regions, can activate the complement system through an electrostatic interaction independent of antibodies [190]. This can be seen with β-amyloid fibrils binding to arginine-rich segments within the β chain of C1q [191]. Consequently, the fragments not only create further inflammation attracting glial cells, but can also activate classical pathway triggering the release of more pro-inflammatory components. In a study done with APPQ-/- mice, those lacking C1q are unable to activate the classical pathway because the fibrillary Aβ interaction with C1q is not possible [192]. In AD pathology, factors leading to neurodegenerative pathways of complement activation include C1q interaction with not only the β-sheet fibrils, but also hyperphosphorylated tau [190]. Though these fibrils would normally be cleared by microglia, binding of C1q to $Aβ_{1-42}$ peptide strands make it increasingly difficult for microglia to clear out neurotoxic debris [193]. The general trend toward increased complement

activation causes the activated microglia to further exacerbate inflammation as C1q upregulation positively correlates with the quantity of reactive astrocytes making the blood-brain barrier vulnerable [183].

Collectively, our results indicate that CBS contains proteins that promote α-secretase like enzymatic activity (Figure 3-2). LC-MS/MS analysis in CBSF and AgBSF revealed the presence of 142 proteins of which complement protein C1 subunits and alpha-2-macroglobulin showed significantly greater levels in αCBSF compared with AgBSF (Figure 3-3). Upon further study, complement protein C1 subunits showed enhanced sAPPα production and Aβ reduction in cell culture studies (Figure 3-5 & 3-6). As discussed previously, C1q is known to have proinflammatory and detrimental effect on neuronal tissue, which will limit the therapeutic application of C1q. There may be other components in αCBSF contributing the beneficial effects observed in transgenic AD mice. In addition, C1 has α-secretase activity, which may also compete with amyloidogenic β-secretase pathway and reduce β-cleavage of APP when αCBSF was administered in mice. There is much to be learned about the exact mechanisms of action of C1q, especially how its neurotrophic effects may shift in AD pathology and instead lead to further acceleration of neuro-detrimental inflammation. Nevertheless, our research identified an additional and novel function in CBS by enhancing α-secretase-like activity and that the overall reduction in β-amyloid plaques incites a therapeutic potential for attenuating AD pathology.
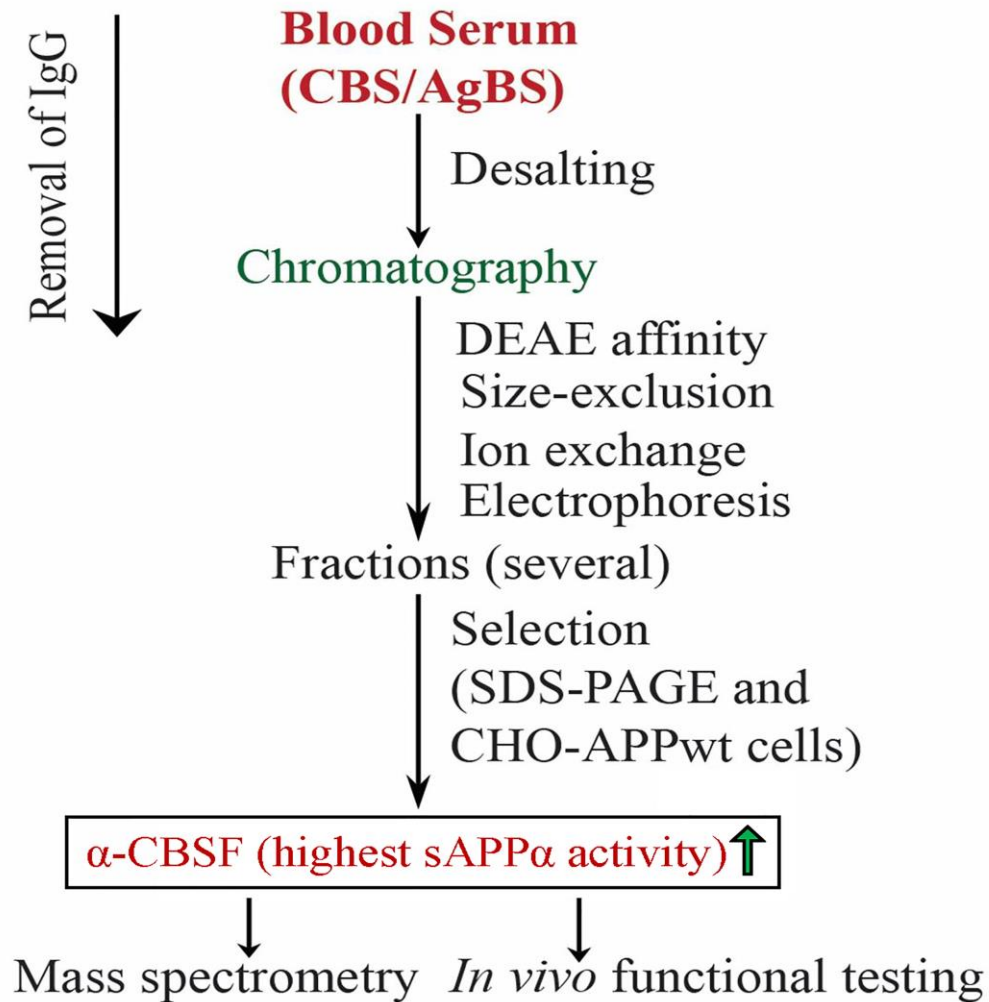
Figure 3-1 Work-flow for αCBSF and AgBSF fractionation.

Initially, CBS and AgBS were desalted followed by sequential chromatographic separation using DEAE column, size-exclusion, and ion-exchange chromatography. Each fraction was collected followed by efficacy testing by treating CHO/APPwt cells for sAPPα release. Eventually a fraction (αCBSF) was chosen based on the highest capacity for sAPPα generation. LC-MS/MS was performed to identify the source of the protein function.
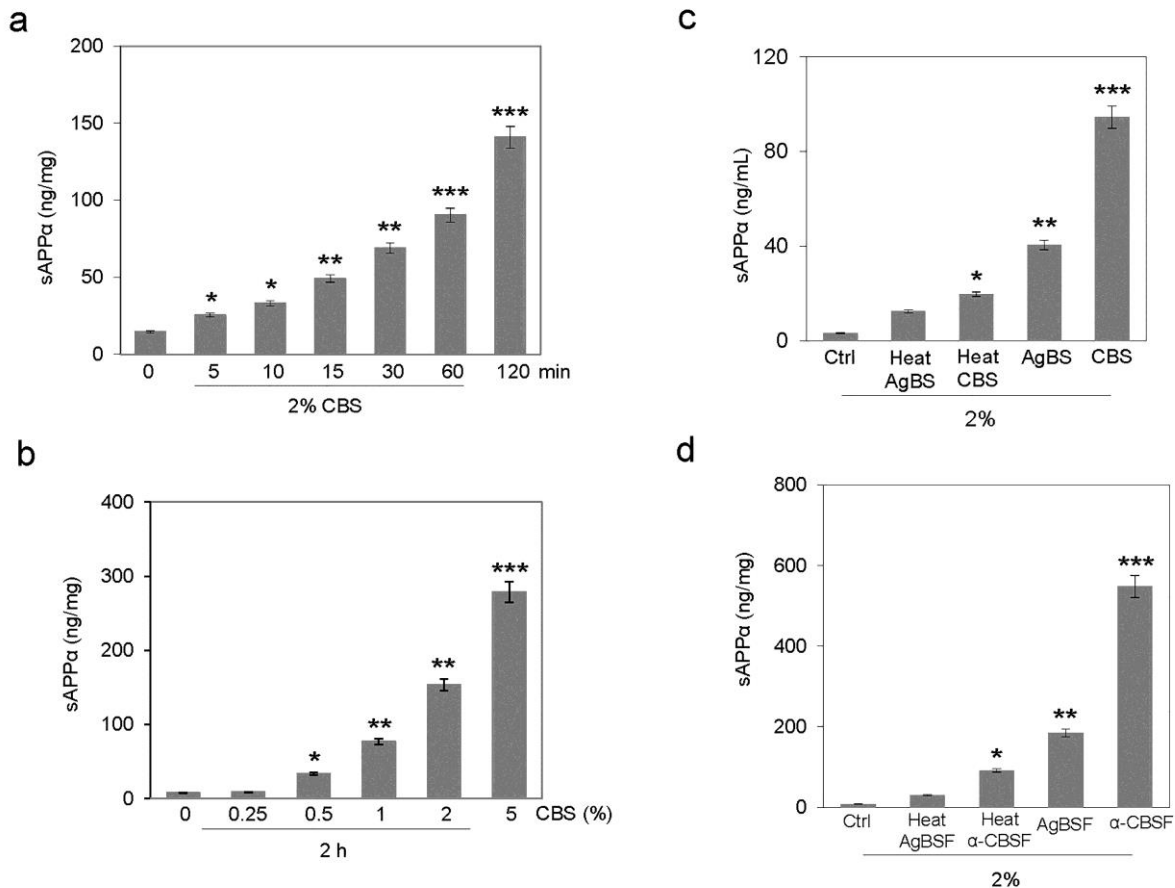
Figure 3-2 CBS significantly enhances APP α-cleavage in CHO/APPwt cells.

(a) Chinese hamster ovary cells overexpressing human wild-type APP (CHO/APPwt cells) were treated for 0 - 120 min with CBS (2%). (b) Chinese hamster ovary cells overexpressing human wild-type APP (CHO/APPwt cells) were treated for 2 h with CBS (0, 0.25, 0.5, 1, 2, and 5) %. (c). Chinese hamster ovary cells overexpressing human wild-type APP (CHO/APPwt cells) were treated for 2 h with CBS (0%, Ctrl), heated-inactivated CBS (2%), heated-inactivated AgBS (2%), AgBS (2%), and CBS (2%). (d) Chinese hamster ovary cells overexpressing human wild-type APP (CHO/APPwt cells) were treated for 2 h with CBS (0%, Ctrl), heated-inactivated CBSF (2%), heated-inactivated AgBSF (2%), fraction isolated from AgBS (AgBSF, 2%), and fraction isolated from CBS (αCBSF, 2%) after purification as briefly described under "Materials and Methods". Then sAPPα release into the conditioned medium was analyzed by ELISA as described under "Materials and Methods". Data are presented as mean (± SEM.) of sAPPα produced (ng/mL or ng/mg) from 3 independent experiments performed in triplicate where the asterisk (*) represent following: *$p < 0.05$, **$p < 0.01$, ***$p < 0.001$), indicating a significant difference from control treatment.
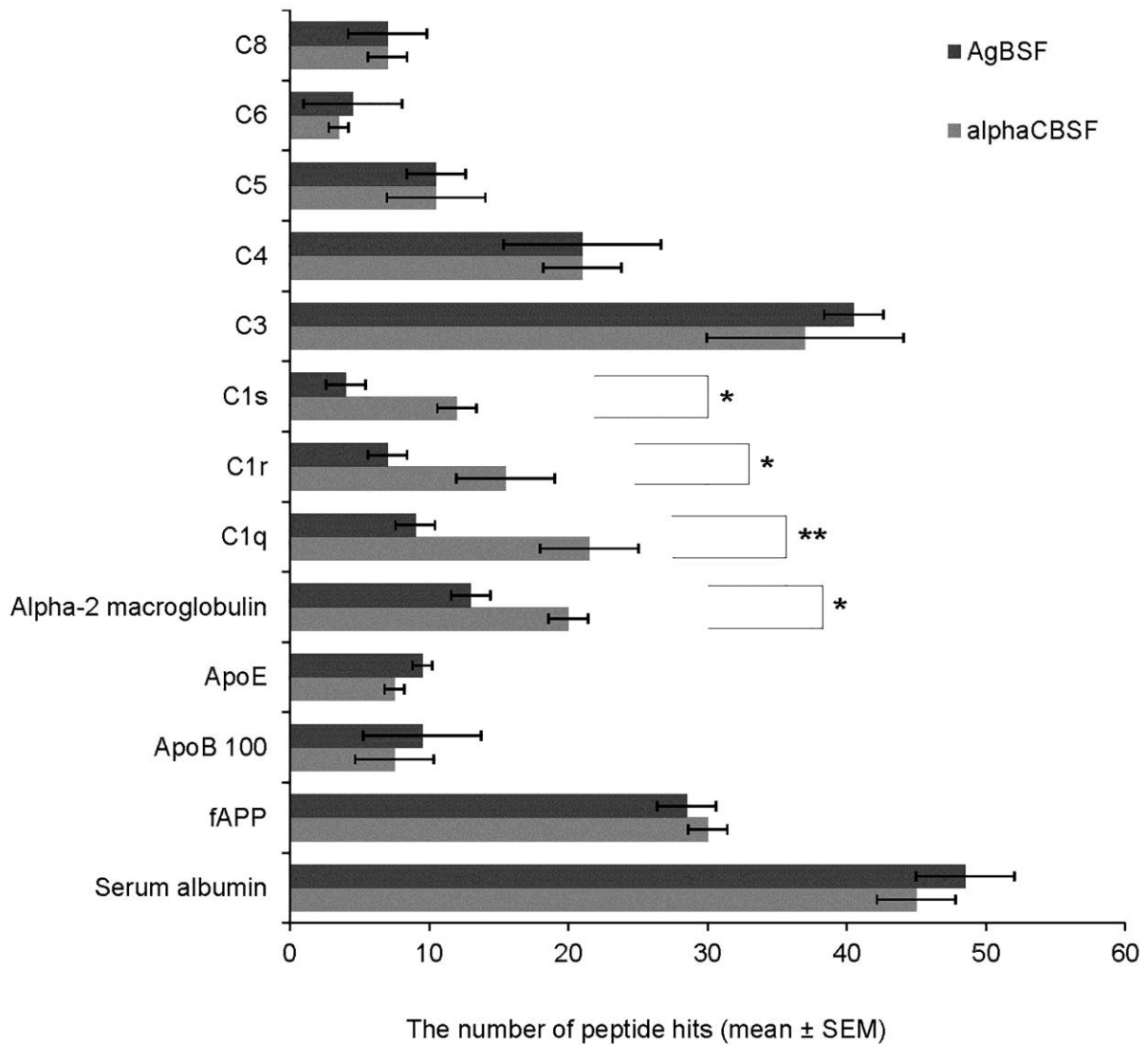
Figure 3-3 Identification of proteomic profile of αCBSF and AgBSF.

The proteome of αCBSF and AgBSF were analyzed by LC-MS/MS. From 142 major proteins identified, those exhibiting proteolytic and therefore potential α-secretase-like activity were selected. Of these proteins, the subunits of complement protein C1q (**$p < 0.001$), C1r (*$p < 0.05$) and C1s (*$p < 0.05$) and alpha-2-macroglobulin (*$p < 0.05$) showed significantly greater levels in αCBSF compared with AgBSF. Data are presented as mean (± SEM.) of number of peptide hits from 3 independent experiments where the asterisk (*) represent following: *$p < 0.05$, **$p < 0.001$, ***$p < 0.01$), indicating a significant difference.
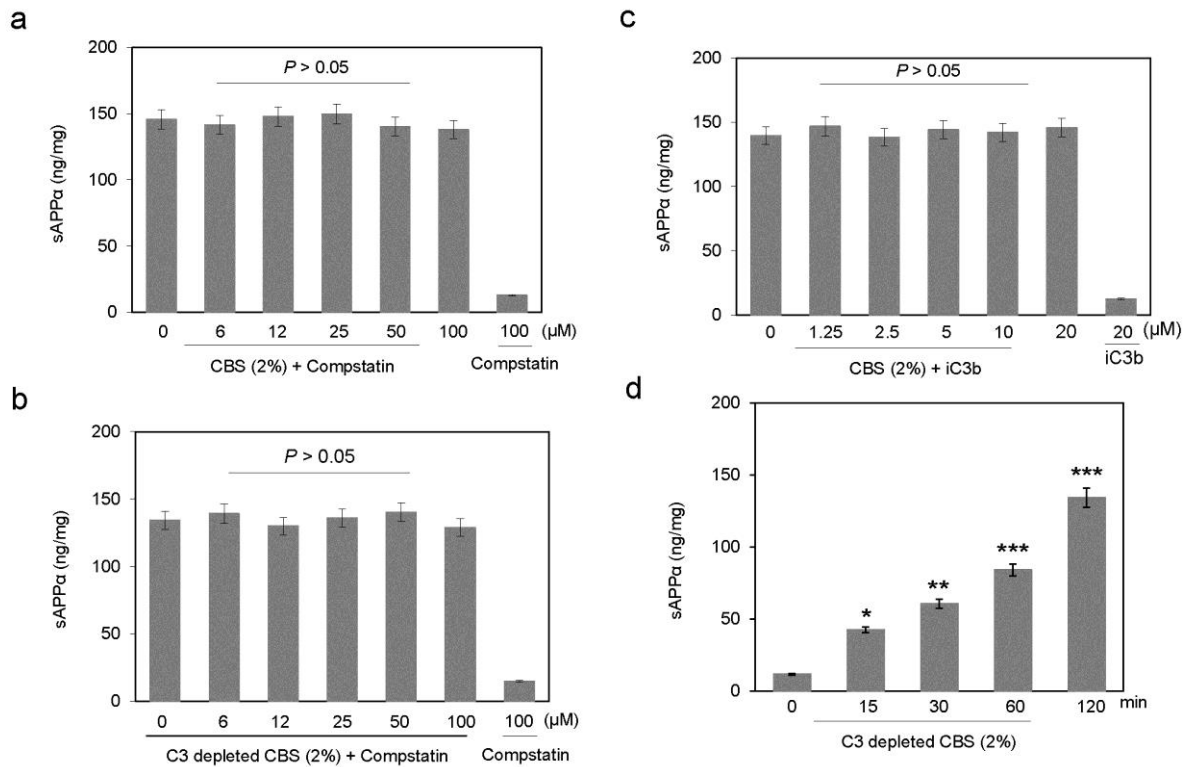
Figure 3-4 CBS mediated sAPPα release by CHO/APPwt cells is independent of complement protein C3b.

C3b inhibitor at indicated concentration (0, 6, 12, 25, 50, and 100 µM) pre-incubated with CBS (2%) as well as C3 depleted CBS (2%) for 15 min. (a). CHO/APPwt cells were treated for 2 h with CBS (2%) + Compstatin (C3b inhibi). (b) CHO/APPwt cells were treated for 2 h with C3 depleted CBS (2%) + Compstatin (C3b inhibi). Then sAPPα release into the conditioned medium was analyzed by ELISA as described under "Materials and Methods". (**c**) In addition, CBS (2%) incubated with iC3b at indicated concentration (0, 1.25, 2.5, 5, 10, and 20 µg/mL) and treated CHO/APPwt cells for 2 h followed by sAPPα determination in the medium by ELISA. (d). CHO/APPwt cells were treated with C3 depleted CBS (2%) for indicated time (0, 15, 30, 60, and 120) min. The sAPPα ELISA results are presented as mean (± SEM.) of sAPPα produced (ng/mL or ng/mg of total intracellular protein) from 3 independent experiments performed in triplicate where the asterisk (*) represent following: $*p < 0.05$, $**p < 0.01$, $***p < 0.001$), indicating a significant difference from control treatment.
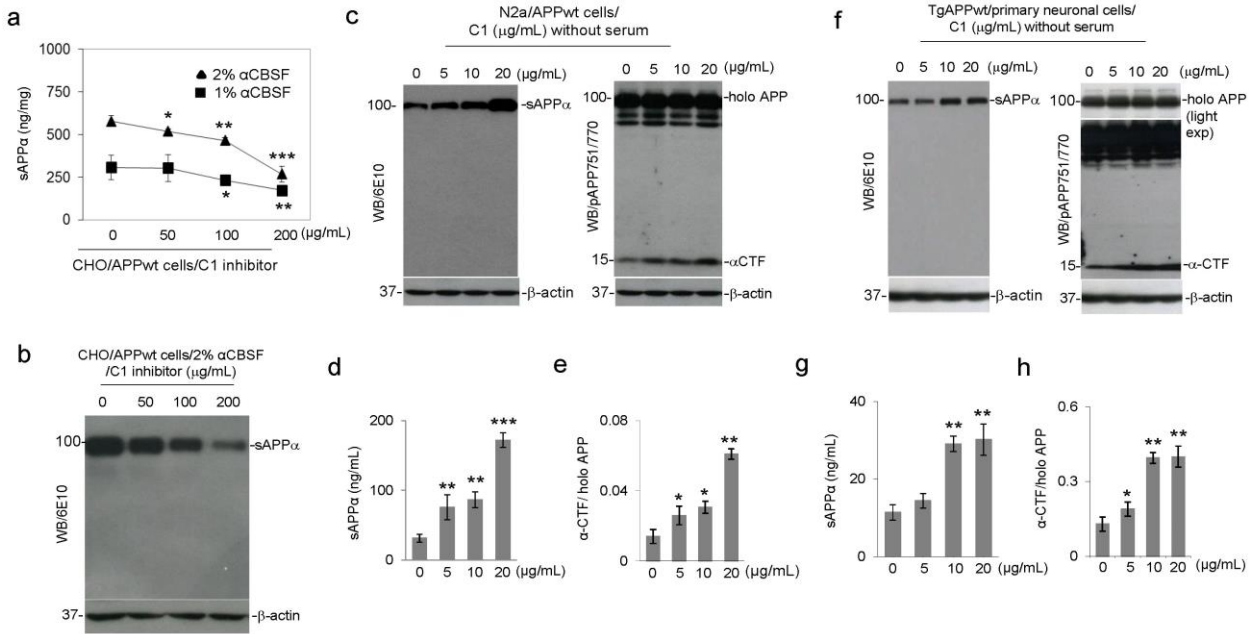
Figure 3-5 A specific complement C1 protein inhibitor significantly reduces APP α-cleavage induced by CBS.

(**a**) CHO/APPwt cells were treated for 2 h with CBS (1 and 2%) in the presence of C1 inhibitor at indicated concentration (0, 50, 100, and 200) µg/mL, followed by analysis of sAPPα in conditioned media by ELISA. (b). In addition, cell lysates from CHO/APPwt cells treated for 2 h with CBS (2%) in the presence of complement protein C1 inhibitor at indicated concentration (0 - 200 µg/mL) were subjected to WB analysis of sAPPα levels. (c) N2a/APPwt cells and (f) TgAPPwt/mouse primary neuronal cells were treated with purified human complement C1 protein complex at indicated dose (0, 5, 10, and 20) µg/mL in serum free condition for 4 h followed by analysis of holo APP, sAPPα and αCTF in cell lysates by WB (c & f). The levels of sAPPα in conditioned media as determined by ELISA (d & g) and band density radios of α-CTF to (full-length) holo APP (e & h) are presented below each blot. The sAPPα ELISA results were presented as mean (± SEM., ng/mL or ng/mg of total intracellular protein, $*p < 0.05$, $**p < 0.01$, $***p < 0.005$).

84
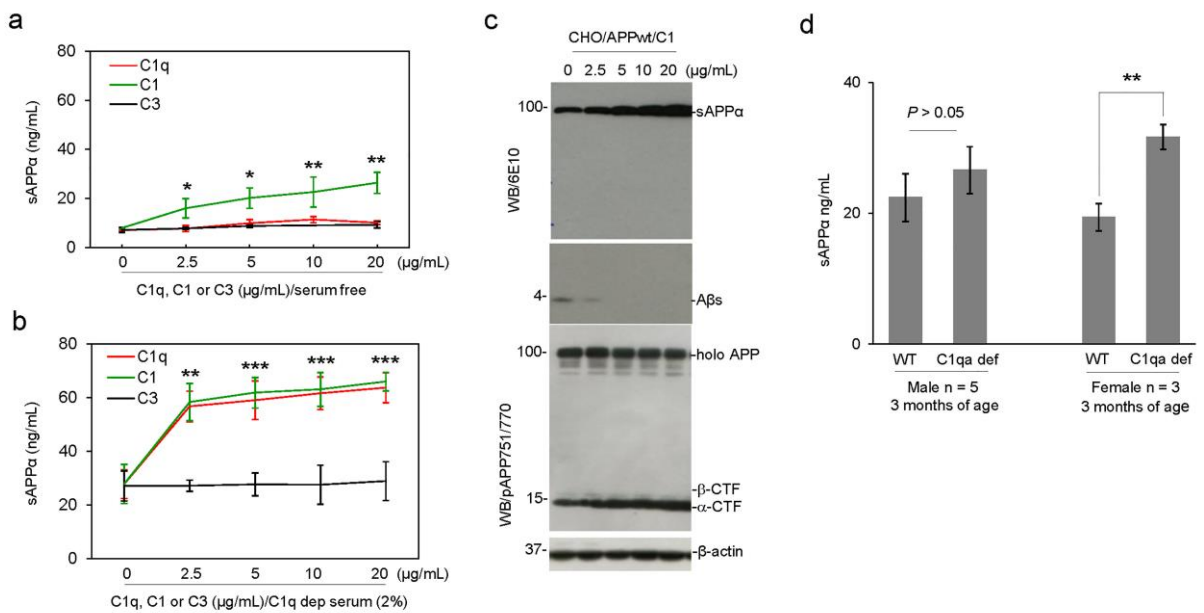
Figure 3-6 The purified human complement C1 protein complex promotes APP α-cleavage.

(a) CHO/APPwt cells were treated for 4 h with purified human complement C1q subcomponent, C1, and C3, at indicated concentration (0, 2.5, 5, 10, and 20) µg/mL in serum free media followed by analysis of sAPPα in conditioned media by ELISA. (b) CHO/APPwt cells were treated for 2 h with purified human complement C1q subcomponent, C1, and C3, at indicated concentration (0, 2.5, 5, 10, and 20) µg/mL in C1q depleted serum followed by analysis of sAPPα in conditioned media by ELISA. (c) In order to further determine the effect of complement C1 protein on APP processing, CHO/APPwt cells were treated for 2 h with purified complement C1 protein at indicated concentration (0, 2.5, 5, 10, and 20) µg/mL in the absence of whole serum and cell lysates were prepared from each treated cell culture for analysis of holo APP, sAPPα, Aβ and α- and β-CTF by WB. The sAPPα ELISA results are presented as mean (± S.E.M) (ng/mL). (d) Evaluation of C1qa deficient mouse sera in APP α-cleavage processing. CHO/APPwt cells were treated for 2 h with plasma (2%) obtained from C1qa knockout mice or wild-type littermates at 3 months of age (n = 5 males or 3 females for each group) followed by determination of sAPPα in conditioned media by ELISA. The sAPPα ELISA results were presented as mean (± SEM., ng/mL or ng/mg of total intracellular protein, *$p < 0.05$, **$p < 0.01$, ***$p < 0.005$).

CHAPTER 4

Ionic co-crystal of lithium salicylate proline (LISPRO) mitigates β-amyloid and associated pathologies in Alzheimer's mice

Permission statement

Habib A, Sawmiller D, Li S, Xiang Y, Rongo D, Tian J, Hou H, Zeng J, Smith A, Fan S, Giunta B, Mori T, Currier G, Shytle DR, Tan J. "LISPRO mitigates β-amyloid and associated pathologies in Alzheimer's mice" <u>Cell Death and Disease</u>; 2017 Jun 15; 8(6):e2880. doi: 10.1038/cddis.2017.279.

Chapter synopsis

Lithium has been marketed in the United States of America since the 1970s as a treatment for bipolar disorder. More recently, studies have shown that lithium can improve cognitive decline associated with Alzheimer's disease (AD). However, the current United States Food and Drug

Administration-approved lithium pharmaceutics (carbonate and citrate chemical forms) have a narrow therapeutic window and unstable pharmacokinetics that, without careful monitoring, can cause serious adverse effects. Here, we investigated the safety profile, pharmacokinetics, and therapeutic efficacy of LISPRO (ionic co-crystal of lithium salicylate and l-proline), lithium salicylate, and lithium carbonate (Li_2CO_3). We found that LISPRO (8-week oral treatment) reduces β-amyloid plaques and phosphorylation of tau by reducing neuroinflammation and inactivating glycogen synthase kinase 3β (GSK3β) in transgenic Tg2576 mice. Specifically, cytokine profiles from the brain, plasma, and splenocytes suggested that 8-week oral treatment with LISPRO down-regulates pro-inflammatory cytokines, up-regulates anti-inflammatory cytokines, and suppresses renal COX2 expression in transgenic Tg2576 mice. Pharmacokinetic studies indicated that LISPRO provides significantly higher brain lithium levels and more steady plasma lithium levels in both B6129F2/J (2-week oral treatment) and transgenic Tg2576 (8-week oral treatment) mice compared to Li_2CO_3. Oral administration of LISPRO for 28 weeks significantly reduced β-amyloid plaques and tau-phosphorylation. In addition, LISPRO significantly elevated pre-synaptic (synaptophysin) and post-synaptic protein (postsynaptic density protein 95) expression in brains from transgenic 3XTg-AD mice. Taken together, our data suggest that LISPRO may be a superior form of lithium with improved safety and efficacy as a potential new disease modifying drug for AD.

Background

Alzheimer's disease (AD) affects memory and cognition irreversibly, and is one of the most critical public health concerns for the elderly. Extracellular amyloid plaques (mostly amyloid-β, Aβ) [194] and intracellular neurofibrillary tangles (NFTs; paired helical filament of hyperphosphorylated tau) [195] are neuropathological hallmarks of AD which severely affect the

hippocampus and neocortex [196]. Currently, the United States Food and Drug Administration (FDA) has approved acetylcholinesterase inhibitors (*i.e.*, donepezil, rivastagmine, and galantamine) and/or *N*-methyl D-aspartate antagonists (*i.e.*, memantine) for AD intervention [197]. However, no pharmacological or non-pharmacological intervention is wholly-available that is effective in preventing or slowing the progression of the disease. Therefore, large numbers of AD patients and their care givers urgently await better alternatives.

Lithium has been used to treat mania and depression since the mid-20th century [198] and, despite the advent of newer medications, it is still considered the gold standard for the treatment of bipolar disorder [199][200]. While lithium is currently FDA approved as a mood stabilizer for the treatment of bipolar disorder, it is also commonly prescribed off-label for other neuropsychiatric symptoms including suicidality and impulsive aggression, [199] as well as neurodegenerative diseases such as AD [201]. Nunes and colleagues observed in a 18-month clinical study that AD patients treated daily with micro-doses of lithium performed at a consistent level on the mini-mental status exam (MMSE), indicating arrested cognitive decline compared to the placebo-group [202]. Moreover, Forlenza and colleagues reported in their 1-year clinical trial study that patients with amnestic mild cognitive impairment treated with chronic low-dose lithium progressed less to AD compared to the placebo-group [200]. The treated patients performed higher on the cognition subscale of the AD Assessment Scale and had decreased concentrations of phosphorylated tau in their cerebrospinal fluid (CSF), indicating lithium as a potential therapeutic for AD [200].

Several mechanisms may underlie lithium's potential neuroprotective efficacy for AD. An important mechanism of lithium is that it inhibits certain enzymes in a noncompetitive manner by displacing the required divalent cation, magnesium [88]. Klein and Melton identified glycogen

synthase kinase 3β (GSK3β) as one such molecular target of lithium [89]. In the context of AD, this enzyme phosphorylates tau at most serine and threonine residues in the paired helical filaments. GSK3 activity contributes both to Aβ production and Aβ-mediated neuronal cell death [90]. Aβ is derived from amyloid precursor protein (APP) by sequential proteolysis, catalyzed by the aspartyl protease β-site amyloid precursor protein cleaving enzyme 1 (BACE1), followed by presenilin-dependent γ-secretase proteolysis [56]. Therapeutic doses of lithium block the production of Aβ peptides by interfering with APP cleavage at the γ-secretase step, without inhibition of Notch processing, by targeting GSK3α [91]. Lithium also blocks the accumulation of Aβ in brains of mice overexpressing APP by inhibition of GSK3β, implicating its requirement for maximal processing of APP [92]. Since GSK3β also phosphorylates tau protein, inhibition of GSK3β offers a new approach to reduce the formation of both β-amyloid plaques and NFTs. Interestingly, combined transgenic mice overexpressing GSK3β with transgenic mice expressing tau with a triple FTDP-17 mutation develop prefibrillar tau-aggregates that are averted by lithium [93].

Despite its medicinal advantages, current lithium pharmaceutics (*i.e.*, carbonate and citrate chemical form) approved by FDA are known to cause serious short- and long-term side effects in humans. The drugs have a narrow therapeutic window (0.6-1.5 mM), as the commonly used lithium salts cross the blood-brain-barrier slowly, [203][204] requiring multiple doses throughout the day to reach safe therapeutic plasma levels. Moreover, required therapeutic doses oftentimes lead to excess accumulation of lithium ions in peripheral organs, particularly the kidney and heart. Dehydration, in the setting of lithium therapy, may result in renal and cardiac toxicity, hypothyroidism, hyperparathyroidism, weight gain, and nephrogenic diabetes insipidus [205]. Lithium intoxication ensues with supratherapeutic serum concentrations, producing symptoms

such as loss of consciousness, muscle tremor, epileptic seizures, and pulmonary complications [206]. As such, lithium administration requires frequent monitoring of blood chemistry and lithium plasma levels, which can discourage physicians from prescribing lithium in favor of other therapeutics which do not require monitoring plasma levels to avoid the potential side-effects noted. This is especially true in the elderly who often have an array of comorbidities that necessitate polypharmacy. Hence, there is a demand for a safer and better lithium formulation to treat AD.

We have previously reported the development of a novel ionic cocrystal of lithium with an organic anion, salicylic acid, and l-proline (LISPRO, LP). The unique crystal structure of LISPRO does not negatively affect the bioactivity of lithium at several potential therapeutic targets related to AD treatment, namely induction of brain-derived neurotrophic factor (BDNF) from neurons, inhibition of lipopolysaccharide induced nitric oxide (NO) production from microglia, neural differentiation, and inhibition of GSK3β in neural stem cells. While LISPRO either outperformed or matched the efficacy of equimolar concentrations of lithium salt controls at these targets *in vitro*, the cocrystal distinctly modulated lithium pharmacokinetics *in vivo*. For example, rats administered with a single oral high dose of LISPRO had detectable brain lithium levels at 48 h, while those receiving the equimolar equivalent of conventional carbonate chemical form of lithium did not. In addition, LISPRO produced a steady plasma lithium plateau over a 48-h period whereas carbonate chemical form of lithium produced the typical plasma lithium spike thought to be associated with adverse events [87][149]. Moreover, salicylic acid in the crystal reduces neuroinflammation associated with AD, being the active metabolite of aspirin. These data point to the potential for increased safety and efficacy profile of LISPRO.

In this study, we more thoroughly evaluated the therapeutic efficacy and safety profile of LISPRO on ameliorating AD-like pathology in cell culture systems and transgenic AD mouse models (*i.e.*, Tg2576 and 3XTg-AD mice). We found that LISPRO has a superior pharmacokinetic and safety profile compared to traditional lithium chemical form, promoting us to further investigate the therapeutic efficacy for AD treatment.

Materials and methods

Reagents

For preparation of LISPRO (LP), lithium salicylate (LS) [$\geq$ 98% pure, anhydrous, 1 mM (Sigma-Aldrich, St. Louis, MO, USA)] and L-proline ($\geq$ 99% pure, Sigma-Aldrich, 1 mM) were dissolved in 2.0 ml of hot deionized water. The resulting solution was maintained on a hot plate (75-90 °C) to allow slow evaporation of solvent until colorless crystals had formed, which were collected and dried (evaporation at 1 atmospheric pressure). For preparation of lithium carbonate (LC), [$\geq$ 99% ACS grade, 1 mM (Sigma-Aldrich)] were suspended in 1-2% methylcellulose [12-18 cP, 1-2% in H_2O (20 °C) (Sigma-Aldrich)] solution.

Antibodies

Primary antibodies include anti-A$\beta_{1\text{-}16}$ (6E10, Covance Research Products, Emeryville, CA, USA), anti-A$\beta_{17\text{-}24}$ (4G8, Covance Research Products), anti-p-tau (Thr^{231}, EMD Millipore, Billerica, MA, USA), anti-p-tau (Ser^{202}, AT8, Thermo Fisher Scientific, Waltham, MA, USA), anti-p-tau (Ser^{404}), anti-p-tau (Thr^{181}, AT270, AnaSpec, Fremont, CA, USA), anti-total tau (tau46, Cell Signaling Technology, Danvers, MA, USA), anti-synaptophysin (Cell Signaling Technology), anti-GSK3β (Ser^{9}, Thermo Fisher Scientific), anti-cyclooxygenase 2 (COX2) (Thermo Fisher Scientific), anti-light chain 3B (LC3B) (Thermo Fisher Scientific), anti-β-tubulin III (Thermo Fisher Scientific), anti-p-synapsin I (Thermo Fisher Scientific), anti- microtubule

associated protein 2 (MAP2) (Thermo Fisher Scientific), anti- glial fibrillary acidic protein (GFAP) (Thermo Fisher Scientific), anti- neuronal nuclei (NeuN) (Thermo Fisher Scientific), anti- post synaptic density protein 95 (PSD95) (Thermo Fisher Scientific), and anti-glyceraldehyde-3-phosphate dehydrogenase (GAPDH) (Thermo Fisher Scientific) antibodies.   Paired helical filament 1 (PHF1) antibody was kindly provided by Dr. Peter Davies (Albert Einstein University).

Cell culture

HeLa cells stably transfected with wild-type 4R0N human tau [HeLa/tau cells; kindly provided by Dr. Chad Dickey, University of South Florida (USF) (Tampa, FL, USA)], human neuroblastoma SH-SY5Y cells (ATCC, Manassas, VA), murine neuroblastoma cells (N2a cells), murine neuronal stem cells (ATCC), human neural stem cells (H9-Derived, ATCC) were cultured in Dulbecco's modified Eagle's medium (DMEM) with 10% fetal bovine serum, 1 mM sodium pyruvate, and 100 U/ml of penicillin/streptomycin. Kidney cells were cultured in *InVitro*GRO medium (BioreclamationIVT, ATCC). Splenocytes from individual mice were prepared and treated as previously described [207]. Primary neuronal cells were obtained from cerebral cortices of Tg2576 mouse embryos, between 15 and 17 days *in utero*, as described previously [208][209]. These cells were treated with LP or LC at 0, 2.5, 5, 10, 20, or 30 mM for 12 h, supernatants were collected and cells were washed with ice cold PBS 3X and lysed with cell lysis buffer (20 mM Tris, pH 7.5, 150 mM NaCl, 1 mM EDTA, 1 mM EGTA, 1% v/v Triton X-100, 2.5 mM sodium pyrophosphate, 1 mM β-glycerolphosphate, 1 mM Na_3VO4, 1 µg/ml leupeptin, and 1 mM PMSF) (Sigma-Aldrich).

In addition, murine primary culture microglia was isolated from mouse cerebral cortices, as described previously [37][210]. Briefly, cerebral cortices from newborn mice (1-day old) were isolated under sterile conditions and mechanically dissociated at 4 °C. Cells were grown in RPMI

1640 medium supplemented with 5% fetal calf serum, 2 mM glutamine, 100 U/ml penicillin, 0.1 μg/ml streptomycin, and 0.05 μM 2-mercaptoethanol for 14 days, after which only glial cells remained. Astrocytes were separated from microglial cultures using a mild trypsinization protocol as described [211]. Greater than 98% of these glial cells stained positive for anti-Mac-1 antibody (Roche Diagnostics, Indianapolis, IN, USA) by fluorescence activated cell sorting (FACS) analysis [212].

Enzyme-linked immunosorbent assay

Enzyme-linked immunosorbent assay (ELISA) was performed according to the manufacturer's instruction. Total Aβ species, including $Aβ_{40,42}$ in cell conditioned media and brain homogenates were detected by $Aβ_{1-40/42}$ ELISA kits (IBL America, Minneapolis MN, USA) according to the manufacturer's instructions. In addition, cytokines [TNFα, IL-10, and IL-12 (p70) levels in brain homogenates and or in cell conditioned media were measured by ELISA (R &D Systems, Minneapolis, MN) according to the manufacturer's instructions. Aβ levels are represented as pg/mg (mean ± SEM) of total cellular protein.

Microglial inflammatory activity analysis

To determine the effect of LP on microglial pro-inflammatory activity, primary microglial cells were treated with LP (0-20 mM) in the presence of interferon γ (IFNγ) (100 U/ml) and/or CD40 ligand (CD40L, 1 μg/ml) for 8 h, and then pro-inflammatory microglial activation was assessed by fluorescence-activated cell sorting (FACS) and ELISA analyses of CD40, tumor necrosis factor α (TNFα), and interleukin-12 protein 70 (IL-12p70).

Phagocytosis analysis

To determine the effect of LP on microglial Aβ phagocytosis, primary microglia were pretreated with LP at 10 mM or vehicle (1% dimethyl sulfoxide) for 6 h followed by incubation with 1 μM fluorescein isothiocyanate (FITC)-Aβ$_{42}$ for 1 h. Cellular supernatants and lysates were analyzed for extracellular and cell-associated FITC-Aβ$_{42}$ using a fluorometer and data were represented as the relative fold of mean fluorescence change, calculated as the mean fluorescence for each samples at 37 °C divided by mean fluorescence at 4 °C.

Autophagy analysis

In addition, the effect of LP and LC on microglial autophagy was determined by pretreating microglial cells with LP, LC (10 mM), or phosphate-buffered saline (PBS) for 18 h, followed by permeabilization, staining with autophagic marker LC3B antibody and determination of fluorescent intensity of autophagosome and cytosol by a Slidebook digital microscopy (Version 5.0.0.1, Olympus America Inc., NY USA).

Mice

Triple transgenic (3XTg-AD) mice harboring APP$_{SWE,}$ PSEN1 (PS1/M146V) and tau (P301L) mutations (3XTg-AD, the Jackson Laboratory, Bar Harbor, ME, USA), Tg2576 mice harboring APP$_{SWE}$ (Taconic, Hudson, NY, USA) and wild-type B6129F2/J mice (the Jackson Laboratory) were housed under standardized 12 h-light/12-h dark cycle at ambient temperature and humidity with diet and water available *ad libitum* at the USF vivarium. The mice were allowed to acclimate for a period of one week before any treatment. All experiments were conducted in accordance with USF Institutional Animal Care and Use Committee approved protocols and guidelines of the National Institutes of Health.

Lithium treatment

Adult male B6129F2/J mice (2-month old) were treated for 2 weeks (acute) with one of six diets, consisting of normal mice chow diet (Teklad 2018) containing low or high doses of LP (0.18 or 0.35%; equivalent to 292 or 583 mg/kg/day), LS (0.10 or 0.20%; equivalent to 162 or 325 mg/kg/day), or LC (0.025 or 0.05%; equivalent to 42 or 83 mg/kg/day), yielding 1.125 or 2.25 mM Li/kg/day, respectively, for all forms of lithium. In addition, both male and female Tg2576 (8-month old) and 3XTg-AD mice (5-month old) were fed for 8 and 28 weeks (chronic) with one of four diets respectively, consisting of normal mice chow alone or normal chow supplemented with LC (0.05%), LS (0.20%), or LP (0.35%). These doses were chosen based on the literature and a pilot study conducted at our laboratory using low- and high-doses of lithium salts.

Plasma and brain lithium measurement

After LP, LS, or LC treatment, mice were anesthetized with isoflurane, blood was collected by cardiac puncture, the heart and vasculature were carefully perfused with ice-cold PBS containing heparin (10 U/ml) and brain tissue was removed for lithium determination using atomic absorption spectroscopy (AAS). Blood was centrifuged at 1,600 x g at room temperature for 10 min and 100 µl plasma was diluted 10 fold in 10% isopropyl alcohol containing 5% trichloroacetic acid (IPA), vortexed, and incubated for 10 min to precipitate proteins. Supernatants were clarified at 3,000 x g for 30 min prior to measuring lithium content (AA-6200, Shimadzu, Kyoto, Japan at the Interdisciplinary Research Facility at USF). Each brain was divided coronally, the front half was rinsed with PBS, weighed, suspended in an equal volume of concentrated HNO_3, heated for 1 h at 100 °C, cooled to room temperature, centrifuged at 3,000 x g for 1 h, and the supernatant was diluted 10 fold in 10% isopropyl alcohol prior to measuring lithium content using AAS (Shimadzu

AA-6200). Peak absorbance were determined referring to values obtained for standards 1% HNO_3

lithium solution (HIGH-PURITY STANDARDS, Charleston, SC, USA)

Western blot analysis

The posterior half of each brain was equally divided sagittally and one portion (one-fourth

of brain) was immediately frozen at liquid nitrogen, and stored at -80 °C for Western blot (WB)

analyses. Brains were homogenized (Minilys homogenizer, Bertin Technologies) in RIPA lysis

buffer (Cell Signaling Technology) containing protease and phosphatase inhibitor cocktail

(Thermo Fisher Scientific) and centrifuged at 14,000 rpm for 1 h at 4 °C. For WB analyses,

supernatants from cell lysates or homogenized tissue were electrophoretically separated using 10%

bicine/tris gel (8 M urea) for proteins less than 5 kD or 10% tris/SDS gels for larger proteins.

Electrophoresed proteins were transferred to nitrocellulose membranes (Bio-Rad, Richmond, CA,

USA), washed and blocked for 1 h at room temperature in tris-buffered saline containing 5% (w/v)

nonfat dry milk (TBS/NFDM). After blocking, membranes were hybridized overnight with

various primary antibodies, washed and incubated for 1 h with the appropriate HRP-conjugated

secondary antibody in TBS/NFDM. Blots were developed using the luminol reagent (Thermo

Fisher Scientific) and densitometry analysis was performed using an ImageJ software (Java

1.6.0_20, NIH, USA) as used previously.

Immunohistochemical analysis

The other posterior portion (one-fourth) of each brain was fixed in fresh 4%

paraformaldehyde solution for cryostat sectioning and free-floating 25-μm coronal sections were

collected and stored in PBS with 100 mM sodium azide at 4 °C. Immunohistochemical (IHC)

staining was conducted according to the manufacturer's instruction using a Vectastain ABC *Elite*

kit (Vector Laboratories, Burlingame, CA, USA) coupled with the diaminobenzidine substrate. Biotinylated anti-phospho-tau antibodies against different phospho-tau residues were used as primary antibodies. Images were acquired as digitized tagged-image format files to retain maximum resolution using a BX60 bright field microscope with an attached CCD camera system (Olympus DP-70, Tokyo, Japan). Digital images were routed into a Windows PC for quantitative analyses using an ImageJ software after obtaining a threshold optical density that discriminated staining from background. Each anatomic region of interest was manually edited to eliminate artifacts and selection bias was controlled for by analyzing each region of interest in its entirety.

Immunocytochemical analysis

After 30 min fixation with fresh 4% paraformaldehyde solution, immunocytochemical (ICC) staining was conducted by indirect method and visualized by appropriate immunofluorescence dye (*i.e.*, FITC)-labeled secondary antibodies. Images were acquired as digitized tagged-image format files to retain maximum resolution using a confocal microscope with an attached CCD camera system (Olympus DP-70).

Statistical analysis

All data were normally distributed; therefore, in instances of single mean comparisons, Levene's test for equality of variances followed by the *t-test* for independent samples were used to assess significance. In instances of multiple mean comparisons, one-way analysis of variance (ANOVA) with *post hoc* Fisher's LSD test was used. Alpha was set at 0.05 for all analyses. The statistical package for the social sciences release IBM SPSS 23.0 (IBM, Armonk, NY) was used for all data analyses.

Results

Lithium pharmacokinetics during chronic LP, LC, and LS treatment

In our previous study, we monitored the pharmacokinetics of lithium following a single dose of LP and LC by oral gavage. Using male Sprague-Dawley rats, the plasma and brain profiles measured by AAS indicated that LP produces a very steady level of lithium at 48 h after treatment, whereas the level of lithium was almost undetectable after 48 h of LC treatment [87]. In the present study, we investigated the plasma and brain pharmacokinetics of lithium upon chronic treatment with LP, LC, or LS to Tg2576 and 3XTg-AD mice, as well as wild-type B6129F2/J mice. Low or high doses of LP, LC, or LS, yielding lithium at 1.125 or 2.25 mM/kg/day respectively, showed steady increases of lithium levels in the plasma and brain between 1 and 2 weeks of treatment in B6129F2/J mice, with the high dose yielding higher lithium levels (Figures 4-1a and b). No statistically significant differences were found between treatments in plasma lithium levels at either dose. By contrast, after 2 weeks of treatment, LP yielded significantly higher brain lithium levels compared to LC and LS.

In Tg2576 mice, LP and LC treatment revealed steady increases of lithium levels in the plasma and brain over an 8-week treatment, with significantly higher plasma lithium levels by LC treatment compared to LP only during the 2-week treatment (Figure 4-1c). However, after 8-week treatment, LP provided significantly higher brain lithium levels compared to LC (Figure 4-1d). In 3XTg-AD mice, no significant difference was observed in both plasma or brain lithium levels after 28 weeks of LP, LC, or LS treatment (Figure 4-1e). Of note, the brain to plasma lithium ratio of LP tended to be higher after 28-week compared to LC and LS treatment (Figure 4-1f), while the difference did not reach significance (LP and LS, $p = 0.98$; LP and LC, $p = 0.84$; LS and LC, $p =$

0.85). Lithium levels showed undetectable levels in both plasma and brain from untreated control mice.

Chronic LP treatment reduces β-amyloid plaques in Tg2576 and 3XTg-AD mice

Lithium treatment has been shown to reduce Aβ generation *in vitro,* [91] while controversial results also exist regarding its ability to reduce Aβ production *in vivo* [213][214]. We determined the effect on β-amyloid plaques by chronic treatment with LC or LP in Tg2576 mice and with LC, LS, or LP in 3XTg-AD mice. In Tg2576 mice, an 8-week treatment with LP significantly reduced Aβ burden (positive area of β-amyloid plaques) compared to LC-treated as well as untreated control Tg2576 mice, as determined by IHC using $Aβ_{17-24}$ specific 4G8 antibody (Figures 4-2a and b). Similarly, LP treatment significantly reduced both soluble and insoluble Aβ levels as determined by ELISA (Figure 4-2c). However, both Aβ burden and Aβ levels did not alter after LC treatment. In 3XTg-AD mice, 28-week LP treatment significantly decreased Aβ burden, as determined by IHC using $Aβ_{17-24}$ specific 4G8 and $Aβ_{1-16}$ specific 6E10 antibodies (Figures 4-2d and e), but Aβ burden was not significantly altered after treatment with LS or LC.

Chronic LP treatment reduces tau phosphorylation through inhibition of GSK3β in Tg2576 and 3XTg-AD mice

In Tg2576 mice, 8-week LP treatment significantly reduced phosphorylation of tau [p-tau (Thr^{231})] compared to untreated controls, as determined by IHC and WB analyses (Figures 4-3a and b). In addition, LP treatment significantly increased GSK3β (Ser^9) inhibitory phosphorylation, as determined by WB (Figure 4-3c). However, tau or GSK3β inhibitory phosphorylation was not altered by treatment with LC. In 3XTg-AD mice, 28-week LP treatment significantly reduced tau phosphorylation [p-tau (Thr^{231})] in CA1 as determined by IHC (Figures 4-3d and f). In addition,

LP treatment tended to reduce tau phosphorylation p-tau (Thr^{231}) in CA3, but this decrease was not statistically significant for p-tau (Thr^{231}) [(Figures 4-3d and g) (LP and LS, $p = 0.771$; LP and LC, $p = 0.31$; LS and LC, $p = 0.233$]. LC or LS treatment did not significantly alter tau phosphorylation in CA1 or CA3 as determined by IHC. In addition, LP treatment significantly reduced tau phosphorylation [p-tau (Ser^{396})], as determined by IHC (Figure 4-3h) and tau phosphorylation [p-tau (Ser^{396}, Ser^{404}, Thr^{181} and Thr^{231})], as determined by WB (Figures 4-3i and j). LC and LS also reduced tau phosphorylation at several sites, notably p-tau (Ser^{396} and Thr^{231}), albeit less than LP.

LP treatment reduces microglial inflammation, while enhancing microglial Aβ phagocytosis and autophagy

In as much as microglial CD40/CD40L signaling can enhance Aβ generation [37] and impair Aβ phagocytosis, [210] we determined the effects of LP on CD40 expression, CD40/CD40L signaling, and Aβ phagocytosis in primary microglial cells. Primary microglial cells were treated with LP (0-20 mM) in the presence of IFNγ (100 U/ml) and/or CD40 ligand (CD40L, 1 µg/ml) for 8 h. LP treatment significantly inhibited IFNγ-induced CD40 expression in a dose-dependent manner (Figure 4-4b), as determined by FACS analysis, as well as IFNγ/CD40L-induced release of pro-inflammatory cytokines (*i.e.*, TNFα and IL-12p70), as determined by ELISA (Figure 4-4c). To assess the effect of LP on microglial Aβ phagocytosis, primary microglial cells were pre-incubated with 10 mM LP or vehicle (1% dimethyl sulfoxide) for 6 h followed by 1-h incubation with fluorescent-tagged Aβ$_{1-42}$ (FITC-Aβ$_{1-42}$). LP significantly increased uptake of Aβ$_{1-42}$ in primary microglial cells, as evidenced by increased cell-associated (intracellular) and decreased extracellular fluorescence (Figure 4-4d). Sarkar et al. (2005) first showed that lithium up-regulates autophagy and clears mutant proteins (huntingtin and α-

synuclein) by inhibiting inositol monophosphatase [215] Subsequently, several cell culture and animal studies demonstrated induction of autophagic pathways by lithium [216] To investigate the effect of LP and LC on autophagy, primary microglial cells were treated with LP or LC (10 mM) for 18 h, followed by permeabilization and staining with autophagic marker LC3B antibody. Both LP and LC treatment significantly enhanced autophagy (Figure 4-4a).

Chronic LP treatment inhibits peripheral and neural inflammation in Tg2576 mice

Given that LP could modify β-amyloid plaque pathology in transgenic AD mice, we wanted to determine whether reduction of Aβ is associated with an anti-inflammatory effect. In Tg2576 mice, 8-week LP treatment significantly increased plasma levels of anti-inflammatory cytokines (*i.e.*, IL-4 and IL-10) compared to untreated controls, as determined by ELISA (Figure 4e). In addition, LP treatment increased IL-10 in splenocytes, while reducing pro-inflammatory cytokines (*i.e.*, TNFα and IL-12p70), as measured by ELISA (Figure 4-4f). LP treatment did not alter plasma IL-2 or IFNγ, as determined by ELISA (Figure 4-4e). LP treatment also increased brain levels of anti-inflammatory cytokines (*i.e.*, TGFβ1 and IL-10) while attenuating the levels of sCD40L (Figure 4-4g and h) as analyzed by ELISA. No cytokine measured was altered by LC treatment. Taken together, these findings indicated that LP dampens pro-inflammatory microglial activation, while promoting Aβ phagocytosis and autophagy.

LP treatment decreases GSK3β activity and tau phosphorylation *in vitro*

Since LP inhibited tau phosphorylation and increased inhibitory GSK3β phosphorylation *in vivo*, we further investigated these activities of LP *in vitro*. HeLa cells overexpressing human wild-type tau (HeLa/tau cells), human neuroblastoma SH-SY5Y cells, and primary neuronal cells were treated with LP at increasing concentrations (0, 2.5, 5, and 10 mM) for 12 h, followed by

analysis of tau and/or GSK3β phosphorylation by WB. LP significantly increased in inhibitory phosphorylation of GSK3β (Ser^9) in HeLa/tau cells (Figure 4-5a). This increase in anti-tau phosphorylation was associated with a decrease at 10 mM, as indicated by PHF1 (recognizes phospho-Ser^{396}) and phospho-tau (Thr^{231}) immunoreactivity in HeLa/tau cells (Figure 4-5b). Similarly, LP (5 and 10 mM) significantly increased inhibitory phosphorylation GSK3β (Ser^9) in human neuroblastoma SH-SY5Y and primary neuronal cells (Figure 4-5c). Taken together, these findings confirm that LP reduces tau phosphorylation through inactivation of GSK3β.

LP treatment enhances neuronal cell differentiation and chronic treatment prevents cortical neuronal and synaptic protein loss

To examine the effect of LP on neuronal cell differentiation, cultured murine neuroblastoma N2a cells were treated with LP and LC at 10 mM for 24 h, followed by analysis of neuronal markers [*i.e.*, β-tubulin III and phospho-synapsin I (Ser$^{62-67}$)] by ICC and WB analyses. LP-treated N2a cells were significantly enhanced differentiation, as evidenced by increased expression of β-tubulin III and phospho-synapsin I (Ser$^{62-67}$) compared to LC (Figures 4-6a-c). In addition, LP treatment significantly enhanced differentiation of cultured murine and human neuronal stem cells (MNSC and HNSC, respectively) compared to LC treatment, as evidenced by enhanced neuronal markers (*i.e.*, MAP2 and phospho-synapsin I). Moreover, LP-treated MNSC cells demonstrated increased expression of Tau46, total tau, and MAP2 compared to LC-treated these cells (Figures 4-6d-g). Taken together, these findings indicate that LP significantly enhanced neuronal stem cell differentiation.

To examine whether LP treatment can prevent neuronal loss, 5-month old 3XTg-AD mice were treated with LP, LC, or LS for 28 weeks, followed by IHC analysis using anti-NeuN antibody. Both LP and LS treatment significantly increased the number of NeuN-labeled positive cells in the

neocortex region compared to untreated control mice (Figure 4-6h). In addition, LP- and LS-treated 3XTg-AD mice showed increased expression of pre- and post-synaptic proteins (*i.e.*, synaptophysin and PSD95) by WB analysis (Figure 4-6i). Collectively, these findings suggest that chronic administration of LP or LS to 3XTg-AD mice significantly prevents neuronal loss and improves expression of pre- and post-synaptic proteins.

Both acute and chronic LP treatment does not increase COX2 expression

Previous *in vitro* and *in vivo* studies have indicated that lithium chloride inhibits constitutive GSK3β activity in the kidney, thereby inducing COX2 expression; producing inflammation and toxicity [217][218][219]. To compare the effect of LP and LC on renal GSK3β activity and COX2 expression, cultured human renal proximal tubule (HRPT) cells were treated with LP or LC at 0, 10, 20, or 30 mM for 12 h. Interestingly, both LP and LC increased inhibitory phosphorylation of GSK3β (Ser^9), while only LC increased COX2 expression (Figures 4-7a and b). Therefore, LC-induced COX2 expression is independent of GSK3β activity.

To compare the effects of LP, LS, and LC treatment on renal COX2 expression *in vivo*, 6-week old B6129F2/J mice were fed for 2 weeks with diets containing LP, LC, or LS at low or high doses (1.125 or 2.25 mM Li/kg/day). As shown by WB and IHC analyses, neither LP, LC, nor LS treatment alter COX2 expression at low dose, although LC-treated B6129F2/J mice showed a tendency to increase. In contrast, only LC significantly increased COX2 expression at the high dose (Figures 4-7c and d). Further, to test whether chronic administration of lithium induces COX2 expression in the context of the pathological condition, transgenic Tg2576 AD mice were treated with LP and LC at 2.25 mM Li/kg/day (high dose) for 8 weeks. As expected, both IHC and WB analyses indicated that only LC treatment shows significant increase of COX2 expression

(Figures 4-7e-g). No statistically significant difference was found between LP-treated Tg2576 AD mice and untreated controls.

Discussion

Despite a narrow therapeutic window (0.6-1.5 mM) and the potential for serious adverse events, lithium has been used as the first line therapy to reduce manic episodes and suicidality in patients with bipolar disorder due to lack of better alternatives [220]. We have previously shown that FDA-approved lithium carbonate produces very sharp peak plasma and brain lithium concentrations after oral dosing, followed by a rapid decline in rats. In contrast, LISPRO showed steady plasma and brain lithium levels out to 48 h without any sharp peak [87]. Based on these findings, we hypothesize that LISPRO may prevent the drastic change of lithium levels in the plasma seen with current lithium drugs, and maintain stable therapeutic doses and, thus, would represent a significant improvement over current lithium medicines for a desired time by slow-release into the peripheral blood. Similar to above findings, our recent data (8-weeks treatment in Tg2576 mice) showed significantly stable plasma lithium levels over the period of time (Figure 4-1c) as well as higher brain lithium levels compared to Li_2CO_3 (Figure 4-1d). More importantly, B6129F2/J mice treated with LISPRO showed significantly higher brain lithium levels at low (1.125 mM/kg/day) and high (2.25 mM/kg/day) concentrations compared to Li_2CO_3 (Figures 4-1a-b). Moreover, our recent study also showed comparable levels of lithium in 3XTg-AD mouse plasma and brain as result of lithium salicylate, Li_2CO_3, or LISPRO (28-week treatment). Furthermore, the brain to plasma lithium ratio in the LP-treated group was slightly higher (LP and LS, $p = 0.98$; LP and LC, $p = 0.84$; LS and LC, $p = 0.85$) versus LS- and LC-treated groups (Figures 4-1e-f). Lithium has been employed in treatment of several neurodegenerative diseases including AD. It has been reported that lithium prevents the generation of Aβ peptides by inhibiting GSK3α

activity, which interferes with APP γ-secretase cleavage [91][221][222]. In terms of LP, we expected that addition of salicylate, which is the primary metabolite derivative of acetyl-salicylic acid (aspirin), could work together synergistically to improve the safety and modify the pharmacological action of lithium for attenuating AD pathology. Study data suggest that aspirin exerts its effects on the inflammatory cascades, irreversibly inhibiting COX1, and modifying enzyme activity of COX2, suppressing production of prostaglandins and thromboxane. Although lithium has anti-inflammatory properties, several studies indicate that chronic lithium might induce COX2 expression through inhibition of GSK3β activity. Our data also showed that both lithium carbonate and LISPRO inactivate GSK3β, but only lithium carbonate activates COX2 whereas LISPRO suppresses COX2 due to the anti-inflammatory properties of salicylate anion. A recent epidemiological study showed that low-dose aspirin with lithium exert synergistic effects by increasing 17-hydroxy-decosahexanoic acid (17-OH-DHA), an anti-inflammatory brain DHA metabolite which significantly reduced the risk of disease deterioration in bipolar patients compared to other non-steroidal anti-inflammatory drugs and glucocorticoids, a COX2 inhibitor [223]. Together, salicylic acid increased brain 17-OH-DHA, [224], and lithium reduced neuroinflammation, [225][99] while zwitterionic l-proline significantly reduced the hygroscopic property of parent salicylate salt by influencing the solid phase formation. Assuming the above hypothesis is true, we wanted to investigate the bioactivities of LISPRO in terms of ameliorating AD pathology in cell culture systems and in transgenic (Tg2576 and 3XTg-AD) mouse models. We showed that 8-week LISPRO-treated Tg2576 AD mice had significantly reduced soluble and insoluble Aβ levels as well as Aβ burden compared to Li_2CO_3- and control-treated Tg2576 AD mice (Figures 4-2a-c). To examine LISPRO's effect on Aβ generation in 5-month old 3XTg-AD mice, we treated them with LISPRO, lithium salicylate, Li_2CO_3, and control-diet for 28 weeks with

equal dosages of lithium (2.25 mM/kg/day). We showed that LISPRO treatment significantly reduced extracellular Aβ plaques, as evidenced by IHC staining using 4G8 and 6E10 antibodies (Figures 4-2d and e). Taken together, these findings demonstrated that LISPRO suppresses generation of both soluble and insoluble Aβ in Tg2576 and 3XTg-AD mouse models.

Moreover, several lines of evidence demonstrated that lithium is a direct inhibitor of GSK3β and also increases the inhibitory serine-phosphorylation of the enzyme [89][226]. Thus, we wanted to examine whether LISPRO could reduce tau phosphorylation in cell culture and AD mouse models. Using human HeLa/tau, human neuroblastoma SHSY-5Y, and primary neuronal cell lines, we found that LISPRO treatment inhibits phosphorylation of tau at 5-10 mM concentrations, which is associated with increasing inhibitory phosphorylation of GSK3β (Ser^9) (Figures 4-5a-c). Taken together, these findings indicated that LISPRO inactivates GSK3β activity, and thereby reduces tau phosphorylation. Since lithium is a suitable inhibitor for inhibiting GSK3β *in vivo*, we also examined whether LISPRO-mediated suppression of GSK3β activity is associated with attenuation of tau phosphorylation in Tg2576 mice. In this model, we showed that an 8-week LISPRO treatment significantly reduces p-tau (Thr^{231}) phosphorylation compared to Li$_2$CO$_3$ and control (Figures 4-3a and b). These findings were also correlated with increased p-GSK3β (Ser^9) inhibitory phosphorylation, indicating inactivation of GSK3β activity (Figure 4-3c). To confirm these data obtained in the Tg2576 AD mouse model, we next investigated whether chronic administration of LISPRO could also reduce tau phosphorylation in 3XTg-AD mice. Thus, we treated 5-month old 3XTg-AD mice with LISPRO, lithium salicylate, Li$_2$CO$_3$, or control-diet for 28 weeks with equal doses of lithium (2.25 mM/kg/day). IHC staining using p-tau (Thr^{231}) and p-tau (Ser^{396}) antibodies as well WB analyses using multiple p-tau [Ser^{396}, Ser^{404}, Thr^{181}, and Thr^{231}] amino acid residues demonstrated that LISPRO, and in many cases

lithium salicylate, significantly attenuates tau phosphorylation compared to Li_2CO_3 and control (Figures 4-3d-j).

Inflammatory processes are thought to play an active role in AD formation and progression. Preclinical as well as postmortem analyses of AD patient brains have provided tons of evidence indicating the dysregulation and/or uncontrolled activation of microglial and astrocytic cells, activation of complement cascade, inflammatory enzymes such as COX2, inducible nitrate oxide synthase, reactive oxygen species, and calcium dysregulation pathways in brain, CSF, and blood [227][228][229]. Although it is inconclusive whether these changes are initiating or secondary consequences, proinflammatory such as IL-1β, IL-6, TNFα, NO and anti-inflammatory cytokines such as IL-4, IL-10, TGFβ elevated in the CSF and blood of AD patients [228][230][231]. Multiple lines of evidence showed that lithium down-modulates the pro-inflammatory cytokine responses in animal models and is of therapeutic benefits in several neurodegenerative diseases [232][233]. Specifically, Nassar and Azab conclude that lithium has anti-inflammatory properties that may contribute to its therapeutic activity by down-regulation of COX2, inhibition of IL-1β, TNFα, and up-regulation of IL-2 and IL-10 [234]. On the other hand, in contrast to above findings, large bodies of evidence indicated that lithium also induces pro-inflammatory cytokines production such as IL-4 and IL-6 in certain disease conditions [235][236]. Based on these reports, we sought to examine if the efficacy of LISPRO for reducing AD-like pathology in transgenic Tg2576 mice is associated with modulation of pro- and anti-inflammatory cytokine responses. We showed that LISPRO treatment significantly increases the expression of anti-inflammatory cytokines such as IL-4, IL-10, and TGF-β1, while it decreases the expression of pro-inflammatory cytokines such as INFγ, IL-12p70, and sCD40L in Tg2576 mouse brains compared to control- and LC-treated Tg2576 mouse brains (Figures 4-4e-h). Taken together, these findings suggest that LISPRO might

reduce Aβ pathology at least in part *via* up-regulated anti-inflammatory and down-regulated pro-inflammatory cytokine responses in Tg2576 mice.

We demonstrated that CD40-CD40L interaction is critical for brain pro-inflammatory responses in aggravating AD-like pathology [237]. As LISPRO treatment reduced Aβ production in cell culture and transgenic (Tg2576 and 3XTg-AD) mouse models, we next hypothesized that reduction of Aβ pathology might correlate with decreased microglial CD40 expression and/or increased phagocytosis by microglia. In this regard, we found that decreased expression of microglial CD40 and brain soluble CD40L expression by LISPRO treatment might help attenuate Aβ associated pathology, suggesting that disruption of CD40-CD40L signaling could also be involved in attenuation of Aβ pathology in Tg2576 and 3XTg-AD mouse models. As expected, LISPRO suppresses IFNγ-induced CD40 expression (Figures 4b and c) and enhances microglial phagocytosis of Aβ (Figure 4-4d) in cultured primary microglial cells. Moreover, multiple lines of evidence demonstrated that lithium enhances autophagy at low doses (10 mM) [215][216]. In this regard, we found that LISPRO treatment enhances autophagy markers LC3B in cultured primary microglial cells (Figure 4-4a). Collectively, our data suggest that LISPRO-mediated attenuation of Aβ pathology is associated with several therapeutic endpoints including up-regulated anti-inflammatory and down-regulated pro-inflammatory cytokines, suppression of CD40 that disrupts CD40-CD40L signaling, increased microglial phagocytosis of Aβ, and up-regulated autophagy.

Furthermore, to investigate whether LISPRO treatment could modulate neuronal cell differentiation, cultured mouse neuroblastoma N2a, as well as murine and human stem cells was treated with LISPRO, Li_2CO_3, and control. Our data from IHC staining and supportive WB analyses using β-tubulin III, phospho-synapsin I (Ser[62-67]), MAP2, and total tau antibodies

demonstrated that LISPRO treatment significantly promotes neuronal cell differentiation compared to Li_2CO_3 (Figures 4-6a-g). Cheng and Chuang reported that lithium increases the expression of p^{53} and Bcl-2 providing neuronal survival [238]. In addition, it has been shown that administration of lithium as well as mood-stabilizing agent valproate, increases Bcl-2 levels in the cortical region [239]. Based on these findings, we also wanted to examine whether LISPRO could prevent cortical neuronal loss in 5-month-old 3XTg-AD mice were treated with LISPRO, lithium salicylate, Li_2CO_3, or control diet for 28 weeks. Quantitative analysis of neuronal cell numbers using the neuronal marker anti-NeuN antibody, displayed that LISPRO and lithium salicylate treatments respectively yield an increased survival neurons in the neocortex region of 3XTg-AD mice (Fig. 4-6h). We further examined whether LISPRO treatment could modulate the expression of synaptic proteins in 3XTg-AD mice brain, and found that LISPRO and lithium-salicylate significantly increase the protein expression of synaptophysin (Pre-synaptic) and PSD95 (Post-synaptic) in these transgenic mice (Figure 4-6i).

Finally, one of the major side effects of lithium includes renal toxicity secondary to increased expression of COX2 and ensuing inflammation. It has been shown that acute and chronic administration of lithium could enhance COX2 expression by suppressing GSK3β activity in renal cell lines and mouse models [217][218]. We observed the effect of LISPRO on COX2 expression in renal cells from the Tg2576 AD as well as wild-type B6129F2/J mouse models. We treated human renal proximal tubule cells (HRPT) with LISPRO and Li_2CO_3. IHC staining and supportive WB data indicated that LISPRO treatment does not enhance COX2 expression in HRPT renal cells (Figures 4-7a and b). To further test the effect of LISPRO treatment on COX2 expression *in vivo*, we orally fed B6129F2/J and Tg2576 mouse lines with LISPRO, lithium salicylate, and Li_2CO_3 for 2, and 8 weeks, respectively with low (1.125 mM/kg/day) and high doses (2.25 mM/kg/day).

Our IHC and supportive WB findings indicated that LISPRO treatment does not increase COX2 expression (Figures 4-7c-g).

In sum, our data supports our hypothesis that LISPRO is a better alternative formulation of lithium in terms of safety and efficacy in ameliorating AD pathology in cell culture and two different transgenic mouse models. Nevertheless, further translational research is warranted to fully validate LISPRO as a safe and effective disease modifying therapy for AD and other neurodegenerative diseases.
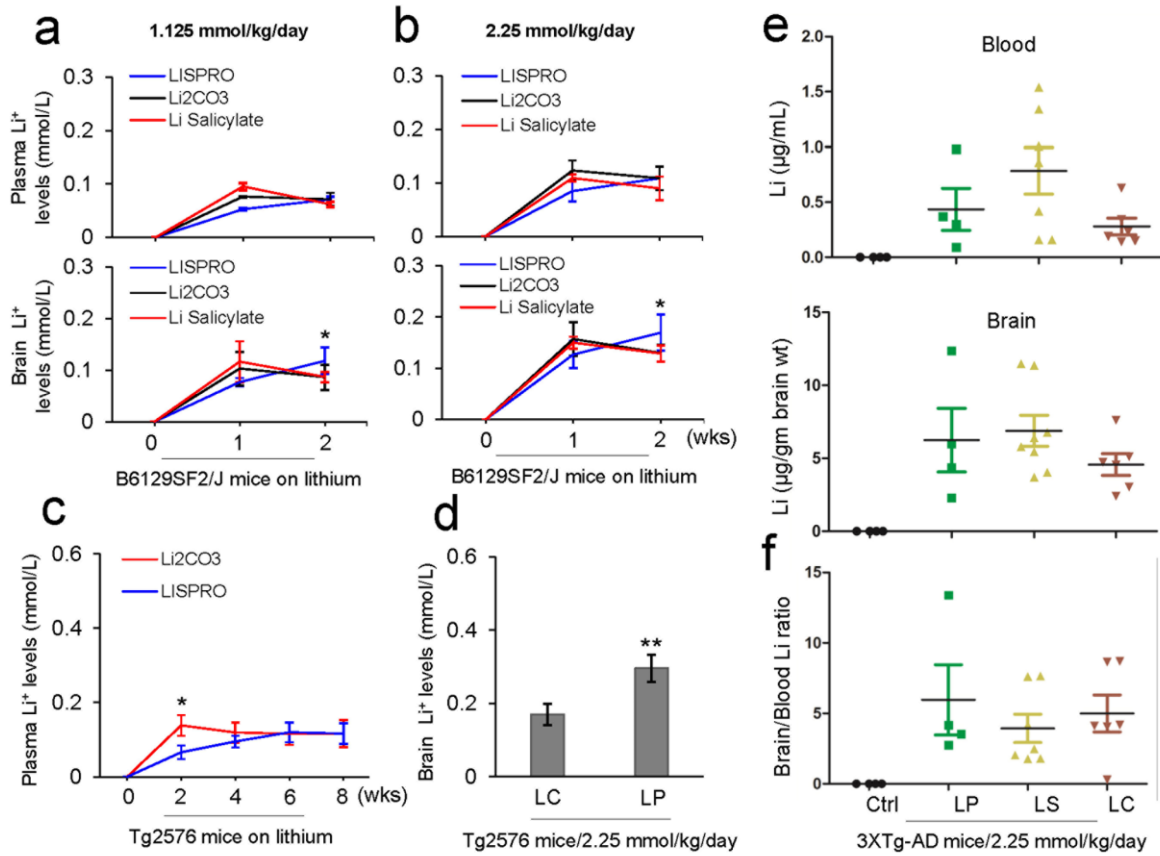
Figure 4-1 Plasma and brain lithium pharmacokinetics following chronic oral treatment with LISPRO (LP), lithium salicylate (LS), and Li₂CO₃ (LC) in B6129SF2/J, Tg2576 and 3XTg-AD mice

(a & b) B6129SF2/J mice (n = 2- 4 mice/group, male) at 2 months of age were treated for 1 or 2 weeks (wks) with 3 diets containing LP, LC, or LS, yielding lithium at 1.125 or 2.25 mM/kg/day. (c & d) Tg2576 mice (n = 8, 4 female/4 male) at 6 months of age were treated for 8 weeks with 2 diets containing LP or LC, yielding lithium at 2.25 mM/kg/day. (e & f) Further, 3XTg-AD female mice (n = 4 - 8 mice/group) at 5 months of age were treated for 28 weeks with 3 diets containing LP, LS or LC, yielding lithium at 2.25 mM/kg/day, or normal mouse chow (Teklad 2018). Blood and brain lithium levels were measured using atomic absorption spectroscopy (AAS). Brain over plasma lithium ratio calculated for each individual 3XTg-AD mouse (f). All mice received normal drinking water and chow *ad libitum*. Statistical analysis was carried out using ANOVA with *post* analysis with Fisher's LSD test (*$p < 0.05$; **$p < 0.01$). There was no significant difference in plasma or brain lithium levels between LC- and LS-treated B6129SF2/J mice ($p > 0.05$). There was no detectable lithium in plasma and brain homogenates in control Teklad 2018 diet-fed B6129SF2/J, Tg2576, and 3XTg-AD mice (Ctrl, data not shown).
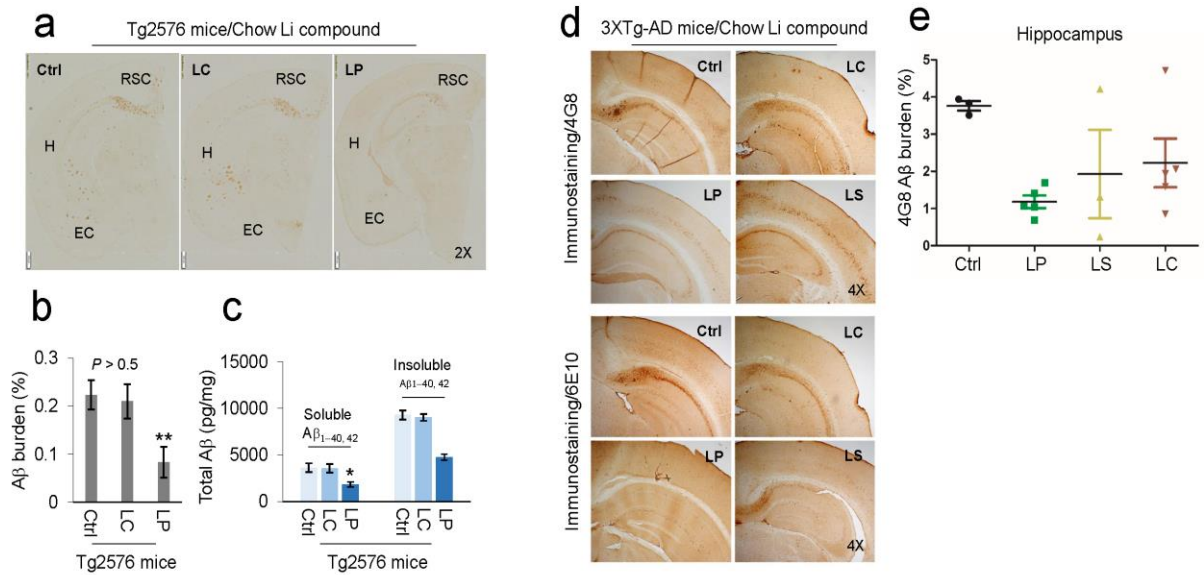
Figure 4-2 Oral LP treatment reduces β-amyloid pathology in Tg2576 and 3XTg-AD mice

Tg2576 mice at 8 months of age (n = 9; 5 male/4 female) and 3XTg-AD female mice at 5 months of age (n = 4 - 8 mice/group) were treated for 8 or 28 weeks, respectively, with diets containing LP, LS or LC, yielding lithium at 2.25 mM/kg/day, or normal mouse chow as indicated. These dosages were chosen to give brain lithium concentrations of 0.25 - 0.50 mM, which fall in a range of clinical therapy for AD. [7, 15] All mice received chow and normal drinking water *ad libitum*. Mouse brain tissue sections and homogenates were prepared from each mouse after treatment. (a and d) Half-brain coronal sections were analyzed by anti-Aβ antibody (4G8) staining. (b and e) Percentage of 4G8 positive plaques (mean ± SEM) was quantified by image analysis as described previously. (**c**) Total soluble and insoluble $A\beta_{1-40, 42}$ peptides from homogenates were analyzed by ELISA and represented as picograms of Aβ peptides per mg of total protein. LP but not LC treatment markedly reduced total soluble and insoluble $A\beta_{1-40,42}$ levels. A *t*-test for two samples and one-way ANOVA-test for multiple independent samples revealed significant differences between LP and LC (b and c) and among LP, LS and LC compared with control diet (Ctrl) (**e**, *p < 0.05, **p < 0.01). There was no notable or significant difference in both 4G8 positive Aβ plaques and cerebral soluble/insoluble $A\beta_{1-40,42}$ levels in brain sections and homogenates between LC-treated and control Teklad 2018 diet-fed Tg2576 mice (Ctrl, *p* > 0.05).
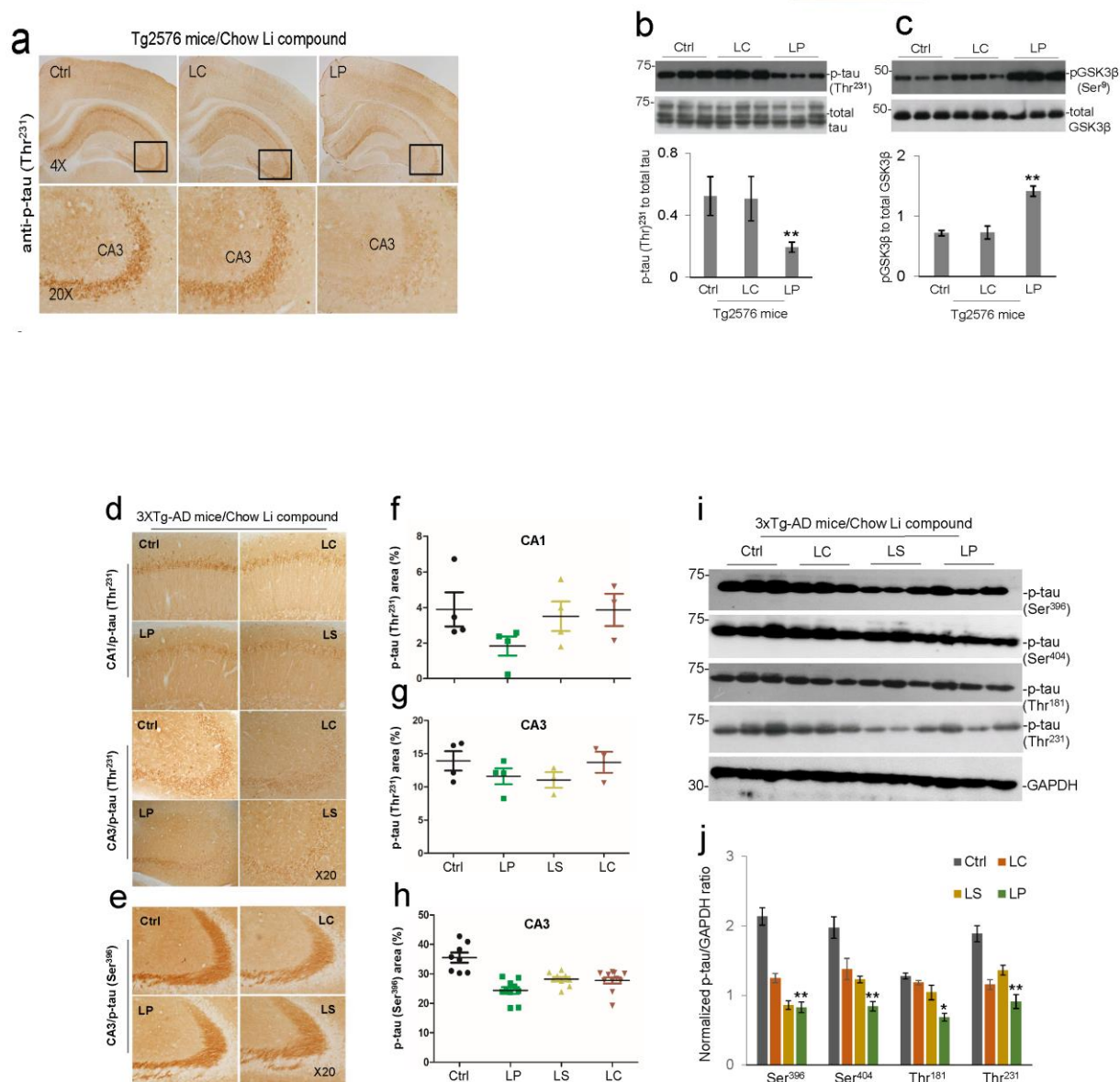
Figure 4-3 Oral LP treatment reduces tau hyper-phosphorylation in Tg2576 and 3XTg-AD mice

Representative micrographs showing IHC staining of brain sections from Tg2576 and 3XTg-AD mice orally treated for 8 and 28 weeks, respectively, with diets containing LP, LS or LC, yielding lithium at 2.25 mM/kg/day, or control Teklad 2018 diet, as detailed in Figure 4-1 above. Shown are IHC staining and quantification of p-tau (Thr[231], a, d) and p-tau (Ser[396], e) immunoreactivity in CA3 of Tg2576 (a) and CA1/CA3 of 3XTg-AD mice brain sections (d and e). Percentage of p-tau (Thr[231]) or p-tau (Ser[396]) positive areas (mean ± SEM) was quantified by image analysis in CA1/CA3 of 3XTg-AD mice (f - h). ANOVA with *post hoc* analyses using Fisher's LSD test for multiple samples reveals significant differences in phosphorylated tau between LP treated and control mince (*$p < 0.05$, **$p < 0.01$). The mouse brain homogenates were subjected to western

113

blot (WB) analysis with antibodies against p-tau (Thr^{231}), p-tau (Ser^{396}), p-tau (Ser^{404}), p-tau (Thr^{181}), total tau, GAPDH (b and i), pGSK3β (Ser^9) or total-GSK3β (c). As shown below WB, densitometry analysis shows the band density ratios of p-tau to total tau (b, bottom panel) or GAPDH (j) and pGSK3β to total GSK3β (c, bottom panel). Statistical *t*-test analyses of WB data revealed a significant decrease in the ratios of p-tau (Thr^{231}) to total tau (b) and increase in pGSK3β (Ser^9) to total GSK3β (**c**) in LP compared with LC-treated Tg2576 mice (**$p < 0.01$). One-way ANOVA and *post hoc* analyses revealed significant differences in the ratio of p-tau to GAPDH (j) compared to control treatment (Ctrl, *$p < 0.05$, **$p < 0.01$). Similar results from both immunochemistry staining and WB analyses were also obtained with PHF-1 antibody (data not shown) in the LISPRO-treated Tg2576 mice. There was no notable and significant difference in both p-tau (Thr^{231}) and inactivated p-GSK3β (Ser^9) levels in brain homogenates between LC- and control Teklad 2018 diet-fed Tg2576 mice ($p > 0.05$).
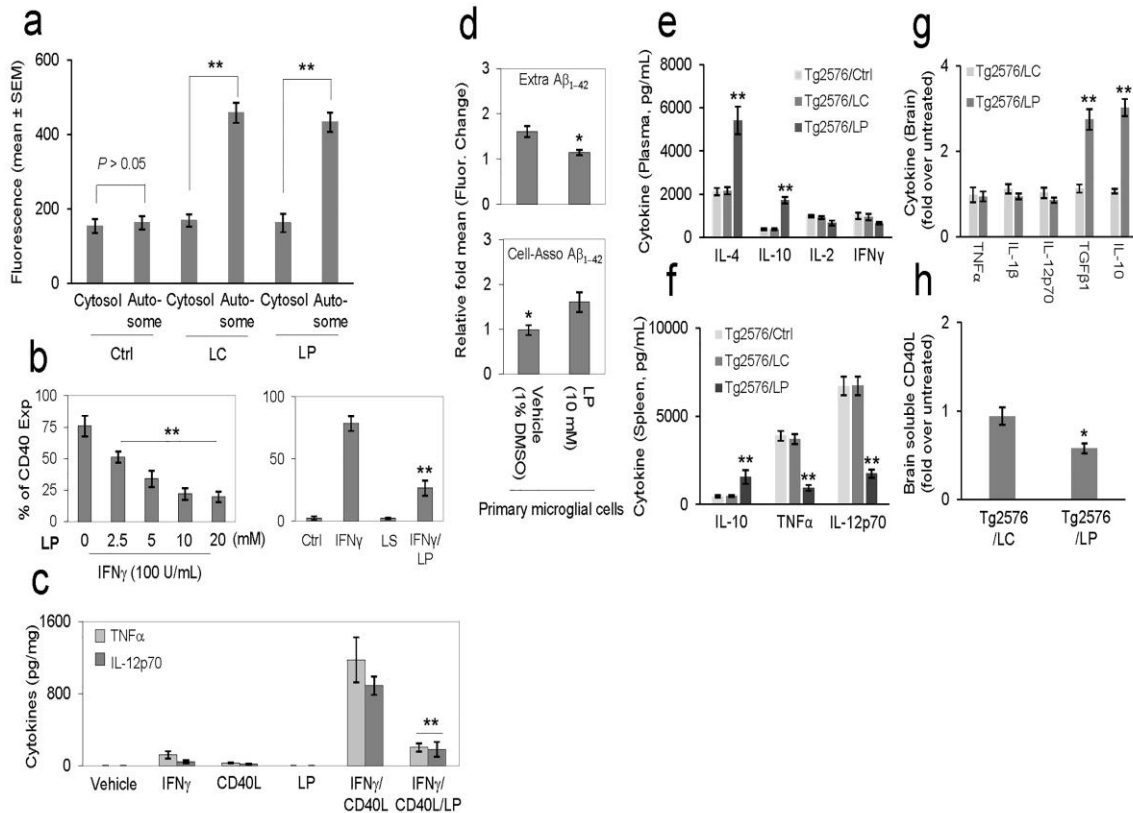
Figure 4-4 LP inhibits peripheral and neuroinflammation, while promoting microglial autophagy and Aβ phagocytosis

(a) For determination of microglial autophagy, mouse primary microglial cells were pretreated with LP, LC, LiCl, or L-proline at 10 mM or PBS (Ctrl) for 18 h, followed by permeabilization, staining with LC3B rabbit polyclonal antibody, and visualization with Alexa Fluor® 647 goat anti-rabbit IgG (LC3B antibody kit, Molecular Probes®). The fluorescence intensity of the autophagosomes (Autosome) and the cytosol were quantified using Slidebook™ digital microscopy software (mean ± SD). Both LP and LC treatments significantly enhanced microglial autophagy (**$p < 0.01$). Note that there was no significance difference in the fluorescence intensity of the autophagosomes and the cytosol between LC, LP, and LiCl ($p > 0.05$). L-proline failed to promote any notable autophagy. In addition, mouse primary microglial cells were treated with LP (0-20 mM) in the presence of IFNγ (100 U/ml) or/and CD40 ligand (CD40L, 1 μg/ml) for 8 h and then examined for pro-inflammatory microglial activation as assessed by flow cytometric (FACS) analysis and ELISA. (b) FACS analysis showed LP induced significant dose dependent decreases in IFNγ-induced CD40 expression. Data are represented as mean percentage of CD40 expressing (CD40 Exp) cells (± SEM) from two independent experiments. (c) Microglial cell culture supernatants were collected and subjected to cytokine ELISA as indicated. Data are represented as mean pg of TNFα or IL-12p70 per mg of total cellular protein (± SEM) from three independent experiments.

For determination of microglial Aβ phagocytosis, primary microglial cell were pre-treated with LP at 10 mM or vehicle (1% DMSO in medium) for 6 h and then incubated with 1 μM FITC-

115

Aβ$_{1-42}$ for 1 h (d). Cellular supernatants and lysates were analyzed for extracellular (Extra, top panel) and cell-associated (Cell-Asso, bottom panel) FITC-Aβ$_{1-42}$ using a fluorometer. Data are represented as the relative fold of mean fluorescence change (mean ± SEM), calculated as the mean fluorescence for each sample at 37°C divided by mean fluorescence at 4°C (n = 4 for each condition presented) (**$p < 0.01$). LDH assay showed no significant increase in cell toxicity induced by LISPRO up to 20 mM in primary microglial cells (data not shown).

For determination of peripheral and neuroinflammation, blood plasma (**e**), splenocyte cultured media (**f**) and brain homogenates (g and h) from LP- and LC-treated and untreated Tg2576 mice (Ctrl) were subjected to cytokine and sCD40L ELISA. Data are presented as mean ± SEM values of cytokines (pg/ml plasma or medium) (e and f) or fold increase of brain tissue-derived cytokines or sCD40L for LC or LP-treated over untreated mice (g and h, n = 9 for LP- and LC-treated mice; n = 6 mice for untreated mice, *$p < 0.05$; **$p < 0.01$). There was no notable or significant difference in cytokine levels in plasma and splenocyte cultured media between LC-treated and control untreated mice ($p > 0.05$).
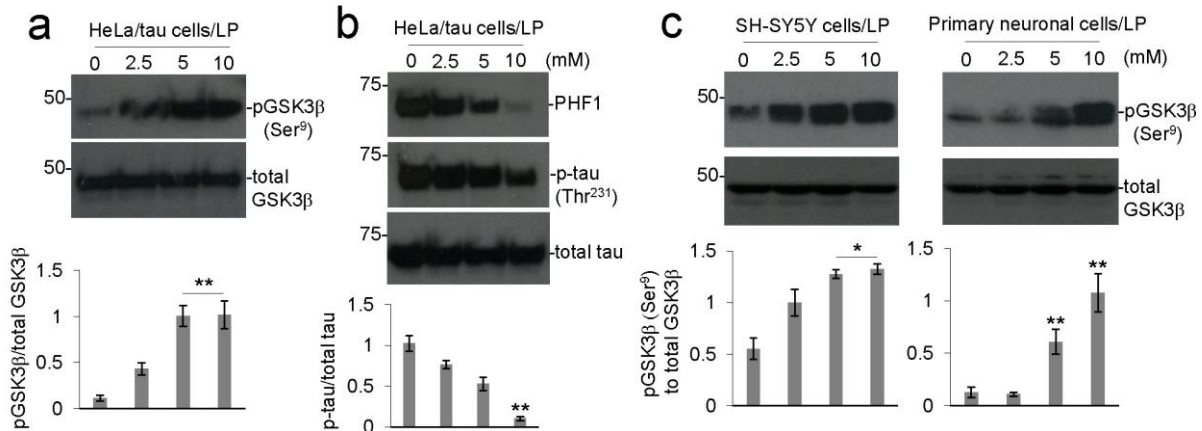
Figure 4-5 LP decreases tau phosphorylation while increasing inhibitory GSK3β (Ser^9) phosphorylation in cultured cells

Human tau stably transfected HeLa cells (HeLa/tau cells) (a and b), human neuroblastoma (SH-SY5Y) cells (c, left panel), and primary neuronal cells (c, right panel) were treated with LP at the indicated concentrations (0-10 mM) for 12 h, followed by analysis of cell lysates by WB. Inhibitory phosphorylation status of GSK3β was detected by anti-phospho-GSK3β (Ser^9) and total GSK3β antibodies (a). Phosphorylation status of tau was detected by anti-phospho-tau [p-tau (Thr^{231})] and PHF1 antibodies as used previously (b). Total tau (phosphorylated and non-phosphorylated) was detected by tau-46 (b). WB results are representative of two independent experiments for pGSK3β (Ser^9) and total GSK3β, and three experiments respectively for PHF1, p-tau (Thr^{231}) and total tau with triplicates for each treatment condition. Densitometry analysis below each WB figure panel shows the band density ratio of pGSK3β (Ser^9) to total GSK3β as well as p-tau (Thr^{231}) to total tau. A *t*-test revealed a significant increase in the ratio of pGSK3β (Ser^9) to total GSK3β and decrease in p-tau to total tau for HeLa/tau cells treated with 10 mM LISPRO compared to control (0 mM) (*$p < 0.05$; **$p < 0.01$). In addition, a significant increase in the ratio of pGSK3β (Ser^9) to total GSK3β was observed for both SH-SY5Y cells and differentiated neuronal cells treated with either 5 or 10 mM LISPRO compared to control (0 mM) (*$p < 0.05$) (c). The secreted Aβ$_{1-40,42}$ peptides were undetectable by Aβ ELISA of the conditioned media from HeLa/tau cells with or without LISPRO treatment (data not shown).

117
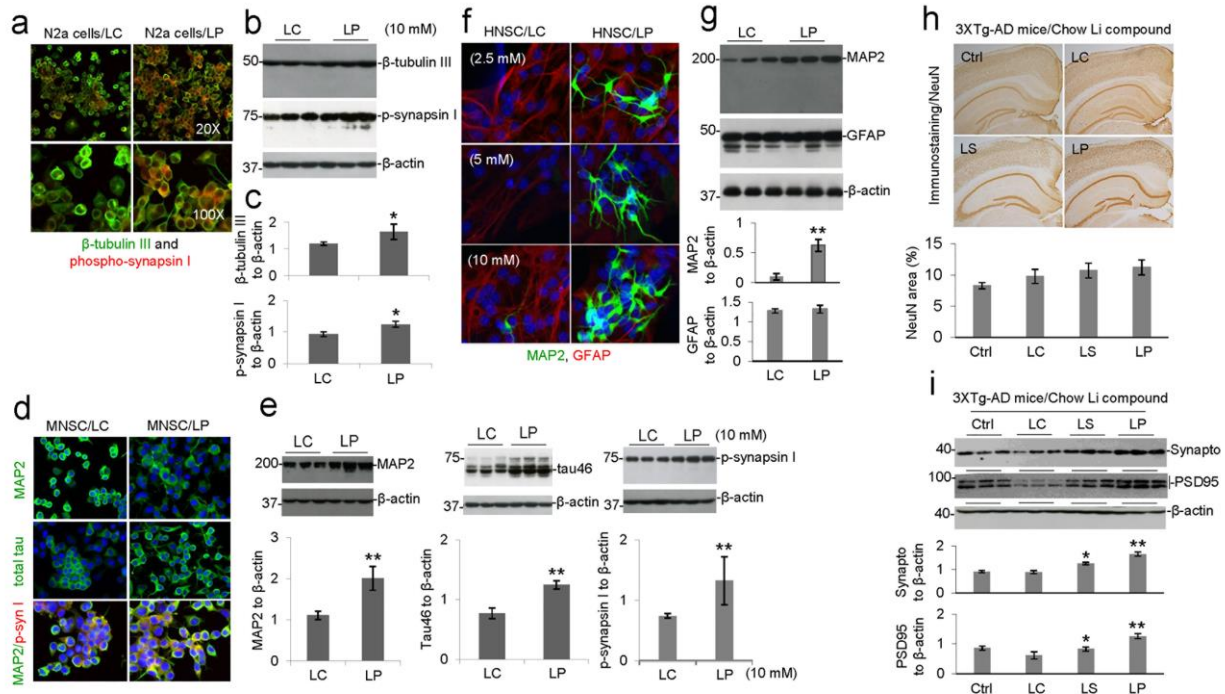
Figure 4-6 LISPRO markedly promotes neuronal cell differentiation and prevent neuronal and synaptic protein loss in 3XTg-AD mice

Murine neuroblastoma (N2a cells, a), murine neuronal stem cells (MNSC, d) and human neural stem cells (HNSC, H9-Derived, f) were treated with LP, LC, LiCl, or L-proline (10 mM) for 24 h, 4 days, or 14 days respectively. These cells were then permeabilized with 0.05% Triton X-100 for 5 min, washed, and stained with mouse anti-β-tubulin III monoclonal antibody, rabbit anti-phospho-synapsin I (Ser^{62} and Ser^{67}) polyclonal antibody, mouse anti-MAP2 monoclonal antibody, mouse anti-total tau (tau46) antibody or rabbit anti-GFAP polyclonal antibody overnight at 4 °C. Alexa Fluor® 488 goat anti-mouse IgG (green) was used to detect β-tubulin III, MAP2 and total tau and Alexa Fluor® 594 donkey anti-rabbit IgG (red) were used to detect phospho-synapsin I and GFAP, respectively (a and d). DAPI staining was used to detect nuclear DNA. Confocal images were taken by Olympus Fluoview™ FV1000 laser scanning confocal microscope. In parallel, N2a cells (b), MNSC (e) and HNSC (g) were treated with LP, LC, LiCl, or L-proline at 10 mM, lysed with cell lysis buffer, and then subjected to WB analysis of β-tubulin III, phospho-synapsin I, MAP2, total tau and GFAP. As indicated below each WB panel, the band density ratios of β-tubulin III and phospho-synapsin I (p-synapsin I) to β-actin (c), MAP2, total tau and phospho-synapsin I to β-actin (e) and MAP2 and GFAP to β-actin (g) are presented as mean ± SEM These data are representative of three independent experiments with similar results (*$p < 0.05$; **$p < 0.01$). There was no notable or significant difference in β-tubulin III, phospho-synapsin I, MAP2, total tau and GFAP immunofluorescence and WB analysis between LC, LiCl, or L-proline treatment ($p > 0.05$) for all three differentiated N2a cells, MNSC and HNSC respectively.

The brain tissue sections and homogenates prepared from LP-, LS-, or LC-treated, or untreated control 3XTg-AD mice, were subjected to IHC staining and WB analyses of neuronal and pre- and post-synaptic proteins, using NeuN, synaptophysin and PSD95 antibodies, respectively. No statistically significant but increased changes in total number of immunoreactive (NeuN) positive cells were observed in LP- and LS-treated compared with untreated control mice (h). (i) However, synaptophysin (Synapto) and PSD95 protein levels were significantly elevated in LP- and LS-treated mice compared with LC-treated and untreated control mice. As indicated below IHC and WB panels, percentage of NeuN immunoreactive positive cells, synaptophysin, and PSD95 to GAPDH band density ratios were determined by image analysis (mean $\pm$ SEM). Data were analyzed by a one-way ANOVA and *post* testing with Fisher's LSD test (*$p < 0.05$; **$p < 0.01$).
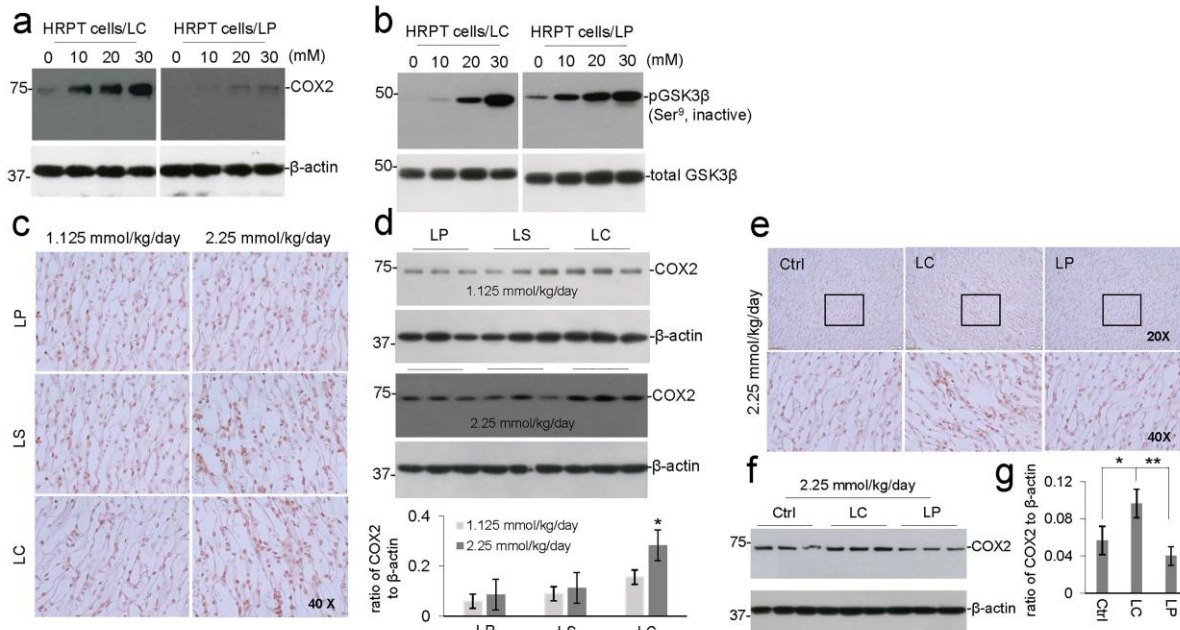
Figure 4-7 LISPRO does not increase COX2 expression *in vitro* and *in vivo*

Human primary renal proximal tubule cells (ATCC® PCS-400-010™) were cultured in *InVitro*GRO medium (BioreclamationIVT) and treated with LP, LC, LiCl, or L-proline at 0 to 30 mM for 12 h. These cells were then lysed with cell lysis buffer and analyzed by WB for COX2, total GSK3β and phospho GSK3β (Ser[9] and Thr[390]) expression using anti-COX2 antibody (a) and anti-phospho- and total GSK3β antibodies (b). Note that there were no notable differences in COX2 expression or GSK3β phosphorylation between LC and LiCl treatments. L-proline treatment induced no change in COX2 expression and GSK3β phosphorylation.

B6129F2/J male mice (weighing 20-25 g, 2-month old) were treated with 3 diets containing LP, LC, or LS, or control Teklad 2018 diet, for 1 or 2 weeks, yielding lithium at 1.125 or 2.25 mM/kg/day. All mice received normal drinking water and chow *ad libitum*. (c) Kidneys were collected after treatment and analyzed by IHC for COX2 expression in the renal medulla. (d) In addition, the kidney microsomal proteins were extracted to assess COX2 expression by WB analysis. COX2 to β-actin band density ratio of WB were determined by ImageJ analysis (mean ± SEM) in duplicates from six mice in each group. Statistical analysis was carried out using ANOVA (*$p < 0.05$, n = 6 for LP, LC and LS; n = 3 for control diet). Furthermore, Tg2576 mice were treated with 2 diets containing LP or LP, yielding lithium at 2.25 mM/kg/day for 8 weeks. (e) Kidneys were collected after treatment and analyzed by IHC for COX2 expression in the renal medulla. (f) The kidney microsomal proteins were extracted to assess COX2 expression by WB. (g) Quantification of COX2 to β- actin band density ratio of WB among ctrl, LP and LC treatments were determined by ImageJ analysis. Statistical analysis was carried out using ANOVA followed post hoc by Fishers LSD (*$p < 0.05$, **$p < 0.01$, n = 9 per treatment).

CHAPTER 5

Ionic co-crystal of lithium salicylate proline (LISPRO), a novel formulation of lithium, prevents cognitive and neuropsychiatric behavioral deficits in the APPswe/PS1dE9 transgenic mouse model of Alzheimer's disease

Chapter synopsis

Alzheimer's disease (AD) is a neurodegenerative disorder characterized by progressive decline of cognition and associated neuropsychiatric symptoms including weight loss, anxiety, agitation, depression, irritation, and aggressiveness. To date, no pharmacological or non-pharmacological intervention has yet been shown to delay or stop progression of the disease. Lithium carbonate (Li_2CO_3), a drug widely used for treating bipolar disorder, has been shown to effect neuroprotection in a number of models of neurodegenerative disease, but may induce inflammation and toxicity in its current formulation. Recently we have shown that a novel ionic co-crystal of lithium salicylate l-proline (LISPRO) is an improved alternative formulation of lithium as compared to lithium carbonate or lithium salicylate in terms of safety and efficacy in ameliorating AD pathology in cell culture and transgenic mouse models. The present study was designed to evaluate and compare the efficacy of LISPRO (LP) with lithium carbonate (LC) and lithium salicylate (LS) for ameliorating cognitive impairments and associated neuropsychiatric signs, including depression, anxiety, irritability, and impaired locomotor function, in

APP$_{SWE}$/PS1dE9 mice, a commonly used transgenic model of AD. Female APP$_{SWE}$/PS1dE9 mice at 4 months of age were orally treated with LP, LS, or LC for 9 months at 2.25 mmol lithium/kg/day followed by determination of body weight, growth of internal organs, and cognitive and non-cognitive behavior. Untreated age-matched non-transgenic littermates (B6C3F1/J) served as wild-type (WT) controls. No significant differences in body weight, brain, heart, lung, spleen, liver or kidney were found between lithium treated- and untreated APP$_{SWE}$/PS1dE9 cohorts. LP treatment improved cognitive function, as shown by lower escape latency during training and probe trial of the Morris water maze (MWM) test and longer contextual freezing time during the fear conditioning test. LP treatment also reduced depression, as assessed by tail suspension test, and irritability, as assessed by touch escape test. Moreover, LP treatment afforded superior protection against cognitive impairment as determined by contextual fear conditioning test and irritability in comparison with LC or LS treatment. However, lithium treatment did not alter anxiety or locomotor activity as assessed by open field, elevated plus maze or accelerated rotarod test. We suggest that chronic LISPRO treatment prevent cognitive deficits, depression and irritability in female APP$_{SWE}$/PS1dE9 mice, and is superior in improving associative learning and memory and irritability compared with lithium salicylate or carbonate treatments, supporting the potential of this lithium formulation for the treatment of AD.

Background

Alzheimer's disease (AD) is characterized pathologically by the accumulation of neuritic plaques [1] and neurofibrillary tangles [2] in the brain and clinically by a progressive decline in cognitive function. As total neuronal volumes positively correlated with memory and cognitive function [240], the degeneration of neural synapses especially in the hippocampus and cortical regions is also positively correlated with cognitive decline in patients with AD [241][242]. It is

widely believed that abnormal accumulation of plaques and tangles consisting of amyloid-β (Aβ) [194] and hyperphosphorylated tau [195] proteins, respectively, promotes neurodegeneration [243] which may be involved in the development of cognitive and neuropsychiatric problems [244]. More recently, soluble oligomeric forms of Aβ and tau have been shown as the most toxic form of Aβ and tau aggregate to produce cognitive deficits in the absence of Aβ plaques or insoluble intraneuronal tangles [245][246][247]. In addition, other emotional problems, such as depression, anxiety, apathy, irritation, agitation and aggression, gradually develop in patients with AD [248]. No single drug has been shown to be effective in improving both cognitive and non-cognitive problems.

Lithium salts were initially used in the treatment of gout (including "brain gout") as early as 1859 and then recognized for its beneficial effects on mood by the late 1800's [198]. Despite having a narrow therapeutic window that requires routine blood monitoring to avoid lithium toxicity and associated side effects, lithium salts are still considered even today as the gold standard by many clinicians for preventing the reoccurrence of mania and suicidality in bipolar patients [249][250]. Based in part on evidence that lithium therapy may prevent cognitive decline in bipolar disorder, a growing body of studies using diverse preclinical and clinical models have provided evidence for potential disease modifying properties of lithium in treating neurodegenerative diseases, including AD [251]. Overall, the available evidence suggest that the neuroprotective effects of lithium found in diverse preclinical models of neurodegeneration translate into therapeutic benefits in cognitive function and reduced biomarkers in clinical trials of mild cognitively impaired amnestic and AD patients at lower lithium doses than those typically used for mood stabilization [252]. Other studies also suggest that long-term lithium treatment inhibits or slows down the core pathophysiologic features of AD in preclinical as well in human

study [253][254]. Notably, in a recent review of 28 psychiatric medications, including antipsychotics, anticonvulsants and antidepressants, lithium had the most replicated evidence for neuroprotection in the widest range of neurodegenerative disease models [255]. Despite these potential benefits of lithium pharmaceutics, safety issues remain. Indeed, current Food and Drug Administration (FDA)-approved lithium pharmaceutics have a narrow therapeutic window, producing a sharp peak in the serum blood levels which can cause adverse side effects. In addition, due to competition for sodium reuptake, high levels of lithium can accumulate in the kidney under certain conditions resulting in renal inflammation and toxicity [256].

To improve lithium's therapeutic profile, we have recently investigated the safety, pharmacokinetics, and therapeutic efficacy of LISPRO, a novel ionic co-crystal of lithium salicylate and l-proline [87], in comparison with lithium carbonate and lithium salicylate in preclinical models of AD [150]. We found that 8- as well as 28-week oral treatment with LISPRO produced superior reduction of hippocampal brain pathology, including Aβ plaque deposition, tau hyperphosphorylation, neuroinflammation, and neurodegeneration, in transgenic Alzheimer's-like mice models. Similarly, in cell culture studies, LISPRO reduced tau hyperphosphorylation, microglial inflammation and glycogen synthase kinase 3-beta activity and was superior to lithium carbonate in enhancing neuronal stem cell differentiation. In addition, pharmacokinetic studies indicated that LISPRO treatment provided significantly higher brain lithium levels and more steady plasma lithium levels in both normal and transgenic Alzheimer's-like mice when compared to lithium carbonate. Moreover, a 2-week oral treatment of lithium carbonate in normal mice increased proinflammatory cyclooxygenase-2 expression in the kidneys, while the molar equivalent of lithium administered as LISPRO did not [150]. The purpose of this follow-up study was to compare the effects of chronic oral treatment of LISPRO with lithium carbonate and lithium

124

salicylate on behavioral impairment and various AD-associated neuropsychiatric symptoms, including depression, irritation, anxiety and impaired locomotion, as well as physical growth and development of internal organs in APPswe/PS1dE9 double transgenic mice, the most widely used preclinical animal model in evaluating drug safety and efficacy for AD. For consistency, we employed the same chronic dosing regimen of LISPRO that was used in our prior study [150].

Materials and methods

Animals and treatment

Twelve-week-old (3 months of age) female transgenic (Tg) APPswe/PS1dE9 mice [B6C3-Tg (APPswe/PS1dE9)85Dbo/Mmjax; Stock #034829; n = 28) and wild-type (WT) non-transgenic control littermates (Non-Tg Ctrl, B6C3F1/J; n = 10) were obtained from Jackson Laboratory (Bar Harbor, ME) and housed 3-4 mouse per cage before starting treatment. APPswe/PS1dE9 mice express human amyloid precursor protein (APP) with the K670N/M671L (Swedish) mutation and human presenilin 1 (PS1) with the deltaE9 mutation, both under control of the prion promoter. The Swedish mutation results in an increase in BACE1 cleavage of APP and the deltaE9 mutation increases γ-secretase activity. These mice show plaque deposits at 6 months of age, and increasing cognitive impairment at 12 months of age [257][258]. APP$_{SWE}$/PS1dE9 mice were randomly assigned into four treatment groups, and starting at 4 months of age received normal chow (Tg-Ctrl, Lithium, 0%, n = 8) or chow that contained lithium carbonate (LC, 0.05%, equivalent to 83 mg/kg/day, n = 6), lithium salicylate (LS, 0.20%, equivalent to 325 mg/kg/day, n = 6) or lithium salicylate proline co-crystal (LP, 0.35%, equivalent to 583 mg/kg/day, n = 8) for 9-months. This gave a dose of lithium at 2.25 mmol lithium/kg/day for each formulation. This dosage was chosen to give brain lithium concentrations of 0.25-0.5 mmol/L, which fall in the range of clinical therapy for AD [150] [200]. Non-transgenic wild type (WT) littermates cohort (Non-Tg Ctrl, n = 10) were

fed normal chow diet as a control. At the end of 8-months treatment (12 months of age) comprehensive cognitive and non-cognitive evaluations (Figure 5-1) were conducted by individuals blind to genotype and treatment group [160]. All animal experiments were performed in accordance with the guidelines of the National Institutes of Health and were approved by USF Institutional Animal Care and Use Committee (IACUC reference number: IS000002240).

Behavioral assays

Morris water maze

The Morris Water Maze (MWM) is used to investigate hippocampal spatial memory impairments in rodents. The apparatus consists of a circular tank (150×85 cm) filled with water ($25 \pm 2\ ^0$C). The circular tank was divided into four invisible quadrants (North, South, East, West) using ANY-Maze^{TM} video recording software. To increase the tracking sensitivity, white paint solution was mixed in the water to provide contrast to the dark color of the mouse and facilitate tracking of mouse movement. In the study reported here, a hidden platform was placed 1 cm beneath the water level in North East zone during the training period (4 trials) for two consecutive days, during which time individual mouse was placed in the tank and were allowed to find the platform. Over multiple trials wherein the mouse is placed in the tank at different locations, the mouse learns to find the hidden platform within 60 s by using distal spatial learning cues, here consisting of colored objects placed on the walls outside of the water tank but in view of the mouse. If the mouse failed to locate the hidden platform within 60 s, it was guided to the platform and allowed to stay there for 10 - 20 s. Spatial memory was evaluated by assessing the average latency time (in seconds) and path length of a mouse before reaching the hidden platform. Twenty-four hours following the end of the last trial each mouse was given a 60 s probe trial, which determines the ability of the mouse to retrieve learned information. During probe trial, the hidden platform is

removed, and parameters such as escape latency (time to reach the previous platform position), time spent in the platform quadrant, crossings over the platform and total distance travelled were recorded using automated ANY-Maze™ video software.

Fear conditioning

Fear Conditioning (FC) assesses the ability of rodents to learn and memorize the association between environmental cues (context) and aversive stimuli (cued). This test is used to investigate hippocampal- (contextual), as well as amygdala-dependent (cued) memory functions, as indicated by the freezing response (complete absence of movement except respiration). The mouse learns rapidly in an environment where the aversive stimulus consists of conditioned (white tone) and unconditioned stimuli (shock). The experimental set-up consists of a transparent Plexiglas box with a photo beam detection system and an electric shock generator wired to a grid in the floor on the box. On Day 1 a mouse was placed in the chamber and allowed to explore freely for 6 min during which baseline freezing time (conditioning) was observed using automated video recording software. After 3 min, an auditory stimulus (80 dB tone) was given for 30 s followed by a 0.35 mA mild foot shock for 2s. Two minutes later another conditioned-unconditioned pairing was given. The mouse was then removed from the chamber and returned to the home cage. At Days 2, 7, and 21, each mouse was placed back to the chamber for 6 min without any shock and the freezing time was recorded (contextual response). Similarly, the mouse was the placed in the chamber for 6 min after changing contextual cues with a few drops of vanilla extract, the auditory stimulus (80 dB tone) was delivered during the last 3 min, and freezing time was recorded (cued response).

Elevated plus maze

Elevated Plus Maze (EPM) is used extensively with the open field test to assess anxiety-like behavior. The apparatus is elevated 50 cm above the ground and consists of four arms of 60 x 20 cm at 90°, two open and two closed with elevated walls of 40 cm, and a central square of 10 × 10 cm dimension. In this study, each mouse was placed in the center of the maze facing an open arm and the video tracking software is used to record arm entries for 5 min. Mice that stay in the closed arms of the EPM are thought to be exhibiting anxiety-like behavior, whereas those frequently exploring open arms are considered to be exhibiting less anxiety behavior.

Open field test

The Open Field (OF) test is used to evaluate anxiety-like behavior by placing the mouse in a cubic (1m x 1m x 1m) box with walls to prevent the escape of the mouse. The open field is comprised of peripheral and central areas marked with a grid and square crossings. Video tracking software is used to separate the open field into peripheral and central areas of the grid. The mouse is placed in the center of the open field and allowed to freely move for 10 min under adequate lighting without any background noise and odors, while tracking total distance travelled and times spent in the open and periphery using video tracking software. The amount of time spent or number of entries into central area is indicative of reduced level of anxiety, while more time spent in the periphery indicates higher anxiety level.

Tail suspension test

Depression-related behaviors and antidepressant activity of drugs can be studied in the mouse using tail suspension test. In this test, a mouse is suspended above a surface by anchoring

the tail with tape and is observed for its efforts to escape for 300 s. The duration of periods of attempts to escape (agitation) and immobility is recorded with a stopwatch.

Touch escape test

The Touch Escape test is a non-cognitive behavior test used to analyze the irritability of the animal in response to touch as summarized by SHIRPA (Smithkline Beecham, Harwell, Imperial College, Royal London Hospital, Phenotype assessment) [259]. To determine Touch Escape, each mouse was taken from the home cage and placed on a table. The evaluator brushed the sides and back of the mouse from behind starting from the upper front of the thorax then slowly moving caudally to its tail while evaluating its irritability. A Touch Escape score from 0 to 2 was determined with the following scale: "0" included freezing, or no progression or regression of movement from the evaluator's hand, score "1" comprised of startle responses like agitation, small jump, jerk, twitching followed by a small amount of progression away from the evaluator, score "2" included jumping or quick progressive movements away from the evaluator and/or biting.

Accelerated rotarod test

Briefly, mice were placed on a rotating rod beam, which underwent an acceleration from 4 to 40 rotations per minute (RPM) over 5 min for three consecutive trials separated by a 60 min interval, and latencies to fall as well as maximal speed before falling were determined. The amount of time a mouse remains on the accelerating rotating beam is an index of motor coordination.

Statistical analysis

All data are presented as mean ± SEM. We used t-test for two groups' comparison, while comparison between more than two groups was analyzed by ANOVA followed by Tukey's honest significant difference *post hoc* analyses. Alpha was set at 0.05 for all analyses. Statistical analyses

were performed using the Statistical Package for the Social Sciences (SPSS), release 24.0 (IBM, Armonk, NY).

Results

LISPRO did not affect body weight in female APP$_{SWE}$/PS1dE9 mice

Among the long-term adverse effects, lithium therapy is associated with weight gain in a subset of bipolar patients through an unknown mechanism. But contradictory results also exist regarding effects of lithium treatment on weight gain or loss in both rodents and humans [260]. To investigate whether LP, LS, and LC treatment had any effect on weight gain in APP$_{SWE}$/PS1dE9 mice, body weights of mice were measured at the beginning (4 months age) as well as at the end (13 months of age) of the treatment. Nontransgenic WT control mice weighed significantly more than untreated transgenic APP$_{SWE}$/PS1dE9 cohort both before and after the treatment period (Figure 5-2), presumably due to a significantly greater deposition of fat tissue in nontransgenic WT compared with transgenic APP$_{SWE}$/PS1dE9 mice. However, no statistically significant difference in body weight was found between untreated transgenic APP$_{SWE}$/PS1dE9 mice receiving normal chow and those receiving LP, LS, or LC treatment for 9 months [Before treatment, Age = 4 months, F (4, 36) =13.142; $p < 0.001$; Non-Tg Ctrl vs. Tg-Ctrl: $p < 0.001$; LP vs. Tg-Ctrl: $p = 0.933$; LP vs. LC: $p = 1.000$; LP vs. LS: $p = 0.790$. After treatment, Age = 13 months, F (4, 36) =18.359; $p < 0.001$; Non-Tg vs. Tg-Ctrl: $p < 0.001$; LP vs. Tg-Ctrl: $p = 0.992$; LP vs. LC: $p = 0.995$; LP vs. LS: $p = 0.937$.]

LISPRO did not adversely affect the growth of internal organs in APP$_{SWE}$/PS1dE9 mice

Lithium treatment has been shown to influence the functions of endocrine hormones regulating growth and development of internal organs in mice [261]. Therefore, we wanted to

examine if long-term lithium treatment would adversely affect the growth of internal organs in female transgenic APP$_{SWE}$/PS1dE9 AD mice. To our knowledge, no such data is available on the long-term effect of LP, LC, and LS treatments on organ development in these mice. At sacrifice, post-hoc analysis showed statistically significant decrease in weights of brain (Figure 5-3a, left panel), liver (Figure 5-3b, left panel) and kidneys (Figure 5-3b, center panel) in untreated transgenic APP$_{SWE}$/PS1dE9 cohort compared with non-transgenic WT control mice. However, the weights of heart, lung and spleen were not significantly different between untreated transgenic APP$_{SWE}$/PS1$_{dE9}$ and nontransgenic WT control. In addition, lithium treatment did not significantly alter the weight of any organ in transgenic mice, indicating no adverse effect of lithium treatment on growth of these organs. [Brain, $F (4, 36) = 2.889$; $p = 0.038$; Non-Tg Ctrl vs. Tg-Ctrl: $p = 0.066$; LP vs. Tg-Ctrl: $p = 0.967$; LP vs. LC: $p = 0.688$; LP vs. LS: $p = 0.992$. Heart, $F (4, 36) = 2.048$; $p = 0.111$; Non-Tg Ctrl vs. Tg-Ctrl: $p = 0.763$; LP vs. Tg-Ctrl: $p = 0.630$; LP vs. LC: $p = 0.592$; LP vs. LS: $p = 0.943$. Lung, $F (4, 36) = 0.815$; $p = 0.525$; Non-Tg Ctrl vs. Tg-Ctrl: $p = 1.000$; LP vs. Tg-Ctrl: $p = 0.947$; LP vs. LC: $p = 0.873$; LP vs. LS: $p = 1.000$. Liver, $F (4, 36) = 16.049$; $p = 0.0001$; Non-Tg Ctrl vs. Tg-Ctrl: $p = 0.0001$; LP vs. Tg-Ctrl: $p = 0.442$; LP vs. LC: $p = 0.999$; LP vs. LS: $p = 1.000$. Kidneys, $F (4, 36) = 13.551$; $p = 0.0001$; Non-Tg Ctrl vs. Tg-Ctrl: $p = 0.0001$; LP vs. Tg-Ctrl: $p = 0.998$; LP vs. LC: $p = 0.675$; LP vs. LS: $p = 0.983$. Spleen, $F (4, 36) = 2.813$; $p = 0.042$; Non-Tg Ctrl vs. Tg-Ctrl: $p = 0.711$; LP vs. Tg-Ctrl: $p = 0.366$; LP vs. LC: $p = 0.324$; LP vs. LS: $p = 0.377$.]

Improvement of spatial memory deficits in female APP$_{SWE}$/PS1dE9 mice by LISPRO treatment

Within the medial temporal lobes, the hippocampus has been considered to be critical for spatial memory function and is therefore the focus of this study. In our previous study, we found

that LISPRO treatment prevents the progression of amyloid deposition in the hippocampus and cortex in Tg2576 and 3xTg-AD mice models [150]. Due to abundant amyloid deposition in the cortex and hippocampus by twelve months of age, the transgenic $APP_{SWE}/PS1dE9$ mouse model of AD also shows spatial and stress-induced memory deficits. To examine whether long-term LISPRO treatment ameliorates spatial learning and memory deficits in this AD model, the MWM test was conducted after 8-months of treatment, when the mice were approximately 12 months of age. All groups showed a gradual decrease in escape latency to find the hidden platform in second and third trials of training (Trial 1 vs. Trial 2 and Trial 2 vs. Trial 3: $p < 0.05$; in all five groups; Figure 5-4a), indicating the learning ability of all mice throughout the training period. At probe trial, untreated transgenic $APP_{SWE}/PS1dE9$ mice showed longer escape latencies compared to non-transgenic WT control mice, confirming an AD-associated learning and memory deficit as determined by the MWM test (Figure 5-4b). In addition, LP-treatment significantly reduced the time to find the target platform compared with the untreated transgenic $APP_{SWE}/PS1dE9$ mice, suggesting that LISPRO ameliorates spatial memory deficits in these mice. Although LP treatment reduced the latency to find the target platform compared with LC and LS treatment, this difference was not statistically significant. Thus, long-term treatment with LISPRO, LC, or LS protects against memory loss in transgenic $APP_{SWE}/PS1dE9$ mice. Transgenic mice also spent significantly less time in the target quadrant compared with nontransgenic WT control mice, but this time was not altered with lithium treatment (Figure 5-4c). Swimming distance and speed was not significantly different between untreated and lithium treated transgenic and WT control mice (Figure 5-4d & e). [Latency at probing, F (4, 34) = 7.801; $p = 0.0001$, Non-Tg Ctrl vs. Tg-Ctrl: $p = 0.0001$; LP vs. Tg-Ctrl: $p = 0.003$; LP vs. LC: $p = 0.228$; LP vs. LS: $p = 0.251$. Time in target quadrant, F (4, 34) = 3.824; $p = 0.013$; Non-Tg Ctrl vs. Tg-Ctrl: $p = 0.015$; LP vs. Tg-Ctrl: $p =$

0.437; LP vs. LC: $p = 0.840$; LP vs. LS: $p = 0.720$. Swimming distance, F (4, 34) = 0.389; $p = 0.815$; Non-Tg Ctrl vs. Tg-Ctrl: $p = 1.000$; LP vs. Tg-Ctrl: $p = 1.000$; LP vs. LC: $p = 0.869$, LP vs. LS: $p = 1.000$. Swimming speed, F (4, 34) = 0.265; $p = 0.898$; Non-Tg Ctrl vs. Tg-Ctrl: $p = 0.949$; LP vs. Tg-Ctrl: $p = 1.000$; LP vs. LC: $p = 0.996$, LP vs. LS: $p = 0.999$.]

LISPRO treatment ameliorated contextual associative memory deficits in female APP$_{SWE}$/PS1dE9 mice

FC test is used to examine associative learning and memory in rodent models of AD by measuring their freezing behavior. APP$_{SWE}$/PS1dE9 mice show impaired contextual FC memory at 3 months of age, whereas cued FC is found to be normal [262]. To examine the effect of LISPRO treatment on hippocampal- and amygdala-dependent memory, we examined both contextual and cued fear conditioning in female APP$_{SWE}$/PS1dE9 mice at 12 months of age after 8 months of treatment. At day 1, the baseline freezing responses were recorded where mice were exposed to conditioned stimulus (mild foot shock) paired with an unconditioned stimulus (audio tone). Total baseline freezing time was not significantly different between non-transgenic WT and untreated or lithium treated transgenic APP$_{SWE}$/PS1dE9 mice (Figure 5-5a).   The contextual freezing response was then recorded without tone at 1, 7, and 21 days after conditioning. Freezing times were not significantly different between lithium treated and untreated transgenic APP$_{SWE}$/PS1$_{dE9}$ mice after 1 and 7 days of conditioning ($p > 0.05$ in all case; data not shown). However, untreated transgenic APP$_{SWE}$/PS1dE9 mice exhibited significantly less freezing to the context compared with nontransgenic WT control mice after 21 days of conditioning (Figure 5-5b).   More importantly, LP-treatment significantly increased freezing times compared to untreated or LC or LS-treated transgenic APP$_{SWE}$/PS1dE9 mice at this time point. In addition, we also investigated cued FC, consisting of an audio tone without any foot shock application at days 1, 7, and 21 days

after conditioning training. No statistically significant differences in freezing time were observed among treatment groups for cued FC at any day after training (Figure 5-5c). Taken together, these results indicated that LISPRO improves contextual memory deficits with no change in cued FC, suggesting prevention of hippocampal with maintenance of amygdala-dependent cognitive impairment in female APP_{SWE}/PS1dE9 mice. [Baseline conditioning, $F (4, 36) = 0.508$, $p = 0.730$; Non-Tg Ctrl vs. Tg-Ctrl: $p = 0.998$; LP vs. Tg-Ctrl: $p = 0.998$; LP vs. LC: $p = 0.970$; LP vs. LS: $p = 0.993$. Contextual FC 21 days, $F (4, 36) = 6.828$, $p = 0.0001$; Non-Tg Ctrl vs. Tg-Ctrl: $p = 0.007$; LP vs. Tg-Ctrl: $p = 0.031$; LP vs. LC: $p = 0.039$; LP vs. LS: $p = 0.044$. Cued FC, $F (4, 36) = 1.445$, $p = 0.241$; Non-Tg Ctrl vs. Tg-Ctrl: $p = 0.174$; LP vs. Tg-Ctrl: $p = 0.910$; LP vs. LC: $p = 1.000$; LP vs. LS: $p = 0.999$.]

LISPRO did not reduce anxiety-like behavior in female APP_{SWE}/PS1dE9 mice

It is estimated that more than eighty percent of dementia patients show non-cognitive psychological changes including apathy, depression, anxiety, agitation, and irritability during the progression of AD [263]. Thus, in this study, we examined anxiety by the open field and elevated plus maze tests. APP_{SWE}/PS1dE9 transgenic mice did not exhibit enhanced anxiety compared with WT mice as determined by the open field test, reflected as reduced time in center, center entries or distance traveled in center or enhanced time in periphery or distance traveled in periphery. The transgenic mice also did not exhibit impaired locomotor activity, reflected as altered total time mobile. In addition, no measure of anxiety or locomotor activity was altered by lithium treatment in the transgenic mice. [Time spent in center, $F (4, 36) = 2.985$, $p = 0.034$; Non-Tg Ctrl vs. Tg-Ctrl: $p = 0.973$; LP vs. Tg-Ctrl: $p = 0.189$; LP vs. LC: $p = 0.964$; LP vs. LS: $p = 1.000$; Figure 5-6a. Time spent in periphery, $F (4, 36) = 0.528$, $p = 0.716$; Non-Tg Ctrl vs. Tg-Ctrl: $p = 0.998$; LP vs. Tg-Ctrl: $p = 0.953$; LP vs. LC: $p = 0.958$; LP vs. LS: $p = 1.000$; Figure 5-6b. Center entries, F

(4, 36) = 0.522; p = 0.720, Non-Tg Ctrl vs. Tg-Ctrl: p = 0.721; LP vs. Tg-Ctrl: p = 0.999; LP vs. LC: p = 0.965; LP vs. LS: p = 0.982; Figure 5-6c. Distance travelled in the center, F (4, 36) = 1.242, p = 0.314; Non-Tg Ctrl vs. Tg-Ctrl: p = 0.665; LP vs. Tg-Ctrl: p = 0.596; LP vs. LC: p = 0.990; LP vs. LS: p = 0.421; Figure 5-6d. Distance travelled in periphery, F (4, 36) = 5.369, p = 0.002; Non-Tg Ctrl vs. Tg-Ctrl: p = 0.485; LP vs. Tg-Ctrl: p = 0.880; LP vs. LC: p = 0.481; LP vs. LS: p = 0.931; Figure 5-6e. Total time mobile, F (4, 36) = 4.053, p = 0.009, Non-Tg Ctrl vs. Tg-Ctrl: p = 0.360; LP vs. Tg-Ctrl: p = 0.995; LP vs. LC: p = 0.392; LP vs. LS: p = 0.996; Figure 5-6f.]

In contrast to the open field test, transgenic APP$_{SWE}$/PS1dE9 mice exhibited significantly enhanced anxiety compared with non-transgenic WT control mice, reflected as reduced time spent in the open arms of the elevated plus maze test. However, this level of anxiety was not significantly altered by LC, LS or LP treatment. In addition, no significant difference was found between nontransgenic WT and untreated and lithium-treated transgenic mice in time spent in closed arms or open or closed arm entries. Overall, these results suggest that LISPRO, LC, or LS have no effect on anxiety-like or locomotor behavior in female APP$_{SWE}$/PS1dE9 mice. [Time spent in open arms, F (4, 36) = 5.913, p = 0.001, Non-Tg Ctrl vs. Tg-Ctrl: p = 0.020; LP vs. Tg-Ctrl: p = 0.946; LP vs. LC: p = 1.000; LP vs. LS: p = 0.983; Figure 5-6g. Time spent in closed arms, F (4, 36) = 2.307, p = 0.056; Non-Tg Ctrl vs. Tg-Ctrl: p = 0.054; LP vs. Tg-Ctrl: p = 0.977; LP vs. LC: p = 0.494; LP vs. LS: p = 1.000; Figure 5-6h. Open arms entries, F (4, 36) = 1.630; p = 0.190; Non-Tg Ctrl vs. Tg-Ctrl: p = 0.600; LP vs. Tg-Ctrl: p = 0.996; LP vs. LC: p = 0.976; LP vs. LS: p = 1.000; Figure 5-6i. Closed arm entries, F (4, 36) = 2.756; p = 0.044; Non-Tg Ctrl vs. Tg-Ctrl: p = 0.680; LP vs. Tg-Ctrl: p = 0.580; LP vs. LC: p = 1.000; LP vs. LS: p = 0.759; Figure 5-6j.]

LISPRO prevented depression-like behavior in female APP$_{SWE}$/PS1dE9 mice

The prevalence of depression among AD patients has been reported to be 10 to 50% [264]. Therefore, we assessed whether 12-months old APP$_{SWE}$/PS1dE9 mice with advance state of disease progression show depressive-like behavior and whether LISPRO treatment could reverse this effect as tested by tail suspension test. Mice were individually suspended by the tail from a horizontal stand and immobility time was recorded as an index of depressive-like behavior (Figure 5-7a). While transgenic APP$_{SWE}$/PS1dE9 mice exhibited increased immobility time compared with non-transgenic WT control mice, lithium treatment with LC, LS, or LP reduced immobility time compared in the untreated transgenic mice. No statistically significant difference in immobility time was found between LP, LC, or LS treatment. These data suggest that lithium treatment as LISPRO or carbonate and salicylate salt of lithium reduces depression as a secondary effect in the treatment of AD. [F (4, 36) = 41.093; p = 0.001; Non-Tg Ctrl vs. Tg-Ctrl: p = 0.0001, LP vs. Tg-Ctrl: p = 0.0001; LP vs. LC: p = 0.999; LP vs. LS: p = 0.971; Figure 5-7a.]

LISPRO reduced irritability in female APP$_{SWE}$/PS1dE9 mice

The prevalence of irritability among AD patients was reported from 13-23% in clinical studies. In addition, transgenic APP$_{SWE}$/PS1$_{dE9}$ mice show an increased hypersensitivity to touch indicative of enhanced irritability [265]. Therefore, we examined whether LISPRO treatment reduces irritability in transgenic APP$_{SWE}$/PS1dE9 mice as determined by the touch escape test (Figure 5-7b) While transgenic APP$_{SWE}$/PS1dE9 mice showed higher irritability compared to non-transgenic WT control mice, as shown by its irritability score, LP treatment reduced irritability compared to untreated transgenic APP$_{SWE}$/PS1dE9 mice. In addition, LP treatment produced superior reduction of irritability compared with LC, but not LS, treatment. [F (4, 36) = 6.272, p =

0.001; Non-Tg Ctrl vs. Tg-Ctrl: $p = 0.013$; LP vs. Tg-Ctrl: $p = 0.0001$; LP vs. LC: $p = 0.038$; LP vs. LS: $p = 0.132$; Figure 5-7b.]

LISPRO did not did not alter motor function but lithium carbonate and salicylate treatment improved motor function compared to LISPRO treatment in female APP$_{SWE}$/PS1dE9 mice

Mild tremor and weakness is one of the common side effects for patients receiving chronic lithium treatment [266]. Therefore, we determined whether or not long-term LISPRO treatment changes motor coordination and performance in transgenic APP$_{SWE}$/PS1$_{dE9}$ mice, as determined using the accelerated rotarod test. All mice showed learning of motor functions as indicated by longer time spent on the rod and higher speed at fall over the course of three consecutive trials (Trial 1 vs. Trial 2: $p < 0.05$, within each cohort; Trial 2 vs. Trial 3: $p < 0.05$, within each cohort except LS, Figure 5-8c & d). There was no significant difference in time spent on the rod or speed at fall (RPM) between nontransgenic WT and untreated and LP-treated transgenic APP$_{SWE}$/PS1dE9 mice. However, LC and LS treatment significantly increased motor function compared to LP treatment as shown by increased latency to fall and higher speed at fall. Therefore, LP treatment did not alter motor function in APP$_{SWE}$/PS1dE9 mice, but LC and LS treatment showed improved motor function compared to LP treatment. [Latency to fall, F (4, 107) = 3.633; $p = 0.008$; Non-Tg Ctrl vs. Tg-Ctrl: $p = 0.943$; LP vs. Tg-Ctrl: $p = 0.623$; LP vs. LC: $p = 0.018$; LP vs. LS: $p = 0.024$; Figure 5-8a. Speed at fall, F (4, 107) = 3.587; $p = 0.009$; Non-Tg Ctrl vs. Tg-Ctrl: $p = 0.962$; LP vs. Tg-Ctrl: $p = 0.568$; LP vs. LC: $p = 0.016$; LP vs. LS: $p = 0.028$; Figure 5-8b.]

Discussion

Currently available medications approved by the FDA for the treatment of Alzheimer's disease only mildly reduce certain cognitive symptoms, but do not prevent the disease or slow its

progression. However, a growing body of both translational and preclinical evidence suggests that lithium may potentially have significant disease modifying therapeutic benefits for patients with mild cognitive impairment or early stage AD [200][92]. Although a few studies reported no effect of lithium chloride on Aβ levels [267][268] or even neurodegeneration induced by tau suppression [269], the overriding evidence indicates that lithium treatment effectively reduces extracellular β-amyloid [150][270] and tau hyperphosphorylation in cell culture and animal models of AD [267][271]. Likewise, intracerebroventricular injection of Aβ in zebrafish embryo impairs cognition which was successfully reversed by lithium administration [271]. Lithium has been shown to ameliorate neuropathology and restore hippocampal neurogenesis in Ts65Dn mice, a transgenic model of Down Syndrome, in which chromosome 21 with its APP gene is inherited in triplicate [272]. Gelfo et al. (2017) recently investigated the potential beneficial effects of a 30-day oral lithium treatment (0.24% lithium in diet) in preventing neuropathology and cognitive dysfunction following basal forebrain cholinergic neurodegeneration in rats. While lithium treatment did not affect choline acetyltransferase and caspase-3 activity, it significantly rescued memory deficits suggesting that lithium's therapeutic effects were not dependent on the cholinergic system [273]. Using a rat hippocampal neuron model, Dwivedi et al. (2015) reported that lithium-induced neuroprotection is associated with epigenetic modification of brain-derived neurotrophic factor (BDNF) gene promoter and altered expression of apoptotic-regulatory proteins [274].

In an initial open label feasibility and tolerability clinical trial in mild to moderate AD patients, no significant effects of lithium on cognition were observed after 1 year of treatment [275]. In another single blind multi-center trial in mild to moderate AD patients, no significant effects on cognition were observed after 10 weeks [276]. However, in these early clinical studies,

the dosage was titrated to reach a target serum lithium level based on the prophylaxis range (0.5-0.8 mmol/L) typically used for the maintenance of bipolar disorder. In a more recent double-blind placebo controlled disease modification trial, subjects with mild cognitive impairment (MCI) who received lower levels of lithium (0.25-0.5 mmol/L) had significantly lower conversion rates to AD than those receiving placebo [200]. Moreover, those who had received lithium had significantly lower CSF phospho-tau levels as well as better compliance and performance on the cognitive subscale of the Alzheimer's disease Assessment Scale [200]. In another double-blind, placebo control trial, microdoses (300 µg) of lithium daily for 15 months prevented cognitive decline in AD patients as measured by the mini-mental state examination (MMSE) compared to placebo, with the benefits starting after 6 months and persisting until the end of trial [202]. In addition, chronic lithium treatment has been also shown to increase the serum levels of BDNF in patients with early AD [277], which could be responsible for cognitive enhancement.

Despite the therapeutic potential for lithium in the treatment of AD neuropathology and cognitive impairment, lithium formulations currently available exhibit a narrow therapeutic window with an increased risk of side effects and noncompliance in elderly populations [278]. With the goal of improving lithium's therapeutic profile, we have been investigating the safety, pharmacokinetics, and therapeutic efficacy of LISPRO, a novel ionic co-crystal of lithium salicylate and l-proline, compared with lithium carbonate and lithium salicylate across a host of preclinical models of AD. Employing the same chronic dosage regimen found to reduce AD-like neuropathology in our previous study, the major findings of the present study was that chronic 8-month oral treatment with LISPRO ameliorated spatial (Figure 5-4b) and contextual memory deficits (Figure 5-5b) typically found in female $APP_{SWE}/PS1dE9$ mice at 12 months of age, without adversely effecting body or internal organ development (Figure 5-3a-b), anxiety (Figure 5-6) or

motor function (Figure 5-8). This improved spatial and associative memory function could be mediated through restoration of pre-and post-synaptic protein functions, which is shown in our previous study [150]. A further electrophysiological study is necessary to reveal the protective synaptic functions of LISPRO treatment.

In addition, LISPRO reduced depressive like behavior as assessed in the tail suspension test and irritability as assessed in the touch escape test. Similar to our previous study which found LISPRO to have a superior therapeutic profile for several neuropathological endpoints in cellular and animal models, LISPRO exhibited superior improvement in contextual memory deficits (Figure 5-5b), and amelioration of irritability (Figure 5-7b), compared with molar equivalent doses of lithium carbonate or lithium salicylate. All three formulation LISPRO, carbonate and salicylate pharmaceutics of lithium, significantly improved spatial memory deficits (Figure 5-4b) and depressive-like behavioral symptoms (Figure 5-7a) in female transgenic APP$_{SWE}$/PS1dE9 mice measured by tail suspension test (Figure 5-7a). Lithium carbonate and salicylate showed improved motor function coordination compared to LISPRO as assessed by accelerated rotarod test (Figure 5-8).

Secondary symptoms such as agitation and psychosis are common in AD and are associated with increased patient distress, increased caregiver burden, more rapid cognitive decline, greater risk of institutionalization and mortality, and increased health care costs. Unfortunately, currently available medications used often off-label to target these secondary symptoms have been reported to have long term adverse effects. For example, the FDA issued a black box warning in 2005 that antipsychotics significantly increased all-cause mortality in dementia. Moreover, valproic acid, a mood stabilizer used often off-label to treat agitation across diverse patient populations was found to significantly accelerate brain atrophy as determined by magnetic resonance imaging as well as

cognitive impairment following 1-year treatment in AD patients [279]. Therefore, the ability of chronic treatment with LISPRO to safely reduce AD-like neuropathology and cognitive deficits but also depressive like behavior and irritability in APP$_{SWE}$/PS1dE9 mice has intriguing implications if these preclinical findings translate into clinically meaningful therapeutic benefits.
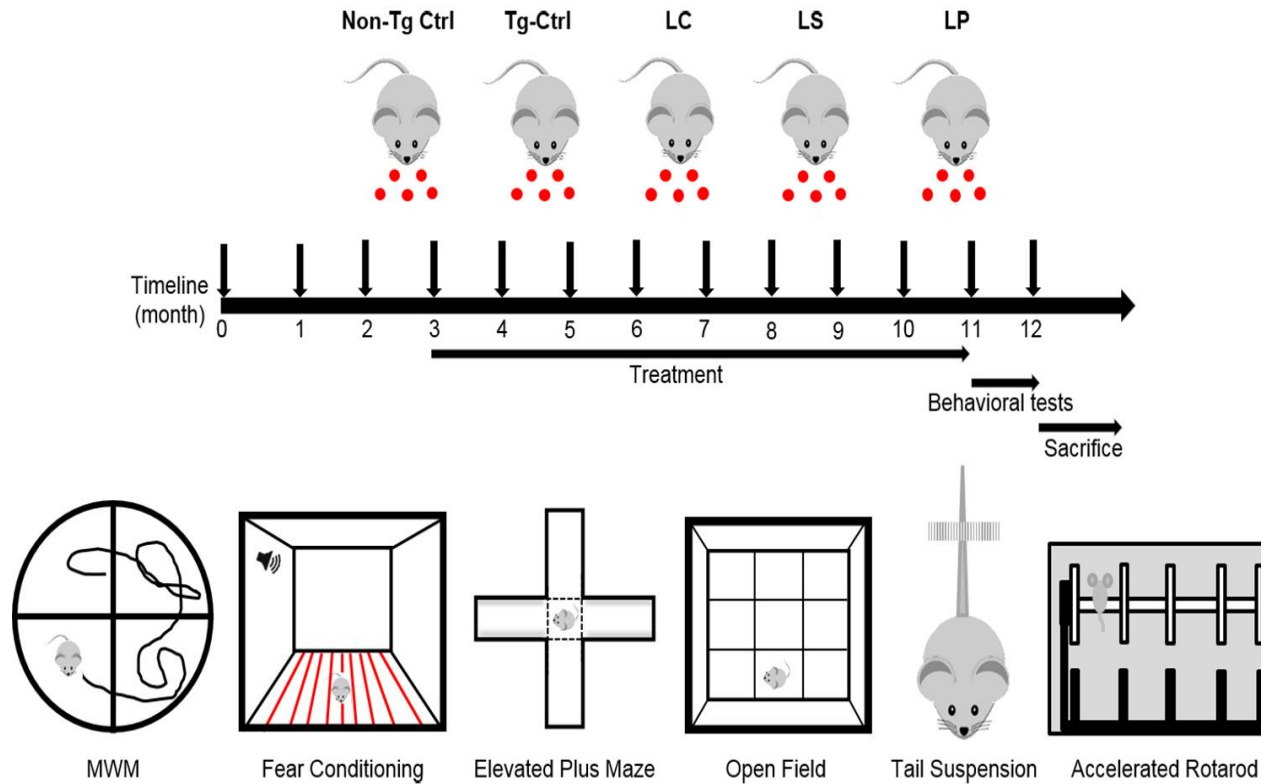
Figure 5-1 Outline of study design.

Female APP$_{SWE}$/PS1dE9 mice at 4 months of age were fed with either regular chow (Tg-Ctrl, n = 8) or chow that contained lithium carbonate (LC, 0.05% equivalent to 83 mg/kg/day, n = 6), lithium salicylate (LS, 0.20% equivalent to 325 mg/kg/day, n = 6) or lithium salicylate proline co-crystal, LISPRO (LP, 0.35% equivalent to 583 mg/kg/day, n = 8) for 9 months. In addition, aged-matched non-transgenic background control mice (B6C3F1/J, Non-Tg Ctrl, n = 10) were fed regular chow for 9 months as control. Each treatment group was subject to a battery of behavioral tests at 12 months of age and mice were sacrificed at 13 months of age.
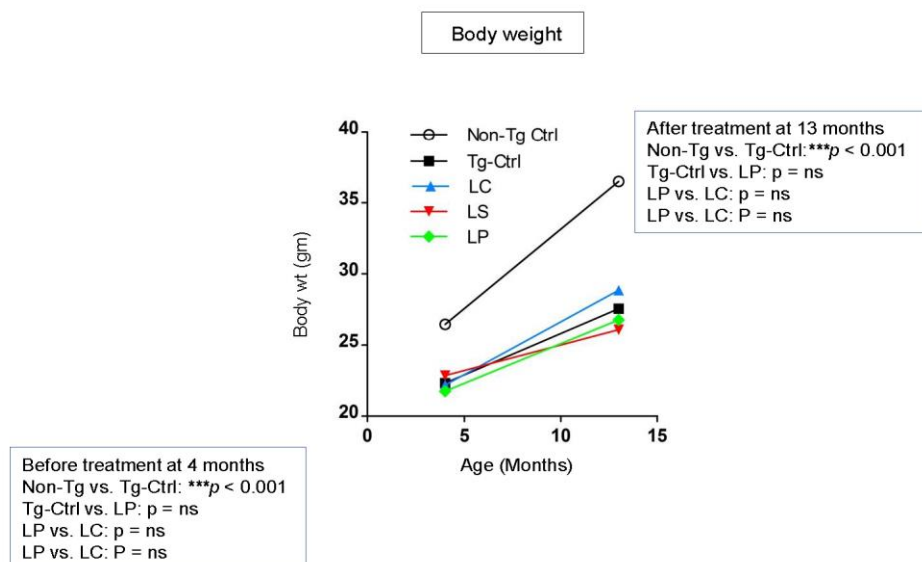
Figure 5-2 Lithium treatment did not affect body weight gain in *female APP$_{SWE}$/PS1dE9* **mice.**

Female transgenic APP$_{SWE}$/PS1dE9 mice were fed with either regular chow (Tg-Ctrl) or chow that contained lithium carbonate (LC), lithium salicylate (LS) or lithium salicylate proline co-crystal, LISPRO (LP), as described for Diagram 1. In addition, age-matched non-transgenic WT mice (B6C3F1/J, Non-Tg Ctrl) were fed normal chow as control. Each treatment group was subjected to body weight measurement at the beginning of treatment (4 months) and at the time of sacrifice (13 months). Lithium treatment (LC, LS, or LP) for nine months had no effect on weight gain compared to transgenic APP$_{SWE}$/PS1dE9 mice ($p > 0.05$ = ns). But, non-transgenic WT cohort control showed significant difference of body weight compared to transgenic cohort before (Non-Tg vs. Tg-Ctrl: ***$p < 0.001$) and after (Non-Tg vs. Tg-Ctrl: ***$p < 0.001$) the treatment. Data shown as means ± SEM. [$p > 0.05$ = non-significant = ns; *$p < 0.05$; **$p < 0.01$; ***$p < 0.001$]

143
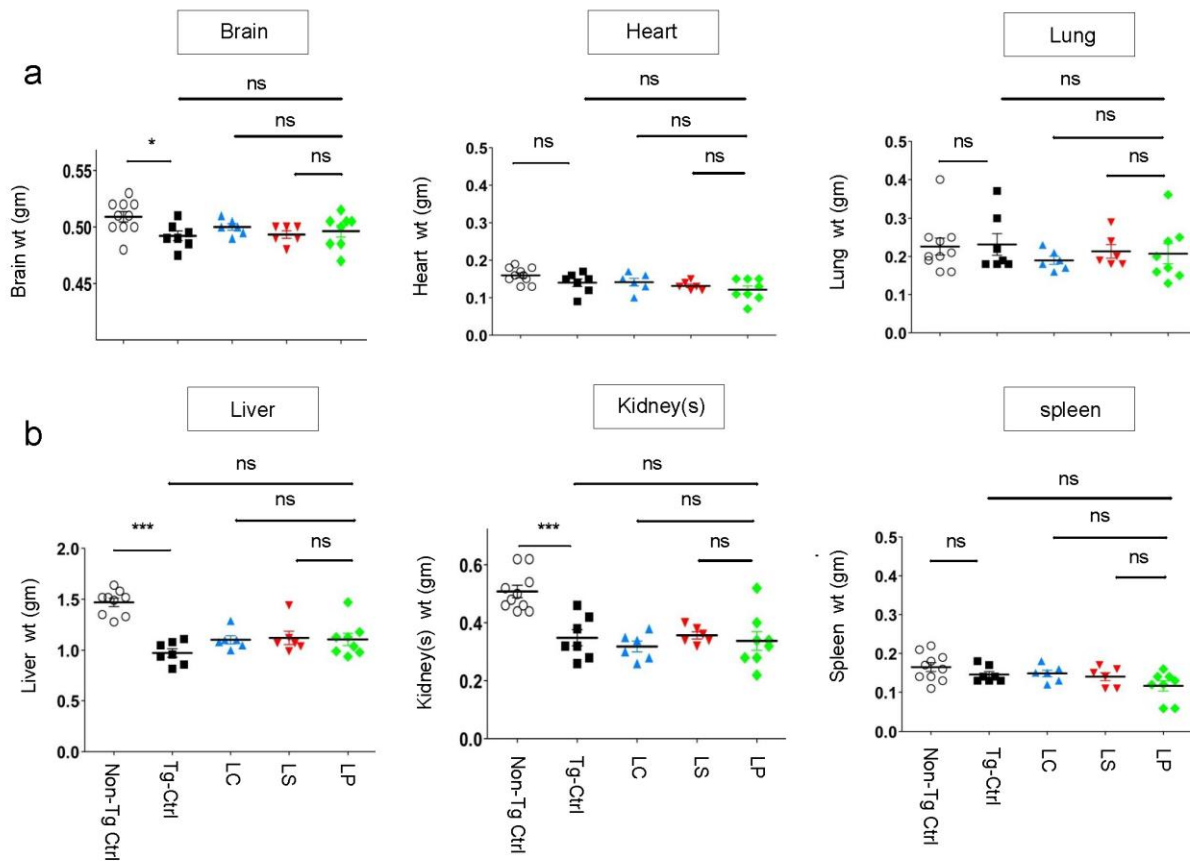
Figure 5-3 LISPRO treatments did not affect growth of internal organs in APP_{SWE}/PS1dE9 mice.

The weight of brain (a**,** left upper panel), heart (a**,** middle upper panel), lung (a**,** right upper panel), liver (b, left lower panel), kidney(s) (b, middle lower panel), and spleen (b**,** right lower panel) were determined at time of sacrifice in female APP$_{SWE}$/PS1dE9 cohort fed normal chow (Tg-Ctrl) or chow containing LC, LS, or LP as well as aged-matched non-transgenic WT control cohort fed normal chow (Non-Tg Ctrl), as described for Diagram 1. No significant differences in the weight of internal organs were observed after 9-months treatment with LP, LC, or LS compared with untreated APP$_{SWE}$/PS1dE9 mice ($p > 0.05$ = ns). Data shown as means ± SEM. [$p > 0.05$ = non-significant = ns; *$p < 0.05$; **$p < 0.01$; ***$p < 0.001$]
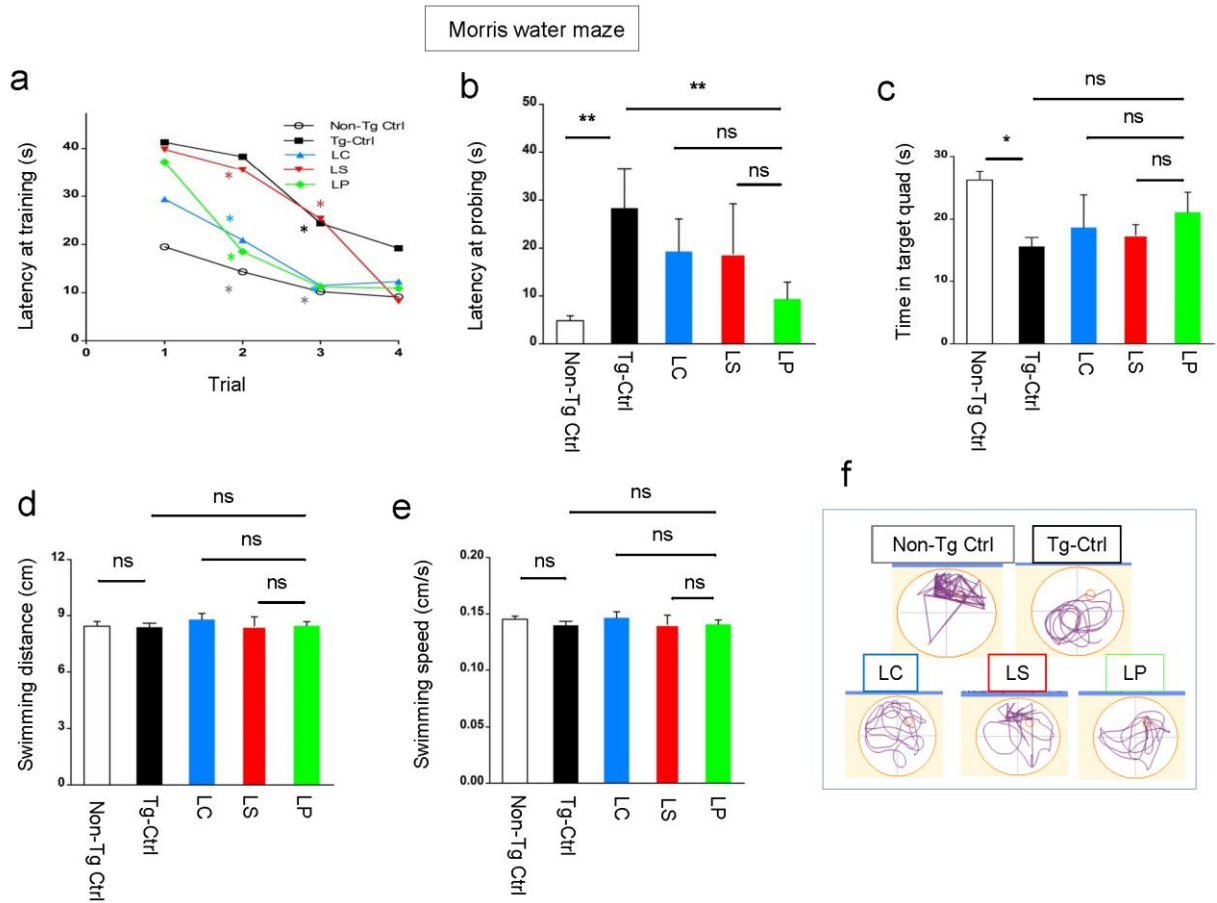
Figure 5-4 Spatial memory deficits in APP_SWE/PS1dE9 mice are improved by chronic LISPRO treatment.

Female APP_SWE/PS1dE9 and non-transgenic WT control mice were fed normal chow or chow containing LC, LS, or LP as described for Diagram 1 followed by MWM testing. (a) Latency to find the hidden platform was determined during the training period during four trials. During the training period, the untreated transgenic APP_SWE/PS1dE9 cohort (Tg-Ctrl) took significantly more time to find the platform compared with the non-transgenic control mice (Non-Tg Ctrl), indicating a deficit in spatial learning. All three lithium treatments (LC, LS, and LP) significantly reduced spatial learning deficit (**$p < 0.01$), as indicated by reduced latency, compared with the previous trial within the same cohort. (b) Latency to find platform target was determined during the probe trial of MWM, performed 24 h after the last training trial. Transgenic APP_SWE/PS1dE9 cohort took more time to find the target platform than the non-transgenic WT cohort (**$p < 0.01$) and LP treatment reversed this learning deficit (**$p < 0.01$). (c) Time spent in target quadrant was determined for probe trial. No significant differences were found in time spent in target quadrant for lithium treated- and transgenic cohort ($p > 0.05 = $ ns). In addition, no statistically significant differences were found in (d) total swimming distance travelled ($p > 0.05 = $ ns) and (e) mean swimming speed ($p > 0.05 = $ ns) during the probe trials. (f) Swim tracking plot during probe trial. Data shown as means $\pm$ SEM. [$p > 0.05 = $ non-significant $= $ ns; *$p < 0.05$; **$p < 0.01$; ***$p < 0.001$]
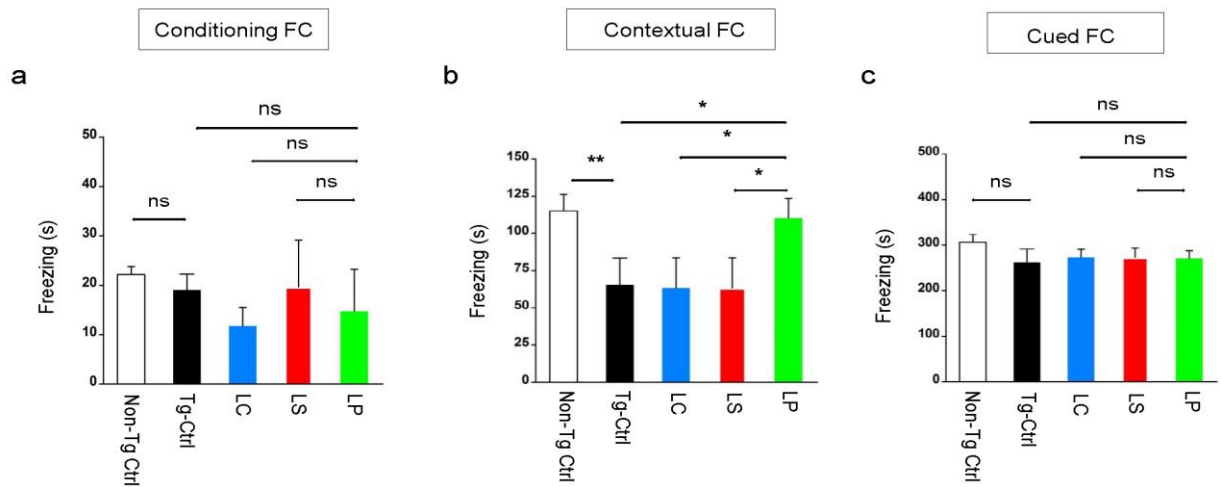
Figure 5-5 LISPRO improves associative-learning and memory on contextual fear conditioning in female APP$_{SWE}$/PS1dE9 mice.

Female transgenic APP$_{SWE}$/PS1dE9 and non-transgenic WT control cohort were fed with normal chow or chow containing LC, LS, or LP as described for Diagram 1, followed by contextual and cued fear conditioning testing. (a) No statistically significant differences for freezing time were found during the conditioning training between non-transgenic WT control (Non-Tg Ctrl) and transgenic APP$_{SWE}$/PS1dE9 control (Tg-Ctrl) or treated with LC, LS, or LP ($p > 0.05$ = ns). (b) No statistically significant difference in contextual freezing times were found among transgenic APP$_{SWE}$/PS1dE9 mice untreated or treated with LC, LS, or LP at 2 or 7 days after conditioning ($p > 0.05$). However, contextual freezing time after 21 days-conditioning was significantly longer for transgenic APP$_{SWE}$/PS1dE9 mice treated with LP compared with transgenic APP$_{SWE}$/PS1dE9 cohort control (*$p < 0.05$), LC (*$p < 0.05$), and LS (*$p < 0.05$) cohort. (c) No statistically significant difference in cued freezing time was found among nontransgenic WT control and transgenic APP$_{SWE}$/PS1dE9 cohort control or treated with LC, LS, or LP ($p > 0.05$ = ns, in all case) in the same time period recorded. Data shown as means ± SEM. [$p > 0.05$ = non-significant = ns; *$p < 0.05$; **$p < 0.01$; ***$p < 0.001$]

146

Open field

a ns / ns / ns / ns — Time in center (s)
b ns / ns / ns / ns — Time in periphery (s)
c ns / ns / ns / ns — Center entries (n)
d ns / ns / ns / ns — Distance travelled in center (m)
e ns / ns / ns / ns — Distance travelled in periphery (m)
f ns / ns / ns / ns — Total time mobile (s)

Open arm

Closed arm

g * / ns / ns / ns — Time spent (s)
h ns / ns / ns / ns — Time spent (s)
i ns / ns / ns / ns — Entries (n)
j ns / ns / ns / ns — Entries (n)

Non-Tg Ctrl, Tg-Ctrl, LC, LS, LP
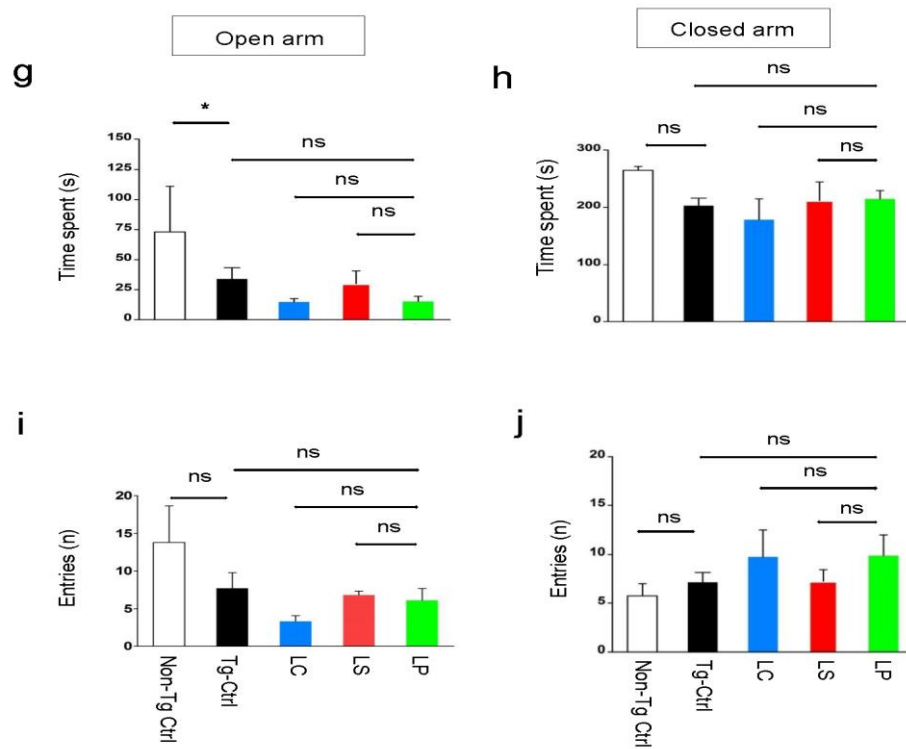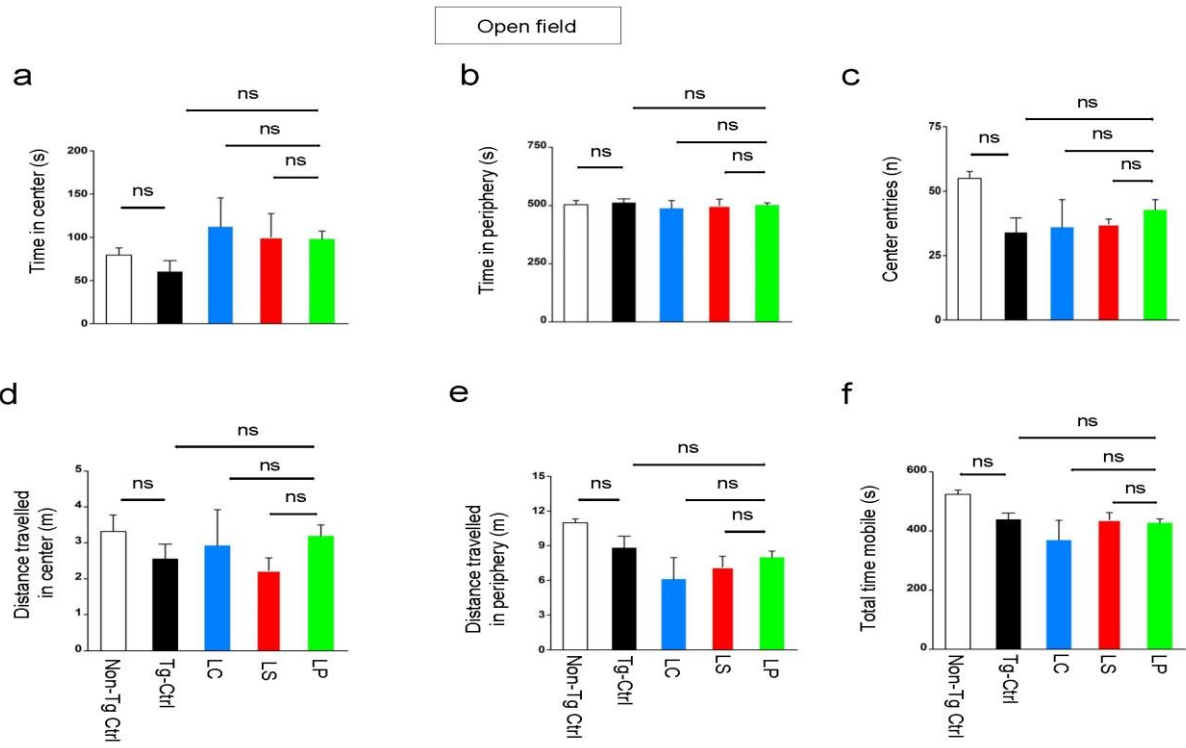
Figure 5-6 LISPRO does not improve anxiety-like behavior or locomotor activity in APP$_{SWE}$/PS1dE9 mice.

Female APP$_{SWE}$/PS1dE9 mice (Tg-Ctrl) exhibited statistically non-significant anxiety-like behavior and locomotor impairment as shown by (c) reduced center entries ($p > 0.05$) and (d) reduced time spent mobile ($p > 0.05$), respectively, compared with non-transgenic WT cohort control during open field testing. No statistically significant differences were observed among transgenic APP$_{SWE}$/PS1dE9 cohort or treated with LC, LS, or LP in (a) time spent in center or (b) periphery, (c) number of center entries, (d) distance travelled in center or (e) periphery or (f) total mobile time. Likewise, transgenic APP$_{SWE}$/PS1dE9 cohort exhibited anxiety as shown by statistically significant reduced (g) time spent (*$p < 0.05$) and (**i**) statistically non-significant but reduced entries in open arms in elevated plus maze test ($p > 0.05$). Similarly, no statistically significant differences were observed among transgenic APP$_{SWE}$/PS1dE9 cohort or treated with LC, LS, or LP in (g) time spent and entries (g & i) in open or (h & j) closed arms ($p > 0.05$; in all case). Data shown as means ± SEM. [$p > 0.05$ = non-significant = ns; *$p < 0.05$; **$p < 0.01$; ***$p < 0.001$]
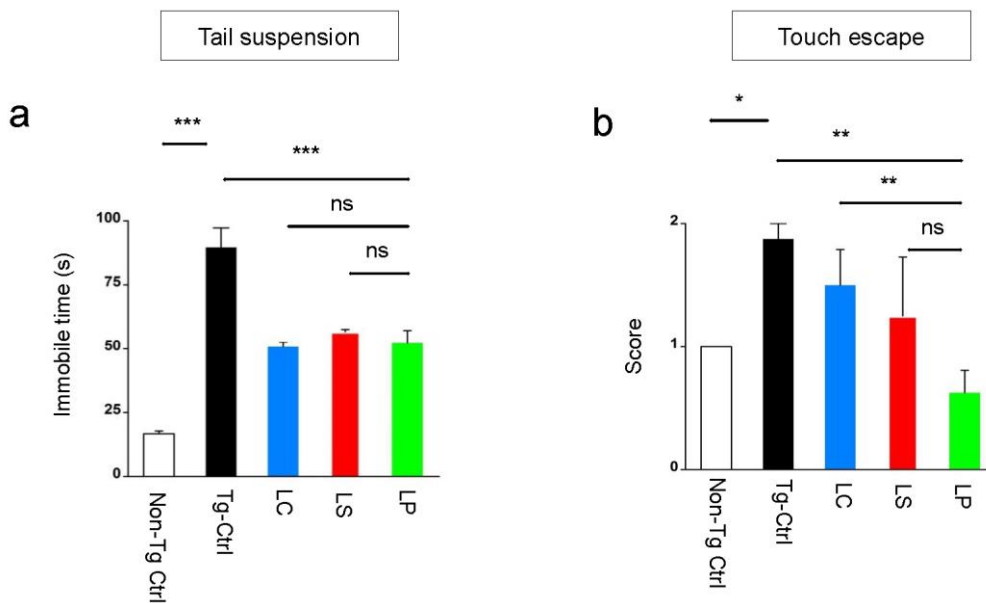
Figure 5-7 LISPRO reduces depressive-like behavior and irritability in APPSWE/PS1dE9 mice.

Female transgenic APPSWE/PS1dE9 cohort (Tg-Ctrl) exhibited depressive-like behavior compared with nontransgenic WT cohort control (Non-Tg Ctrl vs. Tg-Ctrl: ***$p < 0.001$) as shown by increased immobility time in tail suspension test, which was reduced by LC, LS, and LP treatment (a, Tg-Ctrl vs. LP: ***$p < 0.001$).   In addition, transgenic APPSWE/PS1dE9 cohort exhibited increased irritability as shown by increased irritability score in touch escape test compared to nontransgenic WT cohort control (Non-Tg Ctrl vs. Tg-Ctrl: *$p < 0.05$) , which was reversed by LP, and LS treatment (b, **$p < 0.01$). In addition, a statistically significant reduction in irritability score was found between LP and LC treatment (**$p < 0.01$). Data shown as means ± SEM. [$p > 0.05$ = non-significant = ns; *$p < 0.05$; **$p < 0.01$; ***$p < 0.001$]
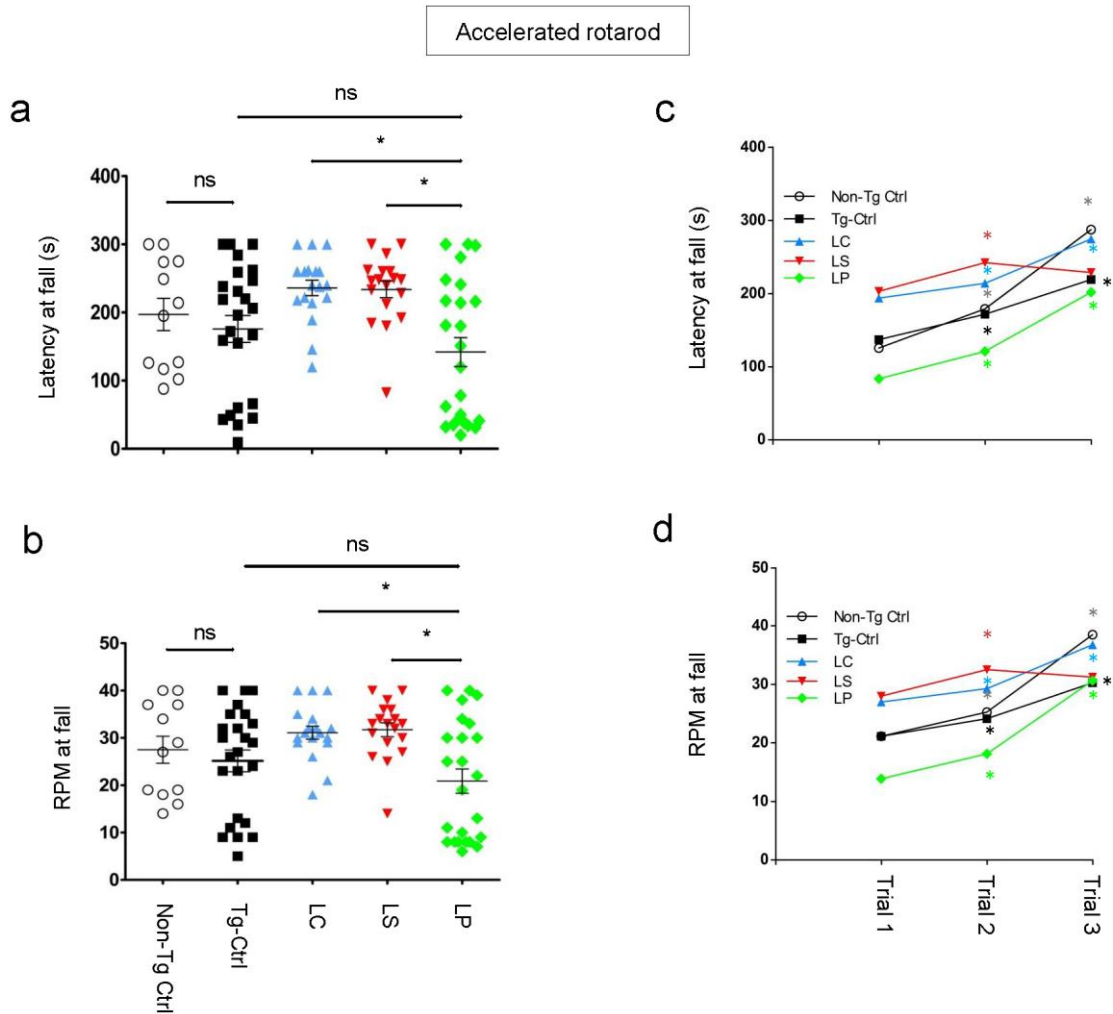
Figure 5-8 Not LISPRO but carbonate and salicylate treatment showed improved motor function compared to LISPRO in female APP$_{SWE}$/PS1dE9 mice.

Female transgenic APP$_{SWE}$/PS1dE9 cohort control (Tg Ctrl) did not exhibit altered motor coordination compared with nontransgenic WT cohort control (Non-Tg Ctrl), as determined by (a) latency to fall (Non-Tg Ctrl vs. Tg-Ctrl: $p > 0.05$ = ns) or (b) RPM at fall (Non-Tg Ctrl vs. Tg-Ctrl: $p > 0.05$ = ns) throughout three consecutive trials of accelerated rotarod testing. In addition, motor coordination did not differ between transgenic APP$_{SWE}$/PS1dE9 and LP treated cohort (LP vs. Tg-Ctrl: $p > 0.05$ = ns). Both LC and LS treatment showed improved motor function compared to LISPRO during (a) latency at fall (LP vs. LC: $p < 0.01$; LP vs. LS: $p < 0.01$) and (b) lower speed at fall [LP vs. LC: $p < 0.01$; LP vs. LS: $p < 0.01$). Both non-transgenic WT control and transgenic treated or control exhibited enhanced motor function learning compared with the previous trials as determined by (**c**) increased latency to fall and (d) increased maximum speed at fall over three consecutive trials. Data shown as means ± SEM. [$p > 0.05$ = non-significant = ns; *$p < 0.05$; **$p < 0.01$; ***$p < 0.001$]

CHAPTER 6

DISCUSSION

AD is the most common cause of dementia among the elderly. APP is strongly implicated in dysregulated amyloidogenic processing, synthesis, and subsequent release of Aβ peptides. The aggregation of Aβ peptides as plaques and accumulation of hyperphosphorylated tau as neurofibrillary tangles are two core AD neuropathological features. Neuronal dysfunction and cell death occurs as a result of protein misfolding and aggregations. Progressive neurodegeneration in the cortex and hippocampus causes atrophy (shrinkage) and ventricular enlargement, particularly involving the frontal, parietal, and temporal lobes. The disease progress is associated with gradual cognitive deterioration and associated decline in different aspects of daily life activities which include working memory, language, and executive functions such as organization and planning. To date, no effective disease-modifying treatments exist for AD. Currently available treatments of AD include acetylcholinesterase inhibitor and NMDA- receptor antagonist, which are safe and reported to show mild to moderate symptomatic benefits in several independent studies. However, these drugs do not stop the deterioration of cognitive functions in AD patients. Therapeutic approaches that lower or inhibit the formation of Aβ and restrain the pathological transformation of tau are capable of slowing down disease progression. The development of novel drugs for AD with strong disease-modifying approaches is one of the biggest unmet clinical needs in global

health care system. Thus, the search for novel biological and pharmacological approaches targeting the molecular events underlying the pathogenesis has been a major goal of our research.

Research in recent years has indicated that blood circulatory system can modulate brain physiology and pathology in normal aging and neurodegenerative conditions such as AD. Factors those are required for maintenance of tissue homeostasis start to decrease, while factors involved in injury-repair and inflammation increase as we get older [40]. In a study of parabiosis, a surgically connecting shared blood system of 3- and 18- month- old mouse study showed increased number of neural stem cells, increased activity of synapses, increased expression of genes involved in formation of new memories, and decreased inflammation in this model of old mouse brain [41]. The same group also discovered that soluble factors responsible for this beneficial effect in young-old parabiosis mouse model, as no evidence of blood cells entry was found in the brain [75]. More interestingly, studies on a mouse model for aging have shown that intravenously transfused young human plasma rejuvenate age-related changes in old mice brain and improve cognitive function as assessed *via* Barnes maze test [156]. Such results indicate that soluble factors in young blood possess enormous potential to reverse age-related impairments in the brain structure and cognitive functions. Beyond aging studies, one of our collaborators also performed a parabiosis study by joining transgenic APPswe/PS1dE9 amyloid and WT aged-matched background control mice. The study data show that peripheral system plays crucial role in the clearance of Aβ in transgenic APPswe/PS1dE9 AD mice [157]. Recent advances in cord blood research emphasize the therapeutic possibility of HUCBC in several CNS disorders including AD. HUCBC possess anti-inflammatory and immune modulatory potential with self-renewal capabilities. We hypothesized that HUCBS may also possess anti-inflammatory immunomodulatory therapeutic potential for AD and other dementias. The study outlined in this PhD dissertation is the first to demonstrate that

152

HUCBS contain α-secretase-like enzyme that has significant potential to produce sAPPα compared to adult and aged blood serum (Chapter 2). In this study, we have isolated and purified a fraction enriched in α-secretase like enzyme (termed as α-CBSF) from HUCBS with thousand-fold more sAPPα producing capacity than the original fraction. Identification and purification of this novel enzyme has enormous therapeutic significance for subset of patients suffering from AD with low levels of sAPPα. The neuroprotective functions of sAPPα in neuronal environment have been evidenced by several independent studies [56]. As outlined in the introduction, sAPPα has neurotrophic and neuroprotective properties by preventing neuronal cell death in AD brain. Additionally, others and we have shown that sAPPα decrease amyloid [42] and tau pathology [43] by inhibiting BACE1 and GSK3β enzyme in rodent models. While the neuroprotective and anti-AD effect of sAPPα is well established, αCBSF infusion for 6 weeks *via* osmotic minipump showed improvement of cognitive functions and reduction of amyloid load in cerebral cortex and hippocampus in transgenic 5XFAD mice. In further studies, we tried to identify the heat-sensitive protein factor(s) from αCBSF. Our study identified a novel role for complement protein C1 in the cell culture system. Multi-step fractionation followed by LC-MS/MS analyses of αCBSF has identified several proteins compared to AgBSF, each of which could potentially generate sAPPα by cleaving APP in cellular system. Utilizing *in vitro* CHO/APPwt, N2a/APPwt, and TgAPPwt primary neuronal cell lines, we found that α-secretase-like enzyme produce sAPPα may be mediated by complement protein C1 (Chapter 3). This result indicates that complement protein C1 might play a crucial role in the brain during APP processing and progression of AD. Although our preliminary data suggest that complement protein C1 is a novel candidate for APP cleavage in cellular condition, further investigation is needed to translate these findings in preclinical models brain.

Lithium has a long history in treating bipolar disorder and other psychiatric conditions. In 1859, Lange used lithium as a prophylactic for depressive illness. After a long break, Cade in 1949 reintroduced lithium salts to treat manic-depressive illness, currently known as bipolar disorder. Subsequently in 1954, Schou and colleagues conducted the first randomized controlled trial and showed that lithium salt has better anti-manic treatment effects compared to electroconvulsive therapy [198]. Despite the strong evidence that lithium salt has neuroprotective potential to treat several diseases, currently available lithium pharmaceutics exhibit a narrow therapeutic window with an increased risk of side effects and noncompliance in elderly populations [278]. To examine lithium's therapeutic profile, we have investigated the safety, pharmacokinetics, and therapeutic efficacy of LISPRO, in comparison with lithium carbonate and the parent lithium salicylate salts in preclinical models of AD. Pharmacokinetic studies indicated that LISPRO provided significantly higher brain lithium levels and more steady plasma lithium levels in both normal and transgenic Alzheimer's-like mice when compared to lithium carbonate. We predict that LISPRO might prevent the drastic change of lithium levels in the plasma seen with current lithium drugs, maintain stable therapeutic doses and, thus, would represent a significant improvement over current lithium medicines for a desired time by slow-release into the peripheral blood. While examining the inflammatory safety profiles, a 2-week oral treatment of lithium carbonate in normal mice increased proinflammatory cyclooxygenase-2 expression in the kidneys, while the molar equivalent of lithium administered as LISPRO did not. Although lithium has anti-inflammatory properties, several studies indicate that chronic administration of lithium might induce COX2 expression through inhibition of GSK3β activity. Our data also showed that both lithium carbonate and LISPRO inactivate GSK3β, but only lithium carbonate activates COX2 whereas LISPRO suppresses COX2 due to the anti-inflammatory properties of the salicylate anion. While

investigating the therapeutic efficacy, we found that 8- as well as 28-week treatment with LISPRO produced superior reduction of hippocampal brain pathology, including Aβ plaque deposition, neuroinflammation, and neurodegeneration in transgenic Alzheimer's-like mice models [150]. It has been reported that lithium prevents the generation of Aβ peptides by inhibiting GSK3α activity, which interferes with APP γ-secretase cleavage. Addition of salicylate, which is the primary metabolite derivative of acetyl-salicylic acid, improves the safety and might modify the pharmacological action of lithium. Moreover, several lines of evidence demonstrated that lithium is a direct inhibitor of GSK3β and also increases the inhibitory serine-phosphorylation. Using human HeLa/tau, human neuroblastoma SHSY-5Y, and primary neuronal cell lines, we found that LISPRO inhibits phosphorylation of tau, which is associated with increasing inhibitory phosphorylation of GSK3β (Ser^9). Additionally, both 8- and 28-week LISPRO treatment significantly reduces p-tau (Thr^{231}) phosphorylation compared to Li$_2$CO$_3$ and control in Tg2576 and 3XTg-AD mice tested using immunohistochemistry [p-tau (Thr^{231}) and p-tau (Ser^{396})] and western blot analyses [p-tau (Ser^{396}, Ser^{404}, Thr^{181}, and Thr^{231})], and in many cases lithium salicylate, significantly attenuates tau phosphorylation compared to lithium carbonate and control. Taken together, these findings indicated that LISPRO inactivates GSK3β activity, and thereby reduces tau phosphorylation, microglial inflammation, GSK3β activity, and was superior to lithium carbonate in enhancing neuronal stem cell differentiation (Chapter 4). While examining the effect of LISPRO and other two lithium drugs on behavioral functions, we found that LISPRO exhibited superior improvement in contextual memory deficits, and amelioration of irritability, compared with molar equivalent doses of lithium carbonate or lithium salicylate. All three formulations LISPRO, carbonate and salicylate pharmaceutics of lithium, significantly improved spatial memory deficits and depressive-like behavioral symptoms in transgenic APPswe/PS1dE9

155

mice measured by tail suspension test. Lithium carbonate and salicylate showed improved motor function coordination compared to LISPRO as assessed by accelerated rotarod test (Chapter 5). Therefore, it is evident that chronic treatment with LISPRO can not only safely reduce AD-like neuropathology and cognitive deficits, but also reduce the depressive like behavior and irritability in APPswe/PS1dE9 mice. These preclinical findings/results have intriguing implications if they translate into clinically meaningful therapeutic benefits.

REFERENCES

[1]   J. Hardy and D. Allsop, "Amyloid deposition as the central event in the aetiology of Alzheimer's disease," *Trends Pharmacol Sci*, vol. 12, no. 10, pp. 383–388, 1991.

[2]   M. Goedert, M. G. Spillantini, and R. A. Crowther, "Tau proteins and neurofibrillary degeneration," *Brain Pathol*, vol. 1, no. 4, pp. 279–286, 1991.

[3]   J. J. Palop and L. Mucke, "Amyloid-β–induced neuronal dysfunction in Alzheimer's disease: from synapses toward neural networks," *Nat. Neurosci.*, vol. 13, no. 7, pp. 812–818, Jul. 2010.

[4]   Alzheimer's Association. 2018, "2018 Alzheimer's Disease Facts and Figures Includes a Special Report on the Financial and Personal Benefits of Early Diagnosis," *Alzheimers Dement* , vol. 14, no. 3, pp. 367–429, 2018.

[5]   C. Haass and D. J. Selkoe, "Cellular processing of beta-amyloid precursor protein and the genesis of amyloid beta-peptide.," *Cell*, vol. 75, no. 6, pp. 1039–42, Dec. 1993.

[6]   J. Kang *et al.*, "The precursor of Alzheimer's disease amyloid A4 protein resembles a cell-surface receptor," *Nature*, vol. 325, no. 6106, pp. 733–736, Feb. 1987.

[7]   T. Jefferson *et al.*, "Metalloprotease Meprin β Generates Nontoxic N-terminal Amyloid Precursor Protein Fragments *in Vivo*," *J. Biol. Chem.*, vol. 286, no. 31, pp. 27741–27750, Aug. 2011.

[8]   J. Bien *et al.*, "The Metalloprotease Meprin β Generates Amino Terminal-truncated Amyloid β Peptide Species," *J. Biol. Chem.*, vol. 287, no. 40, pp. 33304–33313, Sep. 2012.

[9]   C. Schönherr *et al.*, "Generation of aggregation prone N-terminally truncated amyloid β peptides by meprin β depends on the sequence specificity at the cleavage site," *Mol. Neurodegener.*, vol. 11, no. 1, p. 19, Dec. 2016.

[10]   M. Willem *et al.*, "η-Secretase processing of APP inhibits neuronal activity in the hippocampus," *Nature*, vol. 526, no. 7573, pp. 443–447, Oct. 2015.

[11]   S. G. Younkin, "Evidence that Aβ42 is the real culprit in Alzheimer's disease," *Ann. Neurol.*, vol. 37, no. 3, pp. 287–288, Mar. 1995.

[12]   T. Iwatsubo, D. M. A. Mann, A. Odaka, N. Suzuki, and Y. Ihara, "Amyloid β protein (Aβ) deposition: Aβ42(43) precedes Aβ40 in down Syndrome," *Ann. Neurol.*, vol. 37, no. 3, pp. 294–299, Mar. 1995.

[13]   T. Maurice, B. P. Lockhart, and A. Privat, "Amnesia induced in mice by centrally administered beta-amyloid peptides involves cholinergic dysfunction.," *Brain Res.*, vol. 706, no. 2, pp. 181–93, Jan. 1996.

[14]   J. Cleary, J. M. Hittner, M. Semotuk, P. Mantyh, and E. O'Hare, "Beta-amyloid(1-40) effects on behavior and memory.," *Brain Res.*, vol. 682, no. 1–2, pp. 69–74, Jun. 1995.

[15]   B. A. Yankner, L. R. Dawes, S. Fisher, L. Villa-Komaroff, M. L. Oster-Granite, and R. L. Neve, "Neurotoxicity of a fragment of the amyloid precursor associated with Alzheimer's disease.," *Science*, vol. 245, no. 4916, pp. 417–20, Jul. 1989.

[16]   L. Mucke and D. J. Selkoe, "Neurotoxicity of Amyloid -Protein: Synaptic and Network Dysfunction," *Cold Spring Harb. Perspect. Med.*, vol. 2, no. 7, pp. a006338–a006338, Jul.

2012.

[17] T. L. Spires-Jones and B. T. Hyman, "The Intersection of Amyloid Beta and Tau at Synapses in Alzheimer's Disease," *Neuron*, vol. 82, no. 4, pp. 756–771, May 2014.

[18] P. T. Nelson *et al.*, "Correlation of Alzheimer Disease Neuropathologic Changes With Cognitive Status: A Review of the Literature," *J. Neuropathol. Exp. Neurol.*, vol. 71, no. 5, pp. 362–381, May 2012.

[19] S. T. Ferreira, M. V. Lourenco, M. M. Oliveira, and F. G. De Felice, "Soluble amyloid-β oligomers as synaptotoxins leading to cognitive impairment in Alzheimer's disease," *Front. Cell. Neurosci.*, vol. 9, p. 191, May 2015.

[20] M. E. Larson and S. E. Lesné, "Soluble Aβ oligomer production and toxicity," *J. Neurochem.*, vol. 120, pp. 125–139, Jan. 2012.

[21] C. M. Waterman-Storer, "Microtubules and microscopes: how the development of light microscopic imaging technologies has contributed to discoveries about microtubule dynamics in living cells.," *Mol. Biol. Cell*, vol. 9, no. 12, pp. 3263–71, Dec. 1998.

[22] J. Avila *et al.*, "Tau Structures.," *Front. Aging Neurosci.*, vol. 8, p. 262, 2016.

[23] A. Mietelska-Porowska, U. Wasik, M. Goras, A. Filipek, and G. Niewiadomska, "Tau Protein Modifications and Interactions: Their Role in Function and Dysfunction," *Int. J. Mol. Sci.*, vol. 15, no. 3, pp. 4671–4713, Mar. 2014.

[24] L. Martin, X. Latypova, and F. Terro, "Post-translational modifications of tau protein: Implications for Alzheimer's disease," *Neurochem. Int.*, vol. 58, no. 4, pp. 458–471, Mar. 2011.

[25] M. Pevalova, P. Filipcik, M. Novak, J. Avila, and K. Iqbal, "Post-translational modifications of tau protein.," *Bratisl. Lek. Listy*, vol. 107, no. 9–10, pp. 346–53, 2006.

[26] P. T. Nelson, H. Braak, and W. R. Markesbery, "Neuropathology and cognitive impairment in Alzheimer disease: a complex but coherent relationship.," *J. Neuropathol. Exp. Neurol.*, vol. 68, no. 1, pp. 1–14, Jan. 2009.

[27] R. Cacace, K. Sleegers, and C. Van Broeckhoven, "Molecular genetics of early-onset Alzheimer's disease revisited," *Alzheimer's Dement.*, vol. 12, no. 6, pp. 733–748, Jun. 2016.

[28] F. K. Wiseman *et al.*, "A genetic cause of Alzheimer disease: mechanistic insights from Down syndrome.," *Nat. Rev. Neurosci.*, vol. 16, no. 9, pp. 564–74, Sep. 2015.

[29] S. L. Rosenthal and M. I. Kamboh, "Late-Onset Alzheimer's Disease Genes and the Potentially Implicated Pathways.," *Curr. Genet. Med. Rep.*, vol. 2, no. 2, pp. 85–101, 2014.

[30] J. Cummings, G. Lee, T. Mortsdorf, A. Ritter, and K. Zhong, "Alzheimer's disease drug development pipeline: 2017.," *Alzheimer's Dement. (New York, N. Y.)*, vol. 3, no. 3, pp. 367–384, Sep. 2017.

[31] F. Mangialasche, A. Solomon, B. Winblad, P. Mecocci, and M. Kivipelto, "Alzheimer's disease: clinical trials and drug development.," *Lancet. Neurol.*, vol. 9, no. 7, pp. 702–16, Jul. 2010.

[32] A. D. Bachstetter *et al.*, "Peripheral injection of human umbilical cord blood stimulates neurogenesis in the aged rat brain," *BMC Neurosci.*, vol. 9, no. 1, p. 22, Feb. 2008.

[33] D. Ilic, C. Miere, and E. Lazic, "Umbilical cord blood stem cells: clinical trials in non-hematological disorders," *Br. Med. Bull.*, vol. 102, no. 1, pp. 43–57, Jun. 2012.

[34] J. D. Newcomb, P. R. Sanberg, S. K. Klasko, and A. E. Willing, "Umbilical cord blood research: current and future perspectives.," *Cell Transplant.*, vol. 16, no. 2, pp. 151–8, 2007.

[35] P. R. Sanberg *et al.*, "The Treatment of Neurodegenerative Disorders Using Umbilical Cord Blood and Menstrual Blood-Derived Stem Cells," *Cell Transplant.*, vol. 20, no. 1, pp. 85–94, Feb. 2011.

[36] B. R. Achyut, N. R. S. Varma, and A. S. Arbab, "Application of Umbilical Cord Blood Derived Stem Cells in Diseases of the Nervous System," *J. Stem Cell Res. Ther.*, vol. 4, no. 5, 2014.

[37] W. V. Nikolic *et al.*, "Peripherally Administered Human Umbilical Cord Blood Cells Reduce Parenchymal and Vascular beta-Amyloid Deposits in Alzheimer Mice," *Stem Cells Dev.*, vol. 17, no. 3, pp. 423–439, Jun. 2008.

[38] D. Darlington *et al.*, "Human Umbilical Cord Blood-Derived Monocytes Improve Cognitive Deficits and Reduce Amyloid-β Pathology in PSAPP Mice," *Cell Transplant.*, vol. 24, no. 11, pp. 2237–2250, Nov. 2015.

[39] Y. Xing, Y. Wu, L. Wang, and X. Meng, "Human umbilical cord blood cell transplantation improves cardiac function in a myoardial infarction rat model but induces intestinal graft versus host disease.," *Cell. Mol. Biol. (Noisy-le-grand).*, vol. 60, no. 2, pp. 6–12, Jun. 2014.

[40] S. A. Villeda *et al.*, "The ageing systemic milieu negatively regulates neurogenesis and cognitive function," *Nature*, vol. 477, no. 7362, pp. 90–94, Sep. 2011.

[41] S. A. Villeda *et al.*, "Young blood reverses age-related impairments in cognitive function and synaptic plasticity in mice," *Nat. Med.*, vol. 20, no. 6, pp. 659–663, Jun. 2014.

[42] D. Obregon *et al.*, "Soluble amyloid precursor protein-alpha modulates beta-secretase activity and amyloid-beta generation," *Nat Commun*, vol. 3, p. 777, 2012.

[43] J. Deng *et al.*, "Soluble amyloid precursor protein alpha inhibits tau phosphorylation through modulation of GSK3beta signaling pathway," *J Neurochem*, vol. 135, no. 3, pp. 630–637, 2015.

[44] L. Lannfelt, H. Basun, L. O. Wahlund, B. A. Rowe, and S. L. Wagner, "Decreased alpha-secretase-cleaved amyloid precursor protein as a diagnostic marker for Alzheimer's disease.," *Nat. Med.*, vol. 1, no. 8, pp. 829–32, Aug. 1995.

[45] K. Sennvik, J. Fastbom, M. Blomberg, L. O. Wahlund, B. Winblad, and E. Benedikz, "Levels of alpha- and beta-secretase cleaved amyloid precursor protein in the cerebrospinal fluid of Alzheimer's disease patients.," *Neurosci. Lett.*, vol. 278, no. 3, pp. 169–72, Jan. 2000.

[46] Y. Goodman and M. P. Mattson, "Secreted Forms of β-Amyloid Precursor Protein Protect Hippocampal Neurons against Amyloid β-Peptide-Induced Oxidative Injury," *Exp. Neurol.*, vol. 128, no. 1, pp. 1–12, Jul. 1994.

[47] M. Gralle, M. G. Botelho, and F. S. Wouters, "Neuroprotective Secreted Amyloid Precursor Protein Acts by Disrupting Amyloid Precursor Protein Dimers," *J. Biol. Chem.*, vol. 284, no. 22, pp. 15016–15025, May 2009.

[48] A. Ishida, K. Furukawa, J. N. Keller, and M. P. Mattson, "Secreted form of beta-amyloid precursor protein shifts the frequency dependency for induction of LTD, and enhances LTP in hippocampal slices.," *Neuroreport*, vol. 8, no. 9–10, pp. 2133–7, Jul. 1997.

[49] M. Hick *et al.*, "Erratum to: Acute function of secreted amyloid precursor protein fragment APPsα in synaptic plasticity," *Acta Neuropathol.*, vol. 129, no. 1, pp. 161–162, Jan. 2015.

[50] W. Araki *et al.*, "Trophic effect of beta-amyloid precursor protein on cerebral cortical neurons in culture.," *Biochem. Biophys. Res. Commun.*, vol. 181, no. 1, pp. 265–71, Nov. 1991.

[51] N. Gakhar-Koppole *et al.*, "Activity requires soluble amyloid precursor protein α to promote neurite outgrowth in neural stem cell-derived neurons via activation of the MAPK pathway," *Eur. J. Neurosci.*, vol. 28, no. 5, pp. 871–882, Sep. 2008.

[52] I. Ohsawa, C. Takamura, T. Morimoto, M. Ishiguro, and S. Kohsaka, "Amino-terminal region of secreted form of amyloid precursor protein stimulates proliferation of neural stem cells.," *Eur. J. Neurosci.*, vol. 11, no. 6, pp. 1907–13, Jun. 1999.

[53] M. P. Demars, A. Bartholomew, Z. Strakova, and O. Lazarov, "Soluble amyloid precursor protein: a novel proliferation factor of adult progenitor cells of ectodermal and mesodermal origin," *Stem Cell Res. Ther.*, vol. 2, no. 4, p. 36, Aug. 2011.

[54] T. Saitoh *et al.*, "Secreted form of amyloid beta protein precursor is involved in the growth regulation of fibroblasts.," *Cell*, vol. 58, no. 4, pp. 615–22, Aug. 1989.

[55] C. U. Pietrzik *et al.*, "From differentiation to proliferation: the secretory amyloid precursor protein as a local mediator of growth in thyroid epithelial cells.," *Proc. Natl. Acad. Sci. U. S. A.*, vol. 95, no. 4, pp. 1770–5, Feb. 1998.

[56] A. Habib, D. Sawmiller, and J. Tan, "Restoring Soluble Amyloid Precursor Protein alpha Functions as a Potential Treatment for Alzheimer's Disease," *J Neurosci Res*, vol. 95, no. 4, pp. 973–991, 2017.

[57] M. P. Mattson, B. Cheng, A. R. Culwell, F. S. Esch, I. Lieberburg, and R. E. Rydel, "Evidence for excitoprotective and intraneuronal calcium-regulating roles for secreted forms of the beta-amyloid precursor protein.," *Neuron*, vol. 10, no. 2, pp. 243–54, Feb. 1993.

[58] K. Furukawa, S. W. Barger, E. M. Blalock, and M. P. Mattson, "Activation of K+ channels and suppression of neuronal activity by secreted β-amyloid-precursor protein," *Nature*, vol. 379, no. 6560, pp. 74–78, Jan. 1996.

[59] K. Furukawa and M. P. Mattson, "Secreted amyloid precursor protein alpha selectively suppresses N-methyl-D-aspartate currents in hippocampal neurons: involvement of cyclic GMP.," *Neuroscience*, vol. 83, no. 2, pp. 429–38, Mar. 1998.

[60] S. W. Barger, R. R. Fiscus, P. Ruth, F. Hofmann, and M. P. Mattson, "Role of cyclic GMP in the regulation of neuronal calcium and survival by secreted forms of beta-amyloid precursor.," *J. Neurochem.*, vol. 64, no. 5, pp. 2087–96, May 1995.

[61] V. L. Smith-Swintosky, L. C. Pettigrew, S. D. Craddock, A. R. Culwell, R. E. Rydel, and M. P. Mattson, "Secreted forms of beta-amyloid precursor protein protect against ischemic brain injury.," *J. Neurochem.*, vol. 63, no. 2, pp. 781–4, Aug. 1994.

[62] M. P. Bowes, E. Masliah, D. A. C. Otero, J. A. Zivin, and T. Saitoh, "Reduction of Neurological Damage by a Peptide Segment of the Amyloid β/A4 Protein Precursor in a Rabbit Spinal Cord Ischemia Model," *Exp. Neurol.*, vol. 129, no. 1, pp. 112–119, Sep. 1994.

[63] E. Thornton, R. Vink, P. C. Blumbergs, and C. Van Den Heuvel, "Soluble amyloid precursor protein α reduces neuronal injury and improves functional outcome following diffuse traumatic brain injury in rats," *Brain Res.*, vol. 1094, no. 1, pp. 38–46, Jun. 2006.

[64] F. Corrigan *et al.*, "The neuroprotective domains of the amyloid precursor protein, in traumatic brain injury, are located in the two growth factor domains," *Brain Res.*, vol. 1378, pp. 137–143, Mar. 2011.

[65] F. Corrigan, R. Vink, P. C. Blumbergs, C. L. Masters, R. Cappai, and C. van den Heuvel, "sAPPα rescues deficits in amyloid precursor protein knockout mice following focal traumatic brain injury," *J. Neurochem.*, vol. 122, no. 1, pp. 208–220, Jul. 2012.

[66] F. Corrigan *et al.*, "The neuroprotective activity of the amyloid precursor protein against traumatic brain injury is mediated via the heparin binding site in residues 96-110," *J. Neurochem.*, vol. 128, no. 1, pp. 196–204, Jan. 2014.

[67] G. Cheng, Z. Yu, D. Zhou, and M. P. Mattson, "Phosphatidylinositol-3-Kinase–Akt Kinase and p42/p44 Mitogen-Activated Protein Kinases Mediate Neurotrophic and Excitoprotective Actions of a Secreted Form of Amyloid Precursor Protein," *Exp. Neurol.*, vol. 175, no. 2, pp. 407–414, Jun. 2002.

[68] S. Jimenez *et al.*, "Age-dependent Accumulation of Soluble Amyloid β (Aβ) Oligomers Reverses the Neuroprotective Effect of Soluble Amyloid Precursor Protein-α (sAPPα) by Modulating Phosphatidylinositol 3-Kinase (PI3K)/Akt-GSK-3β Pathway in Alzheimer Mouse Model," *J. Biol. Chem.*, vol. 286, no. 21, pp. 18414–18425, May 2011.

[69] N. Milosch *et al.*, "Holo-APP and G-protein-mediated signaling are required for sAPPα-induced activation of the Akt survival pathway," *Cell Death Dis.*, vol. 5, no. 8, pp. e1391–e1391, Aug. 2014.

[70] Q. Guo, N. Robinson, and M. P. Mattson, "Secreted beta-amyloid precursor protein counteracts the proapoptotic action of mutant presenilin-1 by activation of NF-kappaB and stabilization of calcium homeostasis.," *J. Biol. Chem.*, vol. 273, no. 20, pp. 12341–51, May 1998.

[71] S. M. Greenberg, W. Q. Qiu, D. J. Selkoe, A. Ben-Itzhak, and K. S. Kosik, "Amino-terminal region of the beta-amyloid precursor protein activates mitogen-activated protein kinase.," *Neurosci. Lett.*, vol. 198, no. 1, pp. 52–6, Sep. 1995.

[72] D. Kögel, R. Schomburg, E. Copanaki, and J. H. M. Prehn, "Regulation of gene expression by the amyloid precursor protein: inhibition of the JNK/c-Jun pathway," *Cell Death Differ.*, vol. 12, no. 1, pp. 1–9, Jan. 2005.

[73] T. D. Stein, N. J. Anders, C. DeCarli, S. L. Chan, M. P. Mattson, and J. A. Johnson, "Neutralization of Transthyretin Reverses the Neuroprotective Effects of Secreted Amyloid Precursor Protein (APP) in APPSw Mice Resulting in Tau Phosphorylation and Loss of Hippocampal Neurons: Support for the Amyloid Hypothesis," *J. Neurosci.*, vol. 24, no. 35, pp. 7707–7717, Sep. 2004.

[74] D. Hartl *et al.*, "Soluble Alpha-APP (sAPPalpha) Regulates CDK5 Expression and Activity in Neurons," *PLoS One*, vol. 8, no. 6, p. e65920, Jun. 2013.

[75] J. M. Castellano *et al.*, "Human umbilical cord plasma proteins revitalize hippocampal function in aged mice," *Nature*, vol. 544, no. 7651, pp. 488–492, Apr. 2017.

[76] B. Dean, "Understanding the role of inflammatory-related pathways in the pathophysiology and treatment of psychiatric disorders: evidence from human peripheral studies and CNS studies.," *Int. J. Neuropsychopharmacol.*, vol. 14, no. 7, pp. 997–1012, Aug. 2011.

[77] J. M. Frischer *et al.*, "The relation between inflammation and neurodegeneration in multiple sclerosis brains.," *Brain*, vol. 132, no. Pt 5, pp. 1175–89, May 2009.

[78] Q. Wang, Y. Liu, and J. Zhou, "Neuroinflammation in Parkinson's disease and its potential as therapeutic target," *Transl. Neurodegener.*, vol. 4, no. 1, p. 19, Dec. 2015.

[79] I. G. Barbosa, R. Machado-Vieira, J. C. Soares, and A. L. Teixeira, "The immunology of bipolar disorder.," *Neuroimmunomodulation*, vol. 21, no. 2–3, pp. 117–22, 2014.

[80] M. T. Heneka *et al.*, "Neuroinflammation in Alzheimer's disease," *Lancet Neurol.*, vol. 14, no. 4, pp. 388–405, Apr. 2015.

[81] H. Neumann, M. R. Kotter, and R. J. M. Franklin, "Debris clearance by microglia: an essential link between degeneration and regeneration.," *Brain*, vol. 132, no. Pt 2, pp. 288–95, Feb. 2009.

[82] D. J. Loane and A. Kumar, "Microglia in the TBI brain: The good, the bad, and the dysregulated.," *Exp. Neurol.*, vol. 275 Pt 3, no. 0 3, pp. 316–327, Jan. 2016.

[83] D. Sawmiller *et al.*, "Luteolin Reduces Alzheimer's Disease Pathologies Induced by Traumatic Brain Injury," *Int. J. Mol. Sci.*, vol. 15, no. 1, pp. 895–904, Jan. 2014.

[84] D. Sawmiller *et al.*, "Diosmin reduces cerebral Aβ levels, tau hyperphosphorylation, neuroinflammation, and cognitive impairment in the 3xTg-AD mice," *J. Neuroimmunol.*, vol. 299, pp. 98–106, Oct. 2016.

[85] K. Rezai-Zadeh *et al.*, "Green tea epigallocatechin-3-gallate (EGCG) modulates amyloid precursor protein cleavage and reduces cerebral amyloidosis in Alzheimer transgenic mice," *J Neurosci*, vol. 25, no. 38, pp. 8807–8814, 2005.

[86] M. Vendrame *et al.*, "Infusion of Human Umbilical Cord Blood Cells in a Rat Model of Stroke Dose-Dependently Rescues Behavioral Deficits and Reduces Infarct Volume," *Stroke*, vol. 35, no. 10, pp. 2390–2395, Aug. 2004.

[87] A. J. Smith *et al.*, "Improving Lithium Therapeutics by Crystal Engineering of Novel Ionic Cocrystals," *Mol. Pharm.*, vol. 10, no. 12, pp. 4728–4738, Dec. 2013.

[88] C. J. Phiel and P. S. Klein, "M OLECULAR T ARGETS OF L ITHIUM A CTION," *Annu. Rev. Pharmacol. Toxicol.*, vol. 41, no. 1, pp. 789–813, Apr. 2001.

[89] P. S. Klein and D. A. Melton, "A molecular mechanism for the effect of lithium on development.," *Proc. Natl. Acad. Sci. U. S. A.*, vol. 93, no. 16, pp. 8455–9, Aug. 1996.

[90] M. A. Mines and R. S. Jope, "Glycogen synthase kinase-3: a promising therapeutic target for fragile x syndrome.," *Front. Mol. Neurosci.*, vol. 4, p. 35, 2011.

[91] C. J. Phiel, C. A. Wilson, V. M.-Y. Lee, and P. S. Klein, "GSK-3α regulates production of Alzheimer's disease amyloid-β peptides," *Nature*, vol. 423, no. 6938, pp. 435–439, May 2003.

[92] O. V Forlenza, V. J. De-Paula, and B. S. Diniz, "Neuroprotective effects of lithium: implications for the treatment of Alzheimer's disease and related neurodegenerative disorders," *ACS Chem Neurosci*, vol. 5, no. 6, pp. 443–450, 2014.

[93] T. Engel, P. Goñi-Oliver, J. J. Lucas, J. Avila, and F. Hernández, "Chronic lithium administration to FTDP-17 tau and GSK-3beta overexpressing mice prevents tau hyperphosphorylation and neurofibrillary tangle formation, but pre-formed neurofibrillary tangles do not revert," *J. Neurochem.*, vol. 99, no. 6, pp. 1445–1455, Dec. 2006.

[94] J. A. Quiroz, R. Machado-Vieira, C. A. Zarate, H. K. Manji, and H. K. Manji, "Novel insights into lithium's mechanism of action: neurotrophic and neuroprotective effects.," *Neuropsychobiology*, vol. 62, no. 1, pp. 50–60, 2010.

[95] W. J. Ryves and A. J. Harwood, "Lithium Inhibits Glycogen Synthase Kinase-3 by Competition for Magnesium," *Biochem. Biophys. Res. Commun.*, vol. 280, no. 3, pp. 720–725, Jan. 2001.

[96] J. S. Rao, H.-J. Lee, S. I. Rapoport, and R. P. Bazinet, "Mode of action of mood stabilizers: is the arachidonic acid cascade a common target?," *Mol. Psychiatry*, vol. 13, no. 6, pp. 585–596, Jun. 2008.

[97] D. L. Murphy, C. Donnelly, and J. Moskowitz, "Inhibition by lithium of prostaglandin E1 and norepinephrine effects on cyclic adenosine monophosphate production in human platelets.," *Clin. Pharmacol. Ther.*, vol. 14, no. 5, pp. 810–4.

[98]   M. C. Chang and C. R. Jones, "Chronic lithium treatment decreases brain phospholipase A2 activity.," *Neurochem. Res.*, vol. 23, no. 6, pp. 887–92, Jun. 1998.

[99]   M. Basselin *et al.*, "Lithium modifies brain arachidonic and docosahexaenoic metabolism in rat lipopolysaccharide model of neuroinflammation.," *J. Lipid Res.*, vol. 51, no. 5, pp. 1049–56, May 2010.

[100]   S. Hong, K. Gronert, P. R. Devchand, R.-L. Moussignac, and C. N. Serhan, "Novel Docosatrienes and 17 *S* -Resolvins Generated from Docosahexaenoic Acid in Murine Brain, Human Blood, and Glial Cells," *J. Biol. Chem.*, vol. 278, no. 17, pp. 14677–14687, Apr. 2003.

[101]   B. Voutsinos-Porche *et al.*, "Temporal patterns of the cerebral inflammatory response in the rat lithium–pilocarpine model of temporal lobe epilepsy," *Neurobiol. Dis.*, vol. 17, no. 3, pp. 385–402, Dec. 2004.

[102]   C. J. Yuskaitis and R. S. Jope, "Glycogen synthase kinase-3 regulates microglial migration, inflammation, and inflammation-induced neurotoxicity," *Cell. Signal.*, vol. 21, no. 2, pp. 264–273, Feb. 2009.

[103]   S. Moncada and J. P. Bolanos, "Nitric oxide, cell bioenergetics and neurodegeneration," *J. Neurochem.*, vol. 97, no. 6, pp. 1676–1689, Jun. 2006.

[104]   G. Bagetta, R. Massoud, P. Rodinò, G. Federici, and G. Nisticò, "Systemic administration of lithium chloride and tacrine increases nitric oxide synthase activity in the hippocampus of rats.," *Eur. J. Pharmacol.*, vol. 237, no. 1, pp. 61–4, Jun. 1993.

[105]   M. Ghasemi and A. R. Dehpour, "The NMDA receptor/nitric oxide pathway: a target for the therapeutic and toxic effects of lithium," *Trends Pharmacol. Sci.*, vol. 32, no. 7, pp. 420–434, Jul. 2011.

[106]   G. Wegener *et al.*, "Combined chronic treatment with citalopram and lithium does not modify the regional neurochemistry of nitric oxide in rat brain.," *J. Physiol. Pharmacol.*, vol. 55, no. 3, pp. 575–86, Sep. 2004.

[107]   S. Maruta *et al.*, "Effects of intraperitoneally injected lithium, imipramine and diazepam on nitrate levels in rat amygdala," *Psychiatry Clin. Neurosci.*, vol. 59, no. 3, pp. 358–361, Jun. 2005.

[108]   E. S. Kleinerman, R. D. Knowles, M. B. Blick, and L. A. Zwelling, "Lithium chloride stimulates human monocytes to secrete tumor necrosis factor/cachectin.," *J. Leukoc. Biol.*, vol. 46, no. 5, pp. 484–92, Nov. 1989.

[109]   M. Hull, E. Lee, T. Lee, N. Anand, V. LaLone, and N. Parameswaran, "Lithium chloride induces TNFα in mouse macrophages via MEK-ERK-dependent pathway.," *J. Cell. Biochem.*, vol. 115, no. 1, pp. 71–80, Jan. 2014.

[110]   M. Martin, K. Rehani, R. S. Jope, and S. M. Michalek, "Toll-like receptor–mediated cytokine production is differentially regulated by glycogen synthase kinase 3," *Nat. Immunol.*, vol. 6, no. 8, pp. 777–784, Aug. 2005.

[111]   Y. Wang *et al.*, "Inhibiting glycogen synthase kinase-3 reduces endotoxaemic acute renal failure by down-regulating inflammation and renal cell apoptosis.," *Br. J. Pharmacol.*, vol. 157, no. 6, pp. 1004–13, Jul. 2009.

[112]   K. Kang *et al.*, "Lithium pretreatment reduces brain injury after intracerebral hemorrhage in rats," *Neurol. Res.*, vol. 34, no. 5, pp. 447–454, Jun. 2012.

[113]   E. M. Knijff *et al.*, "An imbalance in the production of IL-1β and IL-6 by monocytes of bipolar patients: restoration by lithium treatment," *Bipolar Disord.*, vol. 9, no. 7, pp. 743–753, Nov. 2007.

[114] M. H. Rapaport and H. K. Manji, "The effects of lithium on ex vivo cytokine production.," *Biol. Psychiatry*, vol. 50, no. 3, pp. 217–24, Aug. 2001.

[115] T. F. Tay, M. Maheran, S. L. Too, M. S. Hasidah, G. Ismail, and N. Embi, "Glycogen synthase kinase-3β inhibition improved survivability of mice infected with Burkholderia pseudomallei.," *Trop. Biomed.*, vol. 29, no. 4, pp. 551–67, Dec. 2012.

[116] S. Kishter, F. A. Hoffman, and P. A. Pizzo, "Production of and response to interleukin-2 by cultured T cells: effects of lithium chloride and other putative modulators.," *J. Biol. Response Mod.*, vol. 4, no. 2, pp. 185–94, Apr. 1985.

[117] M. B. Sztein *et al.*, "In vitro effects of thymosin and lithium on lymphoproliferative responses of normal donors and HIV seropositive male homosexuals with AIDS-related complex.," *Clin. Immunol. Immunopathol.*, vol. 44, no. 1, pp. 51–62, Jul. 1987.

[118] M. Maes *et al.*, "In vitro immunoregulatory effects of lithium in healthy volunteers.," *Psychopharmacology (Berl).*, vol. 143, no. 4, pp. 401–7, Apr. 1999.

[119] E. Rocha, M. Achaval, P. Santos, and R. Rodnight, "Lithium treatment causes gliosis and modifies the morphology of hippocampal astrocytes in rats.," *Neuroreport*, vol. 9, no. 17, pp. 3971–4, Dec. 1998.

[120] G. M. Gilad and V. H. Gilad, "Astroglia growth retardation and increased microglia proliferation by lithium and ornithine decarboxylase inhibitor in rat cerebellar cultures: Cytotoxicity by combined lithium and polyamine inhibition," *J. Neurosci. Res.*, vol. 85, no. 3, pp. 594–601, Feb. 2007.

[121] E. M. Toledo and N. C. Inestrosa, "Activation of Wnt signaling by lithium and rosiglitazone reduced spatial memory impairment and neurodegeneration in brains of an APPswe/PSEN1ΔE9 mouse model of Alzheimer's disease," *Mol. Psychiatry*, vol. 15, no. 3, pp. 272–285, Mar. 2010.

[122] K. P. Hoeflich, J. Luo, E. A. Rubie, M.-S. Tsao, O. Jin, and J. R. Woodgett, "Requirement for glycogen synthase kinase-3β in cell survival and NF-κB activation," *Nature*, vol. 406, no. 6791, pp. 86–90, Jul. 2000.

[123] S. Ghosh and M. S. Hayden, "New regulators of NF-κB in inflammation," *Nat. Rev. Immunol.*, vol. 8, no. 11, pp. 837–848, Nov. 2008.

[124] L. Wang, L. Zhang, X. Zhao, M. Zhang, W. Zhao, and C. Gao, "Lithium Attenuates IFN-β Production and Antiviral Response via Inhibition of TANK-Binding Kinase 1 Kinase Activity," *J. Immunol.*, vol. 191, no. 8, pp. 4392–4398, Oct. 2013.

[125] P. Zhang, J. Katz, and S. M. Michalek, "Glycogen synthase kinase-3β (GSK3β) inhibition suppresses the inflammatory response to Francisella infection and protects against tularemia in mice," *Mol. Immunol.*, vol. 46, no. 4, pp. 677–687, Feb. 2009.

[126] E. Beurel and R. S. Jope, "Glycogen synthase kinase-3 promotes the synergistic action of interferon-γ on lipopolysaccharide-induced IL-6 production in RAW264.7 cells," *Cell. Signal.*, vol. 21, no. 6, pp. 978–985, Jun. 2009.

[127] M. Bouskila, M. F. Hirshman, J. Jensen, L. J. Goodyear, and K. Sakamoto, "Insulin promotes glycogen synthesis in the absence of GSK3 phosphorylation in skeletal muscle," *Am. J. Physiol. Metab.*, vol. 294, no. 1, pp. E28–E35, Jan. 2008.

[128] K. Hughes, E. Nikolakaki, S. E. Plyte, N. F. Totty, and J. R. Woodgett, "Modulation of the glycogen synthase kinase-3 family by tyrosine phosphorylation.," *EMBO J.*, vol. 12, no. 2, pp. 803–8, Feb. 1993.

[129] V. Stambolic and J. R. Woodgett, "Mitogen inactivation of glycogen synthase kinase-3 beta in intact cells via serine 9 phosphorylation.," *Biochem. J.*, vol. 303 (Pt 3), pp. 701–4, Nov.

1994.

[130] E.-M. Hur and F.-Q. Zhou, "GSK3 signalling in neural development," *Nat. Rev. Neurosci.*, vol. 11, no. 8, pp. 539–551, Aug. 2010.

[131] M. Hetman, J. E. Cavanaugh, D. Kimelman, and Z. Xia, "Role of glycogen synthase kinase-3beta in neuronal apoptosis induced by trophic withdrawal.," *J. Neurosci.*, vol. 20, no. 7, pp. 2567–74, Apr. 2000.

[132] K. M. Jacobs, S. R. Bhave, D. J. Ferraro, J. J. Jaboin, D. E. Hallahan, and D. Thotala, "GSK-3: A Bifunctional Role in Cell Death Pathways," *Int. J. Cell Biol.*, vol. 2012, pp. 1–11, 2012.

[133] J. Jo *et al.*, "Aβ1–42 inhibition of LTP is mediated by a signaling pathway involving caspase-3, Akt1 and GSK-3β," *Nat. Neurosci.*, vol. 14, no. 5, pp. 545–547, May 2011.

[134] P. T. T. Ly *et al.*, "Inhibition of GSK3β-mediated BACE1 expression reduces Alzheimer-associated phenotypes.," *J. Clin. Invest.*, vol. 123, no. 1, pp. 224–35, Jan. 2013.

[135] M. K. King, M. Pardo, Y. Cheng, K. Downey, R. S. Jope, and E. Beurel, "Glycogen synthase kinase-3 inhibitors: Rescuers of cognitive impairments.," *Pharmacol. Ther.*, vol. 141, no. 1, pp. 1–12, Jan. 2014.

[136] K. Spittaels *et al.*, "Glycogen synthase kinase-3beta phosphorylates protein tau and rescues the axonopathy in the central nervous system of human four-repeat tau transgenic mice.," *J. Biol. Chem.*, vol. 275, no. 52, pp. 41340–9, Dec. 2000.

[137] A. Takashima, "GSK-3 is essential in the pathogenesis of Alzheimer's disease.," *J. Alzheimers. Dis.*, vol. 9, no. 3 Suppl, pp. 309–17, 2006.

[138] C. Hooper, R. Killick, and S. Lovestone, "The GSK3 hypothesis of Alzheimer's disease," *J. Neurochem.*, vol. 104, no. 6, pp. 1433–1439, Mar. 2008.

[139] J. Avila, G. León-Espinosa, E. García, V. García-Escudero, F. Hernández, and J. DeFelipe, "Tau Phosphorylation by GSK3 in Different Conditions," *Int. J. Alzheimers. Dis.*, vol. 2012, pp. 1–7, May 2012.

[140] D. F. Seals and S. A. Courtneidge, "The ADAMs family of metalloproteases: multidomain proteins with multiple functions," *Genes Dev.*, vol. 17, no. 1, pp. 7–30, Jan. 2003.

[141] M. Deuss, K. Reiss, and D. Hartmann, "Part-time alpha-secretases: the functional biology of ADAM 9, 10 and 17.," *Curr. Alzheimer Res.*, vol. 5, no. 2, pp. 187–201, Apr. 2008.

[142] G. Murphy, "The ADAMs: signalling scissors in the tumour microenvironment," *Nat. Rev. Cancer*, vol. 8, no. 12, pp. 932–941, Dec. 2008.

[143] E. E. Gardiner, D. Karunakaran, Y. Shen, J. F. Arthur, R. K. Andrews, and M. C. Berndt, "Controlled shedding of platelet glycoprotein (GP)VI and GPIb-IX-V by ADAM family metalloproteinases," *J. Thromb. Haemost.*, vol. 5, no. 7, pp. 1530–1537, Jul. 2007.

[144] M. Bender *et al.*, "Differentially regulated GPVI ectodomain shedding by multiple platelet-expressed proteinases," *Blood*, vol. 116, no. 17, pp. 3347–3355, Oct. 2010.

[145] P. J. Gough, K. J. Garton, P. T. Wille, M. Rychlewski, P. J. Dempsey, and E. W. Raines, "A disintegrin and metalloproteinase 10-mediated cleavage and shedding regulates the cell surface expression of CXC chemokine ligand 16.," *J. Immunol.*, vol. 172, no. 6, pp. 3678–85, Mar. 2004.

[146] M. J. Mohan *et al.*, "The tumor necrosis factor-alpha converting enzyme (TACE): a unique metalloproteinase with highly defined substrate selectivity.," *Biochemistry*, vol. 41, no. 30, pp. 9462–9, Jul. 2002.

[147] R. Postina, "A closer look at alpha-secretase.," *Curr. Alzheimer Res.*, vol. 5, no. 2, pp. 179–86, Apr. 2008.

[148] M. A. Israel *et al.*, "Probing sporadic and familial Alzheimer's disease using induced pluripotent stem cells," *Nature*, vol. 482, no. 7384, pp. 216–220, Feb. 2012.

[149] A. J. Smith *et al.*, "Plasma and brain pharmacokinetics of previously unexplored lithium salts," *RSC Adv.*, vol. 4, no. 24, pp. 12362–12365, 2014.

[150] A. Habib *et al.*, "LISPRO mitigates β-amyloid and associated pathologies in Alzheimer's mice," *Cell Death Dis.*, vol. 8, no. 6, p. e2880, Jun. 2017.

[151] B. G. Mockett, M. Richter, W. C. Abraham, and U. C. Müller, "Therapeutic Potential of Secreted Amyloid Precursor Protein APPsα," *Front. Mol. Neurosci.*, vol. 10, p. 30, Feb. 2017.

[152] V. J. Spilman P, Jagodzinska B, Bredesen DE, "Enhancement of sAPPα as a Therapeutic Strategy for Alzheimer's and Other Neurodegenerative Diseases," *Alzheimer's Neurodegener. Dis.*, vol. 1, no. 1, pp. 1–10, Aug. 2015.

[153] D. Darlington *et al.*, "Multiple low-dose infusions of human umbilical cord blood cells improve cognitive impairments and reduce amyloid-beta-associated neuropathology in Alzheimer mice," *Stem Cells Dev*, vol. 22, no. 3, pp. 412–421, 2013.

[154] J. Middeldorp *et al.*, "Preclinical Assessment of Young Blood Plasma for Alzheimer Disease," *JAMA Neurol.*, vol. 73, no. 11, p. 1325, Nov. 2016.

[155] L. Katsimpardi *et al.*, "Vascular and Neurogenic Rejuvenation of the Aging Mouse Brain by Young Systemic Factors," *Science (80).* vol. 344, no. 6184, pp. 630–634, May 2014.

[156] J. M. Castellano *et al.*, "In vivo assessment of behavioral recovery and circulatory exchange in the peritoneal parabiosis model," *Sci. Rep.*, vol. 6, no. 1, p. 29015, Sep. 2016.

[157] Y. Xiang *et al.*, "Physiological amyloid-beta clearance in the periphery and its therapeutic potential for Alzheimer's disease," *Acta Neuropathol.*, vol. 130, no. 4, pp. 487–499, Oct. 2015.

[158] H. Oakley *et al.*, "Intraneuronal beta-Amyloid Aggregates, Neurodegeneration, and Neuron Loss in Transgenic Mice with Five Familial Alzheimer's Disease Mutations: Potential Factors in Amyloid Plaque Formation," *J. Neurosci.*, vol. 26, no. 40, pp. 10129–10140, Oct. 2006.

[159] S. Oddo *et al.*, "Triple-transgenic model of Alzheimer's disease with plaques and tangles: intracellular Abeta and synaptic dysfunction.," *Neuron*, vol. 39, no. 3, pp. 409–21, Jul. 2003.

[160] D. Sawmiller *et al.*, "Beneficial effects of a pyrroloquinolinequinone-containing dietary formulation on motor deficiency, cognitive decline and mitochondrial dysfunction in a mouse model of Alzheimer's disease," *Heliyon*, vol. 3, no. 4, p. e00279, 2017.

[161] R. D. Shytle *et al.*, "Optimized turmeric extracts have potent anti-amyloidogenic effects.," *Curr. Alzheimer Res.*, vol. 6, no. 6, pp. 564–71, Dec. 2009.

[162] C. Hundhausen *et al.*, "Regulated shedding of transmembrane chemokines by the disintegrin and metalloproteinase 10 facilitates detachment of adherent leukocytes.," *J. Immunol.*, vol. 178, no. 12, pp. 8064–72, Jun. 2007.

[163] T. Isozaki *et al.*, "Evidence That CXCL16 Is a Potent Mediator of Angiogenesis and Is Involved in Endothelial Progenitor Cell Chemotaxis: Studies in Mice With K/BxN Serum-Induced Arthritis," *Arthritis Rheum.*, vol. 65, no. 7, pp. 1736–1746, Jul. 2013.

[164] C. Peters-Libeu *et al.*, "sAβPPα is a Potent Endogenous Inhibitor of BACE1," *J. Alzheimer's Dis.*, vol. 47, no. 3, pp. 545–555, Aug. 2015.

[165] C. Haass and D. J. Selkoe, "Soluble protein oligomers in neurodegeneration: lessons from the Alzheimer's amyloid beta-peptide," *Nat Rev Mol Cell Biol*, vol. 8, no. 2, pp. 101–112, 2007.

[166] P. Eikelenboom and F. C. Stam, "Immunoglobulins and complement factors in senile plaques. An immunoperoxidase study," *Acta Neuropathol*, vol. 57, no. 2–3, pp. 239–242, 1982.

[167] P. Damien and D. S. Allan, "Regenerative Therapy and Immune Modulation Using Umbilical Cord Blood-Derived Cells," *Biol Blood Marrow Transpl.*, vol. 21, no. 9, pp. 1545–1554, 2015.

[168] A. H. Habib Mori T. Tian, J. Zeng, J. Fan, S. Giunta, B. Sanberg, P. Sawmiller, D. and Tan, J., "Human Umbilical Cord Blood Serum-derived alpha-Secretase: Functional Testing in Alzheimer's Disease Mouse Models," *Cell Transplant.*, vol. x, no. y, pp. 1–18, 2018.

[169] H. Rus, C. Cudrici, and F. Niculescu, "The role of the complement system in innate immunity," *Immunol Res*, vol. 33, no. 2, pp. 103–112, 2005.

[170] B. Stevens *et al.*, "The classical complement cascade mediates CNS synapse elimination," *Cell*, vol. 131, no. 6, pp. 1164–1178, 2007.

[171] R. Veerhuis, H. M. Nielsen, and A. J. Tenner, "Complement in the brain," *Mol Immunol*, vol. 48, no. 14, pp. 1592–1603, 2011.

[172] R. A. van Schaarenburg *et al.*, "C1q Deficiency and Neuropsychiatric Systemic Lupus Erythematosus," *Front Immunol*, vol. 7, p. 647, 2016.

[173] N. M. Thielens, F. Tedesco, S. S. Bohlson, C. Gaboriaud, and A. J. Tenner, "C1q: A fresh look upon an old molecule," *Mol Immunol*, vol. 89, pp. 73–83, 2017.

[174] K. B. Reid and R. R. Porter, "Subunit composition and structure of subcomponent C1q of the first component of human complement," *Biochem J*, vol. 155, no. 1, pp. 19–23, 1976.

[175] K. Pisalyaput and A. J. Tenner, "Complement component C1q inhibits beta-amyloid- and serum amyloid P-induced neurotoxicity via caspase- and calpain-independent mechanisms," *J Neurochem*, vol. 104, no. 3, pp. 696–707, 2008.

[176] M. E. Benoit and A. J. Tenner, "Complement protein C1q-mediated neuroprotection is correlated with regulation of neuronal gene and microRNA expression," *J Neurosci*, vol. 31, no. 9, pp. 3459–3469, 2011.

[177] D. A. Fraser, A. K. Laust, E. L. Nelson, and A. J. Tenner, "C1q differentially modulates phagocytosis and cytokine responses during ingestion of apoptotic cells by human monocytes, macrophages, and dendritic cells," *J Immunol*, vol. 183, no. 10, pp. 6175–6185, 2009.

[178] H. Rus, C. Cudrici, S. David, and F. Niculescu, "The complement system in central nervous system diseases," *Autoimmunity*, vol. 39, no. 5, pp. 395–402, 2006.

[179] M. I. Fonseca *et al.*, "Treatment with a C5aR antagonist decreases pathology and enhances behavioral performance in murine models of Alzheimer's disease," *J Immunol*, vol. 183, no. 2, pp. 1375–1383, 2009.

[180] D. A. Fraser, K. Pisalyaput, and A. J. Tenner, "C1q enhances microglial clearance of apoptotic neurons and neuronal blebs, and modulates subsequent inflammatory cytokine production," *J Neurochem*, vol. 112, no. 3, pp. 733–743, 2010.

[181] M. E. Benoit, M. X. Hernandez, M. L. Dinh, F. Benavente, O. Vasquez, and A. J. Tenner, "C1q-induced LRP1B and GPR6 proteins expressed early in Alzheimer disease mouse models, are essential for the C1q-mediated protection against amyloid-beta neurotoxicity," *J Biol Chem*, vol. 288, no. 1, pp. 654–665, 2013.

[182] D. A. Loeffler, D. M. Camp, and D. A. Bennett, "Plaque complement activation and cognitive loss in Alzheimer's disease," *J Neuroinflammation*, vol. 5, p. 9, 2008.

[183] J. J. Alexander, A. J. Anderson, S. R. Barnum, B. Stevens, and A. J. Tenner, "The complement cascade: Yin-Yang in neuroinflammation--neuro-protection and -degeneration," *J Neurochem*, vol. 107, no. 5, pp. 1169–1187, 2008.

[184] C. Gaboriaud, W. L. Ling, N. M. Thielens, I. Bally, and V. Rossi, "Deciphering the fine details of c1 assembly and activation mechanisms: 'mission impossible'?," *Front Immunol*, vol. 5, p. 565, 2014.

[185] J. Rogers *et al.*, "Peripheral clearance of amyloid beta peptide by complement C3-dependent adherence to erythrocytes," *Neurobiol Aging*, vol. 27, no. 12, pp. 1733–1739, 2006.

[186] M. Maier, Y. Peng, L. Jiang, T. J. Seabrook, M. C. Carroll, and C. A. Lemere, "Complement C3 deficiency leads to accelerated amyloid beta plaque deposition and neurodegeneration and modulation of the microglia/macrophage phenotype in amyloid precursor protein transgenic mice," *J Neurosci*, vol. 28, no. 25, pp. 6333–6341, 2008.

[187] P. Gasque, Y. D. Dean, E. P. McGreal, J. VanBeek, and B. P. Morgan, "Complement components of the innate immune system in health and disease in the CNS," *Immunopharmacology*, vol. 49, no. 1–2, pp. 171–186, 2000.

[188] F. H. Brennan, A. J. Anderson, S. M. Taylor, T. M. Woodruff, and M. J. Ruitenberg, "Complement activation in the injured central nervous system: another dual-edged sword?," *J Neuroinflammation*, vol. 9, p. 137, 2012.

[189] Y. Shen and S. Meri, "Yin and Yang: complement activation and regulation in Alzheimer's disease," *Prog Neurobiol*, vol. 70, no. 6, pp. 463–472, 2003.

[190] A. Afagh, B. J. Cummings, D. H. Cribbs, C. W. Cotman, and A. J. Tenner, "Localization and cell association of C1q in Alzheimer's disease brain," *Exp Neurol*, vol. 138, no. 1, pp. 22–32, 1996.

[191] M. Li, R. R. Ager, D. A. Fraser, N. O. Tjokro, and A. J. Tenner, "Development of a humanized C1q A chain knock-in mouse: assessment of antibody independent beta-amyloid induced complement activation," *Mol Immunol*, vol. 45, no. 11, pp. 3244–3252, 2008.

[192] M. I. Fonseca, J. Zhou, M. Botto, and A. J. Tenner, "Absence of C1q leads to less neuropathology in transgenic mouse models of Alzheimer's disease," *J Neurosci*, vol. 24, no. 29, pp. 6457–6465, 2004.

[193] S. D. Webster, A. J. Yang, L. Margol, W. Garzon-Rodriguez, C. G. Glabe, and A. J. Tenner, "Complement component C1q modulates the phagocytosis of Abeta by microglia," *Exp Neurol*, vol. 161, no. 1, pp. 127–138, 2000.

[194] C. L. Masters, G. Simms, N. A. Weinman, G. Multhaup, B. L. McDonald, and K. Beyreuther, "Amyloid plaque core protein in Alzheimer disease and Down syndrome," *Proc Natl Acad Sci U S A*, vol. 82, no. 12, pp. 4245–4249, 1985.

[195] I. Grundke-Iqbal, K. Iqbal, Y. C. Tung, M. Quinlan, H. M. Wisniewski, and L. I. Binder, "Abnormal phosphorylation of the microtubule-associated protein tau (tau) in Alzheimer cytoskeletal pathology," *Proc Natl Acad Sci U S A*, vol. 83, no. 13, pp. 4913–4917, 1986.

[196] A. Serrano-Pozo, M. P. Frosch, E. Masliah, and B. T. Hyman, "Neuropathological Alterations in Alzheimer Disease," *Cold Spring Harb. Perspect. Med.*, vol. 1, no. 1, pp. a006189–a006189, Sep. 2011.

[197] A. Lleo, "Current Therapeutic Options for Alzheimers Disease," *Curr. Genomics*, vol. 8, no. 8, pp. 550–558, Dec. 2007.

[198] E. Shorter, "The history of lithium therapy," *Bipolar Disord*, vol. 11 Suppl 2, pp. 4–9, 2009.

[199] J. F. Hayes *et al.*, "Self-harm, Unintentional Injury, and Suicide in Bipolar Disorder During Maintenance Mood Stabilizer Treatment," *JAMA Psychiatry*, vol. 73, no. 6, p. 630, Jun.

2016.

[200] O. V Forlenza, B. S. Diniz, M. Radanovic, F. S. Santos, L. L. Talib, and W. F. Gattaz, "Disease-modifying properties of long-term lithium treatment for amnestic mild cognitive impairment: randomised controlled trial," *Br J Psychiatry*, vol. 198, no. 5, pp. 351–356, 2011.

[201] F. K. Goodwin, B. Fireman, G. E. Simon, E. M. Hunkeler, J. Lee, and D. Revicki, "Suicide Risk in Bipolar Disorder During Treatment With Lithium and Divalproex," *JAMA*, vol. 290, no. 11, p. 1467, Sep. 2003.

[202] M. A. Nunes, T. A. Viel, and H. S. Buck, "Microdose lithium treatment stabilized cognitive impairment in patients with Alzheimer's disease," *Curr Alzheimer Res*, vol. 10, no. 1, pp. 104–107, 2013.

[203] V. D. Davenport, "Distribution of Parenterally Administered Lithium in Plasma, Brain, and Muscle of Rats," *Am. J. Physiol. Content*, vol. 163, no. 3, pp. 633–641, Nov. 1950.

[204] M. S. Ebadi, V. J. Simmons, M. J. Hendrickson, and P. S. Lacy, "Pharmacokinetics of lithium and its regional distribution in rat brain.," *Eur. J. Pharmacol.*, vol. 27, no. 3, pp. 324–9, Aug. 1974.

[205] C. Livingstone and H. Rampes, "Lithium: a review of its metabolic adverse effects," *J. Psychopharmacol.*, vol. 20, no. 3, pp. 347–355, May 2006.

[206] M. Schou, P. C. Baastrup, P. Grof, P. Weis, and J. Angst, "Pharmacological and clinical problems of lithium prophylaxis.," *Br. J. Psychiatry*, vol. 116, no. 535, pp. 615–9, Jun. 1970.

[207] T. Town *et al.*, "Reduced Th1 and enhanced Th2 immunity after immunization with Alzheimer's beta-amyloid(1-42).," *J. Neuroimmunol.*, vol. 132, no. 1–2, pp. 49–59, Nov. 2002.

[208] J. Tan *et al.*, "Role of CD40 ligand in amyloidosis in transgenic Alzheimer's mice," *Nat. Neurosci.*, vol. 5, no. 12, pp. 1288–1293, Dec. 2002.

[209] K. Rezai-Zadeh *et al.*, "Flavonoid-mediated presenilin-1 phosphorylation reduces Alzheimer's disease beta-amyloid production.," *J. Cell. Mol. Med.*, vol. 13, no. 3, pp. 574–88, Mar. 2009.

[210] K. P. Townsend *et al.*, "CD40 signaling regulates innate and adaptive activation of microglia in response to amyloid beta-peptide," *Eur. J. Immunol.*, vol. 35, no. 3, pp. 901–910, Mar. 2005.

[211] J. Saura, J. M. Tusell, and J. Serratosa, "High-yield isolation of murine microglia by mild trypsinization," *Glia*, vol. 44, no. 3, pp. 183–189, Dec. 2003.

[212] Y. Zhu *et al.*, "Mutant presenilin-1 deregulated peripheral immunity exacerbates Alzheimer-like pathology," *J. Cell. Mol. Med.*, vol. 15, no. 2, pp. 327–338, Feb. 2011.

[213] F. Yu, Y. Zhang, and D.-M. Chuang, "Lithium Reduces BACE1 Overexpression, Beta Amyloid Accumulation, and Spatial Learning Deficits in Mice with Traumatic Brain Injury," *J. Neurotrauma*, vol. 29, no. 13, pp. 2342–2351, Sep. 2012.

[214] T. L. Sudduth, J. G. Wilson, A. Everhart, C. A. Colton, and D. M. Wilcock, "Lithium Treatment of APPSwDI/NOS2−/− Mice Leads to Reduced Hyperphosphorylated Tau, Increased Amyloid Deposition and Altered Inflammatory Phenotype," *PLoS One*, vol. 7, no. 2, p. e31993, Feb. 2012.

[215] S. Sarkar *et al.*, "Lithium induces autophagy by inhibiting inositol monophosphatase," *J. Cell Biol.*, vol. 170, no. 7, pp. 1101–1111, Sep. 2005.

[216] Y. Motoi, K. Shimada, K. Ishiguro, and N. Hattori, "Lithium and Autophagy," *ACS Chem. Neurosci.*, vol. 5, no. 6, pp. 434–442, Jun. 2014.

[217] T.-H. Kwon, "Dysregulation of Renal Cyclooxygenase-2 in Rats with Lithium-induced Nephrogenic Diabetes Insipidus," *Electrolyte Blood Press.*, vol. 5, no. 2, p. 68, Dec. 2007.

[218] R. Rao *et al.*, "Lithium treatment inhibits renal GSK-3 activity and promotes cyclooxygenase 2-dependent polyuria," *Am. J. Physiol. Physiol.*, vol. 288, no. 4, pp. F642–F649, Apr. 2005.

[219] R. Rao, C.-M. Hao, and M. D. Breyer, "Hypertonic Stress Activates Glycogen Synthase Kinase 3β-mediated Apoptosis of Renal Medullary Interstitial Cells, Suppressing an NFκB-driven Cyclooxygenase-2-dependent Survival Pathway," *J. Biol. Chem.*, vol. 279, no. 6, pp. 3949–3955, Feb. 2004.

[220] A. Cipriani, K. Hawton, S. Stockton, and J. R. Geddes, "Lithium in the prevention of suicide in mood disorders: updated systematic review and meta-analysis.," *BMJ*, vol. 346, p. f3646, Jun. 2013.

[221] G. Alvarez, J. R. Muñoz-Montaño, J. Satrústegui, J. Avila, E. Bogónez, and J. Díaz-Nido, "Regulation of tau phosphorylation and protection against beta-amyloid-induced neurodegeneration by lithium. Possible implications for Alzheimer's disease.," *Bipolar Disord.*, vol. 4, no. 3, pp. 153–65, Jun. 2002.

[222] G. Alvarez, J. R. Muñoz-Montaño, J. Satrústegui, J. Avila, E. Bogónez, and J. Díaz-Nido, "Lithium protects cultured neurons against beta-amyloid-induced neurodegeneration.," *FEBS Lett.*, vol. 453, no. 3, pp. 260–4, Jun. 1999.

[223] P. Stolk *et al.*, "Is aspirin useful in patients on lithium? A pharmacoepidemiological study related to bipolar disorder," *Prostaglandins, Leukot. Essent. Fat. Acids*, vol. 82, no. 1, pp. 9–14, Jan. 2010.

[224] C. N. Serhan *et al.*, "Resolvins: a family of bioactive products of omega-3 fatty acid transformation circuits initiated by aspirin treatment that counter proinflammation signals.," *J. Exp. Med.*, vol. 196, no. 8, pp. 1025–37, Oct. 2002.

[225] M. Basselin, N. E. Villacreses, H.-J. Lee, J. M. Bell, and S. I. Rapoport, "Chronic lithium administration attenuates up-regulated brain arachidonic acid metabolism in a rat model of neuroinflammation," *J. Neurochem.*, vol. 102, no. 3, pp. 761–772, Mar. 2007.

[226] R. S. Jope, "Lithium and GSK-3: one inhibitor, two inhibitory actions, multiple outcomes," *Trends Pharmacol. Sci.*, vol. 24, no. 9, pp. 441–443, Sep. 2003.

[227] W. S. Griffin *et al.*, "Glial-neuronal interactions in Alzheimer's disease: the potential role of a 'cytokine cycle' in disease progression.," *Brain Pathol.*, vol. 8, no. 1, pp. 65–72, Jan. 1998.

[228] N. Abbas *et al.*, "Up-regulation of the inflammatory cytokines IFN-gamma and IL-12 and down-regulation of IL-4 in cerebral cortex regions of APP(SWE) transgenic mice.," *J. Neuroimmunol.*, vol. 126, no. 1–2, pp. 50–7, May 2002.

[229] G. C. Brown and A. Bal-Price, "Inflammatory Neurodegeneration Mediated by Nitric Oxide, Glutamate, and Mitochondria," *Mol. Neurobiol.*, vol. 27, no. 3, pp. 325–355, Jun. 2003.

[230] W. S. Griffin *et al.*, "Brain interleukin 1 and S-100 immunoreactivity are elevated in Down syndrome and Alzheimer disease.," *Proc. Natl. Acad. Sci. U. S. A.*, vol. 86, no. 19, pp. 7611–5, Oct. 1989.

[231] E. A. van der Wal, F. Gómez-Pinilla, and C. W. Cotman, "Transforming growth factor-beta 1 is in plaques in Alzheimer and Down pathologies." *Neuroreport*, vol. 4, no. 1, pp. 69–72,

Jan. 1993.

[232] M. Sy *et al.*, "Inflammation Induced by Infection Potentiates Tau Pathological Features in Transgenic Mice," *Am. J. Pathol.*, vol. 178, no. 6, pp. 2811–2822, Jun. 2011.

[233] V. De-Paula *et al.*, "Long-Term Lithium Treatment Increases cPLA2 and iPLA2 Activity in Cultured Cortical and Hippocampal Neurons," *Molecules*, vol. 20, no. 11, pp. 19878–19885, Nov. 2015.

[234] A. Nassar and A. N. Azab, "Effects of Lithium on Inflammation," *ACS Chem. Neurosci.*, vol. 5, no. 6, pp. 451–458, Jun. 2014.

[235] E. Beurel and R. S. Jope, "Inflammation and lithium: clues to mechanisms contributing to suicide-linked traits," *Transl. Psychiatry*, vol. 4, no. 12, pp. e488–e488, Dec. 2014.

[236] S. S. Valvassori *et al.*, "Lithium modulates the production of peripheral and cerebral cytokines in an animal model of mania induced by dextroamphetamine," *Bipolar Disord.*, vol. 17, no. 5, pp. 507–517, Aug. 2015.

[237] B. Giunta, K. Rezai-Zadeh, and J. Tan, "Impact of the CD40-CD40L dyad in Alzheimer's disease.," *CNS Neurol. Disord. Drug Targets*, vol. 9, no. 2, pp. 149–55, Apr. 2010.

[238] R. W. Chen and D. M. Chuang, "Long term lithium treatment suppresses p53 and Bax expression but increases Bcl-2 expression. A prominent role in neuroprotection against excitotoxicity.," *J. Biol. Chem.*, vol. 274, no. 10, pp. 6039–42, Mar. 1999.

[239] G. Chen *et al.*, "The mood-stabilizing agents lithium and valproate robustly increase the levels of the neuroprotective protein bcl-2 in the CNS.," *J. Neurochem.*, vol. 72, no. 2, pp. 879–82, Feb. 1999.

[240] J. H. Morrison and P. R. Hof, "Selective vulnerability of corticocortical and hippocampal circuits in aging and Alzheimer's disease," *Prog Brain Res*, vol. 136, pp. 467–486, 2002.

[241] C. A. Davies, D. M. Mann, P. Q. Sumpter, and P. O. Yates, "A quantitative morphometric analysis of the neuronal and synaptic content of the frontal and temporal cortex in patients with Alzheimer's disease," *J Neurol Sci*, vol. 78, no. 2, pp. 151–164, 1987.

[242] S. T. DeKosky and S. W. Scheff, "Synapse loss in frontal cortex biopsies in Alzheimer's disease: correlation with cognitive severity," *Ann Neurol*, vol. 27, no. 5, pp. 457–464, 1990.

[243] L. Crews and E. Masliah, "Molecular mechanisms of neurodegeneration in Alzheimer's disease," *Hum Mol Genet*, vol. 19, no. R1, pp. R12-20, 2010.

[244] C. G. Lyketsos *et al.*, "Neuropsychiatric symptoms in Alzheimer's disease," *Alzheimers Dement*, vol. 7, no. 5, pp. 532–539, 2011.

[245] S. Gandy, "Testing the amyloid hypothesis of Alzheimer's disease in vivo.," *Lancet. Neurol.*, vol. 9, no. 4, pp. 333–5, Apr. 2010.

[246] K. R. Patterson *et al.*, "Characterization of prefibrillar Tau oligomers in vitro and in Alzheimer disease," *J Biol Chem*, vol. 286, no. 26, pp. 23063–23076, 2011.

[247] K. J. Kopeikina, B. T. Hyman, and T. L. Spires-Jones, "Soluble forms of tau are toxic in Alzheimer's disease.," *Transl. Neurosci.*, vol. 3, no. 3, pp. 223–233, Sep. 2012.

[248] K. L. Lanctot *et al.*, "Neuropsychiatric signs and symptoms of Alzheimer's disease: New treatment paradigms," *Alzheimers Dement (N Y)*, vol. 3, no. 3, pp. 440–449, 2017.

[249] S. Sportiche *et al.*, "Clinical factors associated with lithium response in bipolar disorders," *Aust. N. Z. J. Psychiatry*, vol. 51, no. 5, pp. 524–530, 2017.

[250] P. V Nunes, O. V Forlenza, and W. F. Gattaz, "Lithium and risk for Alzheimer's disease in elderly patients with bipolar disorder," *Br J Psychiatry*, vol. 190, pp. 359–360, 2007.

[251] O. V Forlenza, V. J. de Paula, R. Machado-Vieira, B. S. Diniz, and W. F. Gattaz, "Does Lithium Prevent Alzheimer's Disease?," *Drugs Aging*, vol. 29, no. 5, pp. 335–342, 2012.

[252] O. V Forlenza, I. Aprahamian, V. J. de Paula, and T. Hajek, "Lithium, a Therapy for AD: Current Evidence from Clinical Trials of Neurodegenerative Disorders," *Curr Alzheimer Res*, vol. 13, no. 8, pp. 879–886, 2016.

[253] X. Zhang *et al.*, "Long-term treatment with lithium alleviates memory deficits and reduces amyloid-beta production in an aged Alzheimer's disease transgenic mouse model," *J Alzheimers Dis*, vol. 24, no. 4, pp. 739–749, 2011.

[254] V. A. Fajardo, V. A. Fajardo, P. J. LeBlanc, and R. E. K. MacPherson, "Examining the Relationship between Trace Lithium in Drinking Water and the Rising Rates of Age-Adjusted Alzheimer's Disease Mortality in Texas," *J Alzheimers Dis*, vol. 61, no. 1, pp. 425–434, 2018.

[255] E. C. Lauterbach and M. F. Mendez, "Psychopharmacological Neuroprotection in Neurodegenerative Diseases, Part III: Criteria-Based Assessment: A Report of the ANPA Committee on Research," *J. Neuropsychiatry Clin. Neurosci.*, vol. 23, no. 3, pp. 242–260, 2011.

[256] B. Shine, R. F. McKnight, L. Leaver, and J. R. Geddes, "Long-term effects of lithium on renal, thyroid, and parathyroid function: a retrospective analysis of laboratory data," *Lancet*, vol. 386, no. 9992, pp. 461–468, 2015.

[257] M. Garcia-Alloza *et al.*, "Characterization of amyloid deposition in the APPswe/PS1dE9 mouse model of Alzheimer disease," *Neurobiol Dis*, vol. 24, no. 3, pp. 516–524, 2006.

[258] C. Janus, A. Y. Flores, G. Xu, and D. R. Borchelt, "Behavioral abnormalities in APPSwe/PS1dE9 mouse model of AD-like pathology: comparative analysis across multiple behavioral domains," *Neurobiol Aging*, vol. 36, no. 9, pp. 2519–2532, 2015.

[259] D. C. Rogers *et al.*, "Use of SHIRPA and discriminant analysis to characterise marked differences in the behavioural phenotype of six inbred mouse strains," *Behav Brain Res*, vol. 105, no. 2, pp. 207–217, 1999.

[260] S. K. Praharaj, "Metformin for Lithium-induced Weight Gain: A Case Report," *Clin. Psychopharmacol. Neurosci.*, vol. 14, no. 1, pp. 101–103, 2016.

[261] C. F. Giusti, S. R. Amorim, R. A. Guerra, and E. S. Portes, "Endocrine disturbances related to the use of lithium," *Arq Bras Endocrinol Metab.*, vol. 56, no. 3, pp. 153–158, 2012.

[262] C. Bonardi, F. de Pulford, D. Jennings, and M.-C. Pardon, "A detailed analysis of the early context extinction deficits seen in APPswe/PS1dE9 female mice and their relevance to preclinical Alzheimer's disease," *Behav. Brain Res.*, vol. 222, no. 1, pp. 89–97, Sep. 2011.

[263] C. G. Lyketsos, O. Lopez, B. Jones, A. L. Fitzpatrick, J. Breitner, and S. DeKosky, "Prevalence of neuropsychiatric symptoms in dementia and mild cognitive impairment: results from the cardiovascular health study," *Jama*, vol. 288, no. 12, pp. 1475–1483, 2002.

[264] J. H. Park *et al.*, "Depression in vascular dementia is quantitatively and qualitatively different from depression in Alzheimer's disease," *Dement Geriatr Cogn Disord*, vol. 23, no. 2, pp. 67–73, 2007.

[265] M. Filali, R. Lalonde, and S. Rivest, "Cognitive and non-cognitive behaviors in an APPswe/PS1 bigenic model of Alzheimer's disease," *Genes Brain Behav*, vol. 8, no. 2, pp. 143–148, 2009.

[266] M. Gitlin, "Lithium side effects and toxicity: prevalence and management strategies," *Int J Bipolar Disord*, vol. 4, 2016.

[267] A. Caccamo, S. Oddo, L. X. Tran, and F. M. LaFerla, "Lithium reduces tau phosphorylation but not A beta or working memory deficits in a transgenic model with both plaques and tangles," *Am J Pathol*, vol. 170, no. 5, pp. 1669–1675, 2007.

[268] C. Feyt *et al.*, "Lithium chloride increases the production of amyloid-beta peptide independently from its inhibition of glycogen synthase kinase 3," *J Biol Chem*, vol. 280, no. 39, pp. 33220–33227, 2005.

[269] P. Lei *et al.*, "Lithium suppression of tau induces brain iron accumulation and neurodegeneration," *Mol Psychiatry*, vol. 22, no. 3, pp. 396–406, 2017.

[270] L. Trujillo-Estrada *et al.*, "In vivo modification of Abeta plaque toxicity as a novel neuroprotective lithium-mediated therapy for Alzheimer's disease pathology," *Acta Neuropathol Commun*, vol. 1, p. 73, 2013.

[271] L. R. Nery *et al.*, "Brain Intraventricular Injection of Amyloid-beta in Zebrafish Embryo Impairs Cognition and Increases Tau Phosphorylation, Effects Reversed by Lithium," *PLoS One*, vol. 9, no. 9, 2014.

[272] P. Bianchi, E. Ciani, A. Contestabile, S. Guidi, and R. Bartesaghi, "Lithium Restores Neurogenesis in the Subventricular Zone of the Ts65Dn Mouse, a Model for Down Syndrome," *Brain Pathol.*, vol. 20, no. 1, pp. 106–118, 2010.

[273] F. Gelfo *et al.*, "Chronic Lithium Treatment in a Rat Model of Basal Forebrain Cholinergic Depletion: Effects on Memory Impairment and Neurodegeneration," *J. Alzheimers Dis.*, vol. 56, no. 4, pp. 1505–1518, 2017.

[274] T. Dwivedi and H. Zhang, "Lithium-induced neuroprotection is associated with epigenetic modification of specific BDNF gene promoter and altered expression of apoptotic-regulatory proteins," *Front Neurosci*, vol. 8, p. 457, 2014.

[275] A. Macdonald, K. Briggs, M. Poppe, A. Higgins, L. Velayudhan, and S. Lovestone, "A feasibility and tolerability study of lithium in Alzheimer's disease," *Int. J. Geriatr. Psychiatry*, vol. 23, no. 7, pp. 704–711, 2008.

[276] H. Hampel *et al.*, "Lithium Trial in Alzheimer's Disease: A Randomized, Single-Blind, Placebo-Controlled, Multicenter 10-Week Study," *J. Clin. Psychiatry*, vol. 70, no. 6, pp. 922–931, 2009.

[277] T. Leyhe *et al.*, "Increase of BDNF Serum Concentration in Lithium Treated Patients with Early Alzheimer's Disease," *J. Alzheimers Dis.*, vol. 16, no. 3, pp. 649–656, 2009.

[278] A. Nilsson and R. Axelsson, "Psychopathology during long-term lithium treatment of patients with major affective disorders. A prospective study," *Acta Psychiatr Scand*, vol. 80, no. 4, pp. 375–388, 1989.

[279] A. S. Fleisher *et al.*, "Chronic divalproex sodium use and brain atrophy in Alzheimer disease," *Neurology*, vol. 77, no. 13, pp. 1263–1271, 2011.

APPENDIX A

IACUC APPROVAL FOR ANIMAL STUDY

USF UNIVERSITY OF SOUTH FLORIDA

RESEARCH INTEGRITY AND COMPLIANCE
INSTITUTIONAL ANIMAL CARE & USE COMMITTEE

MEMORANDUM

TO: Jun Tan, M.D., Ph.D.

FROM:

Farah Moulvi, MSPH, IACUC Coordinator
Institutional Animal Care & Use Committee
Research Integrity & Compliance

DATE: 7/15/2014

PROJECT TITLE: Role of sAPPalpha binding to Abeta in Alzheimer's pathology

FUNDING SOURCE: USF department, institute, center, etc.

IACUC PROTOCOL #:   R IS00000438

PROTOCOL STATUS: **Amendment APPROVED**

The Institutional Animal Care and Use Committee (IACUC) received your Modification concerning the above referenced IACUC protocol.

On **7/15/2014** the IACUC reviewed and approved your Modification for the following:

Personnel Addition:

Added: Md Habib (#8020)

APPENDIX B

IACUC APPROVAL FOR ANIMAL STUDY

USF UNIVERSITY OF SOUTH FLORIDA

RESEARCH INTEGRITY AND COMPLIANCE
INSTITUTIONAL ANIMAL CARE & USE COMMITTEE

MEMORANDUM

TO: Jun Tan, M.D., Ph.D.

FROM:

Farah Moulvi, MSPH, IACUC Coordinator
Institutional Animal Care & Use Committee
Research Integrity & Compliance

DATE: 3/30/2016

PROJECT TITLE: LISPRO, an ionic cocrystal of lithium, as a potential novel
                   treatment for Alzheimer's disease

FUNDING SOURCE: National Institutes of Health

IACUC PROTOCOL #: R IS00002240

PROTOCOL STATUS: **APPROVED**

The Institutional Animal Care and Use Committee (IACUC) reviewed your application
requesting the use of animals in research for the above-entitled study. The IACUC
APPROVED your request to use the following animals in your **protocol for a one-year
period beginning 3/30/2016:**

Mouse: 3X Tg (PS1M146V, APPswe, tauP301L) (4 mo, both sexes)	256
Mouse: B6129SF2/J (4 mo/ both sexes)	128

Please take note of the following:

• **IACUC approval is granted for a one-year period at the end of which, an annual
renewal form must be submitted for years two (2) and three (3) of the protocol
through the eIACUC system.** After three years all continuing studies must be
completely re-described in a new electronic application and submitted to IACUC for
review.

• **All modifications to the IACUC-Approved Protocol must be approved by the
IACUC prior to initiating the modification.** Modifications can be submitted to the
IACUC for review and approval as an Amendment or Procedural Change through the

eIACUC system. These changes must be within the scope of the original research hypothesis, involve the original species and justified in writing. Any change in the IACUC-approved protocol that does not meet the latter definition is considered a major protocol change and requires the submission of a new application.

• **All costs invoiced to a grant account must be allocable to the purpose of the grant.** Costs allocable to one protocol may not be shifted to another in order to meet deficiencies caused by overruns, or for other reasons convenience. Rotation of charges among protocols by month without establishing that the rotation schedule credibly reflects the relative benefit to each protocol is unacceptable.

3/30/2016

APPENDIX C

COPYRIGHT PERMISSIONS

This Journal is a member of the Committee on Publication Ethics.

This Journal recommends that authors follow the Uniform Requirements for Manuscripts Submitted to Biomedical Journals formulated by the International Committee of Medical Journal Editors (ICMJE).

Please read the guidelines below then visit the journal's submission site https://mc.manuscriptcentral.com/celltransplantation to upload your manuscript. Please note that manuscripts not conforming to these guidelines may be returned.

Only manuscripts of sufficient quality that meet the aims and scope of *Cell Transplantation* will be reviewed.

As part of the submission process you will be required to warrant that you are submitting your original work, that you have the rights in the work, that you are submitting the work for first publication in the Journal and that it is not being considered for publication elsewhere and has not already been published elsewhere, and that you have obtained and can supply all necessary permissions for the reproduction of any copyright works not owned by you.

Please include a cover letter, containing the name, full mailing address, telephone, email address and fax number (if applicable) of the author responsible for correspondence. Follow the Preparing Your Manuscript (section 6) guidelines below to prepare the manuscript, figures, and tables.

1. Open Access

Cell Transplantation is an open access, peer-reviewed journal. Each article accepted by peer review is made freely available online immediately upon publication, is published under a Creative Commons license and will be hosted online in perpetuity. Publication costs of the journal are covered by the collection of article processing charges which are paid by the funder, institution or author of each manuscript upon acceptance. There is no charge for submitting a paper to the journal.

For general information on open access at SAGE please visit the Open Access page or view our Open Access FAQs.

[Return to top]

2. Article processing charge (APC)

If, after peer review, your manuscript is accepted for publication, a one-time article processing charge (APC) is payable. This APC covers the cost of publication and ensures that your article will be freely available online in perpetuity under a Creative Commons license.

[Price change, see underlined below.] At the time of submission you will be asked to confirm that you will pay the open access fees. The page charge fee is based on the page count estimate made after acceptance ($1,100 for less than 5 pages, $2,200 for 5-12 pages and +$100 for each additional page) when billed.

[Price change, see underlined below.] Additional color charges for figures/illustrations may apply. Color charges are $895 for 1 figure; $1,250 for 2 figures; $1,575 for 3 figures; and $2,050 for 4+ figures.

5. Publishing policies

5.1 Publication ethics
SAGE is committed to upholding the integrity of the academic record. We encourage authors to refer to the Committee on Publication Ethics' International Standards for Authors and view the Publication Ethics page on the SAGE Author Gateway.

5.1.1 Plagiarism
Cell Transplantation and SAGE take issues of copyright infringement, plagiarism or other breaches of best practice in publication very seriously. We seek to protect the rights of our authors and we always investigate claims of plagiarism or misuse of published articles. Equally, we seek to protect the reputation of the journal against malpractice. Submitted articles may be checked with duplication-checking software. Where an article, for example, is found to have plagiarized other work or included third-party copyright material without permission or with insufficient acknowledgement, or where the authorship of the article is contested, we reserve the right to take action including, but not limited to: publishing an erratum or corrigendum (correction); retracting the article; taking up the matter with the head of department or dean of the author's institution and/or relevant academic bodies or societies; or taking appropriate legal action.

5.1.2 Prior publication
If material has been previously published, it is not generally acceptable for publication in a SAGE journal. However, there are certain circumstances where previously published material can be considered for publication. Please refer to the guidance on the SAGE Author Gateway or if in doubt, contact the Editor at the address given below.

5.2 Contributor's publishing agreement

Before publication SAGE requires the author as the rights holder to sign a Journal Contributor's Publishing Agreement. *Cell Transplantation* publishes manuscripts under Creative Commons licenses. The standard license for the journal is Creative Commons by Attribution Non-Commercial (CC BY-NC), which allows others to re-use the work without permission as long as the work is properly referenced and the use is non-commercial. For more information, you are advised to visit SAGE's OA licenses page

Alternative license arrangements are available, for example, to meet particular funder mandates, made at the author's request.

6. Preparing your manuscript

6.1 Word processing formats
Preferred formats for the text and tables of your manuscript are Word DOC, RTF, XLS. Papers should be typed in English, double-spaced throughout with at least 3-cm margins on paper

Last updated: January 2018

178

Cell Death & Disease

www.nature.com/cddis

Aims and Scope

Cell Death & Disease is the sister journal of *Cell Death & Differentiation*. It is a peer-reviewed open access online journal that publishes full-length papers, reviews and commentaries describing original research in the field of translational cell death. *Cell Death & Disease* seeks to encompass the breadth of translational implications of cell death, and topics of particular concentration will include, but are not limited to, the following:

- Experimental medicine
- Cancer
- Immunity
- Internal medicine
- Neuroscience
- Cancer metabolism

Contributions of broad biological interest and impact are especially encouraged.

Indexed and abstracted in

MEDLINE (PubMed), Scopus, Web of Science, Google Scholar and relevant subject-specific databases.

Online Archive

Archive available back to January 2010.

Readership

Cell Death & Disease's primary audience is scientists, clinicians and members of the biotechnology and pharmaceutical industry who are interested in the biology of cell death in the pathogenesis of human diseases or relevant animal models.

Open Access

Cell Death & Disease is an open access, online-only journal. Authors of accepted papers pay an article processing charge, and papers are open access immediately upon publication under a Creative Commons license. Access to content is freely available.

MENU ⌄   Cell Death
& Disease

🔍 Search   ✉ E-alert   📄 Submit   👤 Login

Open Access

Cell Death & Disease makes all content freely available to all researchers worldwide, ensuring maximum dissemination of content through the nature.com platform. Content is published online on a weekly basis to provide timely communication to the community and keep publication times to a minimum.

Publishing open access

Cell Death & Disease is an open access journal: authors pay an article processing charge (APC) for their accepted articles to be open access online and freely accessible immediately upon publication, under a Creative Commons license.

To facilitate self-archiving, Springer Nature deposits open access articles in PubMed Central and Europe PubMed Central on publication. Authors are also permitted to post the final, published PDF of their article on a website, institutional repository or other free public server immediately on publication.

Visit our open research site for detailed information about publishing open access in *Cell Death & Disease*:

- About Creative Commons licensing
- Creative Commons license options and article processing charges (APCs) for *Cell Death & Disease*
- APC payment FAQs
- Help in identifying funding for APCs
- Fee waiver policy

Permissions

*PLEASE NOTE: If the links highlighted here do not take you to those web sites, please copy and paste address in your browser.

Permission to reproduce Wiley journal Content:

Requests to reproduce material from John Wiley & Sons publications are being handled through the RightsLink® automated permissions service.

Simply follow the steps below to obtain permission via the Rightslink® system:

- Locate the article you wish to reproduce on Wiley Online Library (http://onlinelibrary.wiley.com)
- Click on the "Request Permissions" link on the content you wish to use. This link can be found next to the book, on article abstracts, tables of contents or by clicking the green "Information" icon.
- Follow the online instructions and select your requirements from the drop down options and click on 'quick price' to get a quote
- Create a RightsLink® account to complete your transaction (and pay, where applicable)
- Read and accept our Terms & Conditions and download your license
- For any technical queries please contact customercare@copyright.com
- For further information and to view a RightsLink® demo please visit www.wiley.com and select Rights & Permissions.

AUTHORS - If you wish to reuse your own article (or an amended version of it) in a new publication of which you are the author, editor or co-editor, prior permission is not required (with the usual acknowledgements). However, a formal grant of license can be downloaded free of charge from RightsLink by selecting "Author of this Wiley article" as your requestor type.
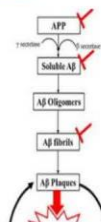
Individual academic authors who are wishing to reuse up to 3 figures or up to 400 words from this journal to republish in a new journal article they are writing should select **University/Academic** as the requestor type. They will then be able to download a free permission license.

Either of the above who are publishing a new journal article or book chapter with an **STM Signatory Publisher** may also select that requestor type and the STM Signatory publisher's name from the resulting drop-down list in RightsLink. This list is regularly updated. The requestor is required to complete the republication details, including the publisher name, during the request process. They will then be able to download a free permissions license.

HOME | ABOUT ∨ | CONTRIBUTE ∨ | BROWSE ∨

Permissions

*PLEASE NOTE: If the links highlighted here do not take you to those web sites, please copy and paste address in your browser.

Permission to reproduce Wiley journal Content:

Requests to reproduce material from John Wiley & Sons publications are being handled through the RightsLink® automated permissions service.

Simply follow the steps below to obtain permission via the Rightslink® system:

- Locate the article you wish to reproduce on Wiley Online Library (http://onlinelibrary.wiley.com)
- Click on the "Request Permissions" link on the content you wish to use. This link can be found next to the book, on article abstracts, tables of contents or by clicking the green "Information" icon.
- Follow the online instructions and select your requirements from the drop down options and click on 'quick price' to get a quote
- Create a RightsLink® account to complete your transaction (and pay, where applicable)
- Read and accept our Terms & Conditions and download your license
- For any technical queries please contact customercare@copyright.com
- For further information and to view a Rightslink® demo please visit www.wiley.com and select Rights & Permissions.

AUTHORS - If you wish to reuse your own article (or an amended version of it) in a new publication of which you are the author, editor or co-editor, prior permission is not required (with the usual acknowledgements). However, a formal grant of license can be downloaded free of charge from RightsLink by selecting "Author of this Wiley article" as your requestor type.

Individual academic authors who are wishing to reuse up to 3 figures or up to 400 words from this journal to republish in a new journal article they are writing should select **University/Academic** as the requestor type. They will then be able to download a free permission license.

Either of the above who are publishing a new journal article or book chapter with an **STM Signatory Publisher** may also select that requestor type and the STM Signatory publisher's name from the resulting drop-down list in RightsLink. This list is regularly updated. The requestor is required to complete the republication details, including the publisher name, during the request process. They will then be able to download a free permissions license.

Submit an Article

Browse free sample issue

Get content alerts

Recommend to a librarian

Subscribe to this journal

Published for the International Society for Neurochemistry

More from this journal

- News
- Pre-clinical Systematic Reviews
- Special Issues
- Mark A Smith Prize
- ISN-Wiley-Blackwell-JNC International Lectureships
- Jobs
- Get Email Alerts

Tell a friend about this journal **Tell a Friend** about this journal

Note to reader : Permission letter for Figure 1-2

Habib, Md

From:	Rights and Permissions <permission@karger.com>
Sent:	Friday, March 02, 2018 7:54 AM
To:	Habib, Md
Subject:	AW: Requested Karger Material

Dear Mr Habib,   *Permission for Figure 1-2*

Thank you for your email. As to your request, I am pleased to inform you that permission is granted hereby to use **Figure 1** from the article

Novel Insights into Lithium's Mechanism of Action: Neurotrophic and Neuroprotective Effects
Quiroz J.A. et al: Neuropsychobiology 2010;62:50–60 (DOI:10.1159/000314310)

to be reproduced in your dissertation, provided that proper credit will be given to the original source and that S. Karger AG, Basel will be mentioned.

Please note that this is a non-exclusive permission, hence any further use, edition, translation or distribution, either in print or electronically, requires written permission again as this permission is valid for the above mentioned purpose only.

This permission applies only to copyrighted content that S. Karger AG owns, and not to copyrighted content from other sources. If any material in our work appears with credit to another source, you must also obtain permission from the original source cited in our work. All content reproduced from copyrighted material owned by S. Karger AG remains the sole and exclusive property of S. Karger AG. The right to grant permission to a third party is reserved solely by S. Karger AG.

Thank you for your understanding and cooperation.

Hopefully, I have been of assistance to you with the above.

Yours sincerely,

Silvia Glücklich
Rights Manager
permission@karger.com

KARGER

S. Karger AG, Medical and Scientific Publishers, Allschwilerstrasse 10, 4009 Basel, Switzerland
t +41 61 306 14 75, f +41 61 306 12 34, www.karger.com

-----Ursprüngliche Nachricht-----
Von: permission@karger.com [mailto:permission@karger.com]
Gesendet: Donnerstag, 1. März 2018 19:16
An: Rights and Permissions <permission@karger.com>
Betreff: Requested Karger Material

1

183

Dear Customer

Thank you for your Requested Karger Material

The following details have been noted:

Delivery address:

Title: Mr
First name: Ahsan
Family name: Habib

Address: 3515 E Fletcher Ave. Tampa, FL 33613

City: Tampa
State (USA only): Florida
Florida
Zip/Postal code:
Country: United States

Fax:
Mailto: mhabib1@health.usf.edu

Requested Karger Material

Primary author(s) and/or editor(s):
Title of book/journal: Neuropsychobiology Citation (year, volume, issue, pages: Neuropsychobiology. 2010;62(1):50-60. doi: 10.1159/000314310. Epub 2010 May 7.

Figure/Table
#
on age

Abstract:

Other media:

Reuse:

Title of your new work:
Publisher:
Type of reuse: I would like to use Fig. 1 in my dissertation with proper citation

Type of format
Print:
Print run:

Posting on a website/intranet:

2

URL of website/intranet:
Secure environment:

Data carrier:
Circulation:
Database:
Software Program:
Circulation:

Translation: No

If yes, please name the relevant language(s):

Are you the author (co-author/editor) of the original work: No

Comment:

Best regards,

3